Regulation and mitotic functions of the PP1 interactors SDS22 and Inhibitor-3

Inaugural-Dissertation

zur

Erlangung des Doktorgrades

Dr. rer. nat.

der Fakultät für

Biologie

an der

Universität Duisburg-Essen

vorgelegt von

Jonas Seiler

aus Gelsenkirchen

April 2016

Die der vorliegenden Arbeit zugrunde liegenden Experimente wurden in der Abteilung für Molekularbiologie I am Zentrum für Medizinische Biotechnologie der Universität Duisburg-Essen durchgeführt.

1. Gutachter: Prof. Dr. Hemmo Meyer

2. Gutachter: Prof. Dr. Stefan Westermann

Vorsitzender des Prüfungsausschusses: Prof. Dr. Andrea Musacchio

Tag der mündlichen Prüfung: 29.08.2016

Table of contents

List of figures

List of tables

Summary

In order to achieve faithful chromosome segregation during mitosis and to avoid aneuploidy, the kinetochores of the two sister chromatids need to form attachments with microtubules emanating from opposite poles of the mitotic spindle. Bipolar attachment of sister kinetochores is regulated by dynamic phosphorylation of kinetochore proteins. Key regulators of this process are the mitotic kinase Aurora B and the counteracting phosphatase PP1. The PP1 interactor SDS22 has been shown to be involved in positively regulating kinetochore-associated PP1 in mammalian cells, however its exact localization and function has remained controversial. SDS22 is known to form a ternary complex with PP1 and inhibitor-3 (I3). While Ypi1/I3 is known to be involved in regulating PP1-mediated counteraction of Ipl1/Aurora kinase in yeast, the function of I3 in mammalian mitosis has thus far been unknown. Findings in yeast furthermore implicate the AAA ATPase Cdc48/p97 with its cofactor Shp1 in positively regulating PP1 and suggest that Cdc48/p97-Shp1 acts on the ternary SDS22-PP1-Ypi1/I3 complex. This study aimed at solving the function of SDS22 at the kinetochore and at elucidating the role of I3 in mammalian mitosis. In addition, we wanted to investigate the interaction of p97 with SDS22-PP1-I3 in mammalian cells.

Our results allow us to draw at least three important conclusions. First, our data reveal a complex role of SDS22 in regulating kinetochore-associated PP1. We confirm that SDS22 is required for PP1 activity at the kinetochore. However, contrary to a previous report, we show that SDS22 does not quantitatively localize to kinetochores under normal conditions and does not function as a PP1 targeting factor to the kinetochore. Instead, while being required for PP1 activity at the kinetochore, SDS22 inhibits PP1-mediated dephosphorylation of Aurora B at T232 when bound to the kinetochore. This is consistent with a model in which SDS22 functions as a PP1 chaperone or maturation factor, mediating a PP1 activation step in solution that is followed by SDS22 dissociation and binding of activated PP1 to KNL1 at the kinetochore.

Second, we elucidate the role of I3 in PP1-mediated balancing of Aurora B. Depletion of I3 leads to quantitative association of SDS22 with PP1 bound to KNL1 at the

kinetochore, accompanied by increased Aurora B activity. This suggests that I3 is required for sequestering and keeping SDS22-PP1 in solution, thus preventing association of inactive SDS22-bound PP1 with KNL1 at the kinetochore. Additionally, we find indications that I3 is required for dissociation of SDS22 from PP1.

Third, we show that the interaction between p97 and the SDS22-PP1-I3 complex is conserved in human cells. Our data provide important first insights on how p97, together with the Shp1 orthologs p37, UBXD4 and p47, may regulate the SDS22-PP1-I3 complex. Our results are consistent with a role of p97 in regulating PP1 by dissociating SDS22 from the ternary PP1 complex.

Zusammenfassung

Um Aneuploidie zu verhindern, müssen während der Mitose die Schwesterchromatiden der duplizierten Chromosomen korrekt auf beide Tochterzellen verteilt werden. Um dies zu gewährleisten, muss es zur Anbindung der Kinetochore der beiden Schwesterchromatiden an Spindelmikrotubuli kommen, die von entgegengesetzten Polen der mitotischen Spindel ausgehen. Diese bipolare Anbindung der Schwesterkinetochore wird durch eine dynamische Phosphorylierung von Kinetochorproteinen ermöglicht und reguliert. Zentrale Regulatoren dieses Prozesses sind die mitotische Kinase Aurora B und die entgegenwirkende Phosphatase PP1. Es wurde bereits gezeigt, dass SDS22, ein Interaktionspartner der Phosphatase PP1, für die volle Aktivität von Kinetochor-gebundenem PP1 vonnöten ist und somit als positiver Regulator der Phosphatase fungiert. Die genaue Lokalisation und Funktionsweise von SDS22 ist allerdings nicht geklärt, da hierzu kontroverse Ergebnisse veröffentlicht wurden. Es ist bekannt, dass SDS22 einen ternären Komplex mit PP1 und Inhibitor-3 (I3) bilden kann. In Hefezellen wurde gezeigt, dass Ypi1/I3 eine Rolle für die der Kinase Ipl1/Aurora entgegenwirkende Aktivität von PP1 spielt. Die Funktion von I3 in der Mitose in Säugerzellen ist allerdings bislang nicht untersucht worden. Ergebnisse aus Hefestudien zeigen darüber hinaus, dass auch die AAA ATPase Cdc48/p97 mit ihrem Kofaktor Shp1 eine Rolle als positiver Regulator von PP1 spielt und deuten darauf hin, dass Cdc48/p97-Shp1 auf den ternären SDS22-PP1-Ypi1/I3-Komplex einwirkt. Ziel dieser Studie war es, die Funktion von SDS22 am Kinetochor aufzuklären und die Rolle von I3 in der Mitose in Säugerzellen herauszufinden. Zudem wollten wir die Interaktion von p97 mit dem SDS22-PP1-I3-Komplex in Säugerzellen untersuchen.

Unsere Ergebnisse lassen mindestens drei wichtige Schlussfolgerungen zu. Zum ersten zeigen unsere Daten, dass die Funktion von SDS22 in der Regulation von PP1 am Kinetochor komplex ist. Unsere Ergebnisse bestätigen, dass SDS22 für die Aktivität von Kinetochor-gebundenem PP1 vonnöten ist. Im Gegensatz zu einer vorherigen Studie zeigen wir allerdings, dass SDS22 unter normalen Bedingungen nicht in quantitativen Mengen am Kinetochor zu finden ist und auch nicht als Rekrutierungsfaktor für PP1 zum Kinetochor fungiert. Obgleich SDS22 für die Funktion von PP1 am Kinetochor gebraucht wird, führt eine quantitative Bindung von

SDS22 an das Kinetochor zur Inhibition der Dephosphorylierung von Aurora B an T232 durch PP1. Diese Ergebnisse lassen sich mit einem Modell erklären, in dem SDS22 eine Rolle als Chaperon oder Reifungsfaktor für PP1 spielt. In diesem Modell wird SDS22 für die Aktivierung von PP1 in Lösung gebraucht, welche der Dissoziation von SDS22 und der Bindung von aktiviertem PP1 an das Kinetochorprotein KNL1 vorausgeht.

Zum zweiten klären wir die Rolle von I3 im Wechselspiel von PP1 und Aurora B auf. Eine Depletion von I3 führt zu einer quantitativen Bindung von SDS22 an PP1, welches an das Kinetochorprotein KNL1 gebunden ist. Dieser Effekt geht mit einer erhöhten Aktivität von Aurora B einher. Dies lässt sich dadurch erklären, dass I3 benötigt wird um SDS22-PP1 zu sequestrieren und in Lösung zu halten, wodurch es eine Assoziation von inaktivem, SDS22-gebundenem PP1 mit KNL1 am Kinetochor verhindert. Zusätzlich finden wir Hinweise darauf, dass I3 für eine Dissoziation von SDS22 von PP1 gebraucht werden könnte.

Zum dritten zeigen wir, dass die Interaktion zwischen p97 und dem SDS22-PP1-I3-Komplex in humanen Zellen konserviert ist. Unsere Daten liefern wichtige erste Einblicke, wie p97, zusammen mit den Shp1 Orthologen p37, UBXD4 und p47, den SDS22-PP1-I3-Komplex regulieren könnte. Unsere Daten deuten darauf hin, dass p97 eine Rolle in der Regulation von PP1 spielen könnte, indem es SDS22 von dem ternären PP1-Komplex dissoziiert.

1 Introduction

In order to achieve faithful chromosome segregation during mitosis, the kinetochores of the two sister chromatids need to form attachments with microtubules emanating from opposite poles of the mitotic spindle. Formation of bipolar kinetochore-microtubule attachments is tightly regulated by opposing activities of the mitotic kinase Aurora B and the phosphatase PP1. In this thesis, we examine the role of the PP1 interacting proteins SDS22 and I3 in regulating PP1 function at the kinetochore. Furthermore, we investigate the regulation and interaction of the ternary SDS22-PP1-I3 complex with the AAA ATPase p97 and its SEP domain cofactors p37, p47 and UBXD4. The following introduction will therefore first give a brief overview on mitosis in mammalian cells, before discussing aspects relevant to our findings in more detail, focussing especially on the kinase Aurora B. The subsequent parts will then give an introduction to PP1 and p97 and their relevant cofactors.

1.1 Mitosis

Mitotic cell division is a highly complex process that results in the separation of a cell into two daughter cells with identical genetic material. It comprises the distribution of replicated chromosomes into two daughter nuclei (mitosis), followed by the physical division of the cytoplasm into two separate daughter cells (cytokinesis). Morphologically, the process of mitosis can be divided into five distinct phases: prophase, prometaphase, metaphase, anaphase and telophase. During prophase, the chromosomes condense within the nucleus, and the two centrosomes separate and start to move towards opposite poles. The mitotic spindle starts to form as microtubules nucleate from the two centrosomes and gradually assemble between them. Nuclear envelope breakdown (NEBD) marks the beginning of prometaphase. During prometaphase, microtubules of the forming spindle start to attach to chromosomes at the kinetochores, which results in an arrangement of the chromosomes in a horse-shoe-like form around the spindle. In metaphase, all chromosomes align in the middle of the spindle, along the cell equator, forming the metaphase plate. When biorientation is achieved, i.e., when both kinetochores on sister chromatids of each chromosome are attached to microtubules from opposite

spindle poles, the cell proceeds to anaphase. During anaphase, the sister chromatids of the replicated chromosomes separate and are then simultaneously pulled towards opposite spindle poles. In telophase, kinetochore-microtubule attachment is lost, chromosomes decondense and new nuclear membranes form around each set of chromosomes. Already in late anaphase, a cleavage furrow begins to form at the cell equator, surrounding the spindle midzone between the two sets of sister chromatids. During telophase, the contractile ring of the cleavage furrow further constricts and the central spindle in the midzone condenses, forming tight bundles of antiparallel microtubules, that overlap at the midbody. Finally, cytokinesis takes place as the two daughter cells are separated by plasma membrane fission at the midbody.

As mentioned above, mitosis is an extremely complex process that involves a tremendous reorganization of all cell components. In order to avoid missegregation of chromosomes, which can lead to cell death or aneuploidy, and therefore, ultimately to cancer (Kops et al., 2005), all steps of mitosis have to be tightly regulated on a molecular level. The intricate regulatory mechanisms governing mitotic entry and progression involve the reversible phosphorylation of a multitude of regulatory and structural proteins, mediated by a number of mitotic kinases and counteracting phosphatases (Ma & Poon, 2011; Bollen et al., 2009), ubiquitin-dependent degradation of key regulators (Musacchio, 2011), and two cell-cycle checkpoints – the G2/M and the spindle assembly checkpoint (SAC) (Ma & Poon, 2011).

Mitotic entry

In order to assure genomic stability, the G2/M checkpoint monitors the DNA replication status and senses DNA damage, preventing cells with unreplicated and / or damaged DNA from entering mitosis (Latif et al., 2001). Satisfaction of the checkpoint leads to activation of the CDK1-cyclin B complex or maturation-promoting factor (MPF), and thereby induces mitotic entry. The CDK1-cyclin B kinase is the main driver of mitosis (Coudreuse & Nurse, 2010; Fung & Poon, 2005). A critical factor for the activation of CDK1 is the amount of cyclin B available for MPF complex formation. In mammalian cells, cyclin B expression is mainly regulated at the levels of transcription and protein degradation (Fung & Poon, 2005). Transcription of cyclin B starts during S-phase and peaks at late G2-phase (Fung & Poon, 2005). Binding of

cyclin B to CDK1 alone, however, does not suffice to activate the kinase, since CDK1 activity is negatively regulated by inhibitory phosphorylation at T14 and Y15 by Wee1 and Mypt1 kinases (Dunphy, 1994; Fung & Poon, 2005). Satisfaction of the G2/M checkpoint allows for CDC25 phosphatases to dephosphorylate CDK1, thereby activating CDK1-cyclin B (Bollen et al., 2009). Activated CDK1-cyclin B phosphorylates a vast number of both regulatory and structural proteins, which leads to a profound reorganization of cellular morphology and structures, including rounding up of the cells, chromosome condensation, mitotic spindle formation, nuclear envelope disassembly, disassembly of the Golgi apparatus and reorganization of the ER (Ma & Poon, 2011; Bollen et al., 2009; Güttinger et al., 2009). In addition to CDK1, a number of other kinases play an important role in regulating mitosis, among them Mps1, Haspin and Aurora A and B kinases (Ma & Poon, 2011). Nuclear envelope breakdown (NEBD) at the beginning of prometaphase allows for many mitotic proteins to gain access to their sites of action. Examples are condensin I that is cytoplasmic in interphase and mediates further chromosome condensation upon NEBD (Güttinger et al., 2009), as well as the spindle assembly checkpoint (SAC) proteins Mad1 and Mad2 (Cheeseman & Desai, 2008). Moreover, and importantly, upon NEBD, spindle microtubules can start to attach to chromosomes at the kinetochores.

Chromosome biorientation

The mitotic spindle is a highly dynamic structure that consists of microtubule fibers and hundreds of regulatory proteins (Walczak and Heald, 2008). The attachment of spindle microtubules to kinetochores is a stochastic process. Microtubules undergo repeated cycles of spontaneous growth and shrinkage, called dynamic instability (Mitchison & Kirschner, 1984). This dynamic instability increases the chance for encounters between microtubules and kinetochores, which has been described as the “search-and-capture” model (Mitchison & Kirschner, 1986). Kinetochores initially attach to the lateral surface of spindle microtubules, are then transported along the microtubules towards the spindle poles, where the lateral attachment is converted to end-on attachment (Tanaka, 2013). In animal cells, bundles of many microtubules are attached to kinetochores in an end-on manner, forming so-called K-fibers (Tanaka, 2013). In order to achieve faithful chromosome segregation, the two

kinetochores on sister chromatids of each chromosome have to form end-on attachments with microtubules emanating from opposite spindle poles. This is termed ‚biorientation'. Formation of bioriented attachments is crucial for chromosome congression to the metaphase plate. However, also monooriented chromosomes can congress to the metaphase plate. This is achieved by a transport mechanism alongside K-fibers attached to already bioriented chromosomes that is mediated by the microtubule motor CENP-E (Kapoor et al., 2006; Kim et al., 2010). Ultimately, however, biorientation of all chromosomes at the metaphase plate has to be achieved before onset of anaphase, in order to avoid missegregation of chromosomes. Two mechanisms exist to sense and correct erroneous microtubule-kinetochore attachments and to halt anaphase onset until correct bipolar attachment of all chromosomes is achieved: error correction (EC) and the spindle assembly checkpoint (SAC) (Musacchio, 2015; Krenn & Musacchio, 2015). The kinase Aurora B plays a decisive role in both pathways (Krenn & Musacchio, 2015). Error correction is a “local” mechanism, that leads to the stabilization of correct, bipolar attachments and to the destabilization of erroneous attachments. It is believed to depend on the ability of the centromere-kinetochore system to detect the tension that occurs upon biorientation, when microtubules pull from opposite spindle poles, or the lack of tension in chromosomes lacking biorientation (Lampson & Cheeseman, 2011; Krenn & Musacchio, 2015). The SAC, on the other hand, generates a “global” signal that prevents cells from entering anaphase before biorientation of all chromosomes is achieved (Krenn & Musacchio, 2015). Briefly, unattached kinetochores function as a recruitment hub for SAC proteins, which leads to the formation of the mitotic checkpoint complex (MCC). As long as the checkpoint is active, the MCC inhibits the anaphase promoting complex or cyclosome (APC/C), a ubiquitin ligase that drives mitotic exit (Musacchio, 2015). The EC and SAC pathways, and the role of Aurora B kinase in these pathways, will be described in more detail in the following chapters.

Mitotic exit

Satisfaction of the SAC leads to activation of the APC/C, a multisubunit E3 ubiquitin ligase that ubiquitinates two key substrates, cyclin B and Securin, thereby targeting them for proteasomal degradation (Musacchio, 2015). Proteolysis of cyclin B inactivates CDK1, thus driving mitotic exit. Inactivation of CDK1 allows for the bulk

dephosphorylation of mitotic substrates by phosphatases including CDC14, PP1 and PP2A (Bollen et al., 2009; Wurzenberger & Gerlich, 2011). The other key APC/C substrate, Securin, is an inhibitor of the protease Separase. Once activated, Separase cleaves Kleisin, a subunit of the Cohesin complex that keeps sister chromatids tightly connected at the centromeres. Cleavage of Cohesin allows for the segregation of sister chromatids to opposite spindle poles (Mehta et al., 2012). Chromosome segregation goes along with, and is facilitated by the assembly of the central spindle that is composed of antiparallel bundles of microtubules that overlap at the central region (Fededa & Gerlich, 2012). The central spindle defines the position of the division plane and contributes to the assembly of the contractile actomyosin ring at the equatorial cell cortex. As the actomyosin ring contracts, the cleavage furrow emerges during anaphase and further ingresses during telophase. In telophase, chromatin decondenses, new nuclear envelopes are assembled and the ER and Golgi apparatus reorganize. The central spindle condenses as ingression of the cleavage furrow progresses, forming an intercellular bridge with the midbody at its center. Cytokinesis is completed by plasma membrane fission at the midbody (Fededa & Gerlich, 2012).

1.2 Chromosome biorientation

1.2.1 The kinetochore

Kinetochores function both as sites for chromosome attachment to spindle microtubules and as recruitment hubs for SAC components. Figure 1.1 shows a schematic structure of a kinetochore attached to microtubules. Kinetochores are highly complex multi-subunit structures that can be structurally divided into an inner and an outer layer (Musacchio, 2015). They assemble on specialized chromatin structures, the centromeres. Centromeres are epigenetically marked by the histone H3 variant CENP-A (Black & Cleveland, 2011). In vertebrate cells, CENP-A nucleosomes interact with a number of CENP proteins that form the constitutive centromere-associated network (CCAN) (Jia et al., 2013). The CCAN establishes the inner kinetochore. CCAN components form several different subcomplexes, e.g. the CENP-T-W-S-X subcomplex that can bind to DNA, possibly forming a nucleosome-like structure (Nishino et al., 2012). As the name indicates, the CCAN constitutively localizes to centromeres throughout the cell cycle. The outer kinetochore, on the other hand, is only formed during mitosis. It is assembled onto the CCAN during late prophase, shortly before NEBD (Jia et al., 2013). The outer kinetochore contains the 10-subunit KMN network that mediates kinetochore-microtubule attachment (Musacchio, 2011). The KMN network is comprised of KNL1 (kinetochore null protein 1), the Mis12 (missegregation 12) complex and the Ndc80 (nuclear division cycle 80) complex. Recruitment of the KMN network to the CCAN is mediated by CENP-C and CENP-T, via binding to the Mis12 complex and the Ndc80 complex, respectively (Screpanti et al., 2011; Przewloka et al., 2011; Schleiffer et al., 2012). The Mis12 complex interacts with both the Ndc80 complex and KNL1 and constitutes the core for KMN network formation (Petrovic et al., 2010). The Ndc80 complex and KNL1 have microtubule-binding activities and were shown to bind microtubules in a cooperative manner (Wei et al., 2007; Cheeseman et al., 2006; Jia et al., 2013).

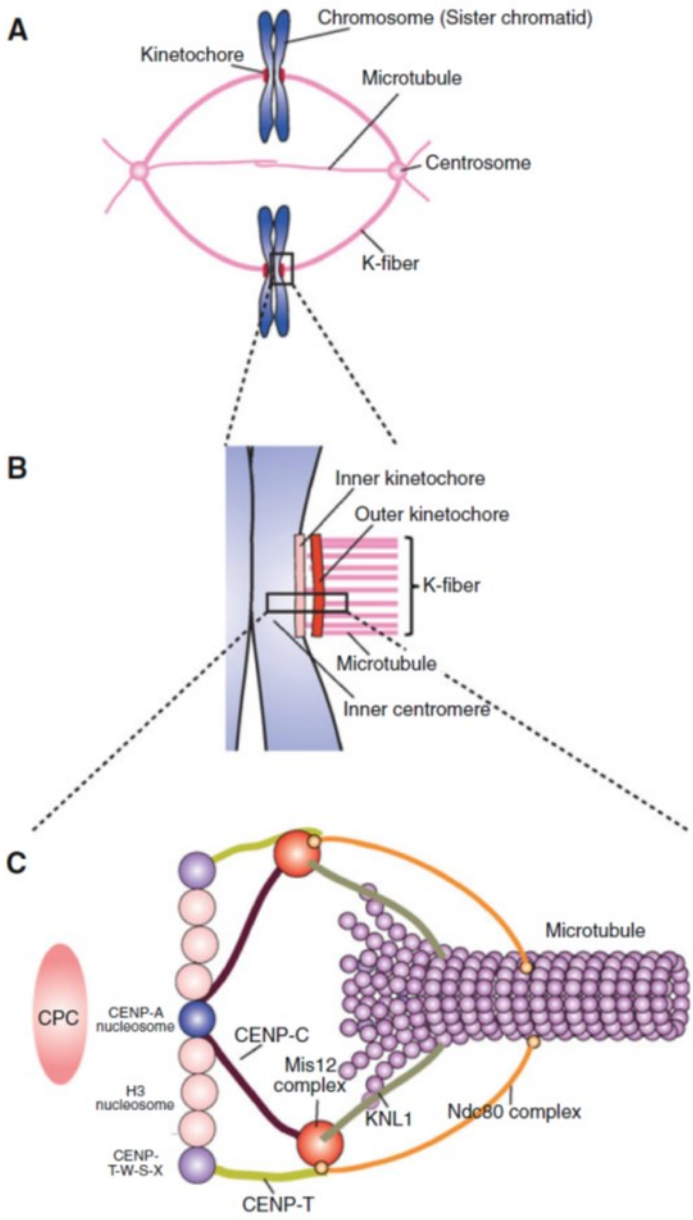

Figure 1.1 Kinetochore structure. A Schematic structure of the mitotic spindle. **B** Schematic morphological structure of a kinetochore attached to microtubules. The boxed area in (**A**) is shown. **C** Schematic molecular structure of a kinetochore attached to microtubules. The boxed area in (**B**) is shown. CPC: Chromosomal passenger complex. (Tanaka, 2013).

Microtubule-kinetochore attachment is a stochastic process. This implies that connection of chromosomes to the mitotic spindle comes about via a mechanism of trial and error. Therefore, erroneous attachments occur relatively frequently (Nicklas, 1997). Besides correct amphitelic (or bipolar) attachment, monotelic, syntelic or merotelic attachments are possible (Figure 1.2).

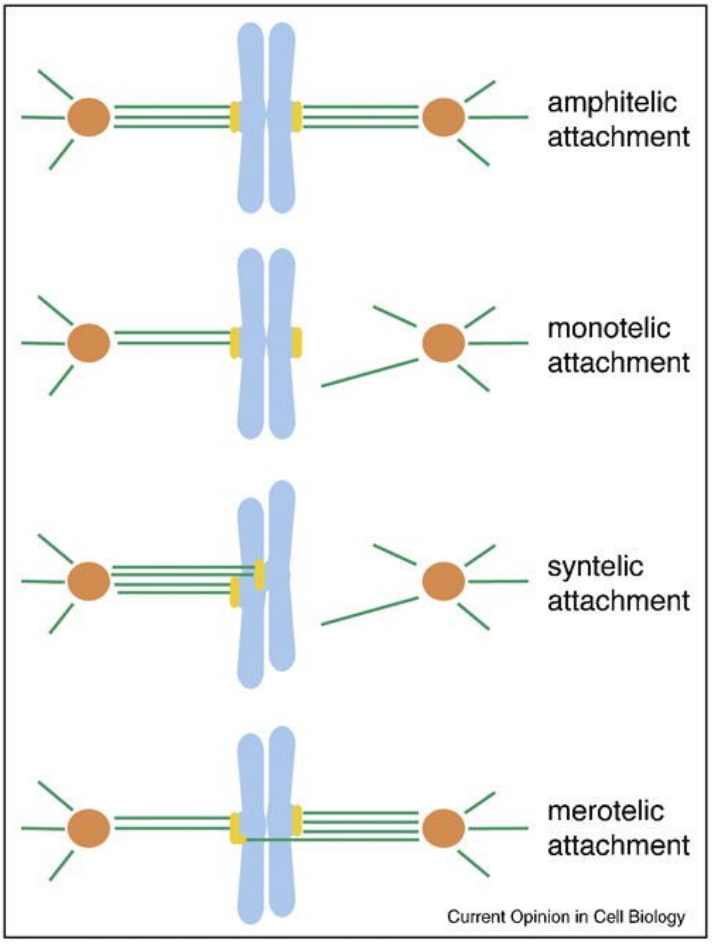

Figure 1.2 Classification of kinetochore-microtubule attachments. Correct attachments are termed ‚amphitelic' or ‚bipolar'. Each sister kinetochore is attached to microtubules emanating from a different spindle pole, and only from that spindle pole. Monotelic attachment: Only one sister kinetochore is attached to microtubules from one spindle pole, the other sister kinetochore is unattached. Syntelic attachment: Both sister kinetochores are attached to microtubules emanating from the same spindle pole. Merotelic attachment: Both sister kinetochores are attached to microtubules from opposing spindle poles, but one kinetochore is additionally attached to microtubules emanating from the other spindle pole. Chromosomes are depicted in blue, kinetochores in yellow, microtubules in green and centrosomes (spindle poles) in orange. (Kelly and Funabiki, 2009).

In order to achieve biorientation, it is essential that erroneous attachments can be detected and corrected. The mechanism that detects and destabilizes incorrect attachments is called error correction (EC). It relies on the detection of inter-kinetochore tension, or the lack thereof, and is mediated by Aurora B kinase (and its counteracting phosphatases, PP1 and PP2A) (Krenn & Musacchio, 2015; Lesage et al., 2011). The EC mechanism will be discussed in detail in chapter 1.3. Briefly, Aurora B, the catalytic subunit of the chromosomal passenger complex (CPC), that localizes to the inner centromere during prometa- and metaphase, dynamically

phosphorylates a number of substrates at the kinetochore in a tension-dependent manner. Monotelic, syntelic and merotelic kinetochore-microtubule attachments lack tension, which enables Aurora B to phosphorylate its kinetochore-localized substrates (Lampson & Cheeseman, 2011; Krenn & Musacchio, 2015). These phosphorylation events destabilize microtubule binding to the KMN network (Lampson & Cheeseman, 2011). Conversely, correct amphitelic attachments generate tension, thereby pulling kinetochore-localized substrates out of the reach of Aurora B. This causes a shift of the dynamic balance of phosphorylation and dephorphorylation towards dephosphorylation, thus stabilizing amphitelic kinetochore-microtubule attachments (Krenn & Musacchio, 2015; Lesage et al., 2011).

1.2.2 The spindle assembly checkpoint

The SAC is a regulatory feedback system that ensures accurate chromosome segregation by preventing anaphase onset until amphitelic attachment of all chromosomes is achieved. Even a single unattached kinetochore is enough to generate a checkpoint signal sufficient to maintain an arrest in metaphase and to halt mitotic exit (Rieder et al., 1995). SAC signaling is mediated by a number of checkpoint proteins. The key players include the kinases Mps1 (monopolar spindle protein1), Aurora B and Bub1 (budding uninhibited by benomyl 1), the pseudokinase BubR1 (Bub-related 1) (Suijkerbuijk et al., 2012) and the non-kinase proteins Bub3, Mad1 (mitotic arrest deficient 1) and Mad2. Kinetochore localization of checkpoint proteins is necessary for proper checkpoint signaling, as targeting of key checkpoint proteins to unattached or improperly attached kinetochores allows for the formation of the mitotic checkpoint complex (MCC) and other diffusible inhibitors (MCC sub-complexes) of the anaphase promoting complex (APC/C) (Jia et al., 2013). The kinases Mps1 and Aurora B function upstream in the checkpoint signaling pathway and positively regulate each other (Saurin et al., 2011; van der Waal et al., 2012). Downstream SAC proteins form three constitutive complexes that are targeted to outer kinetochores via the KMN network: Bub1-Bub3, BubR1-Bub3 and the heterotetrameric Mad1-Mad2 core complex (Jia et al., 2013). Bub1, BubR1 and Bub3 are recruited to kinetochores via KNL1. The Mps1 kinase localizes to kinetochores by binding the Hec1 subunit of the Ndc80 complex (Hiruma et al., 2015) in an Aurora B

dependent manner (Saurin et al., 2011). Mps1 phosphorylates KNL1 on multiple MELT motifs, thereby promoting targeting of Bub1 to KNL1 (London et al., 2012; Shepperd et al., 2012; Yamagishi et al., 2012). This interaction depends on Bub3 (Krenn et al., 2012), suggesting that binding of Bub1-Bub3 to phospho-MELT motifs of KNL1 is mediated by Bub3. Kinetochore targeting of BubR1 depends on both Bub3 and Bub1 (Elowe et al., 2010; Rischitor et al., 2007). Recruitment of the Mad1-Mad2 core complex to kinetochores depends on the Ndc80 complex, Mps1 and Bub1 (Jia et al., 2013). Kinetochore recruitment and activation of checkpoint proteins leads to the assembly of the MCC. The MCC consists of BubR1-Bub3, Mad2 and one or two copies of Cdc20 (cell division cycle 20) (Jia et al., 2013; Izawa & Pines, 2015). Cdc20 has a dual role in SAC signaling – as a component of the MCC and as the activating subunit of the APC/C, a multi-subunit E3 ubiquitin ligase. ActiveAPC/C^{Cdc20} ubiquitinates cyclin B and Securin, thus targeting them for proteasomal degradation. This leads to inactivation of CDK1 and activation of the protease Separase that cleaves the Cohesin complex, thereby driving mitotic exit and chromosome segregation (Figure 1.3 A). Cdc20 activates the APC/C by contributing to the recognition of two APC/C substrate motifs, the KEN box and the destruction box (D box) (Yu, 2007). Two non-mutually exclusive mechanisms have been proposed to explain APC/C inhibition by the MCC (Jia et al., 2013). First, BubR1 acts as a pseudo-substrate that inhibits substrate recruitment by the APC/C^{Cdc20}. BubR1 contains two KEN boxes, that were shown to be involved in MCC assembly and to block substrate binding by the APC/C^{Cdc20}, respectively (Lara-Gonzales et al., 2011). Second, there is evidence that BubR1 and Mad2 alter the mode and site of Cdc20 binding to the APC/C, thereby hindering its ability to activate the APC/C (Herzog et al., 2009; Izawa & Pines, 2011). In order to allow for a quick response to the attachment status of kinetochores, and thus for a rapid checkpoint silencing once biorientation of all chromosomes is achieved, assembly and disassembly of the MCC has to be highly dynamic. Upon MCC binding to the APC/C, Cdc20 in the APC/C^{MCC} complex is autoubiquitinated and subsequently degraded, leading to MCC disassembly (Jia et al., 2013). This mechanism ensures that MCC and APC/C^{Cdc20} concentrations both remain low, rendering the system highly responsive to the kinetochore attachment status (Jia et al., 2013) (Figure 1.3 B).

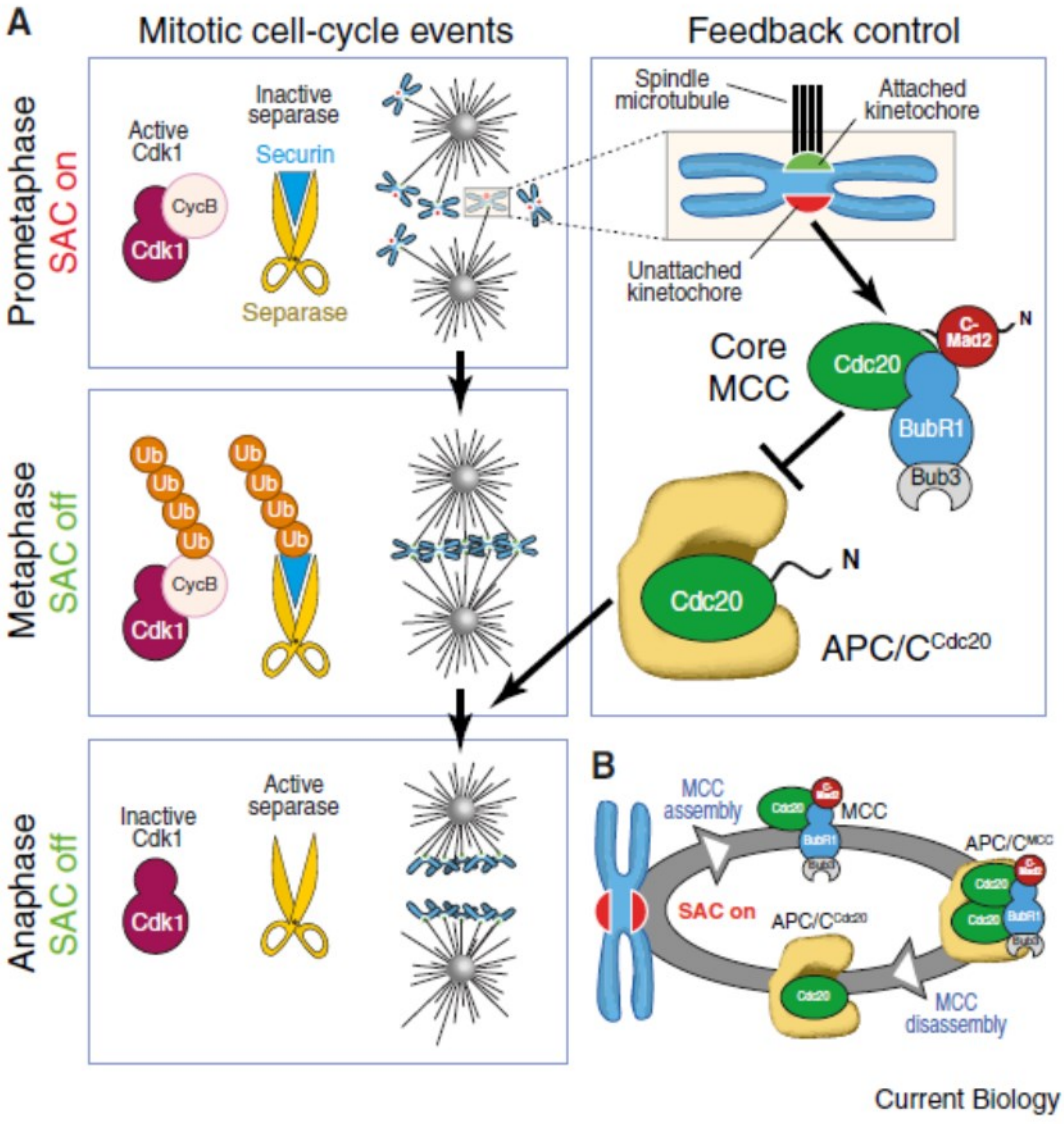

Figure 1.3 The SAC mechanism. A Mitosis is driven by activation of the CDK1-cyclin B kinase. The SAC is active during prometaphase, when chromosomes become attached to the spindle by the formation of microtubule-kinetochore attachments. Properly attached kinetochores (depicted in green) 'satisfy' the SAC and stop signaling. Unattached or improperly attached kinetochores (red) recruit SAC proteins, leading to the assembly of MCC, the SAC effector. MCC binds and inhibits APC/C^{Cdc20}, thereby preventing anaphase onset. When biorientation of all chromosomes is achieved at metaphase, the SAC is satisfied. APC/C^{Cdc20} becomes activated and ubiquitinates cyclin B and Securin, targeting them for proteasomal degradation. This leads to inactivation of CDK1 and activation of the Cohesin-protease separase, and thereby initiates mitotic exit and sister chromatid separation. **B** Assembly and disassembly of MCC is dynamic. When the SAC is active, pathways of MCC assembly and MCC disassembly coexist, rendering the system responsive to the status of kinetochore attachment (Musacchio, 2015).

A key regulated step mediating MCC formation in the presence of unattached or improperly attached kinetochores is the conformational activation of Mad2. Two

Mad2 conformers exist: the inactive O-Mad2 (open Mad2) and the active C-Mad2 (closed Mad2) (Luo & Yu, 2008; Mapelli & Musacchio, 2007). Mad2 in the cytosol has the O-Mad2 conformation, whereas Mad2 incorporated in the Mad1-Mad2 core complex has the C-Mad2 conformation. Only C-Mad2 can be incorporated into the MCC. The Mad1-Mad2 core complex at unattached kinetochores can recruit cytosolic O-Mad2 and induce its conformational transition to C-Mad2, thus facilitating MCC assembly (Jia et al., 2013). Silencing of the SAC once chromosome biorientation is achieved involves the inactivation and removal of SAC proteins from kinetochores and the disassembly of MCC in the cytosol. Kinetochore-microtubule attachment allows for the transport of checkpoint proteins along microtubules towards the spindle poles. This transport is mediated by the dynein/dynactin motor complex (Howell et al., 2001; Gassmann et al., 2010). Additionally, microtubule attachment to kinetochores can directly displace checkpoint proteins from kinetochores through competition for binding sites (Hiruma et al., 2015; Jia et al., 2013). Furthermore, binding of the Mad2 inhibitor p31^{comet} to the Mad1-Mad2 core complex prevents activation of O-Mad2 and thereby inhibits MCC formation (Yang et al., 2007; Mapelli et al., 2006; Fava et al., 2011). Last but not least, the phosphatase PP1 plays a crucial role in checkpoint silencing at the kinetochore by dephosphorylating Aurora B substrates (Lesage et al., 2011) (see chapter 1.4). Furthermore, the phosphorylation of KNL1 MELT motifs by Mps1 is reversed by PP1, decreasing the KNL1 binding affinity for Bub1-Bub3 (London et al., 2012; Shepperd et al., 2012). As mentioned earlier, the MCC is disassembled upon binding to the APC/C, as Cdc20 within the APC/C^{MCC} is autoubiquitinated and thereby targeted for proteasomal degradation, allowing newly synthesized Cdc20 to bind and activate the APC/C (Jia et al., 2013). Additionally, the MCC can be disassembled in a ubiquitination-independent manner (Jia et al., 2011). The Mad2 inhibitor p31^{comet} plays a role in both disassembly pathways (Nilsson et al., 2008; Jia et al., 2011). It has been proposed that the AAA ATPase TRIP13, together with p31^{comet} as an adapter protein, promotes MCC disassembly by catalyzing the conformational switch from C-Mad2 to O-Mad2 (Ye et al., 2015). MCC disassembly also occurs when the SAC is active. Thus far, it is not known if MCC disassembly is accelerated during SAC silencing (Jia et al., 2011).

1.3 Aurora kinases

The Aurora family of Ser/Thr protein kinases plays a pivotal role in the regulation of mitosis and cytokinesis (Carmena et al., 2009). In mammals, three Aurora kinases exist – Aurora A, B and C, whereas only one Aurora homolog is found in budding yeast, called Ipl1 (Increase in PLoidy 1).(Krenn & Musacchio, 2015; Chan & Botstein, 1993). Despite of their high sequence homology and similar substrate consensus motifs, Aurora A and B have very distinct localizations and functions (Carmena et al., 2009; Krenn & Musacchio, 2015): Aurora A localizes to spindle poles during mitosis and regulates mitotic entry, centrosome maturation and spindle formation (Carmena et al., 2009). Aurora B is the catalytic subunit of the chromosomal passenger complex (CPC), that dynamically changes its localization throughout mitosis and plays a crucial role in chromosome biorientation, SAC activation, and contractile ring formation during cytokinesis (Carmena et al., 2012). Aurora C closely resembles Aurora B and is only significantly expressed in cells undergoing meiosis (sperms and oocytes) (Quartuccio & Schindler, 2015).

1.3.1 Aurora B and the chromosomal passenger complex

The CPC is a key regulator of mitosis (Carmena et al., 2012). Besides Aurora B kinase, the CPC contains three non-catalytic subunits that function as regulatory and targeting components: INCENP (inner centromere protein), Survivin and Borealin (Dasra B) (Carmena et al., 2012). All three non-catalytic subunits are required for CPC localization and function, as siRNA-mediated depletions of both INCENP, Survivin and Borealin were shown to perturb CPC targeting to centromeres and caused mitotic defects (Adams et al., 2001; Carvalho et al., 2003; Honda et al., 2003; Gassmann et al., 2004). The structure of the CPC consists of a kinase module, comprising of Aurora B bound to the IN-box segment at the C-terminus of INCENP (Adams et al., 2000), and a localization module, comprising of the INCENP N-terminus, Survivin, and Borealin, associated by the formation of a three-helix bundle (Jeyaprakash et al, 2007). The kinase module and the localization module are connected by the long central region of INCENP (Carmena et al., 2012).

INCENP constitutes the scaffold for CPC assembly. It was the first CPC member to be identified in a screen for novel components of mitotic chromosomes (Cooke et al., 1987). Aurora B binding to the C-terminal INCENP IN-box is required for Aurora B activation (Carmena et al., 2012). Formation of the three-helix bundle of the INCENP N-terminus with Survivin and Borealin is required for CPC localization to centromeres and later to the spindle midzone and the midbody (Vader et al., 2006; Jeyaprakash et al., 2007; Ainsztein et al., 1998; Klein et al., 2006). Furthermore, INCENP binds HP1 (heterochromatin protein 1), mediating CPC localization to heterochromatin during interphase (Ainsztein et al., 1998; Nozawa et al., 2010; Klang et al., 2011).

Survivin belongs to the family of IAP (inhibitor of apoptosis) proteins and contains a BIR (baculovirus IAP repeat) domain that mediates its dimerization (Verdecia et al., 2000), however, in the CPC, Survivin is bound as a monomer. Survivin is phosphorylated by CDK1-cyclin B at T34 (O'Connor et al., 2000; O'Connor et al., 2002). The Survivin BIR domain is involved in CPC targeting to centromeres, as discussed below.

The Borealin N-terminus takes part in the formation of the triple-helix bundle that establishes the CPC localization module (Jeyaprakash et al., 2011). In mitotic cells, essentially all Survivin is associated with Borealin (Gassmann et al., 2004). This heterodimer is incorporated into the CPC by the helix bundle formation with the INCENP N-terminus (Jeyaprakash et al., 2007). Borealin is involved in CPC localization to centromeres by an interaction with Shogoshin proteins (see below).

In order to fulfill its various mitotic functions, localization of the CPC has to be highly dynamic. Indeed, localization of the CPC with its catalytic core, the Aurora B kinase, is highly regulated in space and time and corresponds to its distinct functions throughout mitotic progression. The CPC localizes at chromosome arms during prophase and accumulates at centromeres during prophase and prometaphase, its sole localization site at metaphase. During anaphase, the CPC relocalizes to the spindle midzone and is found at the midbody in telophase (Figure 1.4). CPC targeting and Aurora B activation are complex, multi-step processes, regulated by a number of feedback mechanisms (Carmena et al., 2012). Little is known about CPC function during interphase (Carmena et al., 2012), however, the CPC was shown to localize to

interphase heterochromatin via an interaction of INCENP with HP1 bound to histone H3 trimethylated at K9 (H3 K9me3) (Ainsztein et al., 1998; Nozawa et al., 2010; Klang et al., 2011). During mitosis, phosphorylation of histone H3 at S10 disrupts HP1 binding, possibly contributing to a switch of CPC localization from an HP1-mediated recruitment mode to early mitotic localization mechanisms (Fischle et al., 2005; Hirota et al., 2005; Carmena et al., 2012).

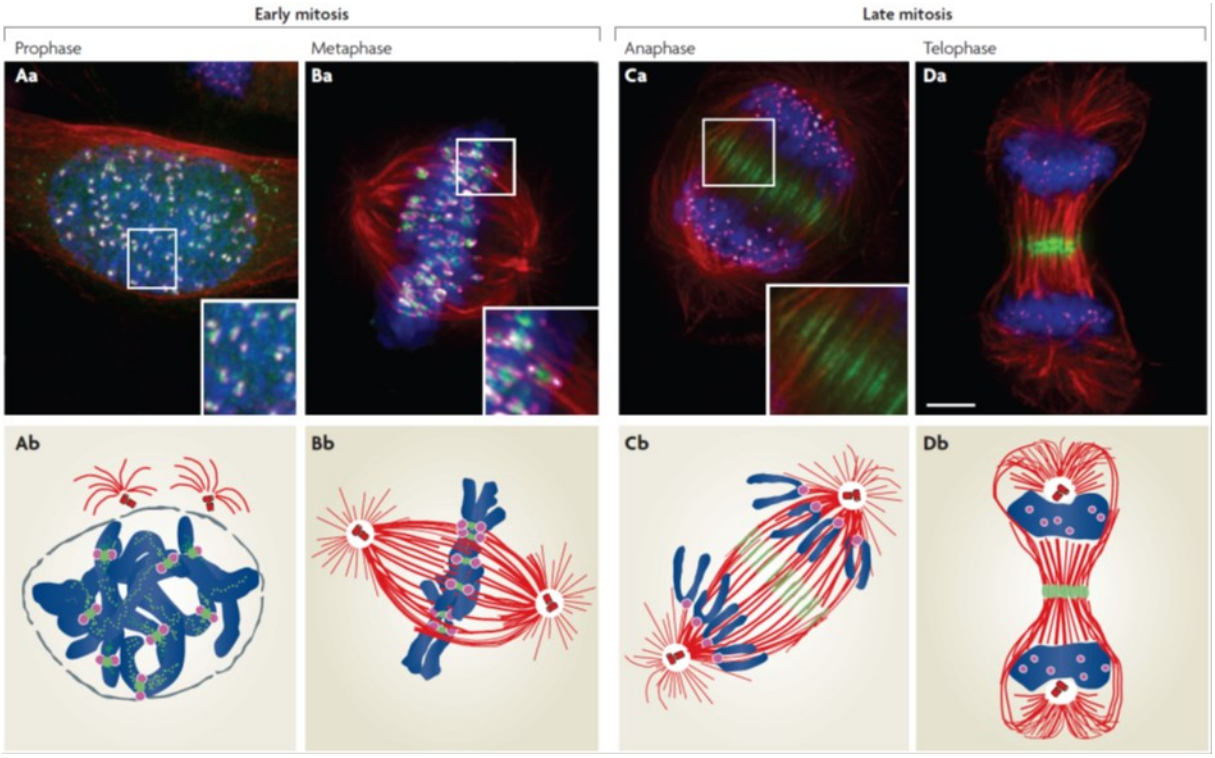

Figure 1.4 CPC localization throughout mitosis. Indirect immunofluorescence (upper panels) and schematic representation (lower panels) of Aurora B localization (green) in HeLa cells throughout mitosis with kinetochores (pink), α-tubulin (red) and chromatin (blue). Aurora B localizes at chromosome arms in prophase and accumulates at centromeres during prophase and prometaphase. In metaphase, Aurora B localization is limited to centromeres. During anaphase, Aurora B relocates to the spindle midzone and is found at the midbody in telophase. Scale bar, 5 μm. (Ruchaud et al., 2007).

CPC enrichment at centromeres during early mitosis is independent of DNA sequence (Bassett et al., 2010), but depends on two mitosis-specific phosphorylation events of histone tails: histone H3 at T3 (H3 T3ph) and histone H2A at T120 (H2A T120ph). The kinase Haspin phosphorylates histone H3 at T3 alongside chromosomes between paired sister chromatids, most prominently at the inner centromere, thus creating a binding site for the Survivin BIR domain (Higgins, 2005; Yamagishi et al., 2010; Polioudaki et al., 2004; Jeyaprakash et al., 2011; Kelly et al.,

2012). Histone H2A at T120 is phosphorylated by Bub1. Due to the localization of Bub1 at the outer kinetochore, this phosphorylation is enriched within the centrosomal regions adjacent to kinetochores (Yamagishi et al., 2010; Kawashima et al., 2007; Kawashima et al., 2010). H2A T120 phosphorylation recruits Shogoshin proteins (Sgo1 and Sgo2), which interact with Borealin that has been phosphorylated by CDK1 (Tsukahara et al., 2010). Maximal concentration of the CPC occurs where histone H3 T3 and histone H2A T120 phosphorylations overlap (Yamagishi et al., 2010). Activation of Aurora B is initiated by its binding to the INCENP IN-Box. The low-level activation caused by this interaction enables Aurora B to phosphorylate the C-terminal TSS motif of INCENP and to autophosphorylate at T232 in the T-loop of its catalytic domain, leading to its further activation (Honda et al., 2003; Bishop & Schumacher, 2002). This phosphorylation likely occurs in trans (Sessa et al., 2005), leading to an increase of Aurora B activity depending on the local density of the CPC (Kelly et al., 2007). A number of other kinases also phosphorylate the CPC at different sites, thereby regulating its localization and activity (Carmena et al., 2012). For example, Chk1 kinase phosphorylates Aurora B at S311, leading to its full activation (Petsalaki et al., 2011). Interestingly, this phosphorylation occurs only in the Aurora B pool adjacent to kinetochores (Zachos et al., 2007). INCENP is phosphorylated at T59 by CDK1 (Goto et al., 2006) and removal of this phosphorylation is required for CPC relocalization to the spindle midzone during anaphase (Hümmer & Mayer, 2009). At mitotic entry, Aurora B phosphorylates histone H3 at S10 (Hsu et al., 2000; Murnion et al., 2001). H3 S10 phosphorylation is a well-established marker for mitotic chromosomes and was shown to contribute to chromosome compaction during anaphase in budding yeast (Neurohr et al., 2011), though, its functions in vertebrates are largely unknown (Carmena et al., 2012). H3 S10 phosphorylation was, however, shown to disrupt HP1 binding to the adjacent trimethylated K9 (Fischle et al., 2005; Hirota et al., 2005) and may therefore also contribute to the switch of CPC localization from an HP1-mediated recruitment mode during interphase to the early mitotic localization mechanisms described above (Carmena et al., 2012).

During early mitosis, the CPC is involved in chromosome compaction and plays a crucial role in error correction and SAC signaling, thus ensuring chromosome biorientation (see also chapter 1.3.2). A proposed function of the CPC in

chromosome compaction is a regulation of the multimeric protein complex condensin (Morishita et al., 2001; Giet & Glover, 2001; Ono et al., 2004; Lipp et al., 2007; Collette et al., 2011). Both in fission yeast and in human cells, Aurora B mediated phosphorylation of Kleisin proteins promotes recruitment of condensin to mitotic chromosomes (Nakazawa at al., 2011; Tada et al., 2011; Ono et al., 2004; Lipp et al., 2007). In fission yeast, Ark1/Aurora and Bir1/Survivin mutants impair chromosome condensation (Petersen & Hagen, 2003; Nakazawa et al., 2008), however this effect is less pronounced in vertebrate cells (Carmena et al., 2012). During the process of chromosome attachment to the spindle, Aurora B destabilizes erroneous kinetochore-microtubule attachments by phosphorylating kinetochore-localized substrates. The KMN network that can form load-bearing attachments to microtubule plus ends (Powers et al., 2009) is phosphorylated by Aurora B at multiple sites (Welburn et al., 2010). Especially phosphorylation of Ndc80/Hec1 at the N-terminus, a main microtubule-binding site, weakens its microtubule binding affinity (Deluca et al., 2006; Ciferri at al., 2008; Cheeseman et al., 2006; Alushin et al., 2010; Guimaraes et al., 2008). Additional phosphorylation events of Mis12 complex components (e.g. Dsn1) and KNL1 can cause a synergistic decrease of the kinetochore-microtubule binding affinity, allowing Aurora B to fine-tune kinetochore-microtubule interactions (Welburn et al., 2010; Hua et al., 2010). In addition to the KMN network, Aurora B regulates further kinetochore proteins that regulate microtubule binding and dynamics. In yeast, the Dam1 complex is negatively regulated by Aurora B phosphorylation (Cheeseman et al., 2002). The Dam1 complex that interacts with the Ndc80 complex is required for the establishment and maintaining of kinetochore-microtubule attachments and carries the ability to processively move with depolymerizing microtubule tips (Gestaut et al., 2008; Tien et al., 2010). Dam1 is conserved only in fungi, however, the Ska complex has been proposed as a functional Dam1 analog in higher eukaryotes and is also negatively regulated by Aurora B (Welburn et al., 2009; Chan et al., 2012). Aurora B mediated phosphorylation also regulates MCAK (mitotic centromere-associated kinesin), facilitating its recruitment to centromeres while inhibiting MCAK binding to microtubule plus ends and its microtubule-depolymerizing activity (Andrews et al., 2004; Lan et al., 2004; Tanenbaum et al., 2011). Furthermore, Aurora B (and Aurora A) regulate CENP-E (kinesin-7), a microtubule plus end directed, kinetochore-

localized motor that transports polar-localized chromosomes towards the forming metaphase plate (Kim et al., 2010).

In order to accurately fulfill its functions, Aurora B activity has to be tightly regulated and balanced. During the process of chromosome-microtubule attachment formation, Aurora B mediated phosphorylation of kinetochore substrates is most prominent at unattached kinetochores and reduced upon microtubule attachment, showing that Aurora B phosphorylation is coordinated with the microtubule attachment status (Welburn et al., 2010; Liu et al., 2010; DeLuca et al.; 2011; Salimian et al., 2011). This is mainly achieved by the recruitment of counteracting phosphatases. The major antagonistic phosphatase for Aurora B is PP1 (Lesage et al., 2011). During early mitosis, PP1 is recruited to kinetochores mainly through binding to the outer kinetochore protein KNL1 (Liu et al., 2010). PP1 binding to KNL1 is counterbalanced by Aurora B itself, as Aurora B phosphorylates the RVSF motif of KNL1, the main PP1 binding site (Welburn et al., 2010; Liu et al., 2010). In addition to KNL1, CENP-E and SDS22 were reported to be involved in PP1 targeting to kinetochores in human cells (Kim et al., 2010; Posch et al., 2010) (see also chapter 1.4.3). At anaphase, PP1 becomes recruited to bulk chromatin by another PP1 interacting protein (PiP), called Repo-Man (Trinkle-Mulcahy et al., 2006). PP1-Repo-Man dephosphorylates histone H3 at T3 and thus helps to dissociate the CPC from centromeres at anaphase onset (Qian et al., 2011). Furthermore, PP1-Repo-Man mediated dephosphorylation of histone H3 at T3 plays a role in regulating CPC targeting already during prometaphase, as siRNA-mediated depletion of Repo-Man caused an increase in H3 T3 phosphorylation on prometaphase chromatin and a partial loss of the centromeric localization of Aurora B with a more diffuse distribution along the chromosome arms (Qian et al., 2011). Aurora B was shown to promote its own centromeric targeting by a positive feedback loop: Aurora B can phosphorylate Repo-Man, thereby inhibiting PP1-Repo-Man mediated dephosphorylation of H3 T3 (Qian et al., 2013). In addition to balancing by counteracting phosphatases, the CPC is regulated on the level of the turnover of its subunits. CPC subunits turn over at centromeres with half-times of less than one minute (Beardmore et al., 2004; Murata-Hori et al., 2002; Ahonen et al., 2009). CPC localization to centromeres was proposed to be regulated by ubiquitination of Survivin. K63-linked ubiquitination of Survivin was reported to promote centromere-association, whereas deubiquitination

mediated by hFAM was reported to be required for Survivin dissociation (Vong et al., 2005). Aurora B is ubiquitinated by the E3 ligase Cullin 3 (Sumara et al., 2007) and subsequently extracted from chromatin by the AAA ATPase p97 with its heterodimeric cofactor Ufd1-Npl4 (Ramadan et al., 2007; Dobrynin et al., 2011). p97-mediated extraction of Aurora B from chromatin was shown to be required for chromatin decondensation and nucleus reformation at the end of mitosis (Ramadan et al., 2007), but also for balancing Aurora B activity in early mitosis during spindle attachment (Dobrynin et al., 2011).

With anaphase onset, a population of the CPC is transferred from centromeres to the spindle midzone. CPC relocalization is facilitated by PP1-Repo-Man-mediated dephosphorylation of histone H3 at T3 (Qian et al., 2011), and by p97-mediated removal of Aurora B from chromosomes (Dobrynin et al., 2011). CPC targeting to the spindle midzone depends on an interaction of INCENP and Aurora B with MKLP2 (mitotic kinesin-like protein 2), that binds microtubules at the central spindle (Gruneberg et al., 2004; Jang et al., 2005; Cesario et al., 2006). MKLP2 interacts with the CPC only during anaphase, when the CDK1-mediated inhibitory phosphorylation of INCENP at T59 is removed (Hümmer & Mayer, 2009). At the central spindle, Aurora B generates a spatial phosphorylation gradient that is centered at the spindle midzone (Fuller at al., 2008). Due to this phosphorylation gradient, during anaphase, Aurora B substrates at chromosome arms exhibit higher phosphorylation levels than substrates at the centromeric regions, as chromosome arms are in closer proximity to the midzone during chromosome segregation. This leads to a further chromosome compaction by axial shortening of the chromosome arms, which is required for proper inclusion of all chromosomes into the daughter nuclei when nuclear envelopes reform (Mora-Bermudez et al., 2007). Furthermore, the CPC at the spindle midzone is involved in stabilizing the central spindle (Douglas et al., 2010). During cytokinesis, the CPC contributes to contractile ring formation and constriction, as Aurora B activity plays a role in regulating cytoskeletal dynamics by an indirect regulation of the small GTPase RhoA, that promotes myosin II activation and actin polymerization (Yuce at al., 2005; Nishimura et al., 2006; Minoshima et al., 2003; Touré et al., 2008).

1.3.2 Roles of Aurora B in error correction and the spindle assembly checkpoint

As mentioned before, Aurora B corrects erroneous kinetochore-microtubule attachments by phosphorylating kinetochore substrates, thereby decreasing their microtubule binding affinity. It is believed that the occurrence of tension upon formation of bioriented attachments leads to the stabilization of these correct attachments, as kinetochore-localized substrates are pulled out of the reach of Aurora B, allowing for their dephosphorylation by the counteracting phosphatase PP1 (Figure 1.5).

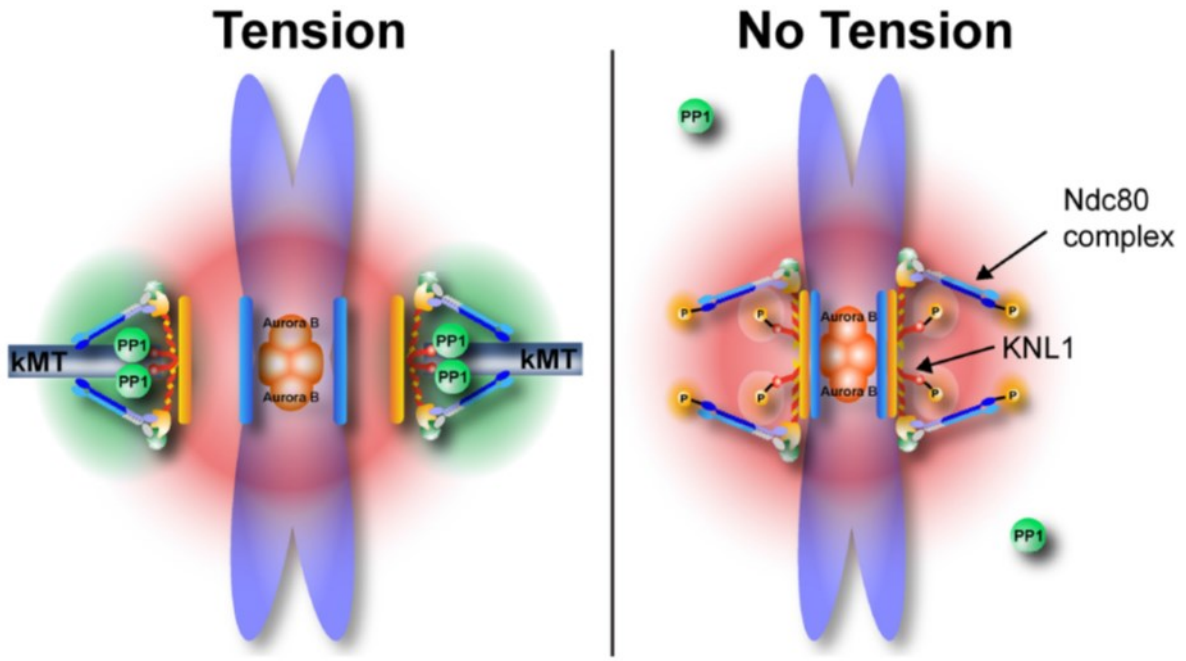

Figure 1.5 Model of tension-dependent regulation of kinetochore-microtubule attachments. In a state of low tension, Aurora B phosphorylates kinetochore-localized substrates, including KNL1 and Hec1, leading to reduced binding of both PP1 and microtubules. When amphitelic attachments form, tension is generated, thus pulling kinetochore-localized substrates out of the reach of Aurora B and allowing for PP1-mediated substrate dephosphorylation, thereby increasing the kinetochore-microtubule binding affinity. (Liu et al., 2010).

A number of findings support this model. Already in 1969, Nicklas and Koch could show that artificially pulling on unipolar attached chromosomes with a glass microneedle stabilized these otherwise unstable attachments. These classical micromanipulation experiments provided the first piece of evidence that stabilization

of kinetochore-microtubule attachments depends on the generation of tension (Nicklas & Koch, 1969). Chemical inhibition of Aurora B was shown to stabilize incorrect kinetochore-microtubule attachments, whereas washout of the inhibitor again destabilized those attachments, allowing for error correction (Hauf et al., 2003; Lampson et al., 2004). A study using FRET-based biosensors provided evidence that phosphorylation of Aurora B substrates at the kinetochore indeed depends on their distance from Aurora B at the inner centromere. A centromere-localized biosensor was highly phosphorylated independently of the kinetochore-microtubule attachment state, whereas a sensor targeted to the outer kinetochore was phosphorylated at unattached kinetochores but dephosphorylated upon achievement of biorientation (Liu et al., 2009). Furthermore, ectopic targeting of Aurora B to the kinetochore increased the phosphorylation level at the outer kinetochore and prevented stabilization of bioriented attachments (Liu et al., 2009). While the concept of tension-dependent Aurora B function in error correction is widely established, it is not understood *how* centromere-localized Aurora B reaches its substrates at outer kinetochores, as outer kinetochore substrates are separated from the inner centromere by a distance of about 100 nm already in the absence of tension (Wan et al., 2009). Two models have been proposed to provide an explanation. Santaguida and Musacchio proposed a “dog leash“ model that explains tension-dependent Aurora B phosphorylation of kinetochore substrates with the physical structure of the CPC (Santaguida & Musacchio, 2009). The CPC scaffold INCENP contains a long, flexible central region with a single alpha helix domain (Samejima et al., 2015), that functions as the “leash“ in this model. The CPC localization module, the “dog owner“ is tethered at the centromere, allowing “the dog“ Aurora B to phosphorylate substrates within limits defined by the length of the “leash“ (Santaguida & Musacchio, 2009; Krenn & Musacchio, 2015). However, overexpression of an INCENP mutant lacking the central region in U2OS cells depleted of endogenous INCENP by RNAi was shown to restore chromosomal alignment and normal mitotic progression (Vader et al., 2007). An alternative model proposed by Lampson and Cheeseman states that active Aurora B molecules diffuse from the inner centromere, thereby generating a diffusion-based phosphorylation gradient, reaching from the centromere to the outer kinetochore (Lampson & Cheeseman, 2011), similar to the phosphorylation gradient observed at the spindle midzone during anaphase (Fuller at al., 2008). This model is supported by the high turnover of CPC subunits at the centromere (Beardmore et al.,

2004; Murata-Hori et al., 2002; Ahonen et al., 2009), however, it has been called into question whether a diffusion gradient could form over such a short distance (Musacchio, 2011; Krenn & Musacchio, 2015).

Another issue that is a matter of intensive research and debate is the role of Aurora B in SAC activation and signaling (Jia et al., 2013; Krenn & Musacchio, 2015). Aurora B appears to play a role upstream in the SAC signaling pathway, as Aurora B inhibition prevents the recruitment of all other SAC components to the kinetochore (Ditchfield et al., 2003; Santaguida et al., 2011; Saurin et al., 2011; Famulski et al., 2007; Vigneron et al., 2004). It has been proposed, however, that this effect could be rather indirect and depend on the generation of unattached kinetochores through Aurora B-mediated error correction (Pinsky et al., 2006). This idea is supported by findings that Aurora B is required for checkpoint activation and mitotic arrest in cells treated with the microtubule-stabilizing drug taxol, but not for mitotic arrest of cells treated with the microtubule-destabilizing drug nocodazole (Ruchaud et al., 2007; Jia et al., 2013). However, recent findings point at a direct role of Aurora B in checkpoint signaling, independent of its function in error correction. Artificial retention of the CPC at anaphase chromosomes, using siRNA-mediated depletion of MKLP2 or a phosphomimetic INCENP mutant (T59E), did not affect kinetochore-microtubule attachments, but led to the recruitment of SAC components (Bub1, BubR1 and Mps1) to anaphase kinetochores (Vázquetz-Novelle & Petronczki, 2010). Furthermore, it was shown that Aurora B is required for mitotic arrest in nocodazole-treated cells, when Mps1 activity is inhibited (Santaguida et al., 2011). Since Aurora B is required for Mps1 recruitment to kinetochores and since artificial tethering of Mps1 to kinetochores was shown to rescue delayed checkpoint activation upon Aurora B inhibition (Saurin et al., 2011), recruitment of Mps1 has been proposed as the primary role of Aurora B in SAC signaling (Saurin et al., 2011; Krenn & Musacchio, 2015).

1.3.3 Aurora A regulates centrosome maturation and mitotic spindle formation and positioning

Besides Aurora B, also Aurora A kinase plays a crucial role in the regulation of mitosis. Aurora A localizes to the spindle poles throughout mitosis and regulates mitotic entry, centrosome maturation and separation as well as spindle assembly (Carmena et al., 2009). Aurora A targeting and function at spindle poles involves a number of interactors and cofactors, including the kinase PAK1 as well as the cofactors Tpx2 and Bora (Barr and Gergely, 2007).Furthermore, Aurora A is regulated by the phosphatases PP2A and PP1. PP1 and Aurora A antagonize each other (Katayama et al., 2001; Ohashi et al., 2006) and Tpx2 was shown to activate Aurora A by preventing its PP1-mediated dephosphorylation (Bayliss et al., 2003). The PP1 interacting protein (PiP) Inhibitor-2 (I2) is involved in this regulation by inhibiting PP1 and allosterically activating Aurora A (Li et al., 2007). Another PiP that was reported to localize to spindle poles, both in interphase and mitosis, is Inhibitor-3 (I3) (Huang et al., 2005), however, its functions at the centrosome are unknown. Aurora A is required for mitotic entry as it phosphorylates the phosphatase CDC25B, thereby promoting its activation, which leads to the activation of centrosome-localized CDK1-cyclin B (Dutertre et al., 2004; Cazales et al., 2005; Hirota et al., 2003). In most animal cells, mitotic spindle assembly is mediated by centrosomes. Centrosomes are specialized organelles that consist of a pair of centrioles surrounded by a pericentriolar matrix (PCM) and function as MTOCs (microtubule-organizing centers). Within the cell cycle, centrosomes duplicate in S phase, simultaneously with DNA replication. Centrosome maturation takes place during late G2 phase and prophase through the recruitment of additional PCM, preparing the centrosomes for their role as spindle poles and increasing their microtubule nucleation potential. Subsequently, the centrosomes separate and move towards opposite sides of the nucleus. This process can be completed either before or after NEBD (Barr and Gergely, 2007). Aurora A is involved in both maturation and separation of centrosomes as well as in spindle formation (Barr and Gergely, 2007). During centrosome maturation, Aurora A activity is required for the recruitment of PCM components such as γ-tubulin, which drives microtubule nucleation (Berdnik & Knoblich, 2002; Hannak et al., 2001; Hirota et al., 2003; Mori et al., 2007; Terada et al., 2003). Furthermore, Aurora-A mediated phosphorylation is required for the

centrosomal recruitment of TACC (transforming acidic coiled-coil containing) proteins (Barros et al., 2005; Kinoshita et al., 2005; Peset et al., 2005), which interact with conserved ch-TOG/XMAP215 proteins, targeting them to microtubule minus-ends (Barr and Gergely, 2007). Binding of TACC-XMAP215 complexes stabilizes centrosome-nucleated microtubules, in particular astral microtubules. XMAP215 stabilizes microtubules and promotes their net growth, mainly by counteracting the microtubule-destabilizing kinesin MCAK (Barr and Gergely, 2007; Peset & Vernos, 2008). The importance of Aurora A for mitotic spindle formation was highlighted by experiments using *Xenopus* egg extracts lacking both centrosomes and chromatin. In this system, Aurora A-coated beads act like MTOCs, as they are sufficient to both nucleate microtubules and even to form the poles of bipolar spindles (Tsai & Zheng, 2005). Positioning of centrosomes and thereby orientation of the mitotic spindle is mediated by the dynamic anchoring of astral microtubules to the cell cortex (Morin & Bellaiche; 2011). Evidently, correct spindle orientation is of particular importance in asymmetrically dividing cells and in cells in polarized tissues. Furthermore, intrinsic mechanisms regulating spindle orientation are also active in cultured cells growing in a monolayer, such as HeLa cells (Toyoshima & Nishida, 2007; Morin & Bellaiche; 2011; Kotak & Gönczy, 2013). In those cells, the mitotic spindle is generally oriented parallel to the substratum (Toyoshima & Nishida, 2007; Thoma et al., 2009). Aurora A has been implicated in spindle orientation in symmetric and asymmetric cell divisions from nematodes to mammals (Morin & Bellaiche; 2011; Regan et al., 2013; Asteriti et al., 2014). A recent study demonstrated that Aurora A activity is required for correct spindle orientation in HeLa cells, as both chemical inhibition and siRNA-mediated depletion of Aurora A led to spindle misorientation (Gallini et al., 2016). In this study, Aurora A-dependent spindle positioning in HeLa cells was shown to depend largely on the cortical recruitment of the large coiled-coil protein NuMA. NuMA is a key regulator of spindle functions, implicated in both spindle orientation as well as spindle organization and maintenance (Radulescu & Cleveland, 2010), that localizes to both spindle poles as well as to cortical regions above the poles (Kiyomitsu & Cheeseman, 2012), and functions as an adaptor for the microtubule motor dynein/dynactin (Kotak et al., 2012). Cortical targeting of NuMA was shown to require Aurora-A mediated phosphorylation at its C-terminus and ectopic NuMA-targeting to the cortex restored spindle orientation defects upon Aurora A inhibition (Gallini et al., 2016).

1.4 Protein phosphatase 1

Dynamic and reversible phosphorylation events play a fundamental role in virtually all cellular processes and signaling pathways. Overall protein phosphorylation is most abundant during mitosis. The global shift in protein phosphorylation that drives the tremendous cellular reorganization required for cell division has to be reversed at mitotic exit. Furthermore, a tight spatiotemporal control of protein (de)phosphorylation is required for proper spindle assembly, chromosome alignment and segregation. While the function and regulation of mitotic kinases has been extensively studied for a long time, the counteracting phosphatases where often thought of as rather static and constitutively active “silent partners“ (Trinkle-Mulcahy and Lamond, 2006). Only for about a decade, more focus has been placed on the role of phosphatases as dynamic and highly regulated counteractors of mitotic kinases (Trinkle-Mulcahy and Lamond, 2006; Bollen et al., 2009). Isoforms of five phosphatases have been implicated in the control of mitosis: PP1, PP2A, PP4, CDC25 and CDC14 (Bollen et al., 2009). While CDC25, CDC14 and PP4 phosphatases apparently function in particular mitotic events in higher eukaryotes, PP1 and PP2A have broader functions during mitosis (Bollen et al., 2009). PP1 and PP2A function in the control and balancing of mitotic kinases, the timely dephosphorylation of specific kinase substrates, and the controlled mass dephosphorylation at mitotic exit (Bollen et al., 2009). (In budding yeast, CDC14 is essential for mitotic exit (Holt et al., 2008), however, this requirement is not conserved in higher eukaryotes (Berdougo et al., 2008).) PP1 and PP2A are structurally related and both have two catalytic metal ions incorporated in the active site (Bollen et al., 2010; Jiang et al., 2013). Together, PP1 and PP2A account for more than 90% of the phosphatase activity in eukaryotic cells (Bollen et al., 2010). During mitosis, PP1 and PP2A have distinct functions, suggesting that their substrates are largely non-overlapping (Bollen et al., 2009). During different mitotic events, PP1 and PP2A holoenzymes can act either antagonistically (e.g. in CDK1 activation) or synergistically (e.g. in balancing Aurora B kinase activity) (Bollen et al., 2009). PP1 has emerged as the main Aurora B-counteracting phosphatase (Lesage et al., 2011). Consistently, global cellular inhibition of PP1 causes an arrest in prometaphase, associated with severe spindle and chromosome alignment effects and these phenotypes can be partially rescued by Aurora B inhibition (Winkler et al., 2015). This chapter focuses on PP1, its

structure and general cellular functions, and, most of all, its role in chromosome biorientation and segregation and the implication of its regulatory subunits SDS22 and Inhibitor-3 (I3) in this process.

1.4.1 Structure and cellular functions of PP1

PP1 belongs to the most conserved eukaryotic proteins (Ceulemans et al., 2002a). It is a member of the PPP (phosphoprotein phosphatases) superfamily of Ser/Thr protein phosphatases. While mammalian genomes encode about 400 Ser/Thr protein kinases, only about 25 Ser/Thr phosphatases exist in mammalian cells (Ceulemans & Bollen, 2004). The number of Ser/Thr phosphatase interactors, however, has increased tremendously during evolution, giving rise to a variety of distinct holoenzymes. When considering these holoenzymes, the numbers of Ser/Thr kinases and Ser/Thr phosphatases are approximately balanced (Ceulemans & Bollen, 2004). The PP1 catalytic subunit forms a compact fold with a central β-sandwich that excludes only the C-terminus and the extreme N-terminus. In the active site, two catalytic metal ions are incorporated, Fe^{2+} and Zn^{2+} (Bollen et al., 2010). *In vitro*, the free PP1 catalytic subunit exhibits a very broad substrate specificity (Bollen et al., 2010). Within the cell, however, PP1 gains substrate specificity through binding to a variety of interactors, so called PiPs (PP1 interacting proteins). PiPs are present in excess in the cell and compete for PP-binding (Ceulemans & Bollen, 2004). So far, nearly 200 PiPs have been identified, that allow for the formation of a vast number of distinct, highly specific PP1 holoenzymes (Heroes et al., 2013). PiPs can function as inhibitors of the catalytic activity, as substrate specifiers, as targeting subunits to direct PP1 to distinct substrates or cellular structures, or as substrates (Figure 1.6). While most PP1 complexes are dimeric, composed of a catalytic subunit and a regulatory PiP, some PP1 holoenzymes contain a second, inhibitory PiP (Bollen et al., 2010).

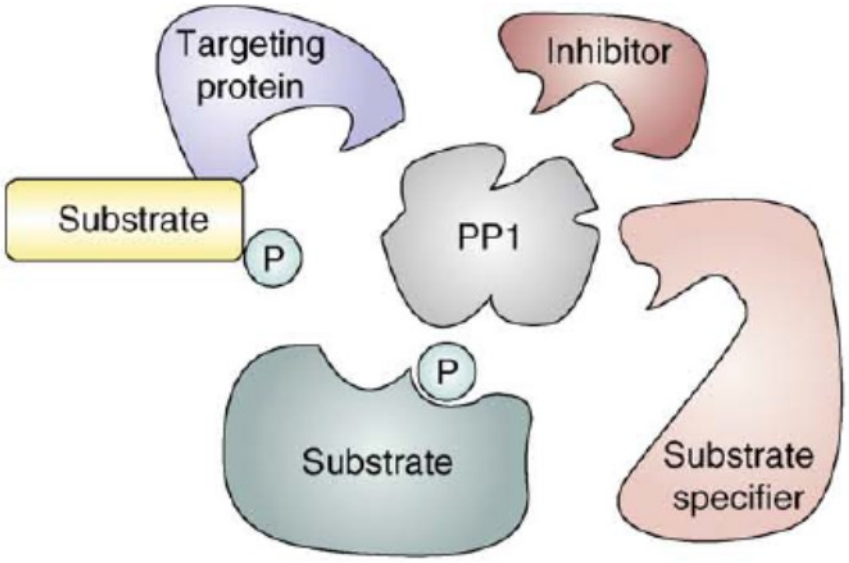

Figure 1.6 Functions of PP1 interacting proteins. PiPs bind to the catalytic PP1 subunit, thus forming heterodimeric or heterotrimeric holoenzymes. PiPs can function as PP1-inhibitors, substrate specifiers, targeting subunits or substrates. Adapted from (Bollen et al., 2009).

Binding of PiPs to PP1 is mediated by short, 4 to 8 aa docking motifs that bind to distinct interaction sites within the PP1 surface (Heroes et al., 2013). Many PiPs share PP1-docking motifs (Ceulemans & Bollen, 2004). Nevertheless, PiPs can interact with PP1 in a highly specific manner, since they combine different numbers and types of PP1-docking motifs (Heroes et al., 2013). Furthermore, PP1-docking motifs are degenerate and different sequence variants can differ considerably in their PP1-binding affinity (Bollen et al., 2010). Additionally, the PP1-binding affinity of some PiPs can be modulated by phosphorylation within or near the docking motif (Liu et al., 2010; Kim et al., 2010; Heroes et al., 2013). These properties allow for a highly complex and dynamic combinatorial control of PP1, depending on the composition and regulation of its interactome (Bollen et al., 2010). The most common and best studied PP1-docking motif is the so-called RVxF motif, which is present in about 70 % of all identified PiPs (Bollen et al., 2010). The RVxF motif binds to a hydrophobic groove remote from the catalytic site of PP1 (Ceulemans & Bollen, 2004). In general, it conforms to the consensus sequence [K/R] [K/R] [V/I] x [F/W], with x being any residue except F, I, M, Y; P, D (Bollen et al., 2010). Binding of the RVxF motif does not per se affect PP1 activity or conformation (Ceulemans & Bollen, 2004). The RVxF motif rather functions as a primary anchor for PP1-binding which

promotes secondary interactions that may further stabilize the binding and / or modulate the activity or substrate specificity of the holoenzyme (Bollen et al., 2010; Heroes et al., 2013). In the case of many PiPs, the RVxF motif is essential for PP1-binding (Bollen et al., 2010). For instance, PP1 targeting to the outer kinetochore protein KNL1 requires the KNL1 RVSF motif. KNL1 also contains another PP1-binding motif, the weaker SILK motif, which is not required for PP1-binding but may stabilize it (Liu et al., 2010).

Besides its role in the regulation of mitosis, PP1 is involved in a variety of cellular processes and pathways, including glycogen metabolism, recovery from starvation responses, protein synthesis, actin and actomyosin reorganization, Ca^{2+}-mediated signaling and apoptosis (reviewed in (Ceulemans & Bollen, 2004)). In mammalian cells, 3 closely related, ubiquitously expressed PP1 isoforms exist: PP1α; PP1β and $PP1\gamma_1$ (in the following referred to as PP1γ). A fourth isoform, $PP1\gamma_2$, an alternative splice variant of PP1γ, is expressed only in the testes. All isoforms exhibit similar enzymatic properties and most PiPs bind to all isoforms (Heroes et al., 2013). Exceptions are for instance Repo-Man and Aurora A, which were reported to interact specifically with PP1γ or PP1α, respectively (Trinkle-Mulcahy et al., 2006; Katayama et al., 2001). However, PP1 isoforms were shown to have distinct subcellular localizations. While all isoforms are present both in the cytoplasm and in the nucleus during interphase, a specific enrichment of PP1α at centrosomes, of PP1γ at nucleoli and of PP1β at non-nucleolar regions of the nucleus has been observed. In mitotic cells, PP1α is found at centrosomes, PP1β on chromatin and PP1γ was shown to be enriched at kinetochores from prometaphase to anaphase and recruited to bulk chromatin during telophase (Andreassen et al., 1998; Trinkle-Mulcahy et al., 2003).

1.4.2 The role of PP1 in chromosome biorientation

As discussed in chapter 1.3, Aurora B kinase activity has to be tightly regulated and balanced in order to accurately fulfill its functions in correcting erroneous kinetochore-microtubule attachments and in SAC signaling. Furthermore, a fast cellular response is required to trigger checkpoint silencing when chromosome biorientation is achieved. A number of studies have established PP1 as the main Aurora B-counteracting phosphatase and shown that PP1-mediated dephosphorylation of kinetochore and checkpoint proteins is essential for SAC silencing (Lesage et al., 2011). First evidence for the importance of the dephosphorylation of kinetochore-localized substrates for chromosome biorientation came from studies using phosphomimetic mutants of KMN or SAC proteins, which caused a constitutive activation of the SAC (Huang et al., 2008; Kemmler et al., 2009). Consistent with these findings, disruption of PP1 recruitment to kinetochores in human cells was shown to disrupt kinetochore-microtubule attachments and to cause a metaphase arrest (Liu et al., 2010). These findings, however, do not clarify whether PP1 is required only for the formation of stable bioriented attachments, thereby influencing the SAC, or whether it also plays a direct role in SAC silencing, once biorientation of all chromosomes is achieved. Using a fission yeast mutant strain that depolymerizes microtubules at the restrictive temperature, Vanoowthuyse and Hardwick showed that Ark1/Aurora B is required for checkpoint activation also in the presence of many unattached kinetochores, and, importantly, that checkpoint escape upon Ark1 inhibition requires PP1 (Vanoosthuyse and Hardwick, 2009). Furthermore, expression of an inactive PP1 mutant in budding yeast made the SAC hypersensitive, whereas PP1 overexpression prevented SAC activation in response to attachment defects (Pinsky et al., 2009). Together, these and other studies have provided evidence for a role of PP1 in both balancing Aurora B activity during the process of kinetochore-microtubule attachment formation, and, furthermore, for a requirement of PP1 for SAC silencing once biorientation is achieved.

The KNM network protein KNL1 has been proposed to be the main anchor for PP1 binding to kinetochores. KNL1 was suggested to be essential for bulk recruitment of PP1 to kinetochores, both in yeast and in human cells (Rosenberg et al., 2011; Liu et al., 2010). KNL1 binds PP1 via its RVSF motif. Mutation of the KNL1 RVSF motif was

reported to cause an (at least nearly) complete loss of PP1 recruitment to kinetochores, leading to an increased phosphorylation of Aurora B kinetochore substrates, a destabilization of kinetochore-microtubule attachments and a persistent activation of the SAC (Rosenberg et al., 2011; Liu et al., 2010). Ectopic targeting of PP1 to the kinetochore, using PP1 fusions to CENP-B or to the PP1-binding deficient KNL1 mutant, was shown to rescue these phenotypes (Rosenberg et al., 2011; Liu et al., 2010). On the other hand, expression of a PP1 fusion to wild type KNL1, which is expected to target twice the amount of PP1 to the kinetochore, is lethal in budding yeast, indicating that the level of PP1 at kinetochores needs to be precisely balanced (Rosenberg et al., 2011). Aurora B mediated phosphorylation of the serine residue within the RVSF motif of KNL1 inhibits binding of PP1 (Liu et al., 2010). This negative feedback mechanism between Aurora B and PP1 makes binding of PP1 to KNL1 tension-dependent, thus allowing for a switch-like response to the formation of stable, bioriented microtubule attachments, which contributes to a fast and definite SAC silencing (Liu et al., 2010; Lesage et al., 2011).

Besides KNL1, a number of other PiPs have been implicated in the regulation and localization of PP1 at kinetochores. SDS22, a main subject of this thesis, was shown to be required for proper chromosomal alignment and PP1-mediated balancing of Aurora B activity (Peggie et al., 2002; Posch et al., 2010; Wurzenberger et al., 2012). Furthermore, SDS22 was reported to localize at kinetochores and, like KNL1, to be required for PP1 targeting to kinetochores (Posch et al., 2010). However, the exact function and localization of SDS22 has remained controversial and will be discussed in detail below. CENP-E, a kinetochore-localized, microtubule plus end directed motor, that transports polar-localized chromosomes along pre-existing K-fibers towards the forming metaphase plate, binds to PP1 via an RVxF motif. Phosphorylation of the CENP-E RVxF motif by Aurora A or Aurora B disrupts PP1 binding and was suggested to be required for the congression of polar-localized chromosomes (Kim et al., 2010). Dephosphorylation of the RVxF motif, which enables PP1 binding, is mediated by PP1 itself and was shown to be required for the formation of stable, bioriented microtubule attachments (Kim et al., 2010). KIF18A (Klp5/6 in fission yeast), another plus end directed motor protein that functions as a kinetochore-targeting PiP, was shown to be required for SAC silencing in fission yeast (Meadows et al., 2011). Yet another kinetochore-localized PiP is Mypt1

(myosin phosphatase-targeting subunit 1). PP1-Mypt1 binds to the mitotic kinase PLK1 (polo-like kinase 1) and limits and balances its activity (Yamashiro et al., 2008). In addition to the kinetochore-localized PP1 anchors, Repo-Man, a vertebrate-specific PiP that targets PP1 to mitotic chromosomes, regulates Aurora B, by dephosphorylating the CPC binding site histone H3 T3 (Qian et al., 2011). Bulk recruitment of PP1-Repo-Man to chromatin occurs at anaphase and was proposed to play a key role in the translocation of the CPC to the spindle midzone (Qian et al., 2011; Qian et al., 2013; Lesage et al., 2011). During (pro)metaphase, PP1-Repo-Man mediated dephosphorylation of histone H3 at T3 at chromosome arms functions to limit CPC targeting to the centromeric region (Qian et al., 2011; Qian et al., 2013). Furthermore, heterokaryon experiments showed that checkpoint silencing must involve the generation of diffusible checkpoint inhibitors (Rieder et al., 1997). While the nature of these soluble inhibitors is not known, it has been suggested that they might be cytoplasmic PP1 holoenzymes (Lesage et al., 2011). In summary, a number of PiPs that are involved in the localization and regulation of PP1 at kinetochores have been identified, however, the exact functions and possible interdependencies of distinct kinetochore-localized PP1 holoenzymes are not well understood. Furthermore, although Aurora B and PP1 were shown to have common substrates, little is known about the exact phosphosites targeted by PP1 at the kinetochore (Lesage et al., 2011). The model shown in Figure 1.7 summarizes the current understanding of the Aurora B- and PP1-mediated regulation of kinetochore-microtubule attachment formation and SAC signaling.

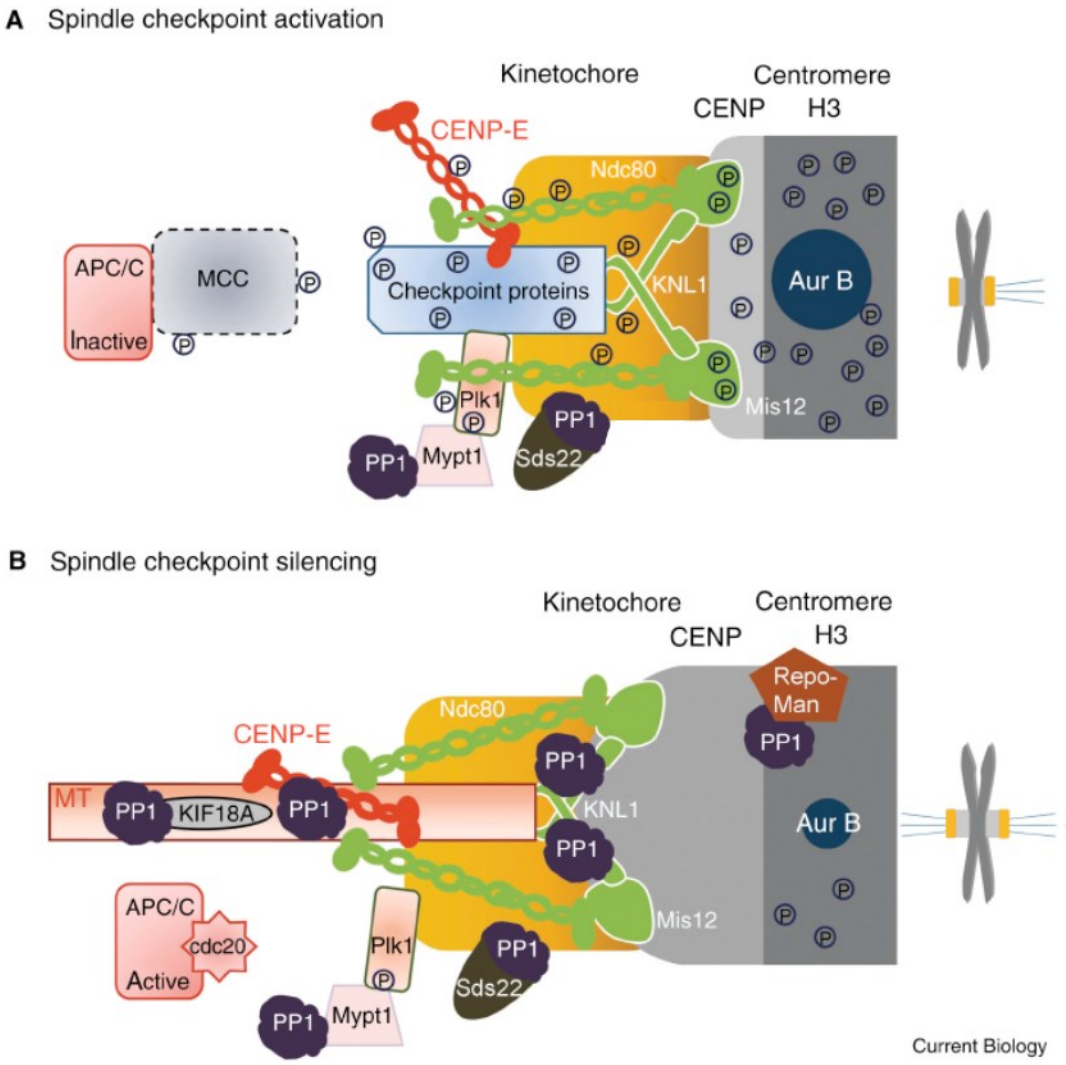

Figure 1.7 Model of PP1 kinetochore-recruitment and PP1-mediated regulation of spindle attachment and SAC signaling. A Unattached or improperly attached kinetochores are tensionless, allowing centromere-localized Aurora B to phosphorylate outer kinetochore proteins. This leads to destabilization of kinetochore-microtubule attachments and activation of checkpoint proteins. Aurora B-mediated phosphorylation of PP1 binding sites on KNL1 and CENP-E inhibits PP1 recruitment. Kinetochore-targeting of PP1 by Mypt1, Repo-Man and SDS22 was proposed to be tension-independent. **B** Formation of amphitelic bipolar microtubule (MT) attachments generates tension, spatially separating Aurora B from its substrates at the outer kinetochore. The ensuing reduced phosphorylation of PP1 binding sites promotes PP1 recruitment by KNL1, CENP-E and KIF18A, leading to a further dephosphorylation of kinetochore substrates, which stabilizes kinetochore-microtubule attachments and promotes SAC silencing. Adapted from (Lesage et al., 2011).

1.4.3 The PP1 interacting proteins SDS22 and Inhibitor-3

Inhibitor-3 (I3) and SDS22 are the two most ancient PiPs and are conserved among all eukaryotes (Ceulemans et al., 2002a). It was shown that mammalian SDS22 and I3, as well as their budding yeast homologs (Sds22 and Ypi1) can form ternary complexes with PP1 (Glc7 in budding yeast) both *in vitro* and *in vivo* (Lesage et al., 2007; Pedelini et al., 2007). Both proteins are essential in yeast (Pedelini et al., 2007) and a number of studies have shown that both Sds22 and Ypi1 play a crucial role in mitosis. Temperature sensitive mutations of Sds22 (*sds22-5* and *sds22-6*), as well as conditional depletions of Ypi1 were shown to cause a cell cycle arrest in metaphase (Pedelini et al., 2007; Bharucha et al., 2008), aberrant mitotic spindles (Pedelini et al., 2007) and chromosome segregation defects (Peggie et al., 2002; Bharucha et al., 2008). However, while mutants of Sds22 and Ypi1 yield similar phenotypes, their functions are not redundant, as overexpression of Sds22 cannot rescue the lethal phenotype of an *ypi1* mutant and vice versa (Pedelini et al., 2007). In the *sds22-6* mutant strain, Glc7/PP1-binding to Sds22 was shown to be impaired at the restrictive temperature (Peggie et al., 2002) and a Glc7/PP1-binding deficient *ypi1* mutant is not able to restore the lethality of a conditional Ypi1 depletion (Bharucha et al., 2008), demonstrating that the essential mitotic functions of Sds22 and Ypi1 are Glc7/PP1-dependend. Furthermore, both Sds22 and Ypi1 are nuclear proteins and were shown to be required for the nuclear enrichment of Glc7/PP1 (as well as Ypi1 for the nuclear localization of Sds22) (Peggie et al., 2002; Pedelini et al., 2007; Bharucha et al., 2008), suggesting that they regulate nuclear functions of Glc7/PP1 during mitosis, as yeast cells undergo closed mitosis in which the nuclear envelope remains intact. In budding yeast, the antagonism between Glc7/PP1 and Ipl1, the sole Aurora kinase in yeast, is well established by genetic interactions, as *glc7* mutants rescue the temperature sensitivity of *ipl1* mutants (Hsu et al., 2000; Peggie et al., 2002; Pinsky et al., 2006). However, findings from Pinsky et al. indicate that Glc7/PP1 does not directly regulate Ipl1/Aurora activity. Ipl1 levels, localization and kinase activity are not altered in a *glc7* mutant background (*glc7-10*) (Pinsky et al., 2006). Instead, Ipl1 and Glc7/PP1 were shown to act on shared substrates, such as Dam1 and histone H3 at S10 (Pinsky et al., 2006; Hsu et al., 2000). Both Sds22 and Ypi1 were shown to affect Ipl1-counteracting functions of Glc7/PP1 (Peggie et al., 2002; Pinsky et al., 2006; Pedelini et al., 2007; Bharucha et al., 2008), however, in what way Sds22 and

Ypi1 regulate Glc7/PP1 activity during mitosis has remained obscure. Like *glc7* mutants, both *sds22* and *ypi1* mutants can suppress the temperature sensitivity of *ipl1* mutants, indicating that Sds22 and Ypi1 positively regulate Glc7/PP1 in order to antagonize Ipl1/Aurora (Peggie et al., 2002; Bharucha et al., 2008). Furthermore, overexpression of Sds22 rescues the temperature sensitivity of *glc7* mutants (*glc7-5* and *glc7-12*), again indicating a positive regulation of Glc7/PP1 by Sds22 (MacKelvie et al., 1995; Peggie et al., 2002). However, on the other hand, the overexpression of either Sds22 or Ypi1 was also shown to rescue the temperature sensitivity of the *ipl1-321* mutant, suggesting an inhibitory function of both Sds22 and Ypi1 towards Glc7/PP1 (Pinsky et al., 2006; Pedelini et al., 2007). Interestingly, in a recent study, conditional depletion of Ypi1 and the temperature sensitive *sds22-6* mutation were found to cause misfolding and aggregation of Glc7/PP1 in the W303 yeast background strain, indicating that Sds22 and I3 are required for the structural integrity of Glc7/PP1 and may have functions in Glc7/PP1 biogenesis and / or maintenance (Cheng & Chen, 2015).

While genetic interaction studies did not yield conclusive results regarding the influence of Sds22 and Ypi1 on Glc7/PP1 activity, both Sds22 and Ypi1 inhibit Glc7/PP1 activity *in vitro* (Pedelini et al., 2007). When added together to Glc7, Sds22 and Ypi1 display an additive inhibitory capacity towards Glc7/PP1 activity (Pedelini et al., 2007). In contrast, human SDS22 and I3 both inhibit PP1 *in vitro*, but do not act synergistically (Lesage et al., 2007). This difference is possibly explained by findings that yeast Sds22 can directly bind to Ypi1, while this direct interaction is lost in mammals (Pedelini et al., 2007; Lesage et al., 2007). Nevertheless, also in mammalian cells, SDS22 and I3 were found to form a ternary sandwich complex with PP1 (Lesage et al., 2007). SDS22, I3 and PP1 were shown to interact physically *in vitro* in pulldown experiments. Additionally, all three components were found in immunoprecipitates of SDS22 or I3 from COS1 cell lysates, demonstrating that the ternary complex exists *in vivo* (Lesage et al., 2007). In yeast two-hybrid experiments, interactions of SDS22 or I3 with PP1 were shown to be stronger when both PiPs are expressed, suggesting that a PP1-complex comprising both SDS22 and I3 is most stable (Pedelini et al., 2007; Lesage et al., 2007).

Complex formation of PP1 and SDS22 with I3 was found to be specific, as SDS22 does not bind to a complex of PP1 with a truncated form of NIPP1 (Nuclear Inhibitor of PP1) that has a similar size as I3 and like I3 binds to PP1 via an RVxF motif (Lesage et al., 2007). The I3 RVxF motif comprises of residues 40-43 (KVEW) and is required for PP1 binding, as a mutation of the RVxF motif abolishes the interaction with PP1 (Lesage et al., 2007). In addition to the RVxF motif, another PP1-binding site of I3 was identified between residues 65-77 in *in vitro* assays using truncations and site directed mutants of I3 and testing for their inhibitory potency towards PP1 (Zhang et al., 2008). This PP1 interaction site was suggested to bind at or near the active site of PP1, thereby inhibiting its activity (Zhang et al., 2008). Similar inhibitory mechanisms have been proposed for other PiPs, such as Mypt1, Inhibitor-2 (I2), DARP-32 and Inhibitor-1 (I1) (Terrak et al., 2004; Hurley et al., 2007; Barford et al., 1998). Interestingly, four residues within the second PP1 interaction site of I3 were shown to be phosphorylated during mitosis in a mass spectrometry screen for mitotic phosphosites (Dephoure et al., 2008), hinting at a possible regulation of I3-binding and the I3-mediated inhibition of PP1 during mitosis. Like other inhibitory PiPs, I3 is a hydrophilic, heat-stable protein and behaves anomalously during SDS-PAGE and gel filtration, suggesting that it has a highly disordered or asymmetric structure (Zhang et al., 2008).

SDS22 does not contain an RVxF motif. It mainly consists of 11 leucine-rich repeats (LRR) that form a superhelical structure. A bipartite PP1-interaction site has been mapped within the concave site of this LRR superhelix. SDS22 binds close to the catalytic site of PP1, at the so-called α4/α5/α6 triangle (Ceulemans et al., 2002b). Point mutations within the PP1 binding site of SDS22 (W302A or E192A) were shown to abolish the interaction with PP1 (Ceulemans et al., 2002; Lesage et al., 2007).

Both SDS22 and I3 inhibit PP1 reversibly and in a substrate-dependent manner. Addition of SDS22 or I3 was shown to inhibit PP-mediated dephosphorylation of casein and glycogen phosphorylase but not of myelin basic protein (MBP) and histone H2A *in vitro*, suggesting that SDS22 and I3 might act as substrate specifiers (Lesage et al., 2007). However, in addition to the reversible inhibition, SDS22 was found to slowly convert PP1 into an inactive form that is sensitive to trypsin digestion, indicating that SDS22 induces a conformational change of PP1. This SDS22-

mediated inactivation of PP1 was shown to be substrate-independent and to reduce the binding affinity of the complex for I3 (Lesage et al., 2007). A similar inactivation mechanism has been described for I2 and was reported to involve the loss of a metal ion from the catalytic site of PP1 (Hurley et al., 2007).

In mammalian cells, SDS22 is found both in the cytoplasm and the nucleus (Lesage et al., 2007). I3 contains a nuclear localization signal (NLS) and is found in the nucleus and especially enriched in the nucleolus in mammalian interphase cells (Huang et al., 2005). During mitosis, I3 was reported to be enriched at centrosomes (Huang et al., 2005). Furthermore, Lee and colleagues reported that I3 selectively interacts with the PP1α and PP1γ isoforms, but not with PP1β (Huang et al., 2005).

The role of SDS22 and I3 in regulating PP1 activity at the kinetochore and thereby in balancing Aurora B kinase is a main subject of this thesis. Little is known about the role of I3 in mammalian cells. Huang and Lee found I3 to be involved in apoptotic response as a caspase-3 substrate (Huang & Lee, 2008), however, the role of I3 during mitosis in mammalian cells has remained unknown. SDS22 on the other hand, has been implicated in two studies to play a role as a positive regulator of PP1 activity at the kinetochore, thereby counteracting Aurora B in human cells (Posch et al., 2010; Wurzenberger et al., 2012). siRNA-mediated depletion of SDS22 was shown to cause chromosomal alignment defects, a delay in mitotic progression and anaphase defects like chromosomal bridges, lagging chromosomes and pauses during poleward chromosome segregation (Posch et al., 2010; Wurzenberger et al., 2012). The localization of SDS22 and its exact function in regulating PP1 activity at the kinetochore, however, has remained controversial. Whereas Swedlow and colleagues reported SDS22 to localize at kinetochores from prometaphase until telophase and to be required for PP1 targeting to kinetochores (Posch et al., 2010), three other groups could not detect it there (Liu et al., 2010; D. Gerlich and M. Bollen, personal communication). Within this study, we found that SDS22 does not quantitatively localize to kinetochores under normal conditions (Eiteneuer et al., 2014) (see Results, chapter 2.1). Also regarding the effect of SDS22 silencing on Aurora B activity, differential results have been published. Upon SDS22 depletion, Swedlow and colleagues observed an increase in Aurora B activity, monitored as an increase in autophosphorylation at T232, but a decrease in Aurora B substrate

phosphorylation (MCAK pS92, Hec1 pS55, CENP-A pS7) (Posch et al., 2010). Consistent with a decreased phosphorylation level of Hec1 and MCAK, Swedlow and colleagues furthermore observed an increase in inter-kinetochore distance in SDS22-depleted cells. They therefore suggest that another phosphatase or another PP1 holoenzyme might dephosphorylate Aurora B substrates (Posch et al., 2010). In contrast, Gerlich and colleagues did not observe an effect on Aurora B T-loop phosphorylation at T232 in SDS22-depleted cells, but an increase in Aurora B substrate phosphorylation (Dsn1 pS100) (Wurzenberger et al., 2012). In addition to its role in counteracting Aurora B, SDS22 has been implicated in the local softening of the cell cortex at cell poles that facilitates elongation of the cell during anaphase (Rodrigues et al., 2015). Baum and colleagues found SDS22 to be required for the dephosphorylation of moesin, a linker between the plasma membrane and the actin cytoskeleton, at the polar cell cortex, thereby promoting polar relaxation in human and *Drosophila* cells (Rodrigues et al., 2015). Like Swedlow and colleagues, Baum's group reported a kinetochore-localization of SDS22 during metaphase and anaphase. They therefore suggest that kinetochore-localized PP1-SDS22 dephosphorylates cortical moesin as chromosomes move towards the polar cortex at mid anaphase, thereby promoting actin clearance and cortical relaxation at the cell poles (Rodrigues et al., 2015).

1.5 The AAA ATPase p97

p97 (also known as VCP (valosin containing protein) in mammals, Cdc48 (cell division cycle protein 48) in yeast, CDC-48 in *C. elegans* and Ter94 in *Drosophila*) is a homohexameric, ATP-driven chaperone that belongs to the family of AAA (ATPases associated with diverse cellular activities) ATPases. It is an essential, highly conserved and abundant protein that is ubiquitously expressed in all eukaryotic cells. p97 accounts for about 1 % of the total cytosolic protein mass and is also found in the nucleus and associated with membranes of various organelles (Ye, 2006). Cdc48/p97 was first identified in budding yeast in a genetic screen for mutants that cause defects in cell cycle progression (Moir et al., 1982). In vertebrate cells, p97 was originally discovered due to its sheer abundance (Peters et al., 1990), foretelling its broad cellular role. Indeed, p97 plays a critical role in a large variety of cellular processes, such as clearance of misfolded proteins by the ubiquitin-proteasome system (UPS), organelle membrane dynamics and a number of intracellular signaling pathways (Schuberth & Buchberger, 2008; Meyer et al., 2012) (see below). Most described p97-associated functions are ubiquitin-dependent (Schuberth & Buchberger, 2008; Meyer et al., 2012). p97 converts the energy of ATP hydrolysis into mechanical force that is used to structurally remodel or unfold substrate proteins or protein complexes. Its molecular function is seen as that of a “segregase“: p97 segregates (ubiquitinated) substrate proteins from protein complexes or cellular surfaces. These substrates are then either degraded by the proteasome or recycled (Ye, 2006; Jentsch & Rumpf, 2007). p97 associates with a large number of protein cofactors that mediate its interaction with ubiquitinated substrates and control p97 activity and localization, thus facilitating its functional diversity (Ye, 2006; Schuberth & Buchberger, 2008; Meyer et al., 2012). Mutations of p97 are linked to a late onset, autosomal dominant multisystemic degenerative disorder termed inclusion body myopathy associated with Paget’s disease of the bone and frontotemporal dementia (IBMPFD) and to amyotrophic lateral sclerosis (ALS) (Watts et al., 2004; Johnson et al., 2010). Symptoms may vary from patient to patient and occur late in life, suggesting that disease-associated p97 mutations do not lead to a global loss of function, but rather have long term effects on protein homeostasis (Meyer & Weihl, 2014). Expression of disease-associated p97 mutants in cultured cells does not affect cell cycle control and cell division (Ju et al., 2008),

suggesting that p97-mediated signaling events are largely unaffected. Instead, disease-associated mutations were found to affect the association of p97 with certain cofactors, suggesting that they might impair a distinct subset of p97 functions (Fernández-Sáiz & Buchberger, 2010; Ritz et al., 2011). p97 expression was found to be elevated in some cancer types (Yamamoto et al., 2004a; Yamamoto et al., 2004b; Tsujimoto et al., 2004; Valle et al., 2011). Because of its essential role in protein homeostasis and since cancer cells are subject to increased proteotoxic stress due to genomic alterations, p97 is considered as a potential cancer therapeutic target (Deshaies, 2014).

1.5.1 Structure and general function of p97

A p97 protomer consists of two ATPase domains (D1 and D2), that are connected by a short linker, a globular N-terminal domain (N domain) and an unstructured C-terminal tail (Ogura & Wilkinson, 2001; DeLaBarre & Brunger, 2003). Both ATPase domains contain a Walker A motif and a Walker B motif which mediate ATP binding and hydrolysis, respectively, and a second region of homology (SRH), that distinguishes AAA ATPases from the wider family of Walker-type NTPases (Ogura & Wilkinson; 2001). Six p97 protomers assemble into a stable, barrel-shaped hexamer, wherein the D1 and D2 domains form two concentric rings that are stacked on top of each other, surrounding a central pore (DeLaBarre & Brunger, 2003). The D1 domain has low ATPase activity and is required for hexamerization, while the main ATPase activity is located in the D2 domain (Rouiller et al., 2002; Song et al., 2003). Consistently, a p97 mutant with a mutation in the Walker B motif of the D2 domain (p97 E578Q) is dominant negative and traps ubiquitinated substrates (Ye et al., 2003; Ramadan et al., 2007). The N domains are positioned at the periphery of the D1 ring (Zhang et al., 2000; DeLaBarre & Brunger, 2003) (Figure 1.8 A) and constitute the primary cofactor binding sites and also contain a low affinity binding site for ubiquitin (Meyer et al., 2012; Ye, 2006). During the ATP hydrolysis cycle the p97 hexamer undergoes major conformational changes, comprising a rotational twist of the D2 ring with respect to the D1 ring and movements of the N Domain between a “down“ conformation in plane with the D1 ring and an “up“ conformation rotated by ~75° relative to the D1 ring. (DeLaBarre and Brunger, 2005; Pye et al., 2006; Banerjee et al., 2016). These conformational changes are believed to generate the

mechanical forces that mediate structural remodeling of substrates, disassembly of protein complexes and segregation of proteins from cellular surfaces or binding partners for proteasomal degradation or recycling (Ye et al., 2003; Stolz et al., 2011). However, the precise mechanisms how p97 remodels and segregates its substrates in different cellular processes are not well understood (Stolz et al., 2011).

In order to fulfill its various cellular functions, p97 associates with a large number of cofactors, several of which contain ubiquitin-binding domains, suggesting that they act as ubiquitin adaptors for p97. The largest subgroup of cofactors interacts with p97 via an UBX (ubiquitin-regulatory X) domain or a UBX-like domain that assumes a ubiquitin-like fold and binds to the p97 N-domain (Schuberth & Buchberger, 2008; Meyer et al., 2012). Furthermore, a number of other p97-binding domains and shorter binding motifs exist, that mediate cofactor-binding to the p97 N-domain or the C-terminal tail. Short p97-binding motifs include the BS1 (binding site 1) motif or SHP box, the VBM (VCP-binding) motif and the VIM (VCP-interacting) motif, which bind to the p97 N-domain. Binding to the C-terminal tail of p97 is mediated by PUB (peptide N-glycosidase / ubiquitin-associated) and PUL (PLAA, Ufd3 and Lub1) domains (Meyer et al., 2012). Some cofactors contain more than one p97-binding site. Different cofactors target p97 to distinct subcellular structures or subsets of substrates, providing specificity for its numerous cellular functions (Schuberth & Buchberger, 2008; Meyer et al., 2012). However, how exactly these distinct cofactors with their particular modes of interaction with p97 relate to its specific functions is not well understood (Meyer et al., 2012). Initially it was suggested that p97 might cooperate with a distinct cofactor in each p97-mediated pathway (Kondo et al., 1997; Meyer et al., 2000). This initial model was extended to a hierarchical model, in which p97 forms core complexes with major cofactors that bind to p97 in a mutually exclusive manner, including the SEP domain cofactors p47 and p37 and the heterodimeric cofactor Ufd1-Npl4, which modulate p97 activity or recruit additional cofactors (Bruderer et al., 2004; Hanzelmann et al., 2011; Meyer et al., 2012). These core complexes can function in several pathways by associating with alternative sets of additional cofactors that may determine the localization and / or bring in additional enzymatic activities (Schuberth & Buchberger, 2008; Yeung et al., 2008; Meyer et al., 2012). Such additional cofactors include E3 ubiquitin ligases, E4 ubiquitin chain extension enzymes and deubiquitinating enzymes (DUBs). Hence, the second major

function of p97 is that of an interaction hub that coordinates ubiquitination and ubiquitin chain editing events. Such modulations of the ubiquitination state may improve the targeting of a substrate protein to the proteasome or facilitate its recycling, thus determining its fate (Jentsch & Rumpf, 2007; Meyer et al., 2012; Meyer & Weihl, 2014) (Figure 1.8 B).

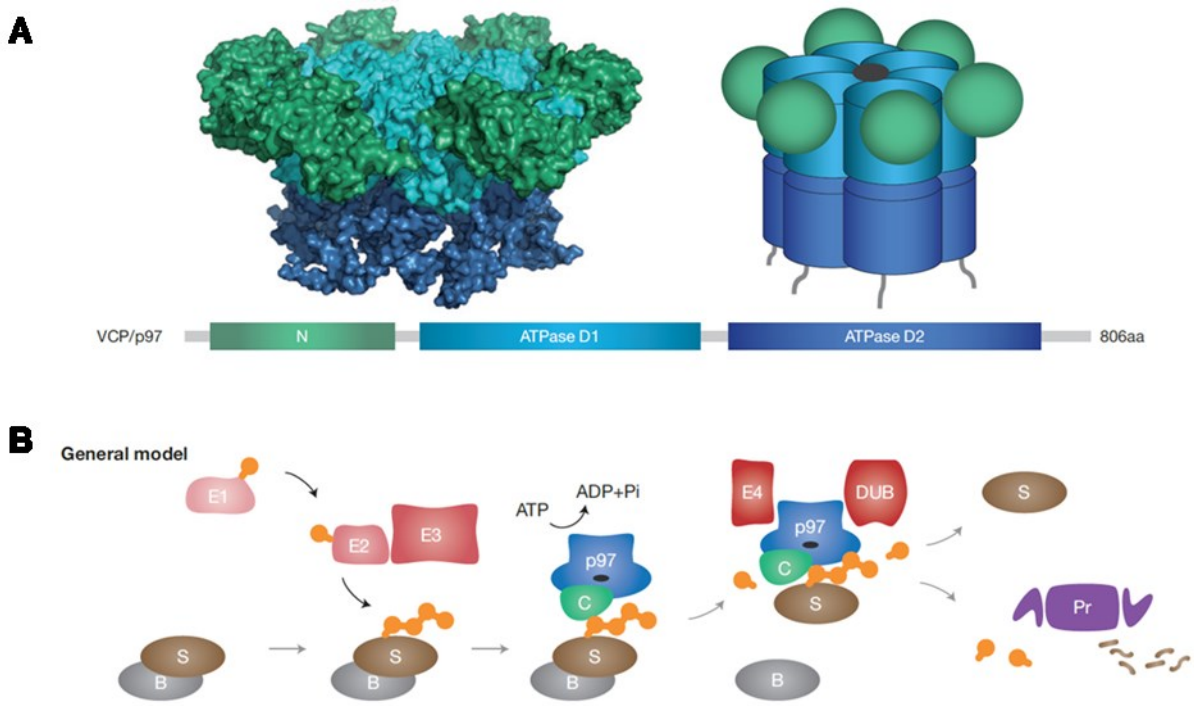

Figure 1.8 p97 structure and general model of p97 function. A Crystal structure and schematic representation of the p97 hexamer and domain structure of the p97 protomer. Each p97 protomer comprises an N domain (green), two ATPase domains D1 (cyan) and D2 (blue) and a less structured C-terminal tail. Six protomers assemble into a p97-hexamer in which the D1 and D2 domains form two concentric rings which are stacked on top of each other. The globular N domains are positioned at the periphery of the D1 ring. **B** Schematic model of the function of p97 in substrate segregation and ubiquitin chain editing. A substrate protein (S) is ubiquitinated by a cascade of the ubiquitin-activating enzyme (E1), a ubiquitin-conjugating enzyme (E2) and a specific ubiquitin ligase (E3). Recognition and binding of the ubiquitinated substrates is mediated by a ubiquitin-binding p97 cofactor (C). ATP hydrolysis by p97 generates mechanical force that structurally remodels the substrate to segregate it from binding partners (B) or cellular surfaces. p97-associated ubiquitin chain extension (E4) or deubiquitinating (DUB) enzymes may modulate the ubiquitination state of the substrate to either facilitate its recycling or target it for degradation by the proteasome (Pr). Subfigures **A** and **B** adopted from (Meyer et al., 2012).

1.5.2 Cellular functions of p97

p97 is an integral element of the UPS. It plays an essential role in individual signaling events as well as for general protein homeostasis, particularly under stress conditions (Meyer et al., 2012). Best understood is the role of p97 in endoplasmic reticulum associated degradation (ERAD), a quality control mechanism for proteins of the secretory pathway (Wolf and Stolz, 2011). In this process, misfolded lumenal and membrane ER proteins are recognized and selectively exported from the ER in a process called retro-translocation. At the outer layer of the ER membrane (in the case of lumenal proteins after their retrograde transport to the ER surface), these proteins are recognized by ER-associated E3 ubiquitin ligases and polyubiquitinated. They are than extracted from the ER membrane by p97 in concert with its heterodimeric cofactor Ufd1-Npl4 and subsequently degraded by the proteasome (Wolf and Stolz, 2011). p97-Ufd1-Npl4 is recruited to the ER membrane by membrane-bound cofactors, such as UBXD8 and Derlin (Wolf and Stolz, 2011; Claessen et al., 2012). Also, p97 has important functions in the extraction and degradation of proteins from mitochondrial membranes and from chromatin and has been linked to the handling and clearance of insoluble protein aggregates (Meyer et al., 2012). Furthermore, more recent findings showed that p97 is involved in co-translational quality control by extracting aberrant translation products from ribosomes for proteasomal degradation and also implicated p97 in the quality control of ribosomes and the disassembly of mRNA-protein complexes (mRNPs) (Meyer & Weihl, 2014). In addition to its role in proteasomal degradation, p97 is also involved in lysosomal degradation via both endosomal sorting and autophagy (Ritz et al., 2011; Kirchner et al., 2013; Tresse et al., 2010; Ju & Weihl, 2010; Chou et al., 2010). Besides its key functions in protein quality control, p97, in complexes with the SEP domain cofactors p47 or p37, has been implicated in membrane-fusion events during Golgi and ER reassembly and nuclear envelope reassembly at the end of mitosis as well as in Golgi and ER maintenance during interphase (Kondo et al., 1997; Meyer et al., 1998; Hetzer et al., 2001; Uchiyama et al., 2006). As mentioned above, the p97 segregase activity plays an important role in controlling several intracellular signaling pathways, both in a degradative and in a non-degradative fashion (Ye et al., 2003; Meyer et al., 2012). For instance, the p97-Ufd1-Npl4 complex acts in DNA damage response where it is required for the extraction of the DNA damage recognition

factors DDB2 and XPC from chromatin, thereby facilitating an effective nucleotide excision repair (NER) and is involved in CDC25A degradation in G2 phase, thereby contributing to a functional G2/M checkpoint (Puumalainen et al., 2014; Riemer et al., 2014). Another important chromatin-associated function of p97 is the counteraction of Aurora B kinase. In *Xenopus* egg extracts, p97 together with Ufd1-Npl4 was shown to extract Aurora B from chromatin at the end of mitosis, thereby promoting nuclear reformation (Ramadan et al., 2007). Furthermore, p97-Ufd1-Npl4 is required for balancing Aurora B activity already in early mitosis during spindle attachment in HeLa cells, where siRNA mediated depletion of Ufd1-Npl4 leads to increased Aurora B localization and activity on prometaphase and metaphase chromatin and causes chromosomal alignment defects and a mitotic delay (Dobrynin et al., 2011).

1.5.3 The SEP domain subfamily of p97 cofactors

Members of the SEP domain subfamily of UBX domain containing p97 cofactors are characterized by a combination of a UBX domain and a SHP box, both mediating binding to the N-domain of p97, and a so-called SEP (after Shp1, eyes closed and p47) domain. The SEP domain was shown to be involved in the trimerization of p47 and suggested to be involved in the putative trimerization of other SEP domain cofactors (Beuron et al., 2006; Yuan et al., 2004; Schuberth & Buchberger, 2008), but further functions of the domain are unknown. Shp1 (suppressor of high-copy PP1), the sole SEP domain protein in budding yeast, furthermore contains a ubiquitin-binding UBA domain. In human cells, four SEP domain proteins exist, namely p47, p37, UBXD4 and UBXD5 (Socius). p47 is the most abundant Shp1 ortholog and, like Shp1, contains a UBA domain. In contrast, the other three human SEP domain proteins lack a UBA domain. p37 and UBXD4 are close p47 homologs, whereas UBXD5 is more distantly related and contains an additional spectrin domain (Schuberth & Buchberger, 2008; Meyer & Weihl, 2014). p47 and p37 were shown to bind to p97 in a mutually exclusive manner, suggesting that the different human SEP domain cofactors form distinct p97-cofactor complexes (Uchiyama et al., 2006). *C. elegans* has only one SEP domain protein, UBXN-2. UBXN-2 has highest sequence homology with p47, but like p37 and UBXD4 lacks a UBA domain (Ye, 2006; Schuberth & Buchberger, 2008) (Figure 1 9).

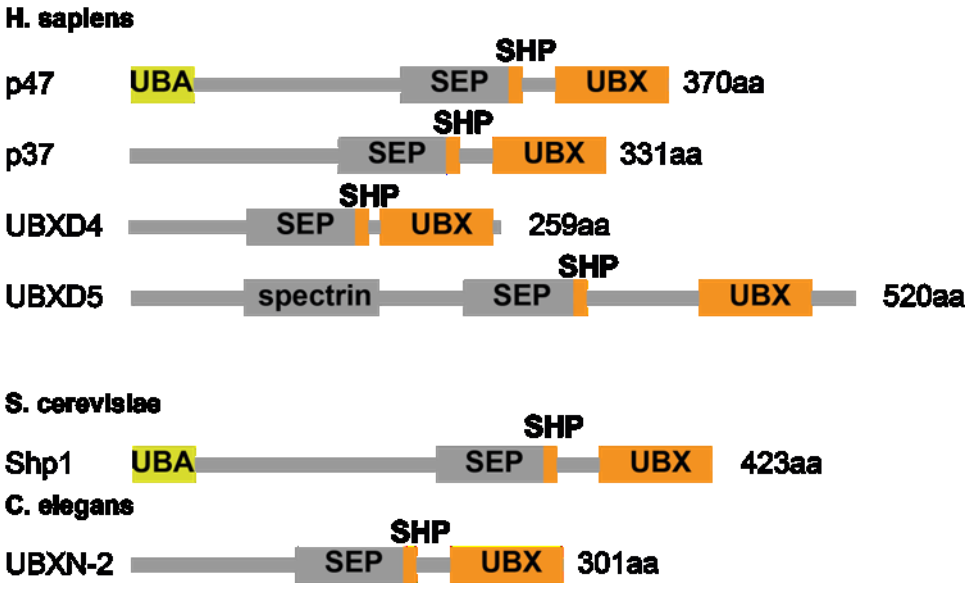

Figure 1.9 The SEP domain subfamily of p97 cofactors. Domain structures of SEP domain proteins in human, budding yeast and *C. elegans*. Four SEP domain proteins exist in humans, whereas only one each in budding yeast and *C. elegans*. The UBX domain and the SHP box bind to the p97 N domain. The UBA domain binds ubiquitin. The SEP domain is involved in the trimerization of p47. Its further functions are unknown. Figure modified from (Meyer & Weihl, 2014).

While the heterodimeric p97 cofactor Ufd1-Npl4 has been implicated in a number of ubiquitin-dependent protein degradation pathways, the SEP domain cofactors were suggested to have mainly non-degradative functions (Schuberth & Buchberger, 2008; Ye, 2006). The p97-p47 complex was shown to predominantly bind mono-ubiquitinated substrates, supporting this notion (Meyer et al., 2002). However, *shp1* mutants in yeast were found to exhibit defects in ubiquitin-dependent degradation of a subset of substrates and have been genetically linked to the proteasome (Hartmann-Petersen et al., 2004; Schuberth et al., 2004).

A mass spectrometry survey in U2OS cells showed highly different expression levels of distinct SEP domain cofactors. With $2.83*10^5$ protein copies detected per cell, p47 is by far the most abundant SEP domain protein, whereas about 100fold less copies of p37 and UBXD4 were found to be expressed (Beck et al., 2011). UBXD5 was not detected in U2OS cells and in another mass spectrometry survey analyzing 11 common human cell lines, raising the possibility that it is tissue specific (Beck et al., 2011; Geiger et al., 2012). In addition to varying expression levels, human SEP domain cofactors differ in their subcellular localization. p47 contains two nuclear

localization signals (NLS) and is strictly nuclear in interphase cells (Uchiyama et al., 2003), whereas p37 and UBXD4 were found to localize to the ER and Golgi compartments (Uchiyama et al., 2006; Rezvani et al., 2009). While little is known about the functions of UBXD4 and UBXD5 (Rezvani et al., 2009; Katoh et al., 2002), p97-cofactor complexes with either p47 or p37 were shown to be required for Golgi and ER reassembly at the end of mitosis, mediating homotypic membrane fusion events by regulating distinct SNARE (soluble NSF attachment protein receptor) complexes, however the exact mechanism has remained unclear (Kondo et al., 1997; Meyer et al., 1998; Hetzer et al., 2001; Uchiyama et al., 2006). Additionally, p37 has been implicated in Golgi and ER maintenance during interphase (Uchiyama et al., 2006). p97-p47 mediated membrane fusion was shown to require ubiquitination of unknown substrate(s), but was not affected by inhibition of the proteasome (Meyer et al., 2002; Wang et al., 2004). In contrast, the activity of the p97-p37 complex in membrane fusion events appears to be independent of substrate ubiquitination (Uchiyama et al., 2006). In mitosis, both p47 and p37 are phosphorylated by CDK1, inhibiting their membrane fusion activity, thus preventing a premature reversion of Golgi fragmentation (Uchiyama et al., 2003; Kaneko et al., 2010). A recent study that we contributed to furthermore showed that p37 in human cells, as well as UBXN-2 in *C. elegans* embryos, are required for limiting centrosomal recruitment of Aurora A kinase in prophase, thereby regulating centrosome maturation and spindle positioning (Kress et al., 2013) (see Results, chapter 2.4). si-RNA mediated depletion of p47 alone showed no defects of spindle positioning and centrosome maturation, but aggravated these phenotypes when co-depleted with p37 (Kress et al., 2013).

The sole budding yeast Cdc48/p97 SEP domain cofactor Shp1 was discovered in a genetic screen searching for mutants that suppress the lethality of Glc7/PP1 overexpression (Zhang et al., 1995). Lysates from *shp1* mutant strains were shown to be deficient in Glc7/PP1 catalytic activity, whereas the expression level and subcellular localization of Glc7 in these mutants was unaltered, suggesting Shp1 to be a positive regulator of overall Glc7/PP1 activity (Zhang et al., 1995). More recent studies furthermore showed that Shp1 is required for Glc7/PP1 to antagonize Ipl1/Aurora (Cheng & Chen, 2010; Böhm & Buchberger, 2013). Cheng and Chen found inducible Shp1 depletion to partially rescue the lethality of a temperature sensitive *ipl1* mutant (*ipl1-321*) and to reverse the hypophosphorylation of the Ipl1

substrate Dam1 in the *ipl1-321* strain (Cheng & Chen, 2010). Consistent with a function of Cdc-48-Shp1 in balancing Ipl1/Aurora, they found Shp1 depletion to cause a metaphase arrest due to SAC activation, chromosomal alignment defects as well as spindle defects and aberrant centrosome numbers in a subset of cells and observed similar phenotypes in a temperature sensitive *cdc48* mutant strain (*cdc48-3*) (Cheng & Chen, 2010). Cheng & Chen furthermore observed a loss of nuclear enrichment of a GFP-Glc7 fusion in Shp1 depleted and *cdc48-3* mutant cells, suggesting Cdc48-Shp1 to be required for Glc7/PP1 function in mitosis by promoting its nuclear targeting (Cheng & Chen, 2010). Böhm and Buchberger confirmed the genetic interactions between *shp1* and *glc7* as well as *shp1* and *ipl1* and also observed a mitotic delay due to SAC activation in *shp1* null mutants (Böhm & Buchberger, 2013). In addition, they could show by co-immunoprecipitation that Shp1 and Glc7 also interact physically (Böhm & Buchberger, 2013). Using Cdc48 binding deficient *shp1* mutants *shp1-a1* and *shp1-b1*, they furthermore showed that Shp1 function in mitotic progression and antagonizing Ipl1/Aurora requires Cdc48/p97 binding (Böhm & Buchberger, 2013). In contrast to the findings by Cheng and Chen, and consistent with the results by Volkert and colleagues, Böhm and Buchberger observed no changes in Glc7/PP1 localization in *shp1* null and Cdc48 binding deficient mutants (Zhang et al., 1995; Böhm & Buchberger, 2013). Instead, they found an increase in Ipl1 substrate phosphorylation (Dam1 and histone H3 at S10) in *shp1* null mutants and decreased binding of Glc7/PP1 to the PiP Glc8 (Inhibitor-2 in vertebrates), suggesting that Shp1 is required for Glc7/PP1 activity and holoenzyme formation (Böhm & Buchberger, 2013). Furthermore, Böhm and Buchberger observed a synthetic lethality between the *shp1-7* null mutant and the *glc7-129* mutant as well as between *shp1-7* and the *sds22-6* mutant (Böhm & Buchberger, 2013). Using an ATPase inactive, substrate-trapping Cdc48 mutant ($Cdc48^{QQ}$), Cheng and Chen recently showed that Cdc48-Shp1 transiently associates with Glc7 as well as Sds22 and Ypi1 (Cheng & Chen, 2015). They furthermore found the ternary Sds22-Glc7-Ypi1 complex to be the main interaction partner of $Cdc48^{QQ}$-Shp1. Their findings also indicate that binding of the Sds22-Glc7-Ypi1 complex to Cdc48-Shp1 is mediated by Sds22, as Glc7 binding to $Cdc48^{QQ}$-Shp1 was abolished in the Glc7 binding-deficient *sds22-6* mutant background (Cheng & Chen, 2015). Using the yeast background strain W303, Cheng and Chen found inducible depletion of Shp1 as well as a temperature-sensitive, Cdc48 binding deficient *shp1* mutant

(*shp1*^{ts}) to cause misfolding of Glc7/PP1, leading to the formation of insoluble Glc7 aggregates that contained the heat shock proteins Hsp104 and Hsp42 and depended on the proteasome for clearance, suggesting Cdc48-Shp1 to be required for the structural integrity of Glc7/PP1 (Cheng & Chen, 2015). Glc7 aggregate formation occurred only within hours after depleting Shp1 and was abolished in the *shp1*^{ts} mutant strain upon addition of the translation inhibitor cycloheximide, suggesting that Cdc48-Shp1 acts on newly synthesized Glc7/PP1 and may be required for Glc7/PP1 biogenesis (Cheng & Chen, 2015). While Sds22 and Ypi1 were not found to co-aggregate with Glc7/PP1 in the *shp1*^{ts} mutant strain, also the *sds22-6* mutant and inducible Ypi1 depletion led to Glc7/PP1 aggregate formation in the yeast W303 background. Whereas Ypi1 depletion, like Shp1 depletion, led to Glc7/PP1 aggregate formation only within hours, Glc7/PP1 aggregates were detected in the *sds22-6* mutant shortly after shifting to the restrictive temperature, suggesting that Sds22 regulates Glc7/PP1 also after biosynthesis (Cheng & Chen, 2015): In contrast to the findings by Cheng and Chen, Böhm and Buchberger did not observe Glc7/PP1 aggregation in a *shp1* null mutant strain, however using a different yeast background strain (DF5) (Böhm & Buchberger, 2013). This discrepancy was suggested to be due to varying capacities of buffering misfolded proteins in different yeast strains (Cheng & Chen, 2015). Together, the published findings indicate that Cdc48-Shp1 is required for the activity and structural integrity of Glc7/PP1 and that it acts on the Sds22-Glc7-Ypi1 complex, possibly being involved in Glc7/PP1 biogenesis, however the underlying mechanism is not understood. While Cheng and Chen proposed that Cdc48-Shp1 may promote the assembly of the Sds22-Glc7-Ypi1 complex, Böhm and Buchberger observed no reduction of Sds22 binding to Glc7/PP1 in a *shp1* null mutant (Cheng & Chen, 2015; Böhm & Buchberger, 2013). Furthermore, it is unclear if the underlying process involves ubiquitination. Cheng and Chen were unable to detect ubiquitinated forms of Glc7/PP1, Sds22 and Ypi1 associated with Cdc48^{QQ}-Shp1. Interestingly, the Shp1 UBA domain was found to be dispensable for cell viability and Glc7/PP1 localization and a *shp1*$^{\Delta UBA}$ mutant did not rescue the temperature sensitivity of the *ipl1-321* mutant (Cheng & Chen, 2015; Böhm & Buchberger, 2013).

In a mass spectrometry screen performed in our research group (Ritz et al., 2011), PP1γ, SDS22 and I3 were identified as interactors of p97 in human cells, indicating

that the interaction between Cdc48/p97 and the ternary PP1 complex is conserved in vertebrates. This finding was confirmed by co-immunoprecipitation experiments. Endogenous PP1γ and SDS22 co-immunoprecipitated with p97-Strep, and, importantly, also with HA-p47, but not with UBXD1-HA, HA-Npl4 and Ufd1-HA (S. Bremer, unpublished data). Furthermore, SDS22, I3 and PP1α and PP1β have been reported as physical interactors of p97, p37 and UBXD4 in a mass spectrometry survey in J.W. Harper's laboratory (Raman et al., 2015), implicating the other two close Shp1 orthologs in the interaction between p97 and the SDS22-PP1-I3 complex. These physical interactions may point at a regulation of the ternary PP1 complex by p97 SEP domain cofactor-complexes and may reveal a functional link between p97 and PP1 in regulating Aurora kinases. siRNA-mediated depletion of p47, the most abundant SEP domain cofactor (Beck et al., 2011), however, was shown to cause no mitotic delay or chromosomal alignment defects (Dobrynin et al., 2011), raising the question of distinct and / or redundant functions of the different p97 SEP domain cofactor-complexes in regulating PP1.

1.6 The aims of the thesis

PP1 functions at the kinetochore by balancing the activity of mitotic kinase Aurora B, thereby regulating its key functions in correcting erroneous kinetochore-microtubule attachments and SAC signaling (Lesage et al., 2011). However, how PP1 activity and localization at the kinetochore is regulated is not well understood. In particular, the role of the PiP SDS22 in regulating PP1 at the kinetochore has remained highly controversial. While two independent studies have shown that SDS22 is relevant for PP1 function at the kinetochore in human cells, contradictory findings have been published on SDS22 localization and on the mode of regulation of kinetochore-associated PP1 by SDS22 (Posch et al., 2010; Wurzenberger et al., 2012; Liu et al., 2010). PP1 can form a ternary complex with both SDS22 and I3 (Lesage et al., 2007; Pedelini et al., 2007). Whereas Ypi1/I3 has been implicated in the regulation of Glc7/PP1 function in balancing Ipl1/Aurora kinase in budding yeast (Pedelini et al., 2007; Bharucha et al., 2008), the role of I3 during mitosis in mammalian cells has remained completely unknown. In initial experiments of our study, we found siRNA-mediated depletions of both SDS22 and of I3 to cause chromosomal alignment defects as well as an increase of active Aurora B kinase on metaphase centromeres (Eiteneuer et al., 2014). Using cell-based and biochemical approaches, we therefore aimed to clarify the functions of SDS22 and I3 in regulating PP1 at the kinetochore.

Results obtained within the course of this study, as well as recent findings in budding yeast furthermore indicate that SDS22 and I3 may have a more general role for PP1 activity and structural integrity, possibly functioning in PP1 biogenesis and / or maintenance (Eiteneuer et al., 2014; Cheng & Chen, 2015). In addition, the AAA ATPase Cdc48/p97 together with its SEP domain cofactor Shp1 is required for PP1 activity and integrity in budding yeast, however the underlying mechanism has remained obscure (Zhang et al., 1995; Cheng & Chen, 2010; Böhm & Buchberger, 2013; Cheng & Chen, 2015). Cdc48/p97-Shp1 was shown to transiently associate with the ternary Sds22-Glc7/PP1-Ypi1/I3 complex (Cheng & Chen, 2015). Importantly, this physical interaction is conserved in human cells, pointing at a conserved role of p97 and its SEP domain cofactors in regulating PP1 (Raman et al., 2015; our unpublished data) We therefore set out to investigate the dynamics and regulation of the ternary SDS22-PP1-I3 complex, and the role of p97 SEP domain cofactor

complexes therein. We thereby aimed to elucidate the possible function of p97 and its SEP domain cofactors in regulating the ternary PP1 complex, and, at the same time, to gain further insights into the mechanism of SDS22- and I3-mediated regulation of PP1.

2 Results

2.1 Part I: The role of SDS22 and I3 in mitotic chromosomal alignment

PP1 has been established as the phosphatase acting antagonistically to mitotic kinase Aurora B (Ceulemans & Bollen, 2004). The PP1 interacting protein (PiP) SDS22 has been implicated in a series of studies to play a role in regulating PP1 activity at the kinetochore and counteracting Aurora B kinase (Peggie et al., 2002; Posch et al., 2010; Wurzenberger et al., 2012). However, whether SDS22 localizes to kinetochores and in whether it affects Aurora B activity and / or Aurora B substrate dephosphorylation has remained controversial (Posch et al., 2010; Wurzenberger et al., 2012; Liu et al., 2010). SDS22 is known to form a ternary complex with PP1 and Inhibitor-3 (I3) (Lesage at al., 2007). However, nothing was known about the role of I3 in mammalian cells. Therefore, we set out to clarify the role of SDS22 in chromosomal attachment and regulation of PP1 at the kinetochore as well as to reveal the potential role of I3 in this process. In the initial phase of our study, we found depletions of both SDS22 and I3 to cause chromosomal alignment defects and a delay in mitotic progression, as well as an increase in Aurora B phosphorylation at T232, indicating that both SDS22 and I3 are required for proper bipolar chromosomal attachment and for PP1 activity at the kinetochore (Eiteneuer et al., 2014). Based on this, we went on to investigate the roles of SDS22 and I3 in regulating kinetochore-associated PP1.

2.1.1 Comparison of SDS22 depletion to global cellular inhibition of PP1 in terms of Aurora B activity

In initial experiments of our study, we could show that siRNA-mediated depletions of both SDS22 and I3 cause a decrease of PP1 activity at kinetochores as evidenced by an increase of Aurora B phosphorylation at T232 on metaphase chromatin (Eiteneuer et al., 2014). Using the example of SDS22 depletion, we wanted to compare this effect to a broader inhibition of PP1. To that end, we made use of HeLa cells inducibly overexpressing a GFP-fusion of the PP1 inhibitor NIPP1 (Nuclear Inhibitor of PP1) with a non-functional substrate-binding FHA (ForkHead Associated) domain (NIPP1-Fm) upon addition of doxycycline. NIPP1 is a potent and highly

specific PP1 inhibitor that inhibits the dephosphorylation of all tested PP1 substrates, except those that are recruited via its FHA domain (Beullens et al., 1992; Vulsteke et al., 1997; Winkler et al., 2015). Cells inducibly overexpressing NIPP1-fm with an additional mutation of the RVxF PP1-binding motif (NIPP1-Fm+Pm) served as a control. HeLa Flp-In NIPP1 cell lines were a kind gift of M. Bollen (KU Leuven) (Winkler et al., 2015). First, we investigated how PP1 inhibition by NIPP1-Fm overexpression affected mitosis and Aurora B phosphorylation. Expression of NIPP1 fusions was induced by addition of doxycycline for 48 h, cells were fixed with formaldehyde and stained with Aurora B pT232 specific antibodies and DAPI to visualize chromatin. Samples were examined by light microscopy. In accordance with a study by Bollen and colleagues, we observed severe chromosomal alignment defects, cells arrested in prometaphase, increased Aurora B phosphorylation on prometaphase and metaphase chromatin as well as a partial loss of the centromeric localization of Aurora B with a more diffuse distribution along the chromatin (Winkler et al., 2015 & data not shown). We then went on to examine the effect of SDS22 depletion on Aurora B phosphorylation in the background of PP1 inhibition by NIPP1-Fm overexpression. HeLa Flp-In NIPP1-Fm or NIPP1-Fm+Pm cells were treated with siRNAs targeting SDS22 or Luciferase, which is absent in mammalian cells, (siLuc) as a control for 48 h. Expression of GFP-NIPP1 fusions was induced by addition of doxycycline for 24 h or not before fixation of cells with formaldehyde. Cells were stained with Aurora B pT232 antibodies and DAPI and the Aurora B pT232 signal intensity on metaphase chromatin was monitored at a laser scanning confocal microscope. In spite of the partial prometaphase arrest upon NIPP1-Fm overexpression, a number of metaphase cells sufficient for statistical analysis was obtained. Aurora B pT232 signal intensities on chromatin were quantified using the automated image analysis software CellProfiler (Carpenter et al., 2006) by creating a threshold-based mask with the DAPI signal to exclude cytoplasmic and centrosomal staining. The mean intensity within this mask was measured for ≥ 36 cells per condition combined from 3 independent experiments. We observed a strong increase in Aurora B phosphorylation in cells overexpressing NIPP1-Fm compared to uninduced and NIPP1-Fm+Pm overexpressing cells, that was not further elevated upon SDS22 depletion, suggesting that PP1 activity on chromatin was fully inhibited. In uninduced and NIPP1-Fm+Pm expressing cells, SDS22 depletion caused an increase in Aurora B phosphorylation compared to siLuc treated controls, consistent

with our results obtained in normal HeLa cells (Eiteneuer et al., 2014). The increase of Aurora B phosphorylation caused by SDS22 depletion was however weaker than the increase observed upon NIPP1-Fm overexpression, indicating that SDS22 is required for full PP1 function at kinetochores, but that its absence does not cause a complete loss of PP1 activity at the kinetochores (Figure 2.1 A and B).

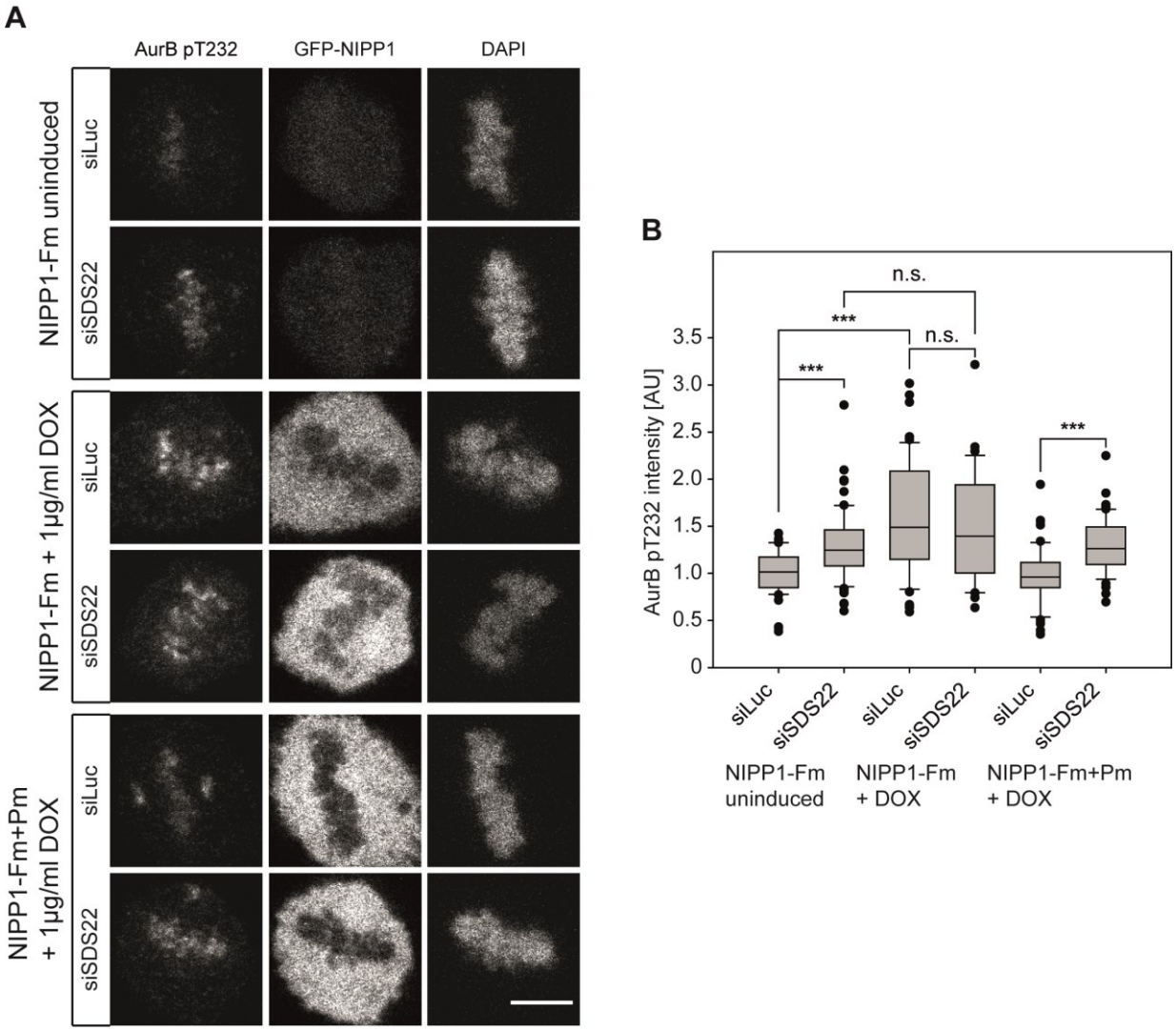

Figure 2.1 siRNA mediated depletion of SDS22 and NIPP1-mediated cellular inhibition of PP1 increase Aurora B activity. A NIPP1-mediated PP1 inhibition and siRNA-mediated SDS22 depletion increase Aurora B autophosphorylation on metaphase chromatin. HeLa Flp-In T-Rex cells inducibly expressing GFP-fusions of the PP1 inhibitor NIPP1-Fm (mutation of the substrate-binding FHA domain) or of NIPP1-Fm+Pm (additional mutation of the RVxF type PP1-binding site) were treated with the indicated siRNAs for 48 h. Expression of NIPP1 fusions was induced by addition of doxycycline for 24 h prior to fixation or not. Cells were fixed with formaldehyde and stained with AurB pT232 antibodies and DAPI. Representative laser-scanning confocal images are shown. Note the unspecific centrosomal staining with the AurB pT232 antibodies. Scale bar, 5 µm. **B** Quantification of (**A**). The AurB pT232 signal intensity on metaphase chromatin was quantified using the software CellProfiler. Box plots show median, lower and upper quartiles (line and box), 10^{th} and 90^{th} percentiles (whiskers) and outliers (●). P-values were calculated using Mann-Whitney *U* test (***, $p \leq 0.001$; n.s., not significant). Data from three independent experiments with a total of ≥ 36 cells per condition.

2.1.2 SDS22, as well as I3 depletion causes increased recruitment of mitotic checkpoint protein BubR1 to metaphase kinetochores

As a part of our study on the role of SDS22 and I3 in regulating kinetochore-associated PP1, we observed chromosomal alignment defects and an increased Aurora B activity in cells depleted for SDS22 or I3 (Eiteneuer et al., 2014). Since an increased Aurora B activity is expected to destabilize microtubule-kinetochore attachments, we asked if silencing of SDS22 and I3 would cause an activation of the spindle assembly checkpoint. To that end, recruitment of the spindle assembly checkpoint protein BubR1 to metaphase kinetochores was monitored. HeLa cells were treated with siRNAs targeting SDS22, I3 or Aurora B for 48 h. siLuc and an siRNA targeting NIPP1, which has no known functions in mitosis (Minnebo et al., 2013; Nuytten et al., 2008), served as negative controls. Cells were formaldehyde-fixed and stained with BubR1 antibodies and CREST serum to visualize kinetochores and with DAPI before analysis at a spinning disc confocal microscope. BubR1 recruitment to kinetochores of aligned metaphase plates was quantified using CellProfiler software (Carpenter et al., 2006). The DAPI and CREST signals were used to identify primary objects (“chromatin“ and “kinetochores“, respectively). The mean intensities of BubR1 and CREST signals on kinetochores were measured and the signal on remaining areas of the chromatin mask was subtracted as background. The ratio of BubR1 to CREST signal intensities on kinetochores was determined for 42 cells per condition combined from 3 independent experiments. We observed an increased recruitment of BubR1 to kinetochores of SDS22 depleted cells, which is in accordance with results published by Swedlow’s group (Posch et al., 2010). Also depletion of I3 caused an increased recruitment of BubR1 to metaphase kinetochores. However, the effect of SDS22 depletion on BubR1 recruitment was slightly stronger than the effect of I3 depletion. In contrast, Aurora B depleted cells had reduced BubR1 signals even on misaligned chromosomes as expected given the importance of Aurora B for spindle assembly checkpoint function (Morrow et al., 2005; King et al., 2007; Saurin et al., 2011; Krenn & Musacchio, 2015) (Figure 2.2 A and B).

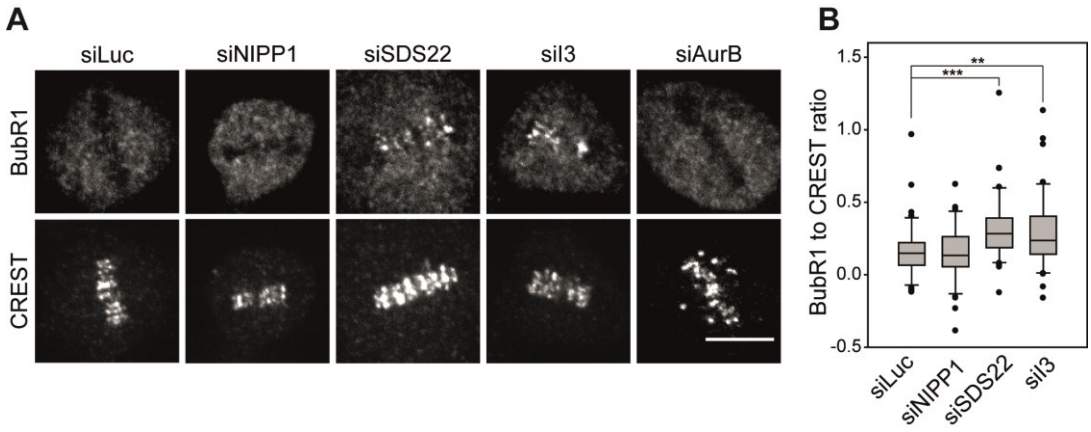

Figure 2.2 siRNA-mediated depletion of SDS22 or I3 causes increased recruitment of the spindle assembly checkpoint protein BubR1 to metaphase kinetochores. A HeLa cells were treated with the indicated siRNAs for 48 h, formaldehyde-fixed and stained with BubR1 and CREST antibodies. Representative spinning disc confocal images are shown. Note for comparison the absence of BubR1 signal in AurB-depleted cells in spite of severe chromosomal misalignment. Scale bar, 10 µm. **B** The ratio of BubR1 versus CREST signal intensity on kinetochores of aligned metaphase plates was quantified using the software CellProfiler. Box plots show median, lower and upper quartiles (line and box), 10th and 90th percentiles (whiskers) and outliers (●). P-values were calculated using Mann-Whitney *U* test (**, $p \leq 0.01$; ***, $p \leq 0.001$). Data from three independent experiments with a total of 42 cells per condition. AurB-depleted cells were not quantified due to absence of metaphase plates.

2.1.3 I3 depletion enhances association of SDS22 with KNL1-bound PP1

The results presented here so far as well as the initial results from our study (Eiteneuer et al., 2014) suggest that both SDS22 and I3 act as positive regulators of PP1 activity towards Aurora B pT232 and therefore as antagonists of Aurora B function during bipolar chromosomal attachment. Therefore, we set out to find the mechanisms how SDS22 and I3 regulate PP1 activity at the kinetochore. We first asked whether SDS22 and / or I3 might be required for PP1 localization to kinetochores. To that end, A. Eiteneuer performed depletion experiments in HeLa cells stably expressing GFP-PP1γ at near endogenous levels (kindly provided by L. Trinkle-Mulcahy; Trinkle-Mulcahy et al., 2003). Unlike reported before (Posch et al., 2010), depletions of either SDS22 or I3 did not affect the localization of PP1γ at metaphase kinetochores, indicating that SDS22 and I3 do not regulate PP1 amounts at the kinetochore (Eiteneuer et al., 2014). We next asked, whether SDS22 and / or I3 localize to the kinetochores themselves and therefore might directly affect PP1 activity at the kinetochores. To that end, A. Eiteneuer generated HeLa cells stably

overexpressing GFP-I3 and made use of a HeLa cell line that stably expresses SDS22-GFP from a bacterial artificial chromosome (BAC) under control of its endogenous promotor (kindly provided by A. Hyman) (Poser et al., 2008). Expression levels of SDS22-GFP and endogenous SDS22 in those cells corresponded to the endogenous expression level in untransfected HeLa cells. In localization studies at a confocal microscope performed by A. Eiteneuer GFP-I3 was not detectable at kinetochores and largely absent from mitotic chromatin. Furthermore, unlike previously reported (Posch et al., 2010), also SDS22-GFP was not detectable at kinetochores, suggesting that SDS22 does not localize to kinetochores when expressed at near endogenous levels (Eiteneuer et al., 2014). Since I3 can form a ternary complex with PP1 and SDS22 (Pedelini et al., 2007; Lesage et al., 2007) we next asked whether I3 might regulate the mitotic localization of SDS22. RNAi experiments were performed in the HeLa SDS22-GFP cells by A. Eiteneuer. Strikingly, SDS22-GFP became enriched at kinetochores upon depletion of I3 but not after control or NIPP1 depletions, showing that SDS22 can localize to kinetochores under certain circumstances and indicating that I3 prevents quantitative localization of SDS22 to the kinetochore (Eiteneuer et al., 2014).

The outer kinetochore protein KNL1 has been suggested as the major binding partner of PP1 at the kinetochore (Liu et al., 2010; Rosenberg et al., 2011). Consistently, RNAi experiments showed a loss of PP1 from kinetochores upon depletion of KNL1 (Liu et al., 2010; Eiteneuer et al., 2014). Like I3, KNL1 binds to PP1 via its RVxF motif. We therefore next asked whether SDS22 recruitment to kinetochores upon I3 depletion was mediated through binding to KNL1-bound PP1. Indeed, co-depletion of KNL1 alongside I3 depletion abolished the kinetochore localization of SDS22 (Eiteneuer et al., 2014). To verify this finding, we made use of stable cell lines expressing GFP-fusions of KNL1. HeLa cells stably expressing full length KNL1 with a C-terminal LAP-tag (Localization and Affinity Purification tag, containing GFP and an S-peptide) from a BAC under control of its endogenous promotor were a kind gift from A. Hyman. HeLa Flp-In cells inducibly expressing amino acids 1-250 of KNL1, that contain the RVxF PP1-binding motif, fused to an N-terminal GFP-tag were kindly provided by A. Musacchio (Krenn et al., 2013). We first examined the cells by spinning disc confocal microscopy. Before imaging, cells were fixed with formaldehyde and stained with DAPI. Expression of GFP-KNL1 (1-250)

was induced by addition of doxycycline 24 h prior to fixation. Full length KNL1-LAP was found to be absent from nuclei in interphase cells and appeared to accumulate in the ER / Golgi apparatus. In mitotic cells from prophase to anaphase full length KNL1-LAP showed a clear localization to kinetochores (Figure 2.3 A). GFP-KNL1 (1-250) was shown to be soluble, as it was distributed throughout the nuclei and cytoplasm in interphase cells. In mitotic cells GFP-KNL1 (1-250) was mainly cytoplasmic. Surprisingly, however, targeting to kinetochores of the truncated KNL1 was not completely abolished, as evidenced by sporadic green punctae on mitotic chromatin, even though it lacks the C-terminal region required for interaction with the Mis12 complex (Krenn et al., 2013) (Figure 2.3 B).

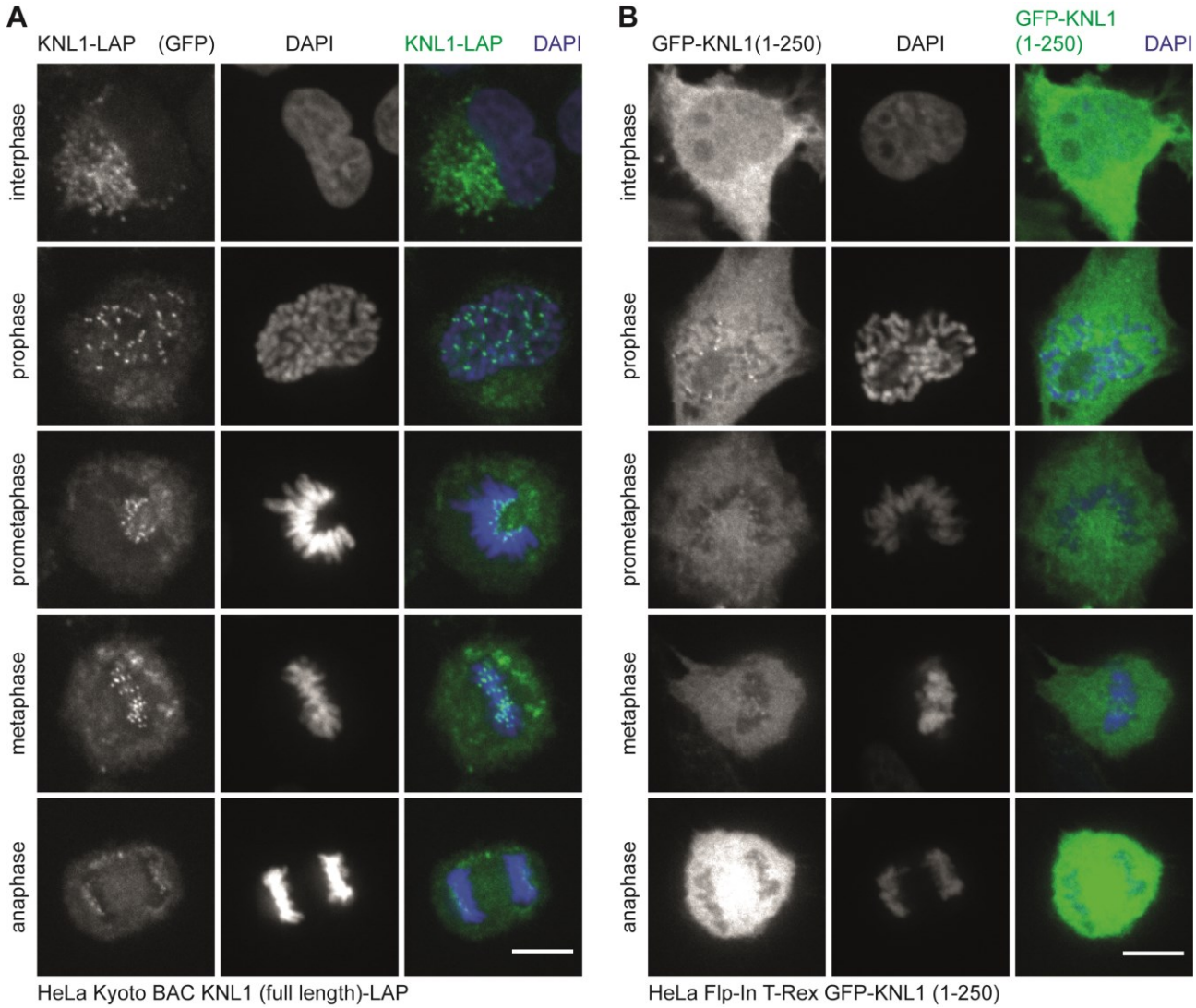

Figure 2.3 Localization of GFP-fusions of KNL1 in stably expressing HeLa cells. A HeLa cells stably expressing KNL1 (full length)-LAP (Localization and Affinity Purification tag, containing GFP and an S-peptide) from a BAC were formaldehyde-fixed and stained with DAPI, before imaging at a spinning disc confocal microscope. Representative images of cells in interphase and in mitosis are shown. Scale bar, 10 µm. **B** Expression of GFP-KNL1 (1-250) was induced in HeLa Flp-In T-Rex cells by addition of doxycycline for 24 h. Cells were fixed with formaldehyde and stained with DAPI, before imaging at a spinning disc confocal microscope. Representative images of cells in interphase and in mitosis are shown. Scale bar, 10 µm.

Next we wanted to confirm by co-immunoprecipitation whether depletion of I3 increases association of SDS22 with KNL1. We decided to use the soluble, truncated form of KNL1 for these experiments, since it could be isolated more efficiently and in larger amounts than the full length KNL1-LAP. HeLa Flp-In GFP-KNL1 (1-250) cells were treated with siRNA targeting I3 for 48 h. siLuc and an siRNA targeting NIPP1 that also binds PP1 via an RVxF motif, served as controls. Expression of GFP-KNL1

(1-250) was induced for 24 h prior cell lysis. Control cells inducibly expressing GFP alone were used to test whether co-immunoprecipitates were specific. GFP-KNL1 (1-250) or GFP were immunoprecipitated using beads coupled to GFP nanobodies. IP samples together with 2.5 % inputs were analyzed by Western blotting. As expected, PP1γ specifically co-immunoprecipitated with GFP-KNL1 (1-250), but not with GFP alone. PP1γ association with KNL1 was not affected by either I3 or NIPP1 depletion, as comparable amounts of PP1γ were co-isolated in all conditions. Co-immunoprecipitation of SDS22 with KNL1 was also detected in luciferase control depleted samples, suggesting that SDS22 binds to KNL1-bound PP1, however at low levels. Strikingly, the amount of associated SDS22 was markedly increased upon I3 depletion but not in NIPP1 depleted samples, corroborating the finding that I3 limits the association of SDS22 with KNL1-bound PP1 (Figure 2.4 A and B).

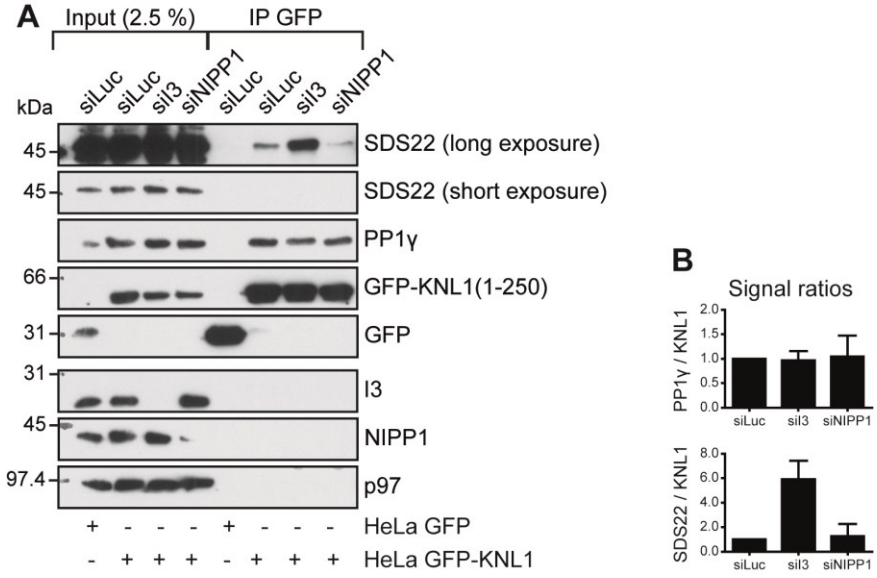

Figure 2.4 siRNA-mediated I3 depletion stimulates SDS22 association with KNL1-bound PP1. A HeLa Flp-In T-Rex cells inducibly expressing GFP or GFP-KNL1 (1-250) were treated with the indicated siRNAs for 48 h. Transgene expression was induced by addition of doxycycline for 24 h prior lysis. GFP or GFP-KNL1 (1-250) was affinity-isolated from cell extracts using anti-GFP nanobodies coupled to sepharose beads. Input samples (2.5 %) and precipitates were analyzed by Western blotting with the indicated antibodies. **B** Quantification of Western blot signals normalized to siLuc. Error Bars represent s.d. with $n = 3$. Note the increase of SDS22 association with GFP-KNL1 (1-250) specifically upon I3 depletion, while PP1γ binding to KNL1 is unaffected.

2.1.4 SDS22 inhibits PP1-mediated dephosphorylation of Aurora B *in vitro*

Using siRNA-mediated depletion, we found I3 silencing to cause a recruitment of SDS22 to KNL1-bound PP1 at the kinetochore. This effect coincided with an inhibition of PP1 activity at the kinetochore, as evidenced by an increased activating phosphorylation of Aurora B kinase at T232 (Eiteneuer et al., 2014). Furthermore, transient overexpression of SDS22 also resulted in an accumulation of SDS22 at kinetochores, accompanied by an increased Aurora B phosphorylation at T232 (Eiteneuer et al., 2014). Together, these findings suggest that SDS22, while being required for full PP1 activity at the kinetochore, acts inhibitory when quantitatively bound to kinetochore-associated PP1. We therefore set out to confirm *in vitro* whether (a) PP1 directly dephosphorylates Aurora B pT232 and whether (b) PP1 activity towards Aurora B is inhibited by SDS22 binding. Recombinant GST-tagged Aurora B in complex with the activating IN-box segment of inner centromere protein (INCENP) was purified from *E. coli* (kindly provided by A. Musacchio, MPI Dortmund). In this complex, Aurora B is autophosphorylated at T232 (Santaguida et al., 2010). As a control, recombinant GST-tagged Survivin was purified from *E. coli*, phosphorylated at T34 by recombinant Cdk1/Cyclin B (kindly provided by Y. Wang, University of Michigan) *in vitro*, and re-purified. Recombinant, purified PP1 is commercially available (New England Biolabs, NEB). Both Aurora B and Survivin were incubated either alone or with increasing concentrations of PP1 for 15 min at 30 °C. The unspecific lambda phosphatase (λPP) (NEB) served as a positive control. Phosphorylation of Aurora B at T232 and Survivin at T34 was monitored by Western blotting with phospho-specific antibodies. We found Aurora B to be dephosphorylated by PP1 in a concentration dependent manner whereas phosphorylation of Survivin was largely unaffected by the same PP1 concentrations. Lambda phosphatase dephosphorylated both Aurora B and Survivin. This shows that PP1 directly and specifically dephosphorylates Aurora B at T232 (Figure 2.5 A). We then went on to test if SDS22 inhibits dephosphorylation of Aurora B T232 by PP1. Recombinant His-tagged SDS22 was purified from *Trichoplusia ni* Tnao38 cells. Aurora B was incubated with PP1 over a time course of 30 min in the presence or absence of SDS22. At 0-, 5-, 10-, 20-, and 30-min time points, samples were taken and analyzed by Western blotting with phospho-specific antibodies. Upon addition of SDS22, the reduction of Aurora B pT232 signal was slowed down and at the 30-min endpoint

there was more residual phosphorylation left than in the absence of SDS22, indicating that SDS22-binding to PP1 indeed inhibits Aurora B dephosphorylation (Figure 2.5 B). To further characterize this inhibition, we incubated Aurora B with PP1 either alone or with increasing SDS22 concentrations for 15 min at 30 °C. Again, phosphorylation levels of Aurora B were monitored by Western blotting, showing that SDS22 inhibits Aurora B dephosphorylation in a dose-dependent manner (Figure 2.5 C). Experiments equivalent to Figure 3.5 C were done by M. Beullens (KU Leuven), using PP1 purified from rabbit skeletal muscle. Since this PP1 was less active than recombinant PP1 from NEB, a higher concentration (40 nM) was used in these experiments. Western blot signals from 3 independent experiments were quantified and normalized to maximum and minimum values. The quantification (Figure 2.5 D) shows the dose-dependent inhibition of Aurora B dephosphorylation by SDS22 with a half-maximal inhibition at a molar ratio of about 1:2 (PP1:SDS22) at the given conditions and concentrations. Consistent with our findings in cells, these data provide evidence that binding of SDS22 to PP1 inhibits its activity towards Aurora B rather than stimulating it.

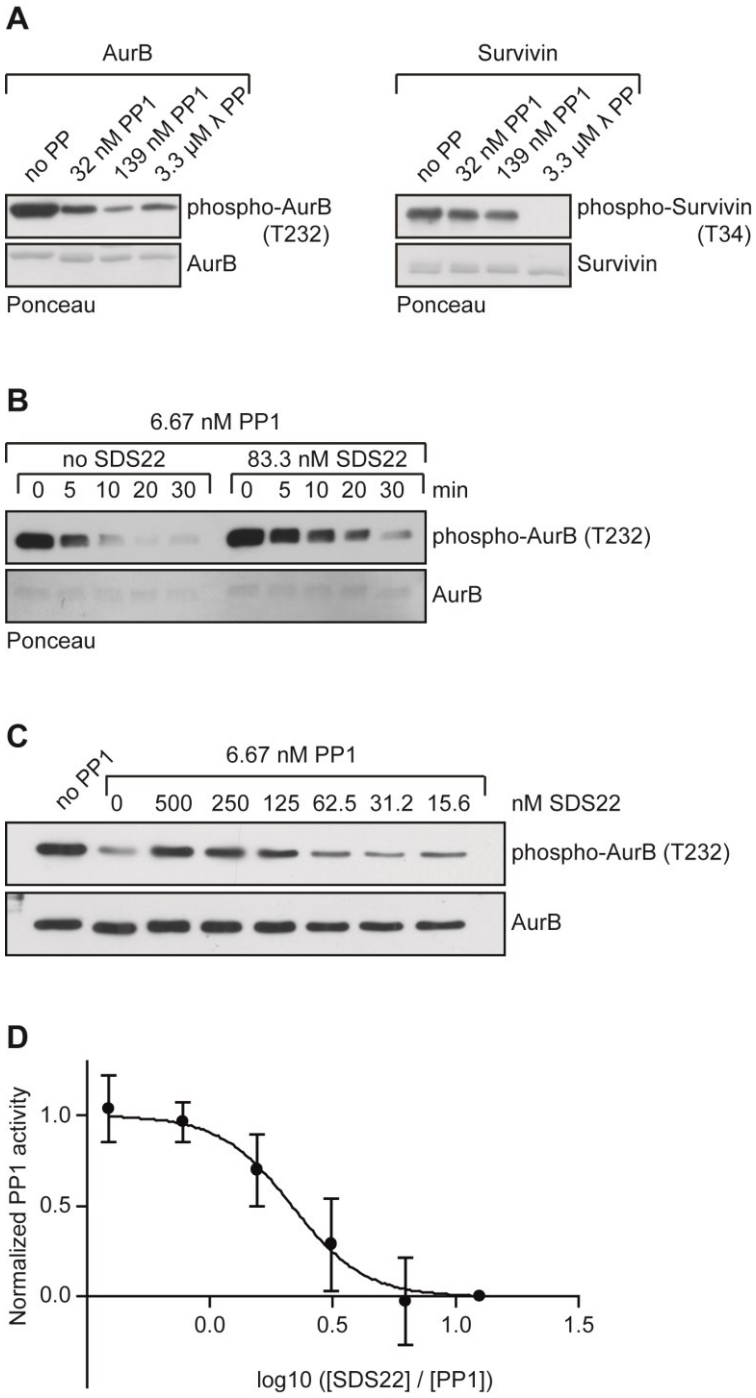

Figure 2.5 Binding of SDS22 to PP1 inhibits dephosphorylation of Aurora B in vitro. A PP1 specifically dephosphorylates Aurora B pT232. Recombinant, autophosphorylated GST-AurB (left panel) or *in vitro* phosphorylated GST-Survivin (right panel) was incubated either alone or with purified PP1 (NEB) at indicated concentrations at 30 ˚C for 15 min. Lambda phosphatase (λPP) (NEB) was used as a positive control. Phosphorylation of AurB at T232 and Survivin at T34 was detected by Western blotting with phospho-specific antibodies and equal loading was confirmed by Ponceau S staining. Note PP1 mediated dephosphorylation of AurB, but not of Survivin. **B** SDS22 inhibits PP1-mediated dephosphorylation of Aurora B at T232. Phosphorylated GST-AurB was incubated with purified PP1 (NEB) with or without recombinant SDS22, purified from *Trichoplusia ni* Tnao38 cells, at indicated concentrations at 30 ˚C for the indicated time spans. Phosphorylation and equal loading were monitored as

in (**A**). **C** SDS22 inhibits PP1-mediated dephosphorylation of Aurora B pT232 in a dose-dependent manner. Phosphorylated GST-AurB was incubated with purified PP1 (NEB) without or with the indicated concentration of purified SDS22 at 30 ˚C for 15 min and phosphorylation monitored as in (**A**). Equal loading was monitored with panAurB antibodies. **D** Experiments equivalent to (**C**) were done by M. Beullens (KU Leuven). 40 nM PP1 purified from rabbit skeletal muscle and SDS22 concentrations as in (**C**) were used. Quantification of Western blot signals from three independent experiments normalized to maximum and minimum values. Error bars represent s.e.m.

2.1.5 Reduction of SDS22 expression partially reverses the increased Aurora B activity on metaphase chromatin caused by I3 depletion

Since we found I3 depletion to cause increased binding of SDS22 to KNL-bound PP1 at the kinetochore accompanied by increased Aurora B phosphorylation and that SDS22 inhibits PP1- mediated dephosphorylation of Aurora B *in vitro*, we reasoned that reduction of SDS22 expression might rescue the effect of I3 depletion on Aurora B activity. To test this assumption, HeLa cells treated with siRNA targeting I3 or luciferase as control for a full period of 48 h were additionally treated with SDS22 or luciferase siRNA for 24 h prior to fixation. Cells were fixed with formaldehyde and stained with antibodies specific for Aurora B pT232 or pan-Aurora B and with DAPI to visualize chromatin and analyzed at a spinning disc confocal microscope. The signal intensity of Aurora B pT232 and pan-Aurora B on metaphase chromatin was monitored. Signal intensities on chromatin were quantified using CellProfiler software (Carpenter et al., 2006) by creating a threshold-based mask with the DAPI signal to exclude cytoplasmic and centrosomal staining. The mean intensities within these DAPI masks were measured and the ratio between phosphorylated Aurora B and whole Aurora B protein signal was calculated for 60 cells per condition combined from 3 independent experiments. Consistent with former experiments, we observed an increase in Aurora B phosphorylation in cells depleted for I3 followed by siLuc control depletion compared to cells treated twice with siLuc. Importantly, this effect was partially, but significantly, reversed in cells depleted for I3 followed by treatment with SDS22 siRNA (Figure 2.6 A and B).

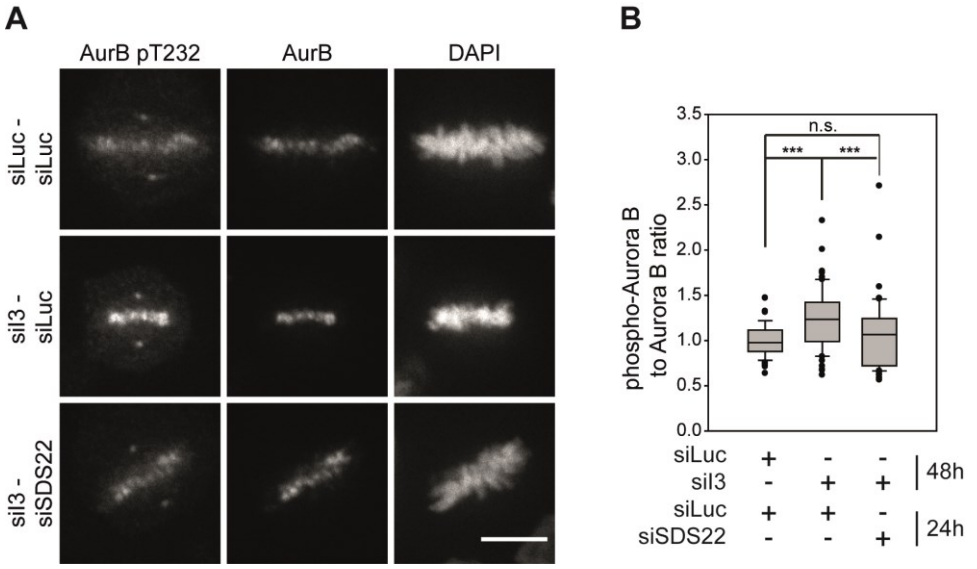

Figure 2.6 Reduction of SDS22 expression partially rescues the effect of I3 depletion on Aurora B activity. A Increased Aurora B autophosphorylation at T232 upon I3 depletion is partially reversed by attenuation of SDS22 expression. HeLa cells were treated with the first siRNA (siLuc or siI3) for 48 h and a second (siLuc or siSDS22) for 24 h before fixation as indicated. Cells were fixed with formaldehyde and stained with panAurB and AurB pT232 antibodies and DAPI. Representative spinning disc confocal images are shown. Note the unspecific centrosomal staining with the AurB pT232 antibodies. Scale bar,10 µm. **B** The ratio of AurB pT232 versus total AurB signal intensity on metaphase chromatin as in (**A**) was quantified using the software CellProfiler. Box plots show median, lower and upper quartiles (line and box), 10^{th} and 90^{th} percentiles (whiskers) and outliers (●).P-values were calculated using Mann-Whitney *U* test (***, $p \leq 0.001$). Data from three independent experiments with a total of 60 cells per condition.

Taken together, the data presented so far show that both SDS22 and I3 are required for full PP1 activity at the kinetochore towards Aurora B pT232 and suggest that SDS22 could be required for a PP1 activation step prior to PP1 association to KNL1 at kinetochores, but that it is inhibitory when bound to kinetochore-associated PP1. They furthermore suggest that the function of I3 in this process is to keep SDS22-PP1 in solution to prevent binding of SDS22-associated PP1 to KNL1 at the kinetochore.

2.2 Part II: Characterization and regulation of the ternary SDS22-PP1-I3 complex

The data presented in the first part of this thesis show that both SDS22 and I3 are required for PP1 function at kinetochores. They are consistent with a model in which SDS22 is required for a PP1 activation step in solution preceding PP1 association to the kinetochore. Since SDS22 keeps PP1 inactive while bound, it has to dissociate prior to the transfer of PP1 to KNL1 at the kinetochore. Our findings furthermore suggest that the function of I3 in this process is to keep SDS22-PP1 in solution to prevent binding of SDS22-associated PP1 to KNL1 at the kinetochore. Additionally, we speculate that I3 might further regulate the SDS22-mediated activation of PP1, possibly by facilitating SDS22 dissociation from PP1. Consistent with this model, it was shown that I3 can form a heterotrimeric complex with PP1 and SDS22 (Pedelini et al., 2007; Lesage et al., 2007). This complex is conserved throughout evolution of eukaryotes (Ceulemans et al., 2002) and was shown to be catalytically inactive within the cell (Lesage et al., 2007), however, further functions of the complex are not known. In the following part we set out to further examine our model and to elucidate the role of I3 in regulating SDS22-PP1 association by further characterizing the interaction between PP1, SDS22 and I3.

2.2.1 SDS22 and I3 are detected both complex-associated and as monomers in gel filtration fractionation of cell lysates

In the study first describing the SDS22-PP1-I3 complex in mammalian cells, gel filtration fractionation of HeLa cell extracts showed comigration of the components of the complex (Lesage et al., 2007). We first wanted to reproduce this finding. HeLa cell extracts were loaded onto a FPLC Superdex 200 10/300 GL gel filtration column to separate the contained proteins and protein complexes according to size. 250 µl fractions were collected. Aliquots of the input extract and the collected fractions were analyzed by Western blotting with SDS22, I3 and PP1γ antibodies. In accordance with the experiment published by Lesage et al., we observed comigration of SDS22, I3 and PP1γ. Importantly, in addition, we found both SDS22 and I3 eluting in two distinct peaks, corresponding to the size of the SDS22-PP1-I3 complex or the monomeric forms, respectively. PP1γ eluted in a broader peak, which was expected,

since it forms a number of different holoenzymes with a variety of different PiPs. For both SDS22 and I3, Western blot signals of the low molecular weight peak were stronger than the complex-associated high molecular weight peak, indicating that large fractions of both PiPs exist as a free pool within the cell (Figure 2.7). Also, this finding established gel filtration fractionation as a suitable experimental approach to further examine the association of SDS22 and I3 with PP1 under different conditions.

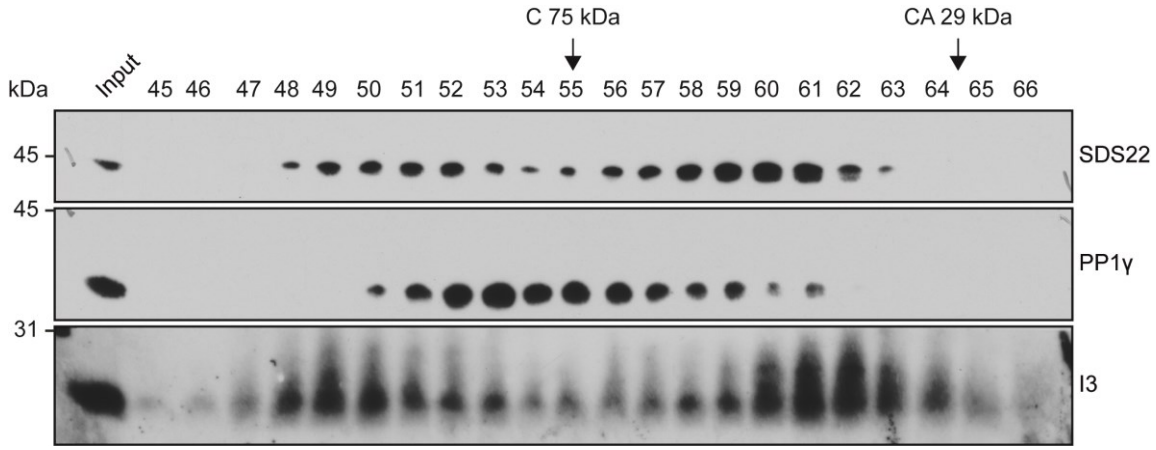

Figure 2.7 Detection of complex-bound and monomeric SDS22 and I3 in gel filtration fractionation. HeLa cell extracts were loaded onto a FPLC Superdex 200 10/300 GL gel filtration column. Aliquots of the input extract and the collected fractions were analyzed by Western blotting with the indicated antibodies. Arrows indicate elution volumes of calibration standard proteins (C, Conalbumin, 75 kDa; CA, Carbonic anhydrase, 29 kDa). Note that both SDS22 and I3 elute in a high and a low molecular weight peak corresponding to the size of the SDS22-PP1-I3 complex or the monomeric forms, respectively.

2.2.2 I3 depletion causes SDS22 to shift towards complex-associated high molecular weight fractions in gel filtration fractionation

We next asked how cellular depletion of I3 would affect association of SDS22 to PP1. To that end, cell extracts of HeLa cells treated with two different siRNAs targeting I3 for 48 h were prepared. Luciferase and NIPP1 depleted cells served as controls. First, depletion efficiencies were verified by Western blotting (Figure 2.8 A). Next, the cell extracts were subjected to gel filtration fractionation on a Superdex 200 10/300 GL column and aliquots of the input extract and the collected fractions analyzed by Western blotting with SDS22, I3 and PP1γ antibodies. For the luciferase and NIPP1 depleted controls, we again observed an elution of both SDS22 and I3 in two peaks with the monomeric low molecular weight forms being more prominent than the high

molecular weight, complex-associated fractions. In the I3 depleted samples, low amounts of residual I3 were found entirely in the high molecular weight fractions. Importantly, upon I3 depletion we observed a shift of SDS22 towards the high molecular weight peak, indicating that I3 depletion increases association of SDS22 to PP1. Also, the high molecular weight SDS22 peak was shifted slightly towards later elution volumes, which can be explained by the absence of I3 from the SDS22-PP1 complex (Figure 2.8 B). For one representative experiment as in Figure 3.8 B, SDS22 Western blot signals were detected with a Typhoon FLA 9000 imager using fluorescence labelled secondary antibodies and quantified, confirming the observed distribution between complex-associated and monomeric SDS22 in control conditions, as well as the shift towards complex-associated fractions upon I3 silencing (Figure 3.8 C). This finding suggests that I3 may be required for a dissociation of SDS22 from PP1.

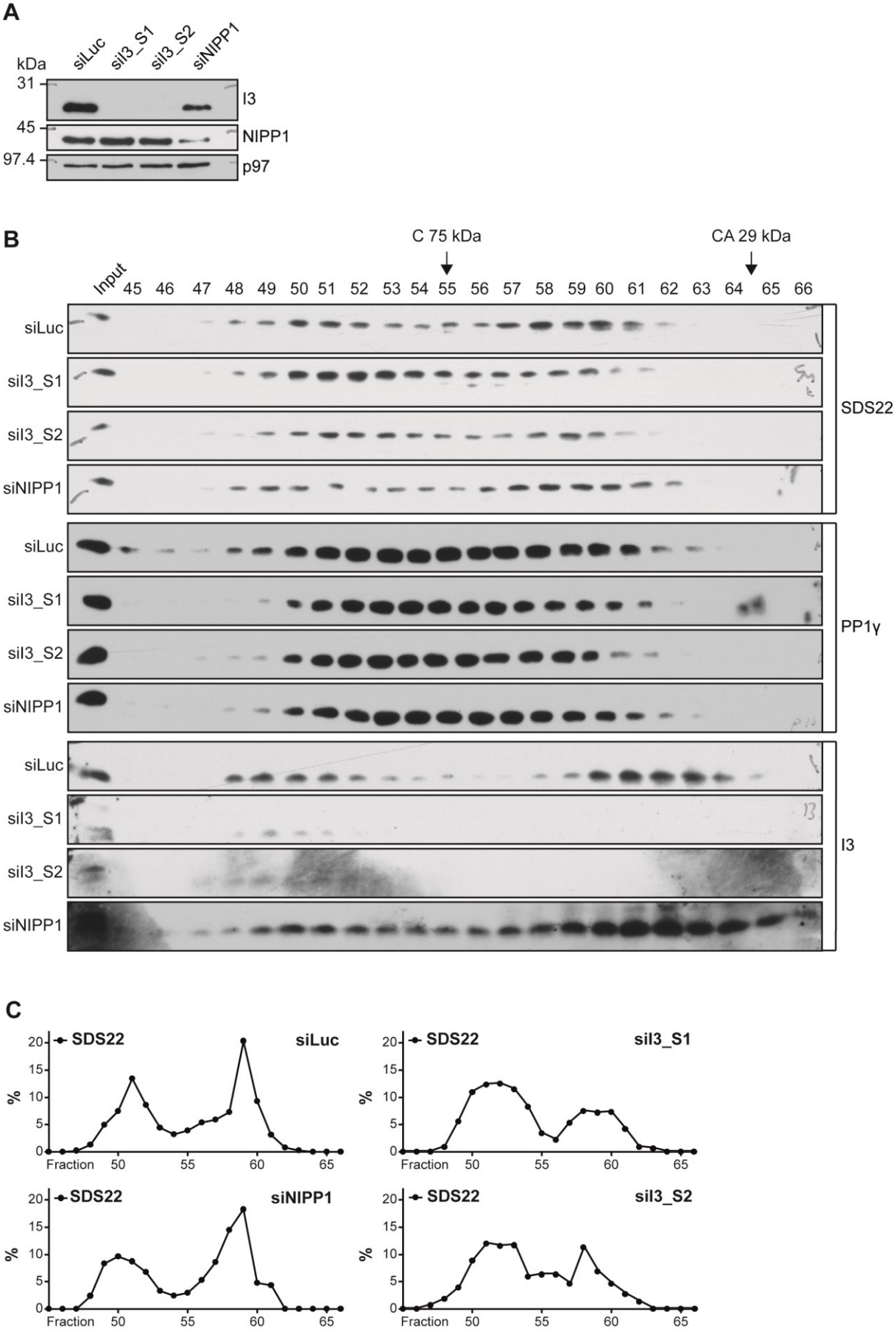
A
kDa
siLuc
sil3_S1
sil3_S2
siNIPP1
31
45
97.4
I3
NIPP1
p97
B
C 75 kDa
CA 29 kDa
Input
45 46 47 48 49 50 51 52 53 54 55 56 57 58 59 60 61 62 63 64 65 66
siLuc
sil3_S1
sil3_S2
siNIPP1
SDS22
PP1γ
I3
C
SDS22
siLuc
sil3_S1
siNIPP1
sil3_S2
%
Fraction
50
55
60
65

Figure 2.8 siRNA-mediated I3 depletion causes SDS22 to shift towards complex-bound high molecular weight fractions in gel filtration fractionation. A HeLa cells were treated with the indicated siRNAs for 48 h, then cell extracts were prepared and analyzed by Western blotting with the indicated antibodies. p97 served as a loading control. **B** Cell extracts as in (**A**) were loaded onto a FPLC Superdex 200 10/300 GL gel filtration column. Aliquots of the input extracts and the collected fractions were analyzed by Western blotting with the indicated antibodies. Arrows indicate elution volumes of calibration standard proteins (C, Conalbumin, 75 kDa; CA, Carbonic anhydrase, 29 kDa). Note that a large fraction of SDS22 is monomeric in control extracts, but mostly complex-bound upon depletion of I3. **C** Quantification of Western blot signals for SDS22. For one representative experiment as in (**B**), SDS22 signals were detected with a Typhoon FLA 9000 imager using fluorescence labelled secondary antibodies. Quantification was done using ImageJ.

2.2.3 High molecular weight SDS22 gel filtration fractions contain SDS22-PP1 complexes

Next, we wanted to verify (a) the assumption that the high molecular weight fractions containing SDS22 and I3 in gel filtration fractionation of HeLa cell extracts comprise the SDS22-PP1-I3 complex and (b) the notion that I3 depletion increases SDS22 binding to PP1. For this purpose we used HeLa cells stably expressing GFP-PP1γ (kindly provided by L. Trinkle-Mulcahy; Trinkle-Mulcahy et al., 2003) to allow for immunoprecipitation of PP1γ from gel filtration peak fractions using anti-GFP nanobodies. Cells were treated with I3 or luciferase siRNAs for 48 h. Expression levels of tagged and endogenous PP1γ and of SDS22 and I3 were monitored by Western blotting. Expression of GFP-PP1γ was at near endogenous level and the depletion of I3 was efficient and did not affect the SDS22 expression level (Figure 2.9 A). Cell extracts were subjected to gel filtration fractionation on a Superdex 200 10/300 GL column and aliquots of the inputs and the collected fractions analyzed by Western blotting with SDS22, I3 and PP1γ antibodies. Again, we observed a shift of SDS22 towards the high molecular weight peak upon I3 depletion. The GFP-PP1γ elution volume peak was about 3 fractions earlier than endogenous PP1γ due to its higher molecular weight. I3 depletion did not affect the elution pattern of both endogenous and GFP-PP1γ (not shown) (Figure 2.9 B). For both the control and the I3 depleted sample, gel filtration fractions containing the high molecular weight peak or the low molecular weight peak of SDS22, respectively, were pooled and subjected to immunoprecipitation using anti-GFP nanobodies coupled to sepharose beads. Precipitates together with 4.5 % inputs were analyzed by Western blotting with SDS22, I3 and PP1γ antibodies. GFP-PP1γ was

immunoprecipitated from both high molecular weight fractions and low molecular weight fractions. Importantly, binding of SDS22 and I3 to GFP-PP1γ could be detected in the high molecular weight fractions but not the low molecular weight fractions of the control depleted sample, showing that the high molecular weight gel filtration peak of SDS22 indeed contains the SDS22-PP1-I3 complex. GFP-PP1γ immunoprecipitates from high molecular weight fractions of the I3 depleted sample contained SDS22 and a small amount of residual I3. The amount of SDS22 bound to GFP-PP1γ immunoprecipitated from I3 depleted high molecular weight fractions was increased compared to the luciferase depleted control, hinting again at an increased association of SDS22 to PP1 in the absence of I3. However, in this experiment, the seemingly increased binding of SDS22 can be at least partially explained by the slightly lower amount of GFP-PP1γ isolated from the siLuc control compared to the I3 depleted sample (Figure 2.9 C).

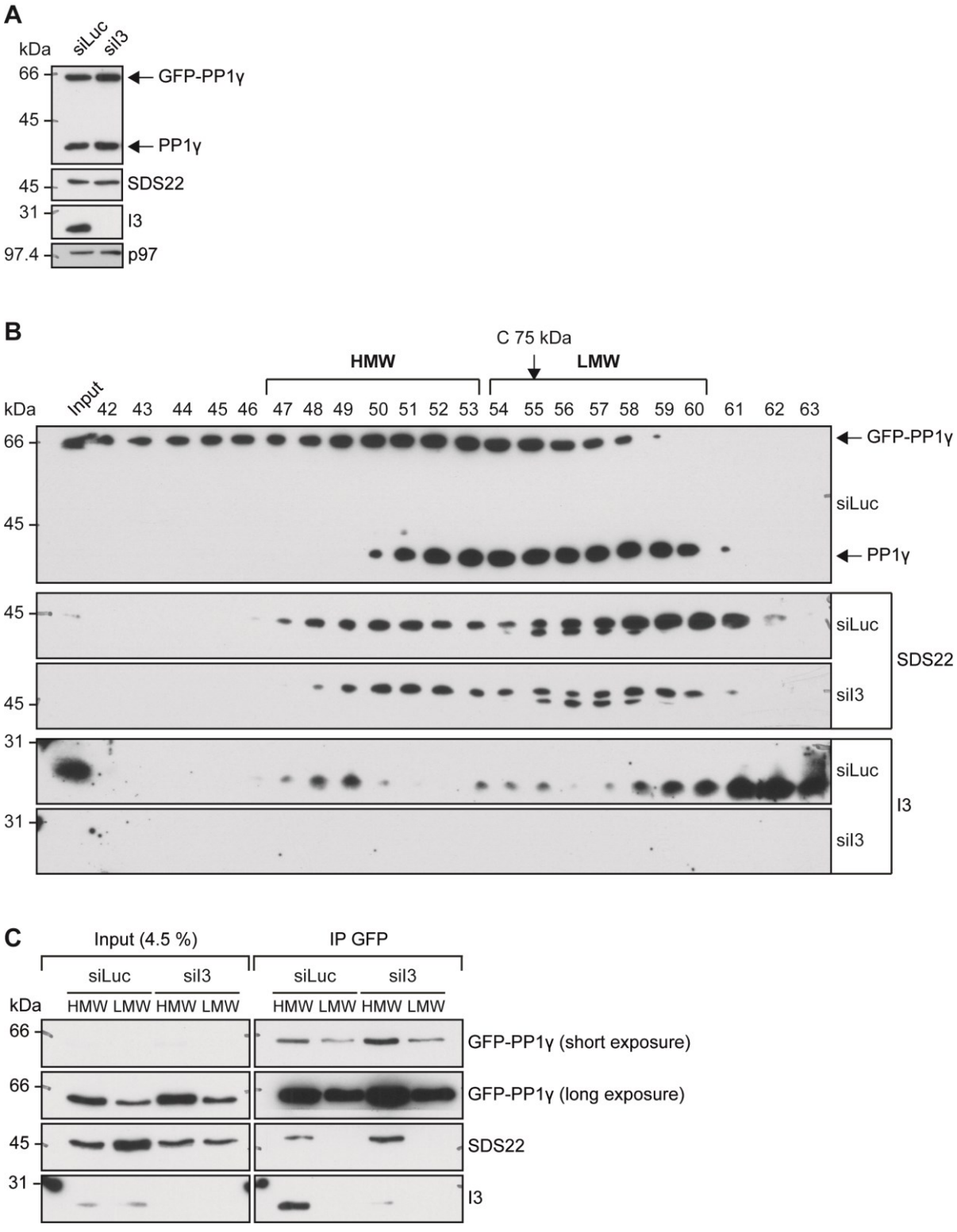

Figure 2.9 SDS22 high molecular weight gel filtration fractions contain SDS22-PP1(-I3) complexes. A HeLa cells, stably expressing GFP-PP1γ, were treated with the indicated siRNAs for 48 h, then cell extracts were prepared and analyzed by Western blotting with the indicated antibodies. p97 served as a loading control. **B** Cell extracts as in (**A**) were loaded onto a FPLC Superdex 200 10/300 GL gel filtration column. Aliquots of the input extracts and the collected fractions were analyzed by Western blotting with the indicated antibodies. Arrows indicate elution volumes of calibration standard proteins (C, Conalbumin, 75 kDa).

C High molecular weight (HMW) and low molecular weight (LMW) fractions indicated in (**B**) were pooled and used for affinity-isolation of GFP-PP1γ using anti-GFP nanobodies coupled to sepharose beads. Input samples (4.5 %) and precipitates were analyzed by Western blotting with the indicated antibodies.

2.2.4 Overexpression of I3 increases formation of the SDS22-PP1-I3 complex

As we found an increased association of SDS22 to PP1 upon I3 depletion in gel filtration fractionation of cell extracts, we next wanted to test whether overexpression of I3 would have the converse effect. A PP1 binding deficient variant of I3 with a mutated RVxF motif (I3 VEW41AEA) was used as a negative control. In a prior experiment we had shown that this mutation is sufficient to completely abolish binding to PP1. To this end, HEK 293 cells were transiently transfected with wild type I3 or I3 VEW41AEA, both with an N-terminal HA tag or with an empty control plasmid carrying a 3*HA-Strep sequence for 24 h, lysed and subjected to immunoprecipitation using HA specific antibodies. Precipitates together with 3 % input and flowthrough (FT) samples were analyzed by Western blotting with I3, SDS22 and PP1γ antibodies. Indeed, both PP1γ and SDS22 bound to wild type I3 but no association of PP1γ or SDS22 above background level was detected with the I3 VEW41AEA mutant (Figure 2.10 A). For gel filtration analysis wild type I3 or I3 VEW41AEA, which were tagged at the N-terminus with GFP or GFP alone were transiently overexpressed in HeLa cells for 48 h. Overexpression of GFP-I3 fusions was verified by Western blotting with I3 specific antibodies (Figure 2.10 B). Next, the cell extracts were subjected to gel filtration fractionation on a Superdex 200 10/300 GL column and aliquots of the input extract and the collected fractions were analyzed by Western blotting with SDS22 and GFP antibodies. GFP eluted at a late elution volume, corresponding to the molecular weight of GFP monomers. Somewhat surprisingly, both GFP-I3 (wild type) and I3 VEW41AEA showed a similar elution pattern with appreciable amounts co-eluting with complex-associated SDS22 in high molecular weight fractions. However, only wild type I3 overexpression but not overexpression of I3 VEW41AEA did affect the elution pattern of SDS22 (see below), indicating that co-elution of the I3 mutant with SDS22 was not due to association of I3 VEW41AEA to SDS22-PP1. For the GFP-transfected sample we again found SDS22 to elute in a high molecular weight peak and a low molecular weight peak, representing the complex-associated or the monomeric form, respectively. This

elution pattern was largely unaffected by the overexpression of PP1 binding deficient GFP-I3 VEW41AEA. Surprisingly, however, overexpression of GFP-I3 (wild type) caused a complete loss of the monomeric SDS22 fractions. The total of SDS22 was shifted towards the complex-associated high molecular weight peak and the peak itself shifted towards an earlier elution volume, due to the higher molecular weight of the ternary SDS22-PP1-I3 complex containing GFP-tagged I3 (Figure 2.10 C). Contrary to our assumption, this finding indicates that overexpression of I3 leads to increased formation of the SDS22-PP1-I3 complex with the total of cellular SDS22 being incorporated in the complex.

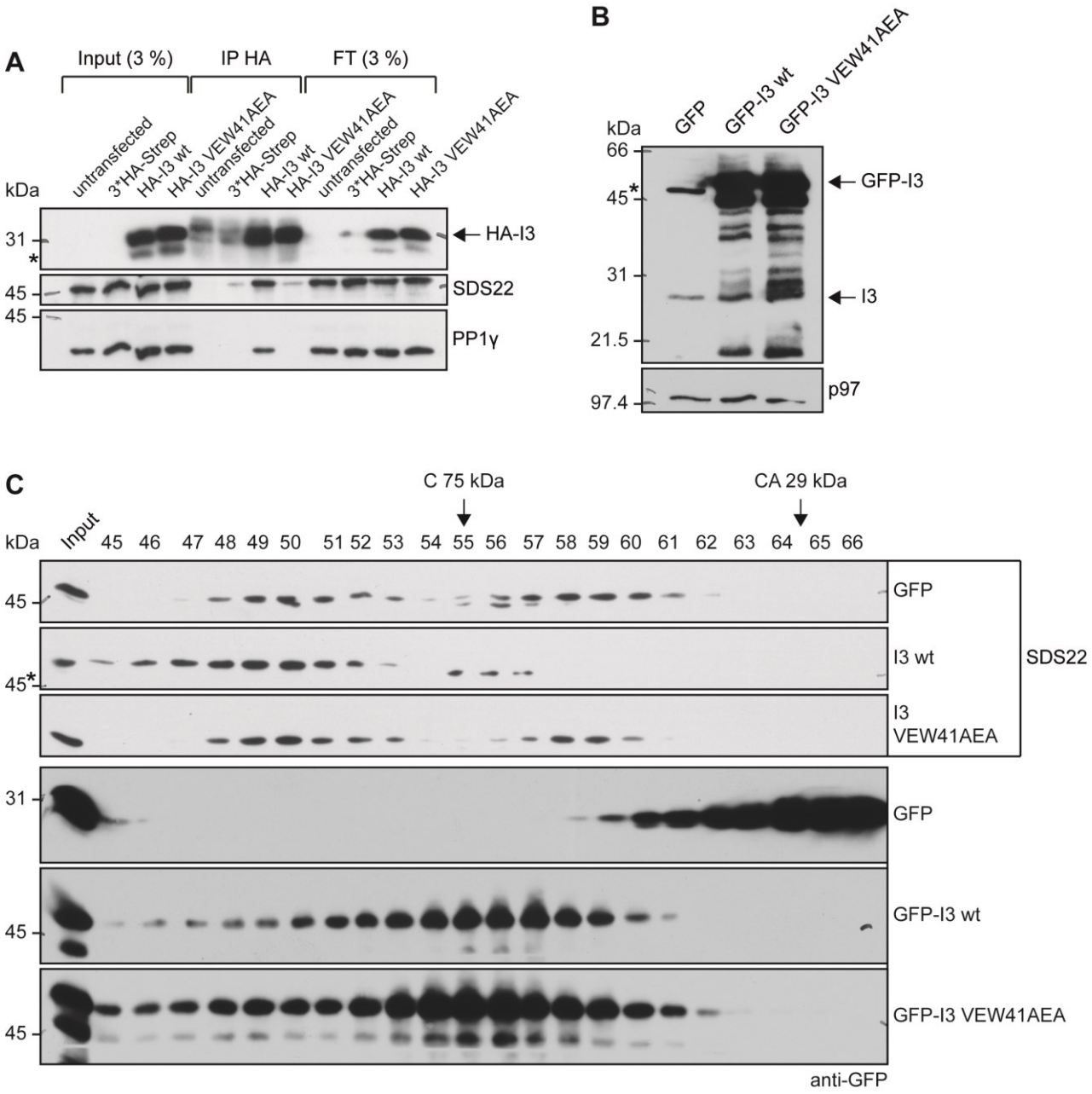

Figure 2.10 Overexpression of I3 increases formation of the ternary SDS22-PP1-I3 complex. A Mutation of the I3 RVxF motif is sufficient to prevent binding of I3 to PP1. HEK 293 cells were transfected with HA-tagged wild type I3 or I3 VEW41AEA for 24 h. Cell extracts were subjected to immunoprecipitation using anti-HA antibodies. Input and flowthrough (FT) samples (2 %) and precipitates were analyzed by Western blotting with the indicated antibodies. Asterisks mark unspecific bands. **B** HeLa cells were transfected with wild type I3 or I3 VEW41AEA tagged with GFP or with GFP alone for 48 h, then cell extracts were prepared and analyzed by Western blotting with the indicated antibodies. p97 served as a loading control. Asterisks mark unspecific bands. **C** Cell extracts as in (**B**) were loaded onto a FPLC Superdex 200 10/300 GL gel filtration column. Aliquots of the input extracts and the collected fractions were analyzed by Western blotting with the indicated antibodies. Arrows indicate elution volumes of calibration standard proteins (C, Conalbumin, 75 kDa; CA, Carbonic anhydrase, 29 kDa). Asterisks mark unspecific bands. Note that a large fraction of

SDS22 is monomeric in control extracts, but completely complex-bound upon overexpression of wild type I3.

2.2.5 *In vitro* reconstitution of the SDS22-PP1-I3 complex

We next wanted to reconstitute the SDS22-PP1-I3 complex *in vitro* with recombinant proteins. Since we found both I3 depletion and I3 overexpression to cause an increased association of SDS22 to PP1 in gel filtration fractionation of cell extracts, we hoped that the recombinant proteins would provide a means to clarify whether I3 has a destabilizing or stabilizing effect on SDS22-PP1 association. Furthermore, they will be valuable tools for future studies of the ternary complex and its interaction with the p97 system (see chapter 2.3). The components of the complex were expressed in insect cells using the baculovirus system. Purified PP1-SDS22 heterodimer coexpressed from a bicistronic baculovirus vector in *Trichoplusia ni* Tnao38 cells was kindly provided by A. Musacchio (MPI Dortmund). His-SDS22 was espressed in *Trichoplusia ni* Tnao38 cells and His-I3 (wild type) and His-I3 VEW41AEA were expressed in *Spodoptera frugiperda* Sf9 cells and purified by affinity chromatography using Ni^{2+} sepharose columns followed by preparative gel filtration. Figure 2.11 A shows Coomassie gels of the purified proteins. As a first application, we wanted to test if purified His-I3 would bind to the purified PP1-SDS22 heterodimer and whether interaction with His-I3 would destabilize the SDS22-PP1 association. To this end, PP1-SDS22 heterodimer was incubated either alone or with a ~7-fold excess of His-I3 (wild type or VEW41AEA) for 30 min on ice and then loaded onto a Superdex 200 Increase 5/150 GL gel filtration column. Aliquots of the input and the collected fractions were analyzed by Western blotting with antibodies specific for SDS22, PP1γ and I3. After incubation and fractionation of PP1-SDS22 alone both SDS22 and PP1 were detected in one elution volume peak that corresponded to the molecular weight of the heterodimer, indicating that binding between PP1 and SDS22 is quite stable. This elution pattern was largely unaffected by the addition of either wild type I3 or I3 VEW41AEA, suggesting that binding of I3 alone is not sufficient to destabilize the interaction between PP1 and SDS22. Importantly, wild type I3 but not I3 VEW41AEA was bound to PP1-SDS22 as a large fraction of wild type I3 co-eluted with PP1 and SDS22. The elution pattern of wild type I3 showed two distinct peaks, comprising the fractions bound to PP1-SDS22 and the monomeric fractions, respectively. I3

VEW41AEA entirely eluted in one monomeric peak, confirming again that the mutation of the RVxF motif completely abolished binding to PP1 (Figure 2.11 B).

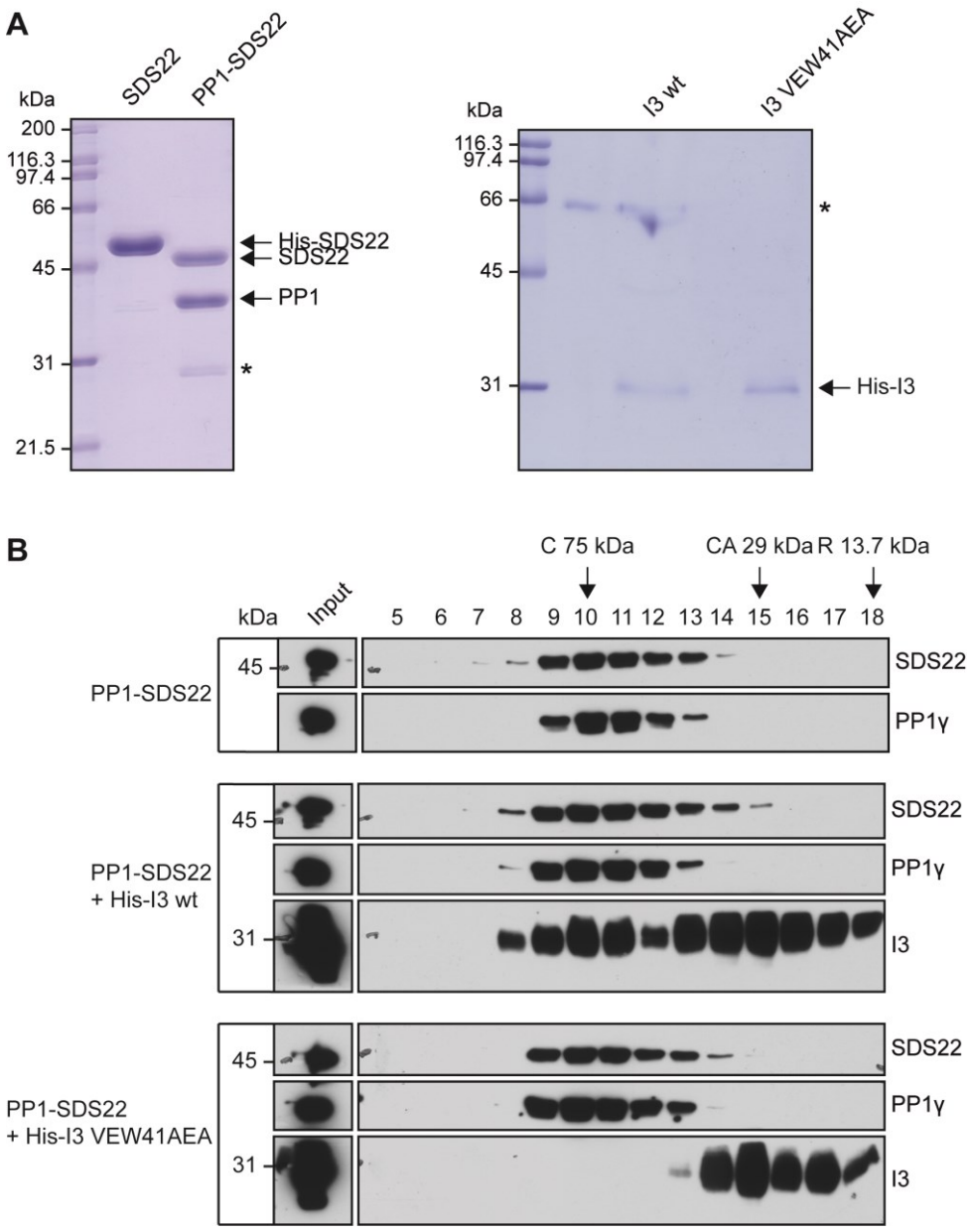

Figure 2.11 *In vitro* reconstitution of the ternary SDS22-PP1-I3 complex. A Recombinant SDS22 and PP1-SDS22 (kindly provided by A. Musacchio, MPI Dortmund) expressed in *Trichoplusia ni* Tnao38 cells and I3 (wild type and VEW41AEA) expressed in *Spodoptera frugiperda* Sf9 cells were purified by affinity chromatography using Ni^{2+} sepharose columns followed by preparative gel filtration. Aliquots of the purified proteins were subjected to SDS-PAGE and coomassie staining. Asterisks mark unspecific bands (in the PP1-SDS22 lane presumably *Trichoplusia ni* I3). **B** PP1-SDS22 was incubated for 30 min on ice either alone or with a ~ 7-fold excess of I3 (wild type or VEW41AEA) and loaded onto a FPLC Superdex 200 Increase 5/150 GL gel filtration column. Aliquots of the input samples and the collected fractions were analyzed by Western blotting with the indicated antibodies. Arrows indicate

elution volumes of calibration standard proteins (C, Conalbumin, 75 kDa; CA, Carbonic anhydrase, 29 kDa; R, Ribonuclease A, 13.7 kDa).

Together, the results in part II revealed that large fractions of SDS22 and I3 exist in the cell in a free form. Overexpression of I3 led to increased formation of the ternary SDS22-PP1-I3 complex, however, also cellular depletion of I3 resulted in an increased association of SDS22 to PP1, indicating that I3 might be involved in dissociating SDS22 from PP1.

2.3 Part III: Interaction of p97 and its SEP domain cofactors p37, p47 and UBXD4 with the SDS22-PP1-I3 complex

In a mass spectrometry shotgun approach performed in our research group (Ritz et al., 2011), PP1γ, SDS22 and I3 were identified as interactors of p97 in human cells. In budding yeast, Cdc48/p97 together with its cofactor Shp1 was shown to positively regulate Glc7/PP1, thereby balancing Ipl1/Aurora kinase activity (Zhang et al., 1995; Cheng & Chen, 2010; Böhm & Buchberger, 2013; Cheng & Chen, 2015). Shp1 was also shown to physically interact with Glc7/PP1, Sds22 and Ypi1/I3 in immunoprecipitation experiments (Cheng & Chen, 2015). Shp1 is the sole member of the SEP domain subfamily of p97 cofactors in budding yeast. In humans four SEP domain proteins exist, namely p47, p37, UBXD4 and UBXD5 (Socius). In the following part we set out to investigate whether the SDS22-PP1-I3 complex is regulated by p97 and which p97 cofactors are involved in this interaction.

2.3.1 The p97 SEP domain cofactors p37, p47 and UBXD4 bind the SDS22-PP1-I3 complex

We first performed immunoprecipitation and pulldown experiments to examine which p97 cofactors bind the SDS22-PP1-I3 complex. p47 was shown to bind SDS22, PP1γ and I3 in initial immunoprecipitation experiments done in our lab by S. Bremer. Therefore, and given the role of Shp1 in yeast, we focussed on the SEP domain cofactors. In a first approach, C-terminal GFP-fusions of p37 and p47 or GFP alone were transiently overexpressed in HEK 293 cells for 24 h, followed by cell lysis and immunoprecipitation with anti-GFP nanobodies. IP samples together with 1.3 % input and flowthrough were analyzed by Western blotting with antibodies specific for GFP, p97, SDS22, PP1γ and I3. p37-GFP and p47-GFP were expressed and precipitated at comparable levels and both showed specific binding of p97. Importantly, GFP fusions of both p37 and p47 showed a weak but specific binding of SDS22, PP1γ and I3. Interestingly, all three components of the PP1 complex associated to p37-GFP more strongly than to p47-GFP (Figure 2.12 A). Immunoprecipitation experiments performed by a master student under my supervision revealed that also UBXD4-GFP bound the PP1 complex to a comparable extent as p37-GFP (Th. Petrik, data not shown). To address more systematically which p97 SEP domain cofactors bind the

SDS22-PP1-I3 complex and to what extent we used HEK 293 Flp-In cell lines inducibly expressing each cofactor with a C-terminal SH(Strep-HA)-tag. These cell lines were generated in our laboratory by E. Vamos and J. Hülsmann. Expression of each p97 SEP domain cofactor (p37, p47, UBXD4 and Socius) and the non-SEP domain cofactor Ufd1 as a control was induced in the respective cell lines by addition of doxycycline for 24 h. Cells inducibly expressing GFP-SH served as a pulldown control. Cell extracts were prepared and subjected to Strep-pulldown with Streptactin sepharose beads. Pulldown samples alongside 0.4 % inputs were analyzed by Western blotting with HA, p97, SDS22, PP1γ and I3 antibodies. Expression levels of the different p97 cofactors varied with p47-SH being expressed most strongly, which was reflected by the amounts of co-precipitated p97. No binding of SDS22, PP1γ and I3 to either GFP-SH or Ufd1-SH was detected. SH-tagged UBXD4, p37 and p47 all bound SDS22, PP1γ and I3, albeit to different extents. Although considerably more p47-SH than p37-SH or UBXD4-SH was expressed and pulled down, less of the PP1 complex was detected in the p47 pulldown. Comparable amounts of the PP1 complex were bound to p37-SH and UBXD4-SH. Socius showed only a weak interaction with SDS22, I3 and PP1γ that was barely above background levels and was therefore not considered in further analyses (Figure 2.12 B). It is worth noting that the interaction of UBXD4, p37 and p47 with the ternary PP1 complex could be shown to be p97 dependent as binding of the complex was abolished in immunoprecipitations of GFP-tagged p97-binding-deficient mutants (Th. Petrik, data not shown). These findings suggest that UBXD4, p37 and p47 may all function, possibly redundantly, in regulating the SDS22-PP1-I3 complex.

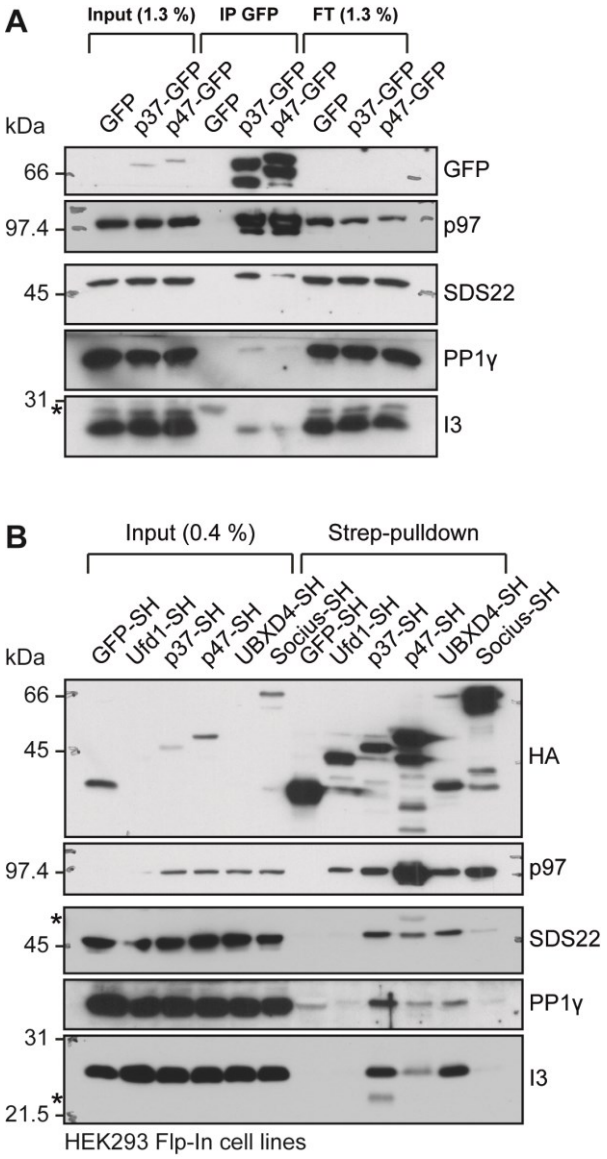

Figure 2.12 The SEP domain proteins p37, p47 and UBXD4 bind the SDS22-PP1-I3 complex. A HEK 293 cells were transfected with p37 or p47 C-terminally tagged with GFP or with GFP alone for 24 h. GFP- fusions were affinity-isolated from cell extracts using anti-GFP nanobodies coupled to sepharose beads. Input and flowthrough (FT) samples (1.3 %) and precipitates were analyzed by Western blotting with the indicated antibodies. **B** Expression of the indicated p97 cofactors, C-terminally tagged with Strep-HA (SH), was induced in HEK 293 Flp-In cells by addition of doxycycline for 24 h. Cells inducibly expressing GFP-SH served as a pulldown control. SH-tagged proteins were affinity-isolated from cell lysates by Strep-pulldown using Streptactin sepharose beads. Inputs (0.4 %) and precipitates were analyzed by Western blotting with the indicated antibodies. Asterisks mark unspecific bands.

2.3.2 Depletions of p97 and p37, p47 and UBXD4, but not of Ufd1 and Npl4, lead to accumulation of PP1 complex-bound SDS22

In order to examine how p97 and its SEP domain cofactors p37, p47 and UBXD4 regulate the SDS22-PP1-I3 complex we again made use of gel filtration fractionation of HeLa cell extracts. HeLa cells were depleted of p97, p37, p47 or UBXD4 with in each case two different siRNAs for 48 h. Cells treated with non-targeting luciferase siRNA or depleted for the non-SEP domain p97 cofactors Ufd1 and Npl4 served as controls. Depletion efficiencies for p97, p37, p47, Ufd1 and Npl4 were assessed by Western blotting with respective antibodies. All proteins tested were effectively downregulated. The depletion efficiency for UBXD4 could not be verified due to lack of an antibody. Another western blot of the cell extracts as above was probed for SDS22, I3 and PP1γ, showing that depletions of p97 and the SEP domain cofactors p37, p47 and UBXD4 did not affect the expression levels of the PP1 complex components (Figure 2.13 A). Next, the cell extracts were subjected to gel filtration fractionation on a Superdex 200 10/300 GL column and aliquots of the input extract and the collected fractions were analyzed by Western blotting with SDS22 antibodies. As observed before, in siLuc treated control samples, SDS22 eluted in a high and a low molecular weight peak, representing complex-associated and monomeric forms, respectively, with the monomeric form being more prominent. Strikingly, p97 depletions with both siRNAs led to a complete loss of the monomeric peak with the total of SDS22 being shifted towards the complex-bound fraction. SEP domain cofactor depletions also caused SDS22 to shift towards the complex-bound fraction, although the effect was less severe than upon p97 depletion. In contrast, depletions of Ufd and Npl4 did not affect the elution pattern of SDS22 (Figure 2.13 B). Taken together, these findings suggest that p97 together with its cofactors p37, p47 and UBXD4 is involved in dissociating SDS22 from PP1. In preliminary analyses we also looked for effects of p97 and SEP domain cofactor depletions on I3 association to PP1 but did not observe changes in the elution pattern of I3 (data not shown).

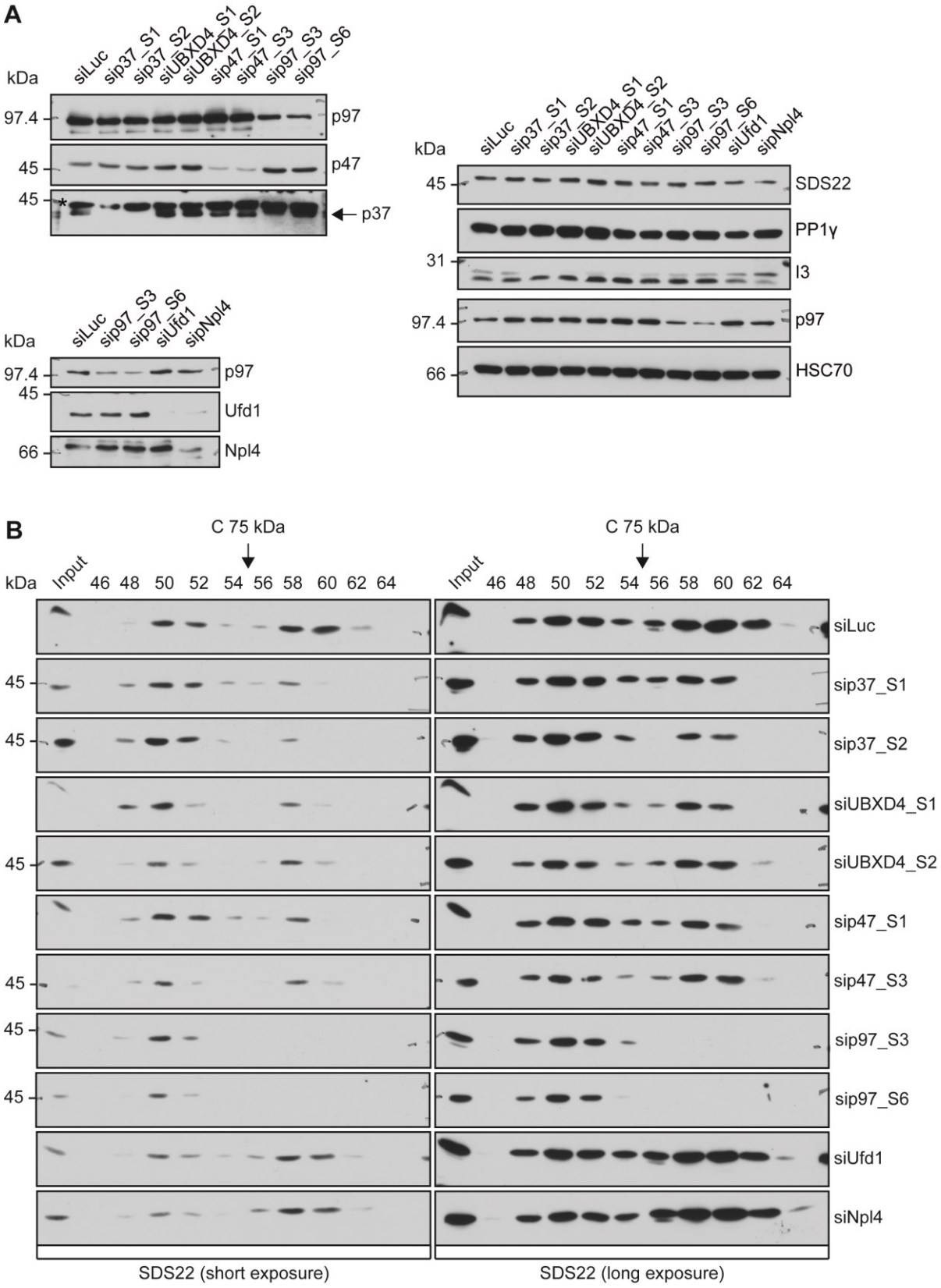
A
kDa
siLuc
sip37_S1
sip37_S2
siUBXD4_S1
siUBXD4_S2
sip47_S1
sip47_S3
sip97_S3
sip97_S6
97.4
p97
45
p47
45
*
p37
siUfd1
sipNpl4
Ufd1
66
Npl4
SDS22
PP1γ
31
I3
HSC70
B
C 75 kDa
Input
46 48 50 52 54 56 58 60 62 64
SDS22 (short exposure)
SDS22 (long exposure)

Figure 2.13 siRNA-mediated depletions of p97 and SEP domain cofactors, but not of Ufd1 and Npl4, lead to accumulation of complex-bound SDS22. A HeLa cells were treated with the indicated siRNAs for 48 h, then cell extracts were prepared and analyzed by Western blotting with the indicated antibodies. HSP70 served as a loading control. Asterisks mark unspecific bands. Note that SEP domain cofactor depletions did not affect expression levels of SDS22, I3 and PP1γ. **B** Cell extracts as in (**A**) were loaded onto a FPLC Superdex 200 10/300 GL gel filtration column. Aliquots of the input extracts and the collected fractions were analyzed by Western blotting with SDS22 antibodies. Arrows indicate elution volumes of calibration standard proteins (C, Conalbumin, 75 kDa). Note the complete loss of monomeric SDS22 low molecular weight fractions upon p97 depletion.

2.3.3 Increased PP1 complex-association of SDS22 upon p37 depletion is reversed by expression of siRNA resistant p37

We next wanted to verify whether the effect of p97 SEP domain cofactor depletions on PP1 complex-association of SDS22 was specific and not due to off-target effects of the siRNAs used. To this end, we used the example of p37 depletion with the sip37_S2 oligonucleotide. Therefore, we generated a HeLa cell line inducibly expressing siRNA-resistant p37 with a 3*HA-Strep tag. Murine p37 cDNA carrying 3 nucleotide mismatches compared to the p37 siRNA fused to a 3*HA-Strep tag was cloned into a pcDNA5/FRT/TO vector and transfected into parental HeLa Flp-In cells (kindly provided by U. Kutay, ETH Zurich). Single clones were selected and tested for expression of $p37^{RNAiRes}$-3*HA-Strep upon doxycycline treatment. Indeed $p37^{RNAiRes}$-3*HA-Strep was expressed upon addition of doxycycline and was able to bind endogenous p97 as verified by immunoprecipitation (data not shown). Figure 2.14 A shows a Western blot of the p37 restoration experiment. HeLa Flp-In $p37^{RNAiRes}$-3*HA-Strep cells were depleted for p37 or control depleted for luciferase for 48 h. 24 h prior cell lysis expression of $p37^{RNAiRes}$ was induced or not. The western blot was probed with antibodies specific for p37 and p97. $p37^{RNAiRes}$ was strongly overexpressed compared to endogenous p37. Importantly, upon p37 siRNA treatment, endogenous p37 was effectively downregulated also in the background of $p37^{RNAiRes}$ expression and the $p37^{RNAiRes}$ expression level was largely unaffected by the siRNA treatment. Next, cell extracts as in Figure 3.14 A were subjected to gel filtration fractionation on a Superdex 200 10/300 GL gel filtration column and aliquots of inputs and collected fractions analyzed by Western blotting with SDS22 antibodies. For the uninduced, siLuc treated control sample we again observed an elution of SDS22 in a high molecular weight (PP1 complex-associated) and a low molecular

weight (monomeric) peak with the monomeric fraction being more prominent. p37 depletion in uninduced cells again led to a shift of SDS22 towards the complex-associated fraction. Importantly, this effect was reversed upon $p37^{RNAiRes}$ overexpression, ruling out an off-target effect. Remarkably, upon $p37^{RNAiRes}$ overexpression in the control depletion background, SDS22 was shifted further towards the monomeric fraction, providing another piece of evidence for a p97-p37 mediated dissociation of SDS22 from the PP1 complex (Figure 2.14 B).

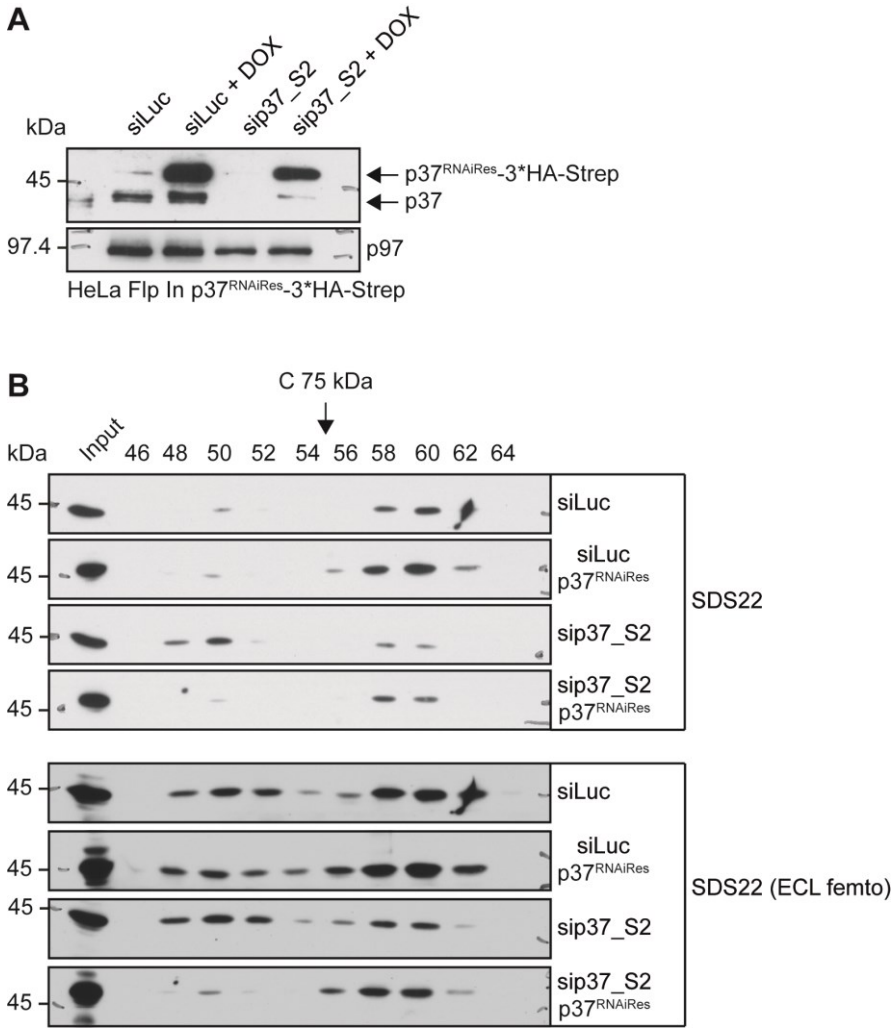

Figure 2.14 Expression of an siRNA-resistant p37 cDNA restores the effect of p37 depletion on SDS22-PP1-I3 complex formation.. **A** Western blot of p37 restoration experiment. HeLa Flp-In cells inducibly expressing siRNA-resistant mouse p37 were treated with the indicated siRNAs for 48 h. Transgene expression was induced by addition of doxycycline for 24 h prior lysis or not. **B** Cell extracts as in (**A**) were loaded onto a FPLC Superdex 200 10/300 GL gel filtration column. Aliquots of the input extracts and the collected fractions were analyzed by Western blotting with SDS22 antibodies. Arrows indicate elution volumes of calibration standard proteins (C, Conalbumin, 75 kDa). Note that the SDS22 shift towards complex-bound high molecular weight fractions upon p37 depletion is reversed after induction of $p37^{RNAiRes}$ expression.

2.3.4 PP1 inhibition combined with p97 SEP domain cofactor depletions does not show synergistic effects on cell proliferation and viability

Since we found p97 with its SEP domain cofactors p37, p47 and UBXD4 to be involved in regulating the SDS22-PP1-I3 complex by facilitating dissociation of SDS22 from PP1, we reasoned that these p97 cofactors could play a role in the

SDS22- and I3-mediated regulation of PP1 at the kinetochore during mitotic chromosomal alignment (see chapter 2.1) and thus be required for balancing Aurora B kinase activity. To test this hypothesis, we used siRNA-mediated depletions of the SEP domain cofactors followed by immunofluorescence stainings for Aurora B pT232 and total Aurora B protein. However, so far, using single depletions of either p37, p47 or UBXD4 we did not detect an increase of either Aurora B phosphorylation or total Aurora B protein level on metaphase chromatin (data not shown). We therefore decided to try a more general approach to test for a functional interaction between PP1 and the p97 SEP domain cofactors. To this end, we combined PP1 inhibition by NIPP1-fm overexpression (Winkler et al., 2015) (see chapter 2.1.1) with siRNA-mediated depletions of SEP domain cofactors and assessed for cell proliferation and viability using a colorimetric MTS assay in order to detect possible synergistic or additive effects. In a first approach, HeLa Flp-In NIPP1-fm cells grown in 96 well plates were depleted for p37, p47 and UBXD4 with two different siRNAs each or for SDS22 for 72 h and full overexpression of NIPP1-fm was induced by addition of 1 µg/ml doxycycline or not for 48 h prior to analysis. We previously had observed cytotoxic effects in cells treated with the sip37_S2 oligonucleotide (data not shown). In contrast to the specific phenotypes observed upon p37 depletion with the sip37_S2 siRNA (see chapters 2.3.3 and 2.4.2), these cytotoxic effects could not be rescued with an siRNA-resistant cDNA and where therefore most likely due to an off-target effect. Therefore, sip37_S1 and sip37_S3 siRNAs were used in this experiment. siLuc control depletion and depletion of the non-SEP domain p97 cofactor UBXD1 served as negative controls. As an internal control for the measurement and for the efficiency of siRNA treatment a cell death control siRNA targeting ubiquitously expressed genes essential for cell survival (Qiagen) was included. To control whether effects upon NIPP1-fm overexpression are due to PP1 inhibition, the experimental setup was reproduced using cells inducibly expressing the PP1 binding deficient NIPP1-Fm+Pm. 1 h prior to measurement MTS reagent was added to the cells and the OD 490 nm was measured on an automated plate reader and normalized to uninduced, untransfected controls. Upon treatment with the cell death control siRNA the OD 490 nm was reduced by about 90 % compared to untreated controls, indicating that the siRNA treatment was efficient and the measurement was reliable. Overexpression of NIPP1-Fm without siRNA treatment led to a reduction of the OD 490 nm by almost 50 % whereas overexpression of

NIPP1-Fm+Pm had no effect, confirming that PP1 inhibition reduces cell proliferation and survival (Winkler et al., 2015). siRNA mediated depletions also caused reduced proliferation and / or survival as the OD 490 nm was decreased between 12 % (siUBXD4_S2) and 37 % (siSDS22) (also treatment with the non-targeting luciferase control siRNA caused a reduction of the OD 490 nm by about 27 %). Nevertheless, we did not observe additive or synergistic effects when combining NIPP1-Fm overexpression with both SEP domain cofactor or SDS22 depletions (Figure 2.15 A). We reasoned that this might be due to the strong overexpression of NIPP1-Fm already causing a full inhibition of PP1. Since the expression level of the NIPP1 fusions was tunable depending on the doxycycline concentration, as evidenced by Western blotting with GFP antibodies (Figure 2.15 C), the experimental setup was repeated using a milder expression of NIPP1-Fm (induction for 24 h prior analysis with 0.5 ng/ml doxycycline). As expected, also the effect on cell proliferation and / or viability upon mild induction of NIPP1-Fm expression was weaker, as the OD 490 nm was only decreased by about 12 % compared to uninduced controls. As in the previous experiment, SDS22 depletion had a stronger effect on the proliferation and / or survival rates than control and p97 cofactor depletions. However, again, we did not observe synergistic or additive effects when combining NIPP1-Fm expression with SDS22 or p97 SEP domain cofactor depletions (Figure 2 15 B).

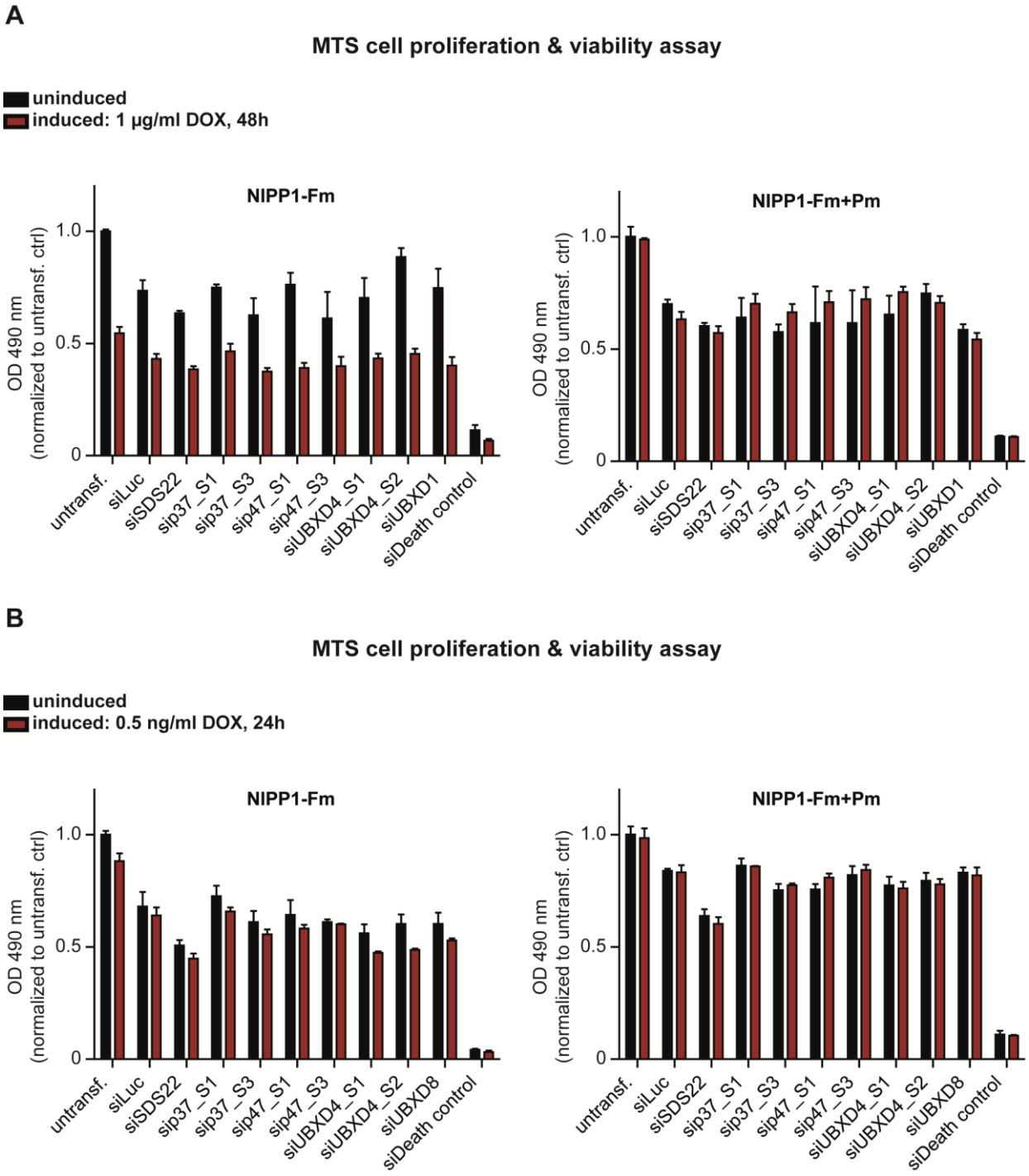
A
MTS cell proliferation & viability assay
uninduced
induced: 1 µg/ml DOX, 48h
NIPP1-Fm
NIPP1-Fm+Pm
OD 490 nm
(normalized to untransf. ctrl)
1.0
0.5
0
untransf.
siLuc
siSDS22
sip37_S1
sip37_S3
sip47_S1
sip47_S3
siUBXD4_S1
siUBXD4_S2
siUBXD1
siDeath control
B
MTS cell proliferation & viability assay
uninduced
induced: 0.5 ng/ml DOX, 24h
NIPP1-Fm
NIPP1-Fm+Pm
OD 490 nm
(normalized to untransf. ctrl)
1.0
0.5
0
untransf.
siLuc
siSDS22
sip37_S1
sip37_S3
sip47_S1
sip47_S3
siUBXD4_S1
siUBXD4_S2
siUBXD8
siDeath control
C
NIPP1-Fm
NIPP1-Fm+Pm
kDa
0 0.1 0.3 0.5 1 1000
0 0.1 0.3 0.5 1 1000
ng/ml DOX
66
GFP-NIPP1
97.4
p97
HeLa Flp In T-Rex GFP-NIPP1

Figure 2.15 Inhibition of PP1 combined with siRNA-mediated depletion of p97 SEP domain cofactors does not show synergistic effects on cell proliferation and viability. MTS cell proliferation & viability assay. HeLa Flp-In T-Rex cells inducibly expressing GFP-fusions of the PP1 inhibitor NIPP1-Fm or of the PP1 binding deficient mutant NIPP1-Fm+Pm as a control were grown in 96 well plates and treated with the indicated siRNAs for 72 h. Expression of NIPP1 fusions was induced by addition of the indicated doxycycline concentrations for the indicated time spans, followed by addition of MTS reagent and incubation at 37 ˚C for 1 h. The OD 490 nm was measured on an automated plate reader and normalized to uninduced, untransfected controls. Graphs show single experiments with technical triplicates. Error bars represent s.d. **A** Expression of NIPP1 fusions was induced by addition of 1 µg/ml doxycycline for 48 h prior to analysis. **B** Expression of NIPP1 fusions was induced by addition of 0.5 ng/ml doxycycline for 24 h prior to analysis. **C** Tunable expression of NIPP1 fusions. Expression of GFP-fusions of NIPP1-Fm or NIPP1-Fm+Pm was induced by addition of the indicated doxycycline concentrations for 48 h. Cell extracts were prepared and analyzed by Western blotting with GFP and p97 antibodies. p97 served as a loading control.

Taken together, using co-immunoprecipitations, we could show that p97 with either of the SEP domain cofactors UBXD4, p37 or p47 binds the SDS22-PP1-I3 complex. Furthermore, gel filtration fractionation analyses indicate that p97 complexes with both UBXD4, p37 or p47 are involved in dissociating SDS22 from PP1. However, so far, we did not find evidence for a p97 SEP domain cofactor-mediated regulation of PP1 at the kinetochore nor could we detect synergistic or additive effects when combining PP1 inhibition with siRNA-mediated SEP domain cofactor depletions.

2.4 Part IV: The role of the p97 SEP domain cofactors p37 and p47 in mitotic spindle orientation

UBXN-2 is the sole CDC-48/p97 SEP domain cofactor in *Caenorhabditis elegans*. It has highest sequence homology with p47 but lacks, like p37 and UBXD4, an N-terminal UBA domain (Schuberth & Buchberger, 2013). We contributed to a study on mitotic functions of UBXN-2 and its mammalian orthologs p37 and p47 that was mainly done by E. Kress and colleagues in M. Gotta's laboratory. In this study, UBXN-2 was shown to be involved in the regulation of centrosome maturation timing and mitotic spindle positioning in *C. elegans* embryos (Kress et al., 2013). The data obtained by E. Kress and colleagues in M. Gotta's laboratory suggest that CDC-48-UBXN-2 regulates these processes by dissociating AIR-1/Aurora A kinase from centrosomes during prophase, thereby limiting its net recruitment. siRNA-mediated depletions of p37 alone and p37/p47 double depletions in human cells done in P. Meraldi's group caused an accumulation of Aurora A at centrosomes during centrosome separation in prophase, a delay in centrosome separation as well as rotating and misoriented mitotic spindles (Kress et al., 2013), suggesting that the role of UBXN-2 in mitotic regulation is conserved. As our contribution to the study by Kress et al., we investigated the mitotic localization and functions of p37 and p47.

2.4.1 p97 SEP domain cofactors p37 and p47 localize to mitotic centrosomes

Given the role of UBXN-2 in regulating the centrosomal recruitment of Aurora A kinase (Kress et al., 2013), we wanted to investigate whether p37 and p47 localize to mitotic centrosomes. We did not test for the localization of UBXD4 since we did not consider it at this time and in the context of this study. We used transient overexpressions of p37 and p47 GFP-fusions. Using live cell imaging and formaldehyde fixations with or without preextraction, we did not observe a specific localization of either p37-GFP or p47-GFP to mitotic centrosomes (data not shown). However, using methanol fixation, we observed a specific enrichment of p37-GFP and p47-GFP at mitotic centrosomes. HeLa cells were transiently transfected with p37-GFP, p47-GFP or GFP alone for 48 h, fixed with ice-cold methanol and stained with γ-tubulin antibodies to visualize centrosomes and with DAPI before imaging at a spinning disc confocal microscope. We found both p37-GFP and p47-GFP to be

enriched at centrosomes from prophase to metaphase (Figure 2.16 A). GFP alone, however, was also enriched at mitotic centrosomes in a certain number of cells. Figure 2.16 B shows a quantification of cells with enriched centrosomal GFP signal. Centrosomal localization was observed in 85.7 % of p37-GFP expressing cells, 52.9 % of p47-GFP expressing cells and in 26.2 % of GFP expressing cells.

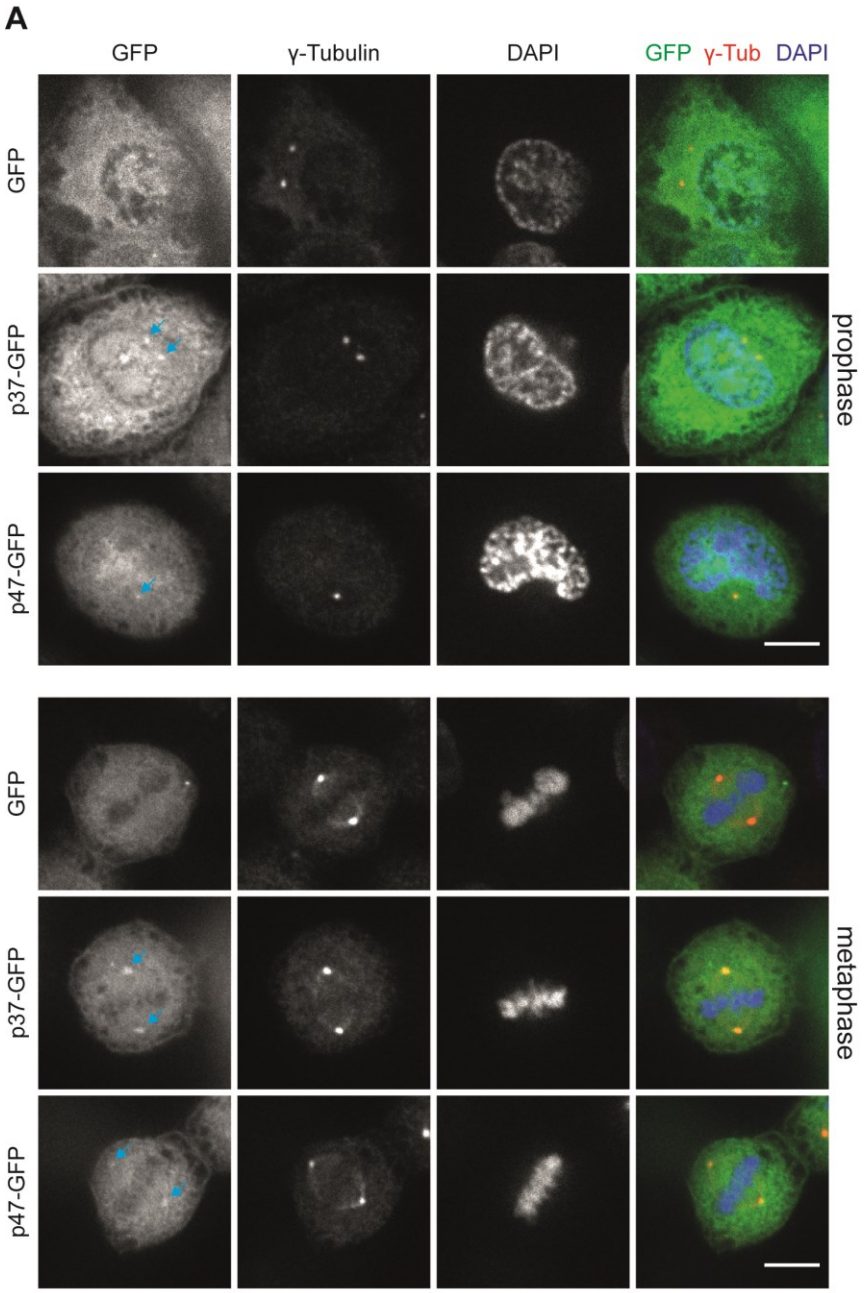
A
GFP
γ-Tubulin
DAPI
GFP γ-Tub DAPI
GFP
p37-GFP
p47-GFP
prophase
GFP
p37-GFP
p47-GFP
metaphase
B
Centrosomal localization
cells with enriched centrosomal GFP signal [%] (prophase to metaphase)
100
80
60
40
20
0
GFP
p37-GFP
p47-GFP

Figure 2.16 The p97 SEP domain cofactors p37 and p47 are enriched at mitotic centrosomes. A HeLa cells were transfected with p37 or p47 C-terminally tagged with GFP or with GFP alone for 48 h, fixed with methanol and stained with γ-tubulin antibodies and DAPI. Representative spinning disc confocal images of prophase and metaphase cells are shown. Arrows indicate the centrosomes in GFP panels. Scale bar, 10 µm. **B** Quantification of (**A**). Centrosomal localization is observed in 85.7 % of p37-GFP expressing cells (*n* = 56), 52.9 % of p47-GFP expressing cells (*n* = 68) and 26.2 % of GFP expressing cells (*n* = 61). Data combined from two independent experiments.

2.4.2 p37 depletion causes mitotic spindle orientation defects

We then went on to examine mitotic phenotypes upon p37 and p47 depletion. HeLa cells were treated with siRNAs targeting p37 or p47 or with a non-targeting control siRNA (siControl) for 48 h, methanol fixed and stained with γ-tubulin antibodies and DAPI before analysis at a spinning disc confocal microscope. We observed an increase of metaphase cells with chromosomal misalignments upon p37 depletion (data not shown). Furthermore, and consistent with findings of P. Meraldi's group (Kress et al., 2013), single depletion of p37 but not p47 led to an increased number of cells with an aberrant mitotic spindle orientation. Consistent with previous studies (Toyoshima & Nishida, 2007; Thoma et al., 2009), in control depleted cells the mitotic spindle generally oriented parallel to the substratum. In contrast, in p37 depleted cells, the orientation of the spindle towards the substratum strongly varied. Figure 2.17 A shows 3D representations of Z-stack confocal images of representative p37 or control depleted anaphase cells. We next wanted to verify whether this phenotype is p37 specific and not due to an off-target effect of the siRNA used (sip37_S2). For the restoration experiment we again used our HeLa Flp-In p37^{RNAiRes}-3*HA-Strep cells. Cells were p37 or control depleted for 48 h and expression of p37^{RNAiRes} was induced by addition of doxycycline for 34-40 h prior analysis or not. Depletion of endogenous p37 and p37^{RNAiRes} overexpression was confirmed by Western blotting (Figure 2.17 B). For analysis of the phenotype, cells were methanol fixed and stained for γ-tubulin and DAPI. The spindle orientation in anaphase cells was scored visually in 3 independent experiments with $n \geq 74$ cells per condition. Anaphase spindles with both centrosomes not visible in one focal plane were scored as misoriented. Under control conditions, about 10 % of the cells had misoriented spindles. p37 depletion caused a significant increase of cells with misoriented spindles (27.54 %; $p < 0.0001$, using Fisher's exact test). Importantly, the phenotype was largely and significantly

($p < 0.01$, using Fisher's exact test) rescued by $p37^{RNAiRes}$ overexpression (Figure 2.17 C), ruling out an off-target effect and confirming that p37 is required for proper mitotic spindle orientation.

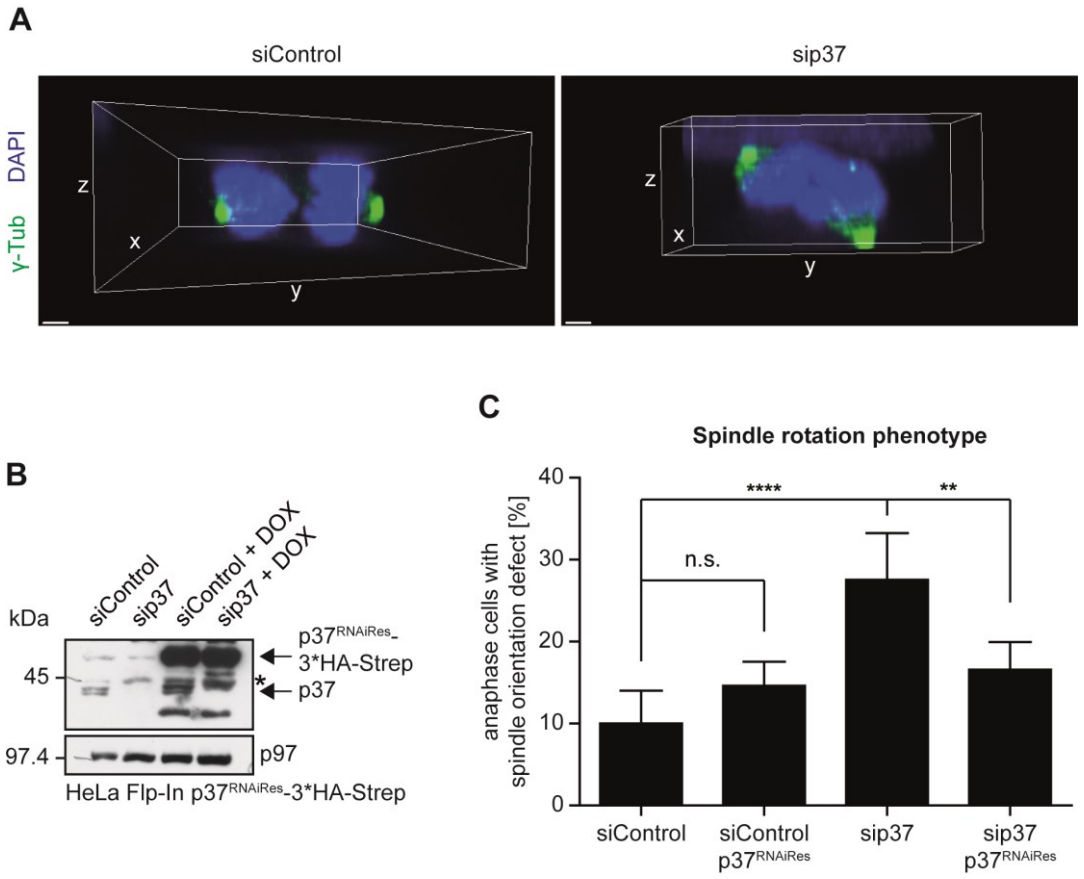

Figure 2.17 siRNA-mediated p37 depletion causes mitotic spindle orientation defects. **A** HeLa cells, treated with siControl or sip37_S2 siRNAs for 48 h, were fixed with methanol and stained with γ-tubulin antibodies and DAPI. Z-stack series of representative anaphase cells were taken at a spinning disc confocal microscope and 3D representations were generated using the software Imaris. Scale bar, 2 µm. Note that the mitotic spindle is oriented parallel to the substratum under control conditions and rotated in the z plane upon p37 depletion. **B** Western blot of p37 restoration experiment. HeLa Flp-In $p37^{RNAiRes}$-3*HA-Strep cells were treated with the indicated siRNAs for 48 h. Transgene expression was induced by addition of doxycycline for 36 h prior lysis or not. Asterisks mark unspecific bands. **C** Restoration of the p37 spindle rotation phenotype. HeLa Flp-In $p37^{RNAiRes}$-3*HA-Strep cells were siRNA treated as in (**A**) and transgene expression was induced by addition of doxycycline for 34-40 h prior fixation or not. Cells were fixed with methanol and stained with γ-Tubulin antibodies and DAPI. The spindle orientation in anaphase cells was scored visually in 3 independent experiments with $n \geq 74$ cells per condition. Error bars represent s.d. P-values were calculated using Fisher's exact test (****, $p \leq 0.0001$; **, $p \leq 0.01$; n.s., not significant).

Together, the data presented in this part show that the p97 SEP domain cofactors p37 and p47 localize to centrosomes during mitosis and that p37 is required for proper mitotic spindle positioning.

3 Discussion

The results presented here and in our study (Eiteneuer et al., 2014) make an important contribution to better understanding the regulation of PP1. In the following, I am going to discuss the complex functional relationship of SDS22 and I3 in regulating kinetochore-associated PP1. Additionally, I will discuss our findings that suggest a p97-mediated regulation of the ternary SDS22-PP1-I3 complex.

Our findings reveal a more complex role of SDS22 in regulating kinetochore-associated PP1 than previously reported. In agreement with two previous independent studies (Posch et al., 2010; Wurzenberger et al., 2012), we find SDS22 to be required for kinetochore-associated PP1 function in counteracting Aurora B kinase, thereby ensuring proper chromosome alignment and progression through mitosis. However, in contrast to findings by J. Swedlow's research group (Posch et al., 2010), we show that SDS22 does not quantitatively localize to the kinetochore under normal conditions and that it does not function as a substrate specifier or targeting factor of PP1 at the kinetochore. Instead, whereas being required for PP1 function at the kinetochore, SDS22 inhibits the activity of kinetochore-associated PP1 when quantitatively bound.

Furthermore, we show for the first time that also I3 is required for the regulation of PP1 function at the kinetochore in human cells. By forming a ternary complex with SDS22-PP1, I3 limits the association of SDS22 with KNL1-bound PP1 at the kinetochore, thereby ensuring PP1 activity and thus balancing of Aurora B kinase. Based on our findings, we propose a model in which SDS22 functions as a PP1 chaperone or maturation factor, mediating a PP1 activation step in solution that is followed by SDS22 dissociation and binding of activated PP1 to KNL1 at the kinetochore. I3 keeps SDS22-PP1 in solution, preventing association of SDS22-PP1 with KNL1 and may regulate or contribute to SDS22-mediated activation of PP1 and / or SDS22 dissociation from activated PP1. Our model predicts SDS22 and I3 to have a more general role in PP1 function and homeostasis, possibly mediating PP1 biogenesis and / or maintenance.

Findings in yeast have implicated the AAA ATPase Cdc48/p97 with its SEP domain cofactor Shp1 in positively regulating PP1 (Zhang et al., 1995; Cheng & Chen, 2010; Böhm & Buchberger, 2013; Cheng & Chen, 2015). Interaction studies furthermore suggest that Cdc48/p97-Shp1 acts on the ternary Sds22-PP1-Ypi1/I3 complex, however, the underlying mechanism has remained elusive (Cheng & Chen, 2015). The data presented here show that this interaction is conserved in humans and provide first indications on how p97 with its SEP domain cofactors p37, UBXD4 and p47 regulates the ternary SDS22-PP1-I3 complex. Our findings are consistent with a role of p97 SEP domain cofactor-complexes in regulating PP1 by dissociating SDS22 from the ternary PP1 complex. While we are just beginning to unravel the role of p97 in regulating PP1, the data presented here provide important first insights that may point to a significant general mechanism in controlling PP1 homeostasis and holoenzyme composition.

3.1 The complex role of SDS22 in regulating PP1 activity at the kinetochore

Two independent studies have previously investigated the role of SDS22 in regulating kinetochore-associated PP1 in human cells (Posch et al., 2010; Wurzenberger et al., 2012). Consistent with findings in yeast, their data provide evidence for a positive role of SDS22 for PP1 activity at the kinetochore and its function in balancing Aurora B (Peggie et al., 2002; Pedelini et al., 2007; Posch et al., 2010; Wurzenberger et al., 2012). Consistent with compromised PP1 function at the kinetochore, both Swedlow and colleagues and Gerlich and colleagues found siRNA-mediated depletion of SDS22 to cause an imbalanced Aurora B activity, accompanied by chromosome segregation defects (Posch et al., 2010; Wurzenberger et al., 2012). However, their findings differ in two important points. Whereas Swedlow and colleagues reported that SDS22 localizes to kinetochores from prometaphase to anaphase and found it to be required for PP1 targeting to kinetochores (Posch et al., 2010), Gerlich and colleagues did not detect SDS22 at the kinetochore (D. Gerlich, personal communication), which is consistent with findings by two other research groups (Liu et al., 2010; M. Bollen, personal communication). Furthermore, data by Swedlow and colleagues and Gerlich and colleagues differ on whether SDS22 affects Aurora B activity and / or Aurora B substrate dephosphorylation. While Swedlow and colleagues observed an increase

in Aurora B phosphorylation at T232 upon SDS22 depletion (Posch et al., 2010), indicating that SDS22-regulated PP1 directly regulates Aurora B activity, Gerlich and colleagues did not detect an increase in Aurora B T232 phosphorylation, but increased Aurora B substrate phosphorylation (Wurzenberger et al., 2012), suggesting that PP1 acts downstream of Aurora B.

Our data confirm that SDS22 is required for proper chromosome alignment, as evidenced by alignment defects (Eiteneuer et al., 2014) and SAC activation (Figure 2.2) upon SDS22 depletion. In agreement with findings by Swedlow and colleagues (Posch et al., 2010), we observe an increase in Aurora B T232 phosphorylation upon SDS22 depletion (Figure 2.1), indicating that Aurora B activity is regulated directly by SDS22-regulated PP1. In addition, we detect a slight increase in total Aurora B protein level at metaphase centromeres and persistence of Aurora B at centromeres during anaphase in cells depleted of SDS22 (or I3) (Eiteneuer et al., 2014). This may be explained by a feedback loop between Aurora B and PP1-Repo-Man, as active Aurora B promotes its own targeting by inhibitory phosphorylation of Repo-Man, thereby preventing dephosphorylation of the CPC targeting site histone H3 pT3 (Qian et al., 2013). Furthermore, using an *in vitro* dephosphorylation assay, we show for the first time that PP1 indeed directly and specifically dephosphorylates Aurora B at T232 (Figure 2.5 A).

However, our findings argue against a direct role of SDS22 in regulating kinetochore-associated PP1, since we do not detect SDS22-GFP at kinetochores when expressed at near endogenous levels (Eiteneuer et al., 2014). Furthermore, we do not observe a decrease in PP1 localization at the kinetochore upon SDS22 depletion (Eiteneuer et al., 2014), speaking against a role of SDS22 as a PP1 targeting factor to the kinetochore. This finding is in contrast to the study by Swedlow and colleagues (Posch et al., 2010) that characterizes SDS22 as a kinetochore-targeting PiP, and consistent with a study showing that KNL1 functions as the major anchor for PP1 at the kinetochore as it is essential for bulk recruitment of PP1 to kinetochores (Liu et al., 2010). However, while we find SDS22 to be absent from kinetochores under control conditions, SDS22 does have the ability to localize to the kinetochore under certain conditions. We find SDS22 to localize to kinetochores when overexpressed (Eiteneuer et al., 2014). Different expression levels are likely to explain the conflicting

results reported on SDS22 localization (Posch et al., 2010; Rodrigues et al., 2015; Liu et al., 2010). More importantly, SDS22 becomes recruited to kinetochores upon I3 depletion, indicating that I3 limits SDS22 association to kinetochores (Eiteneuer et al., 2014). We show that SDS22 binding to kinetochores is mediated by KNL1-associated PP1 as PP1 binding-deficient SDS22 mutants do not localize to kinetochores when overexpressed and kinetochore-recruitment of SDS22 in I3 depleted cells is abolished upon co-depletion of KNL1 (Eiteneuer et al., 2014). We corroborate this finding biochemically by immunoprecipitation of a soluble KNL1 fragment containing the RVxF PP1 binding motif, detecting a low basal level of SDS22 associating with KNL1-bound PP1 under control conditions that is markedly increased upon I3 depletion (Figure 2.4).

We therefore conclude that SDS22 does not act as a targeting factor or substrate specifier for PP1 at the kinetochore. Instead, our findings suggest that SDS22 inhibits PP1 activity at the kinetochore when quantitatively bound as both overexpression of wild type SDS22 as well as I3 depletion lead to an increase of Aurora B T232 phosphorylation (Eiteneuer et al., 2014) (Figure 2.6). The finding that attenuation of SDS22 expression partially reverses the effect of I3 depletion on Aurora B phosphorylation furthermore confirms that I3 depletion indeed negatively affects kinetochore-associated PP1 activity through increased SDS22 binding to kinetochore-bound PP1 (Figure 2.6). In addition, we show that SDS22 inhibits PP1 mediated dephosphorylation of Aurora B at T232 *in vitro* (Figure 2.5). These results are consistent with previous findings that SDS inhibits PP1 activity *in vitro* (Lesage et al., 2007) and with findings in yeast, where SDS22 acts as a dosage suppressor of a temperature sensitive *ipl1*/Aurora mutant (Pinsky et al., 2006).

The seemingly contradictory findings that SDS22 is required for PP1 activity at the kinetochore, yet it inhibits PP1 when bound are best explained by a model in which SDS22 functions as a PP1 chaperone or maturation factor. We propose that SDS22 is required for PP1 activation by binding and stabilizing an inactive structural intermediate of PP1. Consistent with this hypothesis, Sds22 is essential in budding yeast and has been shown to be required for the structural integrity of Glc7/PP1 in the W303 yeast background strain (Pedelini et al., 2007; Cheng & Chen, 2015). SDS22 is one of the most ancient PiPs (Ceulemans et al., 2002a). Unlike RVxF

motif-containing PiPs, SDS22 binds to PP1 via its leucine-rich repeats and in close proximity to the catalytic site of PP1 (Ceulemans et al., 2002b). SDS22-binding has profound effects on the conformation of PP1, as SDS22-binding has been shown to convert PP1 into an inactive form that is sensitive to trypsin digestion *in vitro* (Lesage et al., 2007). Recently, α4, a PP2A interactor, has been characterized as a PP2A chaperone (Jiang et al., 2013). PP2A is structurally related to PP1 and, like PP1, has two catalytic metal ions incorporated in the active site (Bollen et al., 2010; Jiang et al., 2013) α4 was shown to bind and stabilize an inactive, latent form of PP2A (Jiang et al., 2013). Removal of the catalytic metal ions from the PP2A active site increases α4-binding to PP2A (Jiang et al., 2013). α4 may help recharge PP2A with metal ions and was found to be essential for the cellular activity of PP2A (Jiang et al., 2013). Our findings, together with structural and biochemical data from M. Bollen's research group (Ceulemans et al., 2002b; Lesage et al., 2007), suggest that SDS22 may have a similar function with regard to PP1. SDS22 may be required for the biogenesis of newly synthesized PP1 and / or for PP1 regulation and maintenance after biosynthesis, possibly by facilitating (re)charging with catalytic metal ions, or keep a fraction of PP1 bound and inactive as part of a regulatory mechanism. In any case, and consistent with our data, SDS22 would be required for PP1 activation, but keep PP1 in an inactive state while bound. In order to further strengthen this hypothesis, it will be interesting to examine whether inactive and / or metal ion binding deficient forms of PP1 exhibit an increased binding to SDS22. Furthermore, and critically, it will be important to determine whether depletion of SDS22 affects further PP1-mediated functions, as is to be expected for a PP1 chaperone. In a recent study by B. Baum's research group, SDS22 was shown to be required for the dephosphorylation of moesin at the polar cell cortex during anaphase, thereby promoting polar relaxation in human and *Drosophila* cells (Rodrigues et al., 2015). Like Swedlow and colleagues (Posch et al., 2010), Baum and colleagues detected SDS22 at kinetochores, using an overexpression construct, and therefore interpret their finding as a function of kinetochore-associated SDS22-PP1 (Rodrigues et al., 2015). Alternatively, and consistent with our model, impaired moesin dephosphorylation and polar relaxation upon SDS22 depletion may be due to a general impairment of PP1 function in the absence of SDS22. However, we cannot rule out the possibility that SDS22 may have a role as a PP1 substrate specifier in particular pathways, as Baum and colleagues find ectopic targeting of SDS22 to the

polar cell cortex to cause premature cortical relaxation during metaphase (Rodrigues et al., 2015). This is in line with biochemical findings by M. Bollen's research group that show that SDS22 can not only convert PP1 into an inactive conformation, but also transiently inhibit PP1 in a substrate-dependent manner (Lesage et al., 2007).

3.2 I3 limits association of SDS22-bound PP1 to KNL1 at the kinetochore

The data presented here, together with further findings of our study from 2014 (Eiteneuer et al., 2014), explore for the first time the role of I3 in mitosis in human cells and reveal its functional relationship to SDS22 in regulating kinetochore-associated PP1. Our findings reconcile seemingly contradictory results in yeast, where both mutations and overexpression of Sds22 or Ypi1/I3 can rescue the temperature sensitivity of an *ipl1*/Aurora mutant (Peggie et al., 2002; Bharucha et al., 2008; Pinsky et al., 2006; Pedelini et al., 2007). Like SDS22, we find I3 to be required for proper chromosome alignment and balancing of Aurora B activity by kinetochore-bound PP1 (Eiteneuer et al., 2014) (Figure 2.6). Since I3, like KNL1, binds PP1 via an RVxF motif, an obvious assumption would be that I3 may regulate PP1 association to kinetochores by competing with KNL1 for PP1 binding. Indeed, we find I3 overexpression to cause a displacement of PP1 from kinetochores, accompanied by an increase in Aurora B activity (Eiteneuer et al., 2014). This finding likely explains why I3 can act as a dosage suppressor of a temperature sensitive *ipl1*/Aurora mutant in yeast (Pedelini et al., 2007). However, this effect is not specific for I3, and likely not physiologically relevant, as also overexpression of the unrelated RVxF motif containing PiP NIPP1 leads to PP1 displacement from kinetochores and increased Aurora B activity (Eiteneuer et al., 2014). Furthermore, we find that I3 depletion does not increase PP1 binding to KNL1 (Figure 2.4), suggesting that I3 does not regulate the total level of PP1 bound to KNL1 at the kinetochore. Instead, and rather unexpectedly, we find I3 depletion to cause a quantitative association of SDS22 with KNL1-bound PP1 at kinetochores, which leads to inhibition of PP1 activity at the kinetochore (Eiteneuer et al., 2014) (Figure 2.6). This effect is specific to I3, as depletion of NIPP1 does not affect SDS22 localization and Aurora B activity (Eiteneuer et al., 2014), and can be recapitulated biochemically by immunoprecipitation of a soluble KNL1 fragment containing the KNL1 RVxF motif. Consistent with our observations in cells, I3 depletion does not affect the amount of

PP1 co-isolated with the KNL1 fragment but specifically and markedly increases the amount of associated SDS22 (Figure 2.4). These findings can be explained by the fact that I3 can form a ternary complex with SDS22-PP1 in solution and preferentially binds SDS22-PP1 rather than binding PP1 alone (Lesage et al., 2007; Pedelini et al., 2007). I3 therefore is required for sequestering SDS22-PP1, thus preventing binding of SDS22-PP1 to KNL1 at kinetochores and thereby allowing for kinetochore-recruitment of active, SDS22-free PP1. In addition to its requirement for keeping SDS22-PP1 in solution, we find indications that I3 is required for a removal of SDS22 from PP1, as we detect an increased association of SDS22 with PP1 upon I3 depletion using gel filtration chromatography of cell lysates (Figure 2.8). We speculate that I3 may regulate or contribute to an SDS22-mediated activation of PP1 and / or facilitate SDS22 dissociation from activated PP1 (see chapter 3.3). Taken together, based on our findings, we propose a model (Figure 3.1), in which SDS22 binds and stabilizes an inactive form of PP1. SDS22 may thereby activate inactive or newly synthesized PP1, possibly by facilitating (re)charging of PP1 with catalytic metal ions. I3 specifically binds to SDS22-associated PP1 until PP1 is activated and SDS22 dissociates, thus preventing binding of inactive SDS22-PP1 to KNL1 at the kinetochore. This allows for binding of active, SDS22-free PP1 to KNL1 at the kinetochore that can fulfill its function in dephosphorylating and counteracting Aurora B kinase.

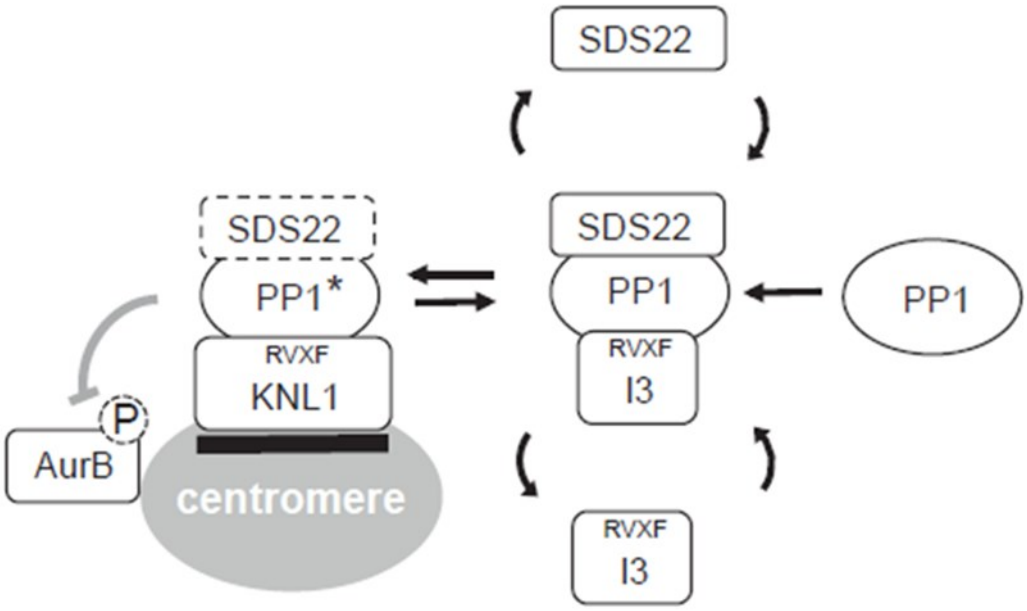

Figure 3.1 Model for the role of SDS22 and I3 in regulating kinetochore-associated PP1. SDS22 binds inactive, possibly newly synthesized PP1 and is required for its activation, but keeps it in an inactive intermediate state while bound. I3 binds SDS22-PP1 in solution, thereby preventing its association with KNL1 at the kinetochore and may contribute to PP1 activation or facilitate SDS22 dissociation from (activated) PP1. Sequestration of SDS22-PP1 by I3 allows for binding of active, SDS22-free PP1 to the kinetochore. Depletion of I3 leads to binding of inactive SDS22-PP1 to KNL1 at the kinetochore, which then fails to properly counteract Aurora B. The asterisk denotes active PP1. (Eiteneuer et al., 2014).

Our model predicts SDS22 and I3 to have a broader role in PP1 function and homeostasis, possibly mediating PP1 biogenesis and / or maintenance. This is supported by findings in budding yeast, where both Sds22 and Ypi1/I3 are essential for survival and have been shown to be required for the structural integrity of Glc7/PP1 (Pedelini et al., 2007; Cheng & Chen, 2015). However, using siRNA-mediated depletion of SDS22 or I3, we do not detect major pleiotropic defects (data not shown). Furthermore, the effects of SDS22 or I3 knockdown on Aurora B activity and chromosome alignment and segregation are relatively mild when compared to global cellular inhibition of PP1 (Eiteneuer et al., 2014; Winkler et al., 2015) (Figure 2.1). This may indicate that SDS22 and I3 merely control a subpopulation of PP1 as part of a specific regulatory mechanism, or, more likely, may be explained by an incomplete knockdown efficiency. This important question may be solved in future studies by generating (conditional) knockout cell lines for SDS22 and I3.

3.3 How does I3 regulate SDS22-PP1?

Our findings show that I3 sequesters SDS22-associated PP1, thereby preventing binding of inactive SDS22-PP1 to KNL1 at kinetochores. In addition, we find indications that I3 is involved in regulating the association of SDS22 with PP1. Using gel filtration chromatography of cell lysates, we reveal that large fractions of both SDS22 and I3 exist as a free pool within the cell, while only a portion is bound in a ternary complex with PP1 (Figures 2.7 & 2.9). Moreover, and unexpectedly, we detect an increased association of SDS22 with PP1 upon I3 depletion (Figures 2.8 & 2.9), suggesting that I3 is involved in dissociating SDS22 from PP1. This finding is rather counterintuitive, as interactions of SDS22 and I3 with PP1 were suggested to be most stable when both PiPs are present, based on yeast triple hybrid approaches. (Pedelini et al., 2007; Lesage et al., 2007). Increased association of SDS22 with PP1 in the absence of I3 within the cell may be explained by one of two possible mechanisms. I3 may function as a protein dissociation or exchange factor and directly promote the dissociation of SDS22 from PP1, or, I3 may be required for an SDS22-mediated activation of PP1, possibly functioning as a co-chaperone. In this case, a lack of I3 would prevent an activation of SDS22-bound PP1 and therefore lead to a persistent binding of SDS22 to the inactive PP1 intermediate, while the removal of SDS22 from (activated) PP1 would require additional factor(s). A role of a “protein exchange factor“ has recently been described for Cand1 (cullin-associated and neddylation-dissociated protein 1), a known interactor of Cullin-RING E3 ubiquitin ligases (CRLs) (Pierce et al., 2013). CRLs are multisubunit complexes that are typified by so-called SCF (Skp1, cullin and F box) complexes (Petroski & Deshaies; 2005; Dye & Schulman, 2007). SCF ubiquitin ligases comprise four subunits, namely the scaffold Cul1, the RING domain protein Rbx1 (the E3 ligase), the adaptor Skp1, and an F box protein that functions as a substrate receptor (Petroski & Deshaies; 2005; Dye & Schulman, 2007). Cand1 associates with SCF complexes and thereby directly facilitates the dissociation and dynamic exchange of substrate-specifying Skp1-F box protein subcomplexes, thus regulating the cellular composition of SCF complexes (Pierce et al., 2013). By analogy, I3 might facilitate the dissociation of SDS22 from (activated) PP1, allowing for a dynamic formation of new PP1 holoenzymes. However, a number of findings speak against this hypothesis. Consistent with yeast triple hybrid data (Pedelini et al.,

2007; Lesage et al., 2007), we find overexpression of I3 to cause an increased formation of the SDS22-PP1-I3 complex, with the total of cellular SDS22 being incorporated in the complex (Figure 2.10), suggesting a quite stable interaction. Furthermore, using recombinant proteins, we do not detect a destabilization of the SDS22-PP1 heterodimer upon addition and binding of I3. (Figure 2.11). In contrast, Cand1 and Skp1-F box protein subcomplexes antagonize each other's binding to Cul1-Rbx1 as an excess of Cand1 generally disrupts the formation of SCF complexes within the cell (Pierce et al., 2013). We therefore conclude that I3 most likely does not function as a direct dissociation or exchange factor for SDS22. Alternatively, we propose that I3 may regulate or contribute to an SDS22-mediated activation of PP1, possibly functioning as a co-chaperone. In this scenario, depletion of I3 would lead to persistent SDS22-PP1 binding due to impaired processing and activation of PP1, while the removal of SDS22 from (activated) PP1 would be mediated by other factor(s), most likely p97 complexes (see chapter 3.4). In addition to its RVxF motif, I3 contains another PP1-interaction site between residues 65-77 that is required for I3-mediated inhibition of PP1 *in vitro* and has been suggested to bind at or near the active site of PP1 (Zhang et al., 2008). In contrast to SDS22, *in vitro* binding and inhibition of PP1 by I3 alone does not induce major conformational changes of PP1 (Lesage et al., 2007). These properties of I3 may to a certain extend resemble those of PTPA (PP2A phosphatase activator), a PP2A activation chaperone (Guo et al., 2014). Unlike the PP2A chaperone α4 that binds and stabilizes a latent, partially unfolded PP2A intermediate, PTPA binds and stabilizes an inactive, but properly folded form of PP2A (Jiang et al., 2013; Guo et al., 2014). PTPA makes extensive contacts with structural elements surrounding the active site of PP2A and facilitates recharging of PP2A with catalytic metal ions in an ATP-dependent manner (Guo et al., 2014). α4 and PTPA could therefore act in concert, mediating refolding of PP2A and chelation of catalytic metal ions, respectively (Jiang et al., 2013; Guo et al., 2014). By analogy, one may speculate that SDS22 and I3 may be required together for a (re)activation of PP1, possibly by preventing PP1 misfolding and facilitating chelation of catalytic ions, respectively.

An important open question is whether the PP1 complex formation with SDS22 and I3 is specifically regulated during mitosis. Four residues within the second PP1 interaction site of I3 are phosphorylated during mitosis (Zhang et al., 2008; Dephoure

et al., 2008), suggesting a mitotic regulation of I3 binding to PP1. Interestingly, we observe a substantial loss of both SDS22- and I3-association with PP1 in lysates of nocodazole treated cells (data not shown). This may indicate a mitosis-specific reduction in SDS22-PP1-I3 complex formation, however, given our findings on the importance of SDS22 and I3 in the regulation of kinetochore-associated PP1, this interpretation seems unlikely. An alternative, more plausible explanation could be that SDS22 and I3 may function in PP1 biogenesis and mainly bind newly synthesized PP1. Halted protein synthesis during mitosis and the prolonged metaphase arrest by nocodazole treatment would hence explain the loss of SDS22-PP1-I3 complex formation.

3.4 The role of p97 and its SEP-domain cofactors in regulating the ternary SDS22-PP1-I3 complex

In budding yeast, it is established that the Cdc48/p97 SEP domain-containing cofactor Shp1 (suppressor of high copy PP1) is required for Glc7/PP1 activity and integrity (Zhang et al., 1995; Cheng & Chen, 2010; Böhm & Buchberger, 2013; Cheng & Chen, 2015). Cdc48/p97-Shp1 is essential for Glc7/PP1 function in counteracting Ipl1/Aurora kinase (Cheng & Chen, 2010; Böhm & Buchberger, 2013). Furthermore, *shp1* mutations have been shown to cause an overall loss of Glc7/PP1 catalytic activity (Zhang et al., 1995), impairment in Glc7/PP1 holoenzyme assembly (Böhm & Buchberger, 2013), and misfolding and aggregation of newly synthesized Glc7/PP1 (Cheng & Chen, 2015). The underlying mechanism, however, has remained elusive. Intriguingly, Cdc48/p97-Shp1 transiently binds the Sds22-Glc7/PP1-Ypi1/I3 complex, suggesting that Cdc48/p97-Shp1 may regulate Glc7/PP1 by modulating or remodeling the ternary Glc7/PP1 complex (Cheng & Chen, 2015). We show here that this interaction is conserved in human cells. Using co-immunoprecipitations, we find that the three mammalian Shp1 orthologs p37, UBXD4 and p47 bind the SDS22-PP1-I3 complex (Figure 2.12), although to different extents, and that this interaction is p97-dependent (data not shown). This is consistent with findings by J.W. Harper and colleagues who find both p97 and the SEP domain cofactors p37 and UBXD4 to interact with PP1 catalytic subunits as well as SDS22 and I3 in a mass spectrometry survey (Raman et al., 2015). Importantly, our findings provide an indication that p97 complexes with the SEP domain cofactors p37,

UBXD4 and p47 function in regulating PP1 by dissociating SDS22 from the ternary SDS22-PP1-I3 complex, as we observe an increased association of SDS22 to the PP1 complex in cell lysates depleted of p97 or either of the three Shp1 orthologs, with a complete loss of a monomeric SDS22 fraction upon p97 depletion (Figures 2.13 & 2.14). Taking into account our findings and our model on the role of SDS22 and I3 in regulating PP1, this suggests that p97 SEP domain cofactor-complexes may function in PP1 biogenesis and / or maintenance by segregating SDS22 from the ternary PP1 complex once newly synthesized and / or inactive PP1 has been activated. This is in contrast to a model proposed by Cheng and Chen, which suggests Cdc48/p97-Shp1 to be required for the assembly of the Sds22-Glc7/PP1-Ypi1/I3 complex rather than its disassembly (Cheng & Chen, 2015). Their model is based on findings that *shp1*, as well as *sds22* and *ypi* mutations lead to the misfolding and insoluble aggregation of Glc7/PP1 in the W303 yeast background strain, with Sds22 being absent from these aggregates and remaining in solution (Cheng & Chen, 2015). These findings, however, may also be explained by a requirement of Cdc48/p97-Shp1 for a dissociation of Sds22 from PP1. In this scenario, a lack of functional Cdc48/p97-Shp1 would lead to a persistent binding and sequestration of Sds22 to a fraction of Glc7/PP1. Therefore, newly synthesized and / or inactive Glc7/PP1 would not be processed by Sds22, leading to Glc7/PP1 misfolding and aggregation.

An important open question is whether p97-mediated dissociation of SDS22-PP1(-I3) leads to recycling and / or degradation of the complex components and whether it is ubiquitination-dependent. We do not observe major changes in the cellular level of SDS22, PP1γ and I3 upon depletion of p97 or p37, p47 or UBXD4 (Figure 2.13 A), speaking for an (at least largely) non-degradative dissociation of SDS22 from the ternary PP1 complex by p97. Furthermore, we observe an increase of free monomeric SDS22 upon overexpression of p37 (Figure 2.14 B), supporting the notion of a non-degradative extraction of SDS22 from the PP1 complex. Glc7/PP1 aggregates observed by Cheng and Chen in *shp1*, *sds22*, or *ypi1* mutant yeast cells require the proteasome for clearance, however, total Glc7/PP1 levels are reduced in Shp1-depleted W303 yeast cells, suggesting that Cdc48/p97-Shp1 is not required for the clearance of misfolded Glc7/PP1 (Cheng & Chen, 2015). Thus far, we have been unable to determine which component of the SDS22-PP1-I3 complex mediates the

interaction with p97 (data not shown). Interaction studies in yeast indicate that Cdc48/p97-Shp1 binds the ternary Glc7/PP1 complex via Sds22 (Cheng & Chen, 2015), which would be consistent with a role of Cdc48/p97 in dissociating Sds22 from Glc7/PP1. Cheng and Chen have been unable to detect ubiquitinated forms of Sds22, Ypi1/I3 or Glc7/PP1 and have found the Shp1 UBA domain to be dispensable for a normal cellular localization of Glc7/PP1 and for cell viability, suggesting that Cdc48-Shp1 may act on the Glc7/PP1 complex in a ubiquitin-independent manner (Cheng & Chen, 2015). Furthermore, SDS22, I3 and PP1 have not been detected in a global mass spectrometry screen for protein ubiquitination in HEK293 cells (Xu et al., 2010). However, Glc7/PP1 has been found to be ubiquitinated in two independent mass spectrometry screens in yeast (Peng et al., 2003; Starita et al., 2012). In the case of the related phosphatase PP2A, binding of the chaperone α4 has been shown to stabilize the catalytic subunit and protect it from polyubiquitination and degradation (Jiang et al., 2013; Kong et al., 2009; McConnell et al., 2010). One may speculate that p97 and SDS22 (and I3) may act in concert in a quality control mechanism for PP1 that would lead to either the activation of PP1 and its assembly into different holoenzymes or its ubiquitination-dependent degradation.

While we find indications that p97 SEP domain cofactor-complexes regulate PP1 by dissociating SDS22, we have so far failed to find evidence for a p97 SEP domain cofactor-mediated regulation of PP1 activity at the kinetochore, as we do not observe an increase in Aurora B T232 phosphorylation in cells depleted of either p37, p47 or UBXD4 (data not shown). Furthermore, we do not observe synergistic or additive effects when combining siRNA-mediated depletion of individual p97 SEP domain cofactors with a (partial) inhibition of cellular PP1 (Figure 2.15). This may be due to the relatively mild effect of SEP domain cofactor depletions on SDS22-PP1 association when compared to p97 depletion (Figure 2.13) and may point to (partially) redundant functions of p37, p47 and UBXD4. In the case of Aurora B activity, another possible explanation may be that depletions of SEP domain cofactors might lead to a shift in p97 complex formation towards p97-Ufd1-Npl4. p97-Ufd1-Npl4 is known to extract Aurora B from chromatin (Ramadan et al., 2007; Dobrynin et al., 2011), which could counteract a possible effect on Aurora B activity due to impaired PP1 activity at the kinetochore. Interestingly, depletion of p47, the by far most abundant p97 SEP domain cofactor (Beck et al., 2011) does not exhibit a stronger effect on SDS22-PP1

association than depletions of either p37 or UBXD4 (Figure 2.13). Furthermore, p47 seems to exhibit a lower binding affinity for SDS22-PP1-I3 when compared to p37 and UBXD4 (Figure 2.12) (Raman et al., 2015), suggesting that p47 may play a minor role in regulating the SDS22-PP1-I3 complex. Combined depletions of the SEP domain cofactors and generation of knockout cell lines shall help to better understand the roles of the individual Shp1 orthologs in future studies.

3.5 The role of the p97 SEP-domain cofactors p37 and p47 in mitotic spindle orientation

Whereas we have thus far failed to clarify a possible role of p97 SEP domain cofactors in regulating Aurora B, we have contributed to a study that shows that UBXN-2 in *C. elegans* embryos, as well as p37 and, to a lesser extent, p47 in human cells are involved in the regulation of Aurora A kinase at the centrosome (Kress et al., 2013). Depletion of UBXN-2 in *C elegans* embryos, as well as depletion of p37 in human cells, leads to an increased accumulation of Aurora A at centrosomes during early prophase, accompanied by centrosome maturation and separation defects and aberrant mitotic spindle orientation (Kress et al., 2013). Depletion of p47 did not result in these phenotypes, but aggravated them when co-depleted with p37 (Kress et al., 2013), suggesting that the human p97 SEP domain cofactors may have (only) partially overlapping functions. These findings suggest that CDC-48-UBXN-2 in *C elegans* and p97-p37 in human cells function by dissociating AIR-1/Aurora A kinase from centrosomes during prophase and thus limiting its net recruitment, thereby regulating centrosome maturation and spindle positioning (Kress et al., 2013). In this context, we show that p37 and p47 localize to centrosomes during mitosis (Figure 2.16) and that siRNA-mediated depletion of p37 causes mitotic spindle orientation defects (Figure 2.17 A). This phenotype is specific, as it can be rescued by the expression of an siRNA-resistant p37 variant (Figure 2.17 B). An increase in Aurora A accumulation and, therefore, activity at the centrosome upon p37 depletion may suffice to explain the effect on spindle orientation, as Aurora A is required for correct spindle positioning by controlling cortical targeting of NuMA, an adaptor of the microtubule motor dynein/dynactin and a key regulator of spindle functions (Gallini et al., 2016). Cortical targeting of NuMA requires its Aurora A mediated phosphorylation

and ectopic targeting of NuMA to the cortex restores spindle orientation defects upon Aurora A inhibition (Gallini et al., 2016). Furthermore, also ectopic targeting of NuMA to the cell cortex alone leads to spindle orientation defects, suggesting that Aurora A activity needs to be tightly balanced in order to achieve correct spindle positioning (Gallini et al., 2016). However, an important open question remains whether the p97-p37-mediated regulation of mitotic spindle orientation involves PP1. This seems plausible, since Aurora A and PP1 antagonize each other (Katayama et al., 2001; Ohashi et al., 2006). Furthermore, cortical targeting of NuMA and spindle orientation has been shown to depend on the phosphorylation state of the membrane-actin linkers ezrin/radixin/moesin (ERM) (Machicoane et al., 2014). Interestingly, dephosphorylation of ERM proteins is mediated by PP1 and requires SDS22 (Grusche et al., 2009; Rodrigues et al., 2015), pointing to a possible link of SDS22-regulated PP1 to mitotic spindle orientation.

4 Material and methods

4.1 Cloning

PCR reactions were done using *PfuUltra* II Fusion HS DNA Polymerase (Agilent Technologies) or Phusion® High-Fidelity DNA Polymerase (New England Biolabs, NEB) according to each supplier's protocol. For insertion of point mutations into plasmid DNA, the QuickChange site-directed mutagenesis kit (Agilent Technologies) was used. For restriction digestions, DNA dephosphorylation reactions and DNA ligations, enzymes from NEB were used according to the manufacturer's recommendations. The NucleoSpin® Gel and PCR Clean-up kit (Macherey-Nagel) was used for DNA extraction from agarose gels and for purification of PCR products. For plasmid amplification, chemically competent *E. coli* DH5-α, XL1-blue or TOP10 cells were transformed according to standard procedures. Amplified plasmid DNA was purified using the NucleoSpin® Plasmid kit (Macherey-Nagel) and the NucleoBond® Xtra Maxi kit (Macherey-Nagel). Generated plasmids were verified by control restriction digestion and sequencing (GATC Biotech).

4.2 Plasmids and constructs

Table 4.1 DNA constructs used in this study.

name	vector	insert	tag	species	source	database entry
pcDNA 3.1(+) 3xHA-Strep	pcDNA 3.1(+)		3xHA-Strep		S. Bremer, Essen	614
pcDNA 5/FRT/TO 3xHA-Strep	pcDNA 5/FRT/TO		3xHA-Strep		A. Riemer, Essen	548
pcDNA 5/FRT/TO GFP	pcDNA 5/FRT/TO		GFP		A. Eiteneuer, Essen	506
pcDNA 3.1(+) HA-I3	pcDNA 3.1(+)	I3	HA	human	M. Welti, Zurich	426
pcDNA 3.1(+) HA-I3 VEW41AEA	pcDNA 3.1(+)	I3	HA	human	M. Welti, Zurich	432
pcDNA 5/FRT/TO GFP-I3	pcDNA 5/FRT/TO	I3	GFP	human	A. Eiteneuer, Essen	606
pcDNA 5/FRT/TO GFP-I3 VEW41AEA	pcDNA 5/FRT/TO	I3	GFP	human	A. Eiteneuer, Essen	607
pFH His-I3	pFH	I3	His	human	A. Musacchio, Dortmund	769
pFH His-I3 VEW41AEA	pFH	I3	His	human	this study	977
pFH His-SDS22	pFH	SDS22	His	human	A. Musacchio, Dortmund	771
pEGFP p37-GFP	pEGFP-N3	p37	GFP	mouse	this study	563
pcDNA 5/FRT/TO p37-3xHA-Strep	pcDNA 5/FRT/TO	p37	3xHA-Strep	mouse	this study	564
pcDNA 5/FRT/TO p37-GFP	pcDNA 5/FRT/TO	p37	GFP	mouse	this study	762
pGEX-4T1 GST-p37	pGEX-4T1	p37	GST	mouse	this study	760
pIRES-puro2b p47-3xHA-Strep	pIRES-puro2b	p47	3xHA-Strep	rat	D. Ritz, Zurich	452
pcDNA 5/FRT/TO p47-GFP	pcDNA 5/FRT/TO	p47	GFP	rat	this study	763
pET41 GST-Survivin	pET41	Survivin	GST	human	S. Knauer, Essen	
pOG44	pOG44	Flp-Recombinase			Invitrogen	197
pOPINE anti-GFP nanobody	pOPINE	anti-GFP nanobody	His	camel	M. Bollen, Leuven	765

pFH His-I3VEW41AEA

pFH His-I3VEW41AEA (clone 977) was generated by site-directed mutagenesis of pFH His-I3 (clone 769) with primers 458 and 459 (Table 4.2)

p37 constructs

Mouse p37 cDNA (IMAGE clone 30637967) was amplified by PCR with primers 715 and 717 introducing BamH1 restriction sites at both 3‘ and 5‘ ends. The amplified cDNA was cloned into pEGFP-N3 (Clontech) to generate clone 563. To generate clones 564, 762 and 760, the p37 sequence was subcloned into pcDNA 5/FRT/TO 3xHA-Strep, pcDNA 5/FRT/TO GFP and pGEX-4T1, respectively, using BamH1 restriction sites.

p47 constructs

Rat p47 cDNA (Meyer et al., 2000) was subcloned from clone 452 into the BamH1 site of pcDNA 5/FRT/TO GFP to generate clone 763. To that end, a BamH1 restriction site was introduced at the 3‘ end of the p47 sequence by site-directed mutagenesis with primers 1132 and 1133.

pOPIN anti-GFP nanobody

The bacterial expression vector for anti-GFP nanobodies was a kind gift from M. Bollen and was originally generated by Alexandrov and colleagues (Kubala et al., 2010).

Table 4.2 DNA primers used in this study.

database entry	orientation	sequence
458	for	GCCAGAGAAAAAGGCAGAAGCGACAAGTGACACTG
459	rev	CAGTGTCACTTGTCGCTTCTGCCTTTTTCTCTGGC
715	for	TGACCTGGATCCATGGGGGAGGGTGGCCGT
717	rev	AGTTCATGGATCCTTTTAGCTGTTGGAGTATCACA
1132	for	CAAGCTTCGAATTCGGATCCATGGCGGAGG
1133	rev	CCTCCGCCATGGATCCGAATTCGAAGCTTG

4.3 Antibodies

Antibodies used in this study for immunofluorescence and Western blotting are listed in Table 4.3. Polyclonal antisera to I3 were raised in rabbits against a C-terminal

peptide (aa 115-126 DPSQPPPGPMQH) and affinity-purified (Eurogentec, animal no. SA7263). Polyclonal antisera to p37 were raised in rabbits against a bacterially expressed GST fusion of mouse p37 (BioGenes, animal no. 20880) and affinity purified using AffiGel resin (Bio-Rad) to which GST-p37 was covalently bound.

Table 4.3 Antibodies used for immunofluorescence and Western blotting.

primary antibodies				
antigen	**species**	**dilution IF**	**dilution WB**	**source**
Aurora B	mouse	1:500	-	BD Biosciences, 611082
Aurora B	rabbit	-	1:5000	R. Bruderer, Zurich, serum 55
Aurora B pT232	rabbit	1:1000	1:2500	Rockland, 600-401-677
BubR1	mouse	1:1000	-	Millipore, MAB3612
CREST	human	1:400	-	Antibody Inc, 15-234-0001
GFP	mouse	-	1:500	Roche, 118144600001
HA	mouse	-	1:1000	Covance, clone 16B12
HSC70	mouse	-	1:10000	Santa Cruz, sc-7298
I3	rabbit	-	1:500	this study
NIPP1	rabbit	-	1:500	Sigma-Aldrich, HPA027452
Npl4	rabbit	-	1:500	H. Meyer, HME16, serum
p37	rabbit	-	1:100	this study
p47	rabbit	-	1:2000	H. Meyer, HME22, serum
p97	rabbit	-	1:2000	H. Meyer, HME08, serum
PP1γ	goat	-	1:500	Santa Cruz, sc-6108
SDS22	goat	-	1:500	Santa Cruc, sc-162164
Survivin pT34	rabbit	-	1:2500	Novus Biologicals, NB500-236
Ufd1	mouse	-	1:500	BD Biosciences, 611966
γ-tubulin	mouse	1:200	-	Sigma-Aldrich, clone GTU-88
secondary antibodies				
antigen	**species**	**dilution IF**	**dilution WB**	**source**
mouse IgG Alexa 488	goat	1:500	-	Invitrogen, A11001
mouse IgG Alexa 568	goat	1:500	-	Invitrogen, A11031
mouse IgG Alexa 633	goat	1:500	-	Invitrogen, A21052
rabbit IgG Alexa 568	goat	1:500	-	Invitrogen, A11011
human IgG Alexa 488	goat	1:500	-	Invitrogen, A11013
goat IgG Alexa 633	donkey	-	1:1000	Invitrogen, A21082
mouse IgG HRP	goat	-	1:10000	Bio-Rad, 170-6516
rabbit IgG HRP	goat	-	1:10000	Bio-Rad, 160-6515
goat IgG HRP	mouse	-	1:10000	Santa-Cruz, sc-2354

Anti-GFP nanobodies

Anti-GFP nanobodies were expressed in *E. coli* BL21 and affinity purified with Ni-NTA Superflow beads (Qiagen), followed by preparative gel filtration on a

HiLoad 16/600 Superdex75 prep grade column (GE). Purified nanobodies were covalently coupled to NHS-activated Sepharose 4 Fast Flow (GE) at 2 mg per ml bead slurry.

4.4 Generation and maintenance of cell lines

All human cell lines were maintained in a humidified incubator at 37 °C and 5 % CO_2. HeLa Kyoto and HEK 293 cells were grown in DMEM (PAN Biotech) supplemented with 10 % FCS (PAN Biotech) and 1 % penicillin/streptomycin (PAN Biotech). HeLa Flp-In GFP-NIPP1-fm and GFP-NIPP1-fm+pm cell lines were a kind gift from M. Bollen (Winkler et al., 2015) and were maintained in DMEM supplemented with 10 % tetracycline free FCS (PAN Biotech), 1 % penicillin/streptomycin as well as 200 µg/ml hygromycin B (PAA) and 5 µg/ml blasticidin S (PAA). HeLa Kyoto cells stably expressing full length mouse KNL1 with a C-terminal LAP-tag (Localization and Affinity Purification tag, containing GFP and an S-peptide) from a BAC under control of its endogenous promotor were a kind gift from A. Hyman and were grown in DMEM supplemented with 10 % FCS, 1 % penicillin/streptomycin, 2mM L-glutamine (Thermo Fisher) and 250 µg/ml G418 (PAA). HeLa Flp-In T-Rex GFP-KNL1 (1-250) and HeLa Flp-In T-Rex GFP cells were a kind gift from A. Musacchio (Krenn et al., 2013) and were grown in DMEM supplemented with 10 % tetracycline free FCS, 1 % penicillin/streptomycin, 2 mM L-glutamine and additionally 250 µg/ml hygromycin B and 4 µg/ml blasticidin S. HeLa cells stably expressing GFP-PP1γ were kindly provided by L. Trinkle-Mulcahy (Trinkle-Mulcahy et al., 2003) and grown in DMEM supplemented with 10 % FCS, 1 % penicillin/streptomycin and 200 µg/ml G418. HEK 293 Flp-In cell lines inducibly expressing Strep-HA fusions of p37, p47, UBXD4, UBXD5, Ufd1 and GFP were generated in our laboratory by E. Vamos and J. Hülsmann. These cell lines were maintained in DMEM supplemented with 10 % tetracycline free FCS, 1 % penicillin/streptomycin, 100 µg/ml hygromycin B and 15 µg/ml blasticidin S. A HeLa Kyoto cell line inducibly expressing mouse p37 (HeLa Flp-In $p37^{RNAiRes}$-3xHA-Strep) was generated based on the Flp-In system (Invitrogen). Parental HeLa Flp-In cells stably expressing HA-tagged tetracycline repressor (TetR) and H2B-mCherry (kindly provided by U. Kutay, ETH Zurich) were co-transfected with the pOG44 Flp-recombinase plasmid (Invitrogen) and pcDNA 5/FRT/TO p37-3xHA-Strep in a 9:1 ratio. 24 h post transfection, cells were

selected with 150 µg/ml hygromycin B. Single clones were picked and seeded in 96 well plates and expanded. Inducible expression of mouse p37-3xHA-Strep was verified by Western blotting. The resulting HeLa Flp-In p37^{RNAiRes}-3xHA-Strep cells were maintained in DMEM supplemented with 10 % tetracycline free FCS, 1 % penicillin/streptomycin, 150 µg/ml hygromycin B and 0.5 µg/ml puromycin (Millipore). Transgene expression in all Flp-In cell lines was induced by addition of doxycycline (Sigma-Aldrich) at 1 µg/ml, unless stated otherwise.

4.5 Transfections

HEK 293 cells were DNA transfected at 60–80 % confluence using a $Ca_3(PO_4)_2$ based protocol and grown for 24 h before analysis. For transfection of a 10 cm dish, 10 µg plasmid DNA were diluted in 1095 µl sterile ddH_2O, followed by addition of 155 µl 2 M $CaCl_2$. 1250 µl 2x HBS buffer (270 mM NaCl, 10 mM KCl, 1.5 mM H_2PO_4, 10 mM glucose, 40 mM HEPES, pH 7.05) were added dropwise and mixed by inverting the reaction tube 10 times. Without further incubation, the transfection mix was added dropwise onto the cells. For DNA transfections of HeLa cells, the JetPEI transfection reagent (Polyplus-transfection) was used according to the manufacturer's protocol. HeLa cells were transfected at 50–60 % confluence and grown for 48 h before analysis. 0.5 µg plasmid DNA and 2 µl jetPEI transfection reagent or 7 µg plasmid DNA and 15 µl jetPEI transfection reagent were used for transfections of 22 mm diameter wells (12 well plate) or 10 cm dishes, respectively.

4.6 RNA interference (RNAi) experiments

For RNAi experiments, cells were transfected with siRNAs at 30–40 % confluence using the Lipofectamine RNAiMAX transfection reagent (Invitrogen) according to the manufacturer's instructions. Cells were either seeded one day in advance (forward transfection) or simultaneously with siRNA transfection (reverse transfection). For immunofluorescence experiments, final siRNA concentrations of 10 nM were used with the exception of the sip37_S2 and siControl oligonucleotides (Figure 2.17) that were transfected at a final concentration of 30 nM. For the MTS cell proliferation and viability assay, cells grown in 96 well plates were transfected with final siRNA concentrations of 20 nM. For biochemical analyses, cells grown in 10 cm dishes were

transfected with final siRNA concentrations of 18 nM. Unless otherwise stated, cells were siRNA treated for 48 h before analysis. siRNAs were purchased from Microsynth, Dharmacon (Dharmacon ON-TARGET*plus*) or Qiagen as detailed in Table 4.4 and diluted to 20 µM stock solutions. All siRNA duplexes contained 3‘ dTdT overhangs.

Table 4.4 siRNA oligonucleotides used in this study.

name	target gene	core sequence	source	supplier	database entry
siControl	-	UUCUCCGAACGUGUCACGU	Ritz et al., 2011	Microsynth	714
siLuc	Luciferase	CGUACGCGGAAUACUUCGA	Microsynth	Microsynth	748
siDeath control	n/s	n/s	Qiagen, SI04381048	Qiagen	838
siAurB	Aurora B	GGUGAUGGAGAAUAGCAGU	Hauf et al., 2003	Microsynth	738
siI3_S1	I3	GUAGAAUGGACAAGUGACA	Eiteneuer et al., 2014	Microsynth	718
siI3_S2	I3	CUGCUGUAUUUAUGAGAAA	Eiteneuer et al., 2014	Microsynth	719
siNIPP1	NIPP1	GGAACCUCACAAGCCUCAGCAAAUU	Stealth RNAi™ siRNA sequence, Invitrogen	Microsynth	837
siNpl4_S1	Npl4	CGUGGUGGAGGAUGAGAUU	Dobrynin et al., 2011	Microsynth	737
sip37_S1	p37	GUGCCGUAAUAUAGAGGAA	Dharmacon siRNA library	Dharmacon	1223
sip37_S2	p37	CUCCAGAAGAGGAGGAUAA	Uchiyama et al., 2006	Microsynth	713
sip37_S3	p37	CUUCAAGAGCCCACGGACA	Dharmacon siRNA library	Dharmacon	1225
sip47_S1	p47	AGCCAGCUCUUCCAUCUUA	Dobrynin et al., 2011	Dharmacon	1226
sip47_S3	p47	GGAGAGACCAGUAAACCGA	Dharmacon siRNA library	Dharmacon	1228
sip97_S3	p97	AAGUAGGGUAUGAUGACAUUG	Wójcik et al., 2004	Microsynth	740
sip97_S6	p97	GGAGUUCAAAGUGGUGGAAACAGAU	Shibata et al., 2012	Microsynth	836
siSDS22_S2	SDS22	AGAGUUCUGGAUGAACGACAA	Wurzenberger et al., 2012	Microsynth	671
siUBXD1_S1	UBXD1	CCAGGUGAGAAAGGAACUU	Ritz et al., 2011	Microsynth	591
siUBXD4_S1	UBXD4	AGAAGAGGUGGACGUUAAA	M. Weith, Essen, modified from Qiagen Hs_UBXD4_7	Dharmacon	1229
siUBXD4_S2	UBXD4	GCUCAGUAUAGUAUCAAGA	Dharmacon siRNA library	Dharmacon	1230
siUBXD8_S1	UBXD8	GAAGUUAUUUCACUAAUAA	Suzuki et al., 2012	Microsynth	891
siUfd1_S2	Ufd1	GUGGCCACCUACUCCAAAU	Dobrynin et al., 2011	Microsynth	594

4.7 Immunofluorescence staining

For immunofluorescence experiments, HeLa Kyoto and HeLa Flp-In p37^{RNAiRes}-3xHA-Strep cells were grown on 18 mm glass cover slips in 12 well culture dishes. HeLa Flp-In GFP-NIPP1 cells were grown on poly-L-lysine coated cover slips (Kleinfeld Labortechnik). For fixation, cells were washed with PBS and then fixed with 4 % formaldehyde in PBS for 15 min or with ice-cold methanol (stored at -20 °C) for 5 min at room temperature. Cells were then washed 3 times for 5 min each in PBS and permeabilized in 0.1 % Triton X-100 in PBS for 10 min followed by another 3 washing steps in PBS. For blocking, cells were incubated in 3 % BSA (Applichem, Albumin Fraction V) in PBS for 30-60 min. Then, the cover slips were placed with the cell side down onto drops of primary antibody solution in 3 % BSA in PBS on parafilm in a humidified chamber and incubated for 90 min. Unbound primary antibodies were removed by washing 3 times in PBS. Cells were then incubated in secondary

antibody solution in 3 % BSA in PBS in a humidified chamber for 30 min in the dark followed by 3 washing steps in PBS. Finally, cells were rinsed with ddH_2O to remove residual salts and mounted on microscopy slides in Mowiol containing 0.5 µg/ml DAPI.

4.8 Fluorescence imaging

Spinning disc confocal imaging was performed on a Nikon Eclipse Ti microscope equipped with a Yokogawa CSU X-1 spinning disc unit using a 100x/1.49 NA oil immersion objective. Images were recorded with an Andor iXon X3 EMCCD camera. Confocal laser scanning microscopy was done on a Leica TCS SP5 AOBS system equipped with PMT and HyD detectors and supported by LASAF software (Leica Microsystems). Images were acquired using an HCX PL APO 63×/1.4NA oil immersion objective. Images were processed using ImageJ software.
Z-stack images were acquired at 0.47 to 0.59 µm intervals by spinning disc confocal microscopy (Nikon Eclipse Ti with Yokogawa CSU X-1) using a 100x/1.49 NA oil immersion objective. 3D image reconstruction was performed using Imaris software (Bitplane).

4.9 MTS cell proliferation and viability assay

To assay for cell proliferation and viability, Hela Flp-In GFP-NIPP1-fm or GFP-NIPP1-fm+pm cells were seeded in 96 well culture dishes at $8*10^3$ cells per well while reverse transfecting with siRNAs at a final concentration of 20 nM. Cells were siRNA treated for 72 h before analysis. Transgene expression was induced by addition of doxycycline 24 or 48 h prior to analysis. For detection, cells were incubated with fresh medium supplemented 1:6 with MTS reagent (Promega) for 1 h at 37 °C and the OD 490 nm was measured on a SPECTRAmax® $PLUS^{384}$ microplate spectrophotometer (Molecular Devices) and normalized to untreated controls.

4.10 Preparation of cell extracts

Cell extracts were prepared from cells grown in 10 cm dishes. All steps were performed on ice using ice-cold (4 °C) buffers. Cells were washed once with PBS,

collected by scraping in 250 µl extraction / IP buffer (150 mM KCl, 50 mM Tris pH 7.4; 5 mM $MgCl_2$, 5 % glycerol, 1 % Triton X-100, 2 mM β-mercaptoethanol, supplemented with Roche complete EDTA-free protease inhibitor and Roche PhosSTOP phosphatase inhibitor) and incubated for 20 min. Insoluble material was removed by centrifugation at 17000 x g for 15 min. Supernatants were collected and the protein concentration was measured using a BCA assay (Interchim). For storage, cell extracts were snap frozen in liquid nitrogen and kept at -80 °C. Cell extracts for analysis by gel filtration chromatography were prepared as described above, but using a different extraction buffer (300 mM NaCl, 50 mM Tris pH 7.4, 0.5 % Triton X-100, 1 mM DTT, supplemented with Roche complete EDTA-free protease inhibitor and Roche PhosSTOP phosphatase inhibitor).

4.11 Immunoprecipitation and pull-down assays

For immunoprecipitations and Strep-pulldowns, cell extracts were adjusted to equal protein concentrations (1.3 to 5.9 mg/ml) and volumina in extraction / IP buffer, supplemented with 1 µg/ml BSA (Interchim) and cleared by centrifugation at 17000 x g for 10 min. Input samples were taken. For HA immunoprecipitation, HA antibody was added to the extracts at 1 µg per mg of total protein and incubated for 1.5 h rotating at 4 °C. Then, protein G agarose beads (Millipore) were washed three times with extraction / IP buffer (1 min at 1000 x g at 4 °C) and 30 µl of protein G bead slurry were added per sample and incubated for 1.5 h rotating at 4 °C. For Strep-pulldown or GFP IPs, 30 µl slurry of pre-washed Strep-Tactin sepharose beads (IBA) or anti-GFP nanobody-coupled sepharose beads, respectively, were added to the extracts and incubated for 1.5 h rotating at 4 °C. After incubation, beads were spinned down at 1000 x g for 1 min at 4 °C and flowthrough samples were taken. Beads were washed 3 times with 500 µl extraction / IP buffer (1 min at 1000 x g at 4 °C). After washing, beads were resuspended in 15 µl extraction / IP buffer and 5 µl of 6x SDS loading buffer was added. Proteins were eluted from beads by boiling for 10 min at 95 °C in SDS loading buffer and analyzed by SDS-PAGE and Western blotting.

4.12 Gel filtration chromatography

Gel filtrations were performed with an FPLC ÄKTApurifier 10 system with UPC-900 UV detector and fraction collector (GE) under isocratic conditions at 4 °C using UNICORN control software (GE). Elution of proteins was monitored by absorbance at 280 nm. To estimate the molecular weight of eluted proteins and protein complexes, standard proteins from LMW and HMW Gel Filtration Calibration kits (GE) were used. HeLa cell extracts for analysis by gel filtration chromatography were prepared with an extraction buffer containing 300 mM NaCl, 50 mM Tris pH 7.4, 0.5 % Triton X-100, 1 mM DTT, supplemented with Roche complete EDTA-free protease inhibitor and Roche PhosSTOP phosphatase inhibitor. Cell extracts were adjusted to equal protein concentrations (1.4 to 7.7 mg/ml) and volumina in extraction buffer and cleared by centrifugation at 17000 x g for 15 min before loading onto an equilibrated Superdex 200 10/300 GL gel filtration column (GE) using a 500 µl loop. The loop was oversaturated by injecting 700 µl sample prior to starting the respective run. TBS (150 mM NaCl, 10 mM Tris pH 7.6) supplemented with 10 µM Leupeptin (Sigma-Aldrich), 10 µM Pepstatin A (Sigma-Aldrich) and 20 mM β-glycerophosphate (Calbiochem) was used as running buffer. Samples were eluted at 0.3 ml/min and 250 µl fractions were collected. For analysis by SDS-PAGE and Western blotting, 45 µl per fraction were used. For affinity isolation of GFP-PP1γ from gel filtration peak fractions HMW fractions (fractions 47-53; ~200-100 kDa) and LMW fractions (fractions 53-60; ~90-45 kDa), respectively, were pooled (80 µl per fraction) and supplemented 1:4 with a 4x IP buffer (150 mM NaCl, 170 mM Tris pH 7.4, 20 % glycerol, 4 % Triton X-100, 8 mM β-mercaptoethanol, 4x Roche complete EDTA-free protease inhibitor), followed by GFP IP with anti-GFP nanobodies coupled to sepharose beads. To assay for interaction of I3 with SDS22-PP1, 1.2 µM recombinant SDS22-PP1 heterodimer purified from *Trichoplusia ni* Tnao38 cells (kindly provided by A. Musacchio, MPI Dortmund) was incubated for 30 min on ice either alone or with a ~7 fold excess of either His-I3 wt or His-I3 VEW41AEA purified from *Spodoptera frugiperda* Sf9 cells in a 50 µl volume in a buffer containing 500 mM NaCl, 20 mM Tris pH 7.9 and 1 mM DTT. Samples were loaded onto an equilibrated Superdex 200 Increase 5/150 GL gel filtration column (GE) using a 15 µl loop. The loop was oversaturated by injecting 30 µl sample prior to starting the respective run. 500 mM NaCl, 20 mM Tris pH 7.9 with 1 mM DTT was used as running buffer.

After 0.3 column volumes 60 µl fractions were collected. 20 µl per fraction were analysed by SDS-PAGE and Western blotting.

4.13 SDS-PAGE and Western blotting

Protein samples were separated by size with standard SDS-PAGE methods using a Tris/glycine/SDS running buffer (200 mM glycine, 25 mM Tris-HCl pH 8.8, 0.1 % SDS) and the Mini-PROTEAN Tetra Cell or Protean II xi Cell systems (Bio-Rad). Samples were run at constant current of 10 to 20 mA per gel. The gels were either stained with Coomassie or used for Western blotting. Western blotting was performed using semi-dry Trans-Blot SD transfer chambers (Bio-Rad). Proteins were blotted onto nitrocellulose membranes (Hybond-C Extra, Amersham) for 1 h at a constant current of 120 mA per gel (300 mA for large Protean II xi gels) using Tris/glycine/SDS running buffer supplemented with 20 % methanol as blotting buffer. Equal protein loading and transfer was verified by Ponceau S staining. Membranes were blocked for 1 h at room temperature in 10 % fat free milk in PBS-T (PBS with 0.05 % Tween 20) or TBS-T (TBS with 0.1 % Tween 20) when probing with phospho-specific antibodies. After blocking, membranes were washed twice for 5 min in PBS-T or TBS-T and incubated in primary antibody dilutions in 3 % BSA in PBS-T or TBS-T over night at 4 °C. Membranes were then washed 3 times for 5 min in PBS-T or TBS-T before incubating in HRP coupled secondary antibodies diluted in 3 % BSA in PBS-T or TBS-T for 1 h at room temperature. Before detection, membranes were again washed 4 times for 5 min in PBS-T or TBS-T. For detection, membranes were incubated for 3 min with SuperSignal West Pico or SuperSignal West Femto enhanced chemiluminescence (ECL) substrates (Thermo Fisher). Light signals were detected on Super RX films (FUJIFILM). Films were developed using a Cawomat 200 IR developing machine (Cawo) and digitalized using a ScanMaker i480 film scanner (Microtek). For detection with a Typhoon FLA 9000 imager (GE), fluorescence-labelled secondary antibodies (Alexa Fluor 633 donkey anti-goat) were used.

4.14 Expression and purification of recombinant proteins

4.14.1 Protein expression and purification from *E. coli*

Recombinant GST-p37 and GST-Survivin were expressed in *E. coli* BL21 and purified by affinity chromatography. Recombinant autophosphorylated Aurora B in complex with the activating IN-box segment of inner centromere protein (INCENP) purified as described (Santaguida et al., 2010) was kindly provided by A. Musacchio, MPI Dortmund.

GST-p37 (for antibody production)

E. coli BL21(DE3)RIL cells were transformed with the GST-p37 expression construct (clone 760) and grown to an OD_{600} of ~0.7 at 37 °C. Expression was induced with 0.4 mM IPTG and carried out at 18 °C for 16 h. Cells were harvested at 3900 x g for 15 min and resuspended in a lysis buffer (PBS supplemented with 1 mM DTT and 0.1 mM PMSF). Cells were lysed using a microfluidizer and cellular debris was removed by centrifugation at 47810 x g for 20 min. Cleared lysate was applied to an equilibrated glutathione-sepharose 4B (GE) gravity flow column. The column was washed with 15 volumes lysis buffer and eluted with lysis buffer supplemented with 20 mM glutathione. Purity of elution fractions was tested by SDS-PAGE and Coomassie staining and protein concentrations were measured by Bradford assay (Bio-Rad). GST-p37 diluted to 1 mg/ml in PBS was used for immunization of rabbits (BioGenes).

GST-Survivin

E. coli BL21 cells harboring the pET41 GST-Survivin plasmid (kindly provided by S. Knauer, University of Duisburg-Essen) were grown to an OD_{600} of ~0.7 at 37 °C. Expression was induced with 1 mM IPTG and carried out at 30 °C for 7 h. Cells were harvested at 3900 x g for 15 min and resuspended in a lysis buffer (150 mM Nacl, 50 mM Tris pH 7.5, 1 mM DTT 1 mM PMSF). Cells were lysed by sonication and cellular debris was removed by centrifugation at 47810 x g for 45 min. Cleared lysate was loaded onto an equilibrated 5 ml GSTrap FF column (GE). The column was washed with 60 volumes lysis buffer and eluted with lysis buffer supplemented with 20 mM glutathione. Purity of elution fractions was tested by SDS-PAGE and Coomassie

staining. Protein was concentrated to about 1 mg/ml using VivaSpin20 concentrators with a molecular weight cut-off of 5 kDa (Sartorius). Protein concentration was determined with a NanoDrop spectrophotometer (NanoDrop Technologies) by measurement of the absorbance at 280 nm using an extinction coefficient of 59360 M^{-1} cm^{-1}. For *in vitro* phosphorylation at T34 by CDK1-cyclin B, buffer was exchanged to kinase buffer (50 mM Tris pH 7.5, 10 mM $MgCl_2$, 0.1 mM EDTA, 1 mM DTT) using 2 ml Zeba Spin desalting columns (Thermo Scientific).

4.14.2 Protein expression and purification from insect cells (Baculovirus system)

Virus generation and expression

Proteins that failed to be expressed and purified in good yields from *E. coli* were expressed and purified from cultured insect cells using the baculovirus-based MultiBac expression vector system (Berger et al., 2004; Fitzgerald et al., 2006; Trowitzsch et al., 2010). This system is based on the integration of gene(s) of interest into a baculoviral genome using Tn7 transposition and / or Cre-*loxP* recombination. Expression vectors were generated by transforming transfer plasmids harboring the gene(s) of interest into an *E. coli* strand containing a modified baculovirus genome on a bacterial artificial chromosome (MultiBac bacmid) into which the gene(s) of interest can be integrated through homologous recombination. Expression viruses were generated and amplified by transfecting bacmids into *Spodoptera frugiperda* Sf9 cells and proteins were expressed and purified from *Spodoptera frugiperda* Sf9 cells or *Trichoplusia ni* Tnao38 cells. pFH transfer plasmids (Fitzgerald et al., 2006; Trowitzsch et al., 2010) containing sequences for His-SDS22 and His-I3 were kindly provided by A. Musacchio (MPI Dortmund). pFH His-I3 VEW41AEA was generated by site directed mutagenesis. Bacmids were produced as described (Trowitzsch et al., 2010). pFH transfer plasmids were transformed into chemically competent *E. coli* DH10EMBacY cells (kindly provided by A. Musacchio, MPI Dortmund) according to standard protocol but with an extended recovery time at 37 °C of 6 h. Transformed cells were plated on LB agar plates with 50 µg/ml kanamycin, 10 µg/ml tetracycline, 7 µg/ml gentamycin, 40 µg/ml IPTG and 100 µg/ml X-Gal. *E. coli* DH10EMBacY contains a helper plasmid that expresses the Tn7 transposon complex upon induction with IPTG. Positive integration events were identified

through blue/white selection. Single positive white clones were used for bacmid amplification in LB medium supplemented with 50 µg/ml kanamycin, 10 µg/ml tetracycline and 7 µg/ml gentamycin. Amplified bacmid DNA was purified using the NucleoSpin® Plasmid kit (Macherey-Nagel), but instead of loading the DNA onto NucleoSpin® Plasmid column, bacmid DNA was precipitated with 50 % isopropanol at -20 °C over night, washed with 70 % ethanol and resuspended in 40 µl sterile TE buffer. *S. frugiperda* Sf9 cells (Invitrogen) were maintained in Sf900^{TM} III serum free medium (Gibco) in adherent and suspension culture at 27 °C according to the supplier's instructions. For virus generation, Sf9 cells seeded in 30 mm diameter wells (6 well plate) at a density of 1*10^6 cells/ml were transfected with bacmid DNA with FuGENE® HD transfection reagent (Promega) according to the manufacturer's instructions using 20 µl bacmid DNA and 5 µl transfection reagent. Viruses were amplified in a three step process in adherent culture in 10 cm dishes (V_0) and in 50 ml suspension cultures (V_1 and V_2), respectively. V_0 and V_1 virus stocks (supernatants of the amplification cultures) were supplemented with 10 % BSA and stored at 4 °C. Production of recombinant proteins was tested by small scale affinity chromatography using the cells from the V_0 culture. V_2 viruses were always prepared freshly and used completely for infection of large scale expression cultures of Sf9 or Tnao38 cells. For protein expression, Sf9 or Tnao38 cells were seeded at 1*10^6 cells/ml in 500 to 1300 ml suspension cultures and V_2 virus was added in an ~1:20 ratio. Expression cultures were incubated at 27 °C and 115 rpm for 48 to 96 h. Cells were harvested for 15 min at 2300 x g and washed in cold PBS for 10 min at 1000 x g. Cells from a 1000 ml expression culture were split into 3 parts before pelleting. Pellets were stored at -80 °C.

His-I3 (wild type & VEW41AEA)

His-tagged I3 (wild type and VEW41AEA) was expressed in Sf9 cells. Pellets were resuspended in 100 ml lysis buffer (200 mM NaCl, 20 mM Tris pH 7.9, 15 mM imidazole, 1 % Triton X-100, 0.5 mM DTT, 0.5 mM PMSF) and lysed by sonication. The relatively low salt concentration was used for lysis to avoid precipitation of endogenous actin. Lysates were cleared by centrifugation at 47810 x g for 45 min followed by filtration through a 0.8 µm filter. Cleared lysates were loaded onto an equilibrated 5 ml HisTrap FF crude column (GE) followed by washing with 5 column volumes of lysis buffer. Since I3 formed aggregates when purified in low salt buffer,

all following purification steps were performed with high salt buffer. The column was washed again with 80 volumes of wash buffer (500 mM NaCl, 20 mM Tris pH 7.9, 15 mM imidazole, 1 % Triton X-100, 0.5 mM DTT) followed by elution with a 50 ml linear 15 to 300 mM imidazole gradient. Elution fractions were tested for recombinant I3 by SDS-PAGE and Coomassie staining. Pooled fractions were concentrated using VivaSpin20 concentrators with a molecular weight cut-off of 5 kDa (Sartorius) and loaded onto an equilibrated HighLoad Superdex 75 16/600 gel filtration column (GE). 500 mM NaCl, 20 mM Tris pH 7.9, 1 % Triton X-100, 1 mM DTT was used as running buffer. Fractions containing His-I3 were concentrated, snap frozen in liquid nitrogen and stored at -80 °C. The concentration of His-I3 VEW41AEA was determined with a NanoDrop spectrophotometer (NanoDrop Technologies) by measurement of the absorbance at 280 nm using an extinction coefficient of 1490 M^{-1} cm^{-1}. The concentration of His-I3 wild type was not measurable with a spectrophotometer due to a lower yield and the absorbance of Triton X-100 in the buffer. Therefore, the His-I3 wild type concentration was estimated on the basis of Coomassie staining intensity. To that end, Coomassie gels were scanned with an Odysse® Clx imaging system (LI-COR biosciences). Band intensities of His-I3 wild type and His-I3 VEW41AEA were quantified using ImageJ software and the His-I3 wild type band intensity was compared to His-I3 VEW41AEA.

His-SDS22

Pellets of Tnao38 cells expressing His-SDS22 were kindly provided by A. Musacchio (MPI Dortmund). Pellets were resuspended in 100 ml lysis buffer (300 mM KCl, 50 mM HEPES pH 7.5, 0.05 % Tween 20, 15 mM imidazole, 1 mM DTT) and lysed by sonication. Lysates were cleared by centrifugation at 47810 x g for 45 min followed by filtration through a 0.8 µm filter. Cleared lysates were loaded onto an equilibrated 5 ml HisTrap FF crude column (GE) followed by washing with 80 column volumes of lysis buffer and elution with 300 mM imidazole. Fractions containing His-SDS22 were concentrated using VivaSpin20 concentrators with a molecular weight cut-off of 10 kDa (Sartorius), loaded onto a 1 ml MonoQ 5/50 GL anion exchange column equilibrated with low salt buffer (50 mM KCl, 50 mM HEPES pH 7.5, 1 mM DTT) and eluted with a 30 ml linear 50 to 1000 mM salt gradient. Fractions containing His-SDS22 were concentrated and further purified by preparative gel filtration on a Superdex 200 10/300 GL gel filtration column (GE). 300 mM KCl, 50 mM HEPES pH

7.5, 0.05 % Tween 20, 1 mM DTT was used as running buffer. His-SDS22 was concentrated, snap frozen in liquid nitrogen and stored at -80 °C. Protein concentration was determined with a NanoDrop spectrophotometer (NanoDrop Technologies) by measurement of the absorbance at 280 nm using an extinction coefficient of 24410 M^{-1} cm^{-1}.

SDS22-PP1

The heterodimeric SDS22-PP1 complex expressed from a bicistronic baculovirus vector in Tnao38 cells was kindly provided by A. Musacchio (MPI Dortmund). The His-tag on SDS22 used for affinity purification of the heterodimer had been subsequently removed by TEV protease cleavage.

4.15 *In vitro* dephosphorylation assays

Recombinant autophosphorylated GST-tagged Aurora B in complex with the activating IN-box segment of inner centromere protein (INCENP) was purified as described (Santaguida et al., 2010) (kindly provided by A. Musacchio, MPI Dortmund). GST-Survivin purified from *E. coli* was phosphorylated *in vitro* with purified CDK1-cyclin B (kindly provided by Y. Wang, University of Michigan) (200 µg CDK1-cyclin B per mg GST-Survivin) in 50 mM Tris pH 7.5, 10 mM $MgCl_2$, 0.1 mM EDTA, 1 mM DTT supplemented with 2 mM ATP at 30 °C for 30 min and re-purified by affinity chromatography with a 5 ml GSTrap FF column (GE). For specificity assays, 12.5 pmol of Aurora B or GST-Survivin was incubated with 0.33 or 1.67 pmol recombinant PP1 (NEB) or with 40 pmol λ phosphatase (NEB) in 1x NEBuffer for PMP supplemented with 1 mM $MnCl_2$ at 30 °C for 15 min in a reaction volume of 10 to 12 µl. For time-course inhibition experiments, 0.33 pmol recombinant PP1 was pre-incubated with or without 4.17 pmol recombinant SDS22 purified from Tnao38 cells for 5 min at 30 °C before adding to 12.5 pmol of autophosphorylated Aurora B in a total reaction volume of 50 µl in 1x NEBuffer for PMP supplemented with 1 mM $MnCl_2$ and incubating at 30 °C. At 0-, 5-, 10-, 20-, and 30-min time points, 10 µl samples were taken for analysis by SDS-PAGE and Western blotting. To assay for dose dependency, 2.5 pmol of autophosphorylated Aurora B was incubated with 0.067 pmol recombinant PP1 without or with the indicated concentrations of SDS22 in 10 µl reaction volume at 30 °C for 15 min before stopping reactions in SDS sample

buffer. Equivalent inhibition experiments were done by M. Beullens (KU Leuven), using PP1 purified from rabbit skeletal muscle. Since this PP1 was less active than recombinant PP1 from NEB, a higher concentration (40 nM) was used in these experiments. 3 independent experiments were analyzed by Western blotting with phospho-specific antibodies and visualized with ECL reagent on a LAS400 imaging system (GE). Signal intensities were quantified with ImageJ software and normalized by subtracting the pT232 signal of Aurora B dephosphorylated by PP1 in the absence of SDS22 (normalized Aurora B pT232 signal = 0) followed by setting the pT232 signal of maximally phosphorylated Aurora B (500 nM SDS22) to 1. The normalized PP1 activity was determined by subtracting the normalized Aurora B pT232 signal from 1. The data points were fitted with a variable slope dose-response equation using GraphPad Prism 5 software.

4.16 Quantification and statistics

Fluorescence intensities were quantified using the automated image analysis software CellProfiler (Carpenter et al., 2006). DAPI and CREST signals were used to identify primary objects in order to measure fluorescence signals on chromatin and / or kinetochores. Statistical analyses were done with SigmaPlot software (Systat) using Mann-Whitney *U* test or Fisher's exact test. Values of $p \leq 0.05$ (*), $p \leq 0.01$ (**), $p \leq 0.001$ (***) and $p \leq 0.0001$ (****) were considered statistically significant. Box plots show median, lower and upper quartiles (line and box), 10^{th} and 90^{th} percentiles (whiskers) and outliers (●). Western blot signal intensities were quantified using ImageJ software.

References

Adams, R. R., Maiato, H., Earnshaw, W. C. & Carmena, M. (2001) Essential roles of Drosophila inner centromere protein (INCENP) and aurora B in histone H3 phosphorylation, metaphase chromosome alignment, kinetochore disjunction, and chromosome segregation. J Cell Biol 153, 865-880.101

Adams, R. R., Wheatley, S. P., Gouldsworthy, A. M., Kandels-Lewis, S. E., Carmena, M., Smythe, C., Gerloff, D. L. & Earnshaw, W. C. (2000) INCENP binds the Aurora-related kinase AIRK2 and is required to target it to chromosomes, the central spindle and cleavage furrow. Curr Biol 10, 1075-1078.105

Ahonen, L. J., Kukkonen, A. M., Pouwels, J., Bolton, M. A., Jingle, C. D., Stukenberg, P. T. & Kallio, M. J. (2009) Perturbation of Incenp function impedes anaphase chromatid movements and chromosomal passenger protein flux at centromeres. Chromosoma 118, 71-84.169

Ainsztein, A. M., Kandels-Lewis, S. E., Mackay, A. M. & Earnshaw, W. C. (1998) INCENP centromere and spindle targeting: identification of essential conserved motifs and involvement of heterochromatin protein HP1. J Cell Biol 143, 1763-1774.109

Alushin, G. M., Ramey, V. H., Pasqualato, S., Ball, D. A., Grigorieff, N., Musacchio, A. & Nogales, E. (2010) The Ndc80 kinetochore complex forms oligomeric arrays along microtubules. Nature 467, 805-810.150

Andreassen, P. R., Lacroix, F. B., Villa-Moruzzi, E. & Margolis, R. L. (1998) Differential subcellular localization of protein phosphatase-1 alpha, gamma1, and delta isoforms during both interphase and mitosis in mammalian cells. J Cell Biol 141, 1207-1215.231

Andrews, P. D., Ovechkina, Y., Morrice, N., Wagenbach, M., Duncan, K., Wordeman, L. & Swedlow, J. R. (2004) Aurora B regulates MCAK at the mitotic centromere. Dev Cell 6, 253-268.159

Asteriti, I. A., Di Cesare, E., De Mattia, F., Hilsenstein, V., Neumann, B., Cundari, E., Lavia, P. & Guarguaglini, G. (2014) The Aurora-A inhibitor MLN8237 affects multiple

mitotic processes and induces dose-dependent mitotic abnormalities and aneuploidy. Oncotarget 5, 6229-6242.219

Banerjee, S., Bartesaghi, A., Merk, A., Rao, P., Bulfer, S. L., Yan, Y., Green, N., Mroczkowski, B., Neitz, R. J., Wipf, P. et al. (2016) 2.3 A resolution cryo-EM structure of human p97 and mechanism of allosteric inhibition. Science 351, 871-875.322

Barford, D., Das, A. K. & Egloff, M. P. (1998) The structure and mechanism of protein phosphatases: insights into catalysis and regulation. Annu Rev Biophys Biomol Struct 27, 133-164.249

Barr, A. R. & Gergely, F. (2007) Aurora-A: the maker and breaker of spindle poles. J Cell Sci 120, 2987-2996.197

Barros, T. P., Kinoshita, K., Hyman, A. A. & Raff, J. W. (2005) Aurora A activates D-TACC-Msps complexes exclusively at centrosomes to stabilize centrosomal microtubules. J Cell Biol 170, 1039-1046.211

Bassett, E. A., Wood, S., Salimian, K. J., Ajith, S., Foltz, D. R. & Black, B. E. (2010) Epigenetic centromere specification directs aurora B accumulation but is insufficient to efficiently correct mitotic errors. J Cell Biol 190, 177-185.117

Bayliss, R., Sardon, T., Vernos, I. & Conti, E. (2003) Structural basis of Aurora-A activation by TPX2 at the mitotic spindle. Mol Cell 12, 851-862.199

Beardmore, V. A., Ahonen, L. J., Gorbsky, G. J. & Kallio, M. J. (2004) Survivin dynamics increases at centromeres during G2/M phase transition and is regulated by microtubule-attachment and Aurora B kinase activity. J Cell Sci 117, 4033-4042.167

Beck, M., Schmidt, A., Malmstroem, J., Claassen, M., Ori, A., Szymborska, A., Herzog, F., Rinner, O., Ellenberg, J. & Aebersold, R. (2011) The quantitative proteome of a human cell line. Mol Syst Biol 7, 549.295

Berdnik, D. & Knoblich, J. A. (2002) Drosophila Aurora-A is required for centrosome maturation and actin-dependent asymmetric protein localization during mitosis. Curr Biol 12, 640-647.207

Berdougo, E., Nachury, M. V., Jackson, P. K. & Jallepalli, P. V. (2008) The nucleolar phosphatase Cdc14B is dispensable for chromosome segregation and mitotic exit in human cells. Cell Cycle 7, 1184-1190.226

Berger, I., Fitzgerald, D. J. & Richmond, T. J. (2004) Baculovirus expression system for heterologous multiprotein complexes. Nat Biotechnol 22, 1583-1587.345

Beullens, M., Van Eynde, A., Stalmans, W. & Bollen, M. (1992) The isolation of novel inhibitory polypeptides of protein phosphatase 1 from bovine thymus nuclei. J Biol Chem 267, 16538-16544.346

Beuron, F., Dreveny, I., Yuan, X., Pye, V. E., McKeown, C., Briggs, L. C., Cliff, M. J., Kaneko, Y., Wallis, R., Isaacson, R. L. et al. (2006) Conformational changes in the AAA ATPase p97-p47 adaptor complex. EMBO J 25, 1967-1976.293

Bharucha, J. P., Larson, J. R., Gao, L., Daves, L. K. & Tatchell, K. (2008) Ypi1, a positive regulator of nuclear protein phosphatase type 1 activity in Saccharomyces cerevisiae. Mol Biol Cell 19, 1032-1045.242

Black, B. E. & Cleveland, D. W. (2011) Epigenetic centromere propagation and the nature of CENP-a nucleosomes. Cell 144, 471-479.60

Bohm, S. & Buchberger, A. (2013) The budding yeast Cdc48(Shp1) complex promotes cell cycle progression by positive regulation of protein phosphatase 1 (Glc7). PLoS One 8, e56486.25

Bollen, M., Gerlich, D. W. & Lesage, B. (2009) Mitotic phosphatases: from entry guards to exit guides. Trends Cell Biol 19, 531-541.39

Bollen, M., Peti, W., Ragusa, M. J. & Beullens, M. (2010) The extended PP1 toolkit: designed to create specificity. Trends Biochem Sci 35, 450-458.227

Bruderer, R. M., Brasseur, C. & Meyer, H. H. (2004) The AAA ATPase p97/VCP interacts with its alternative co-factors, Ufd1-Npl4 and p47, through a common bipartite binding mechanism. J Biol Chem 279, 49609-49616.272

Carmena, M., Ruchaud, S. & Earnshaw, W. C. (2009) Making the Auroras glow: regulation of Aurora A and B kinase function by interacting proteins. Curr Opin Cell Biol 21, 796-805.97

Carmena, M., Wheelock, M., Funabiki, H. & Earnshaw, W. C. (2012) The chromosomal passenger complex (CPC): from easy rider to the godfather of mitosis. Nat Rev Mol Cell Biol 13, 789-803.99

Carpenter, A. E., Jones, T. R., Lamprecht, M. R., Clarke, C., Kang, I. H., Friman, O., Guertin, D. A., Chang, J. H., Lindquist, R. A., Moffat, J. et al. (2006) CellProfiler: image analysis software for identifying and quantifying cell phenotypes. Genome Biol 7, R100.34

Carvalho, A., Carmena, M., Sambade, C., Earnshaw, W. C. & Wheatley, S. P. (2003) Survivin is required for stable checkpoint activation in taxol-treated HeLa cells. J Cell Sci 116, 2987-2998.102

Cazales, M., Schmitt, E., Montembault, E., Dozier, C., Prigent, C. & Ducommun, B. (2005) CDC25B phosphorylation by Aurora-A occurs at the G2/M transition and is inhibited by DNA damage. Cell Cycle 4, 1233-1238.205

Cesario, J. M., Jang, J. K., Redding, B., Shah, N., Rahman, T. & McKim, K. S. (2006) Kinesin 6 family member Subito participates in mitotic spindle assembly and interacts with mitotic regulators. J Cell Sci 119, 4770-4780.176

Ceulemans, H. & Bollen, M. (2004) Functional diversity of protein phosphatase-1, a cellular economizer and reset button. Physiol Rev 84, 1-39.1

Ceulemans, H., Stalmans, W. & Bollen, M. (2002a) Regulator-driven functional diversification of protein phosphatase-1 in eukaryotic evolution. Bioessays 24, 371-381.20

Ceulemans, H., Vulsteke, V., De Maeyer, M., Tatchell, K., Stalmans, W. & Bollen, M. (2002b) Binding of the concave surface of the Sds22 superhelix to the alpha 4/alpha 5/alpha 6-triangle of protein phosphatase-1. J Biol Chem 277, 47331-47337.252

Chan, C. S. & Botstein, D. (1993) Isolation and characterization of chromosome-gain and increase-in-ploidy mutants in yeast. Genetics 135, 677-691.98

Chan, Y. W., Jeyaprakash, A. A., Nigg, E. A. & Santamaria, A. (2012) Aurora B controls kinetochore-microtubule attachments by inhibiting Ska complex-KMN network interaction. J Cell Biol 196, 563-571.158

Cheeseman, I. M., Anderson, S., Jwa, M., Green, E. M., Kang, J., Yates, J. R., 3rd, Chan, C. S., Drubin, D. G. & Barnes, G. (2002) Phospho-regulation of kinetochore-microtubule attachments by the Aurora kinase Ipl1p. Cell 111, 163-172.155

Cheeseman, I. M., Chappie, J. S., Wilson-Kubalek, E. M. & Desai, A. (2006) The conserved KMN network constitutes the core microtubule-binding site of the kinetochore. Cell 127, 983-997.149

Cheeseman, I. M. & Desai, A. (2008) Molecular architecture of the kinetochore-microtubule interface. Nat Rev Mol Cell Biol 9, 33-46.46

Cheng, Y. L. & Chen, R. H. (2010) The AAA-ATPase Cdc48 and cofactor Shp1 promote chromosome bi-orientation by balancing Aurora B activity. J Cell Sci 123, 2025-2034.24

Cheng, Y. L. & Chen, R. H. (2015) Assembly and quality control of the protein phosphatase 1 holoenzyme involves the Cdc48-Shp1 chaperone. J Cell Sci 128, 1180-1192.27

Chou, T. F., Brown, S. J., Minond, D., Nordin, B. E., Li, K., Jones, A. C., Chase, P., Porubsky, P. R., Stoltz, B. M., Schoenen, F. J. et al. (2011) Reversible inhibitor of p97, DBeQ, impairs both ubiquitin-dependent and autophagic protein clearance pathways. Proc Natl Acad Sci U S A 108, 4834-4839.285

Ciferri, C., Pasqualato, S., Screpanti, E., Varetti, G., Santaguida, S., Dos Reis, G., Maiolica, A., Polka, J., De Luca, J. G., De Wulf, P. et al. (2008) Implications for kinetochore-microtubule attachment from the structure of an engineered Ndc80 complex. Cell 133, 427-439.148

Claessen, J. H., Kundrat, L. & Ploegh, H. L. (2012) Protein quality control in the ER: balancing the ubiquitin checkbook. Trends Cell Biol 22, 22-32.280

Collette, K. S., Petty, E. L., Golenberg, N., Bembenek, J. N. & Csankovszki, G. (2011) Different roles for Aurora B in condensin targeting during mitosis and meiosis. J Cell Sci 124, 3684-3694.141

Cooke, C. A., Heck, M. M. & Earnshaw, W. C. (1987) The inner centromere protein (INCENP) antigens: movement from inner centromere to midbody during mitosis. J Cell Biol 105, 2053-2067.107

Coudreuse, D. & Nurse, P. (2010) Driving the cell cycle with a minimal CDK control network. Nature 468, 1074-1079.41

Dai, J. & Higgins, J. M. (2005) Haspin: a mitotic histone kinase required for metaphase chromosome alignment. Cell Cycle 4, 665-668.118

DeLaBarre, B. & Brunger, A. T. (2003) Complete structure of p97/valosin-containing protein reveals communication between nucleotide domains. Nat Struct Biol 10, 856-863.264

DeLaBarre, B. & Brunger, A. T. (2005) Nucleotide dependent motion and mechanism of action of p97/VCP. J Mol Biol 347, 437-452.320

DeLuca, J. G., Gall, W. E., Ciferri, C., Cimini, D., Musacchio, A. & Salmon, E. D. (2006) Kinetochore microtubule dynamics and attachment stability are regulated by Hec1. Cell 127, 969-982.147

DeLuca, K. F., Lens, S. M. & DeLuca, J. G. (2011) Temporal changes in Hec1 phosphorylation control kinetochore-microtubule attachment stability during mitosis. J Cell Sci 124, 622-634.162

Dephoure, N., Zhou, C., Villen, J., Beausoleil, S. A., Bakalarski, C. E., Elledge, S. J. & Gygi, S. P. (2008) A quantitative atlas of mitotic phosphorylation. Proc Natl Acad Sci U S A 105, 10762-10767.251

Deshaies, R. J. (2014) Proteotoxic crisis, the ubiquitin-proteasome system, and cancer therapy. BMC Biol 12, 94.309

Ditchfield, C., Johnson, V. L., Tighe, A., Ellston, R., Haworth, C., Johnson, T., Mortlock, A., Keen, N. & Taylor, S. S. (2003) Aurora B couples chromosome alignment with anaphase by targeting BubR1, Mad2, and Cenp-E to kinetochores. J Cell Biol 161, 267-280.191

Dobrynin, G., Popp, O., Romer, T., Bremer, S., Schmitz, M. H., Gerlich, D. W. & Meyer, H. (2011) Cdc48/p97-Ufd1-Npl4 antagonizes Aurora B during chromosome segregation in HeLa cells. J Cell Sci 124, 1571-1580.173

Douglas, M. E., Davies, T., Joseph, N. & Mishima, M. (2010) Aurora B and 14-3-3 coordinately regulate clustering of centralspindlin during cytokinesis. Curr Biol 20, 927-933.179

Du, J., Kelly, A. E., Funabiki, H. & Patel, D. J. (2012) Structural basis for recognition of H3T3ph and Smac/DIABLO N-terminal peptides by human Survivin. Structure 20, 185-195.123

Dunphy, W. G. (1994) The decision to enter mitosis. Trends Cell Biol 4, 202-207.43

Dutertre, S., Cazales, M., Quaranta, M., Froment, C., Trabut, V., Dozier, C., Mirey, G., Bouche, J. P., Theis-Febvre, N., Schmitt, E. et al. (2004) Phosphorylation of CDC25B by Aurora-A at the centrosome contributes to the G2-M transition. J Cell Sci 117, 2523-2531.204

Dye, B. T. & Schulman, B. A. (2007) Structural mechanisms underlying posttranslational modification by ubiquitin-like proteins. Annu Rev Biophys Biomol Struct 36, 131-150.329

Eiteneuer, A., Seiler, J., Weith, M., Beullens, M., Lesage, B., Krenn, V., Musacchio, A., Bollen, M. & Meyer, H. (2014) Inhibitor-3 ensures bipolar mitotic spindle attachment by limiting association of SDS22 with kinetochore-bound protein phosphatase-1. EMBO J 33, 2704-2720.7

Elowe, S., Dulla, K., Uldschmid, A., Li, X., Dou, Z. & Nigg, E. A. (2010) Uncoupling of the spindle-checkpoint and chromosome-congression functions of BubR1. J Cell Sci 123, 84-94.80

Famulski, J. K. & Chan, G. K. (2007) Aurora B kinase-dependent recruitment of hZW10 and hROD to tensionless kinetochores. Curr Biol 17, 2143-2149.193

Fava, L. L., Kaulich, M., Nigg, E. A. & Santamaria, A. (2011) Probing the in vivo function of Mad1:C-Mad2 in the spindle assembly checkpoint. EMBO J 30, 3322-3336.93

Fededa, J. P. & Gerlich, D. W. (2012) Molecular control of animal cell cytokinesis. Nat Cell Biol 14, 440-447.59

Fernandez-Saiz, V. & Buchberger, A. (2010) Imbalances in p97 co-factor interactions in human proteinopathy. EMBO Rep 11, 479-485.308

Fischle, W., Tseng, B. S., Dormann, H. L., Ueberheide, B. M., Garcia, B. A., Shabanowitz, J., Hunt, D. F., Funabiki, H. & Allis, C. D. (2005) Regulation of HP1-chromatin binding by histone H3 methylation and phosphorylation. Nature 438, 1116-1122.135

Fitzgerald, D. J., Berger, P., Schaffitzel, C., Yamada, K., Richmond, T. J. & Berger, I. (2006) Protein complex expression by using multigene baculoviral vectors. Nat Methods 3, 1021-1032.343

Fuller, B. G., Lampson, M. A., Foley, E. A., Rosasco-Nitcher, S., Le, K. V., Tobelmann, P., Brautigan, D. L., Stukenberg, P. T. & Kapoor, T. M. (2008) Midzone activation of aurora B in anaphase produces an intracellular phosphorylation gradient. Nature 453, 1132-1136.177

Fung, T. K. & Poon, R. Y. (2005) A roller coaster ride with the mitotic cyclins. Semin Cell Dev Biol 16, 335-342.42

Gallini, S., Carminati, M., De Mattia, F., Pirovano, L., Martini, E., Oldani, A., Asteriti, I. A., Guarguaglini, G. & Mapelli, M. (2016) NuMA Phosphorylation by Aurora-A Orchestrates Spindle Orientation. Curr Biol.220

Gassmann, R., Carvalho, A., Henzing, A. J., Ruchaud, S., Hudson, D. F., Honda, R., Nigg, E. A., Gerloff, D. L. & Earnshaw, W. C. (2004) Borealin: a novel chromosomal passenger required for stability of the bipolar mitotic spindle. J Cell Biol 166, 179-191.104

Gassmann, R., Holland, A. J., Varma, D., Wan, X., Civril, F., Cleveland, D. W., Oegema, K., Salmon, E. D. & Desai, A. (2010) Removal of Spindly from microtubule-attached kinetochores controls spindle checkpoint silencing in human cells. Genes Dev 24, 957-971.90

Geiger, T., Wehner, A., Schaab, C., Cox, J. & Mann, M. (2012) Comparative proteomic analysis of eleven common cell lines reveals ubiquitous but varying expression of most proteins. Mol Cell Proteomics 11, M111 014050.296

Gestaut, D. R., Graczyk, B., Cooper, J., Widlund, P. O., Zelter, A., Wordeman, L., Asbury, C. L. & Davis, T. N. (2008) Phosphoregulation and depolymerization-driven movement of the Dam1 complex do not require ring formation. Nat Cell Biol 10, 407-414.154

Giet, R. & Glover, D. M. (2001) Drosophila aurora B kinase is required for histone H3 phosphorylation and condensin recruitment during chromosome condensation and to organize the central spindle during cytokinesis. J Cell Biol 152, 669-682.138

Goto, H., Kiyono, T., Tomono, Y., Kawajiri, A., Urano, T., Furukawa, K., Nigg, E. A. & Inagaki, M. (2006) Complex formation of Plk1 and INCENP required for metaphase-anaphase transition. Nat Cell Biol 8, 180-187.130

Gruneberg, U., Neef, R., Honda, R., Nigg, E. A. & Barr, F. A. (2004) Relocation of Aurora B from centromeres to the central spindle at the metaphase to anaphase transition requires MKlp2. J Cell Biol 166, 167-172.174

Grusche, F. A., Hidalgo, C., Fletcher, G., Sung, H. H., Sahai, E. & Thompson, B. J. (2009) Sds22, a PP1 phosphatase regulatory subunit, regulates epithelial cell polarity and shape [Sds22 in epithelial morphology]. BMC Dev Biol 9, 14.337

Guimaraes, G. J., Dong, Y., McEwen, B. F. & Deluca, J. G. (2008) Kinetochore-microtubule attachment relies on the disordered N-terminal tail domain of Hec1. Curr Biol 18, 1778-1784.151

Guo, F., Stanevich, V., Wlodarchak, N., Sengupta, R., Jiang, L., Satyshur, K. A. & Xing, Y. (2014) Structural basis of PP2A activation by PTPA, an ATP-dependent activation chaperone. Cell Res 24, 190-203.330

Guttinger, S., Laurell, E. & Kutay, U. (2009) Orchestrating nuclear envelope disassembly and reassembly during mitosis. Nat Rev Mol Cell Biol 10, 178-191.44

Hannak, E., Kirkham, M., Hyman, A. A. & Oegema, K. (2001) Aurora-A kinase is required for centrosome maturation in Caenorhabditis elegans. J Cell Biol 155, 1109-1116.208

Hanzelmann, P., Buchberger, A. & Schindelin, H. (2011) Hierarchical binding of cofactors to the AAA ATPase p97. Structure 19, 833-843.273

Hartmann-Petersen, R., Wallace, M., Hofmann, K., Koch, G., Johnsen, A. H., Hendil, K. B. & Gordon, C. (2004) The Ubx2 and Ubx3 cofactors direct Cdc48 activity to proteolytic and nonproteolytic ubiquitin-dependent processes. Curr Biol 14, 824-828.324

Hauf, S., Cole, R. W., LaTerra, S., Zimmer, C., Schnapp, G., Walter, R., Heckel, A., van Meel, J., Rieder, C. L. & Peters, J. M. (2003) The small molecule Hesperadin reveals a role for Aurora B in correcting kinetochore-microtubule attachment and in maintaining the spindle assembly checkpoint. J Cell Biol 161, 281-294.186

Heroes, E., Lesage, B., Gornemann, J., Beullens, M., Van Meervelt, L. & Bollen, M. (2013) The PP1 binding code: a molecular-lego strategy that governs specificity. FEBS J 280, 584-595.230

Herzog, F., Primorac, I., Dube, P., Lenart, P., Sander, B., Mechtler, K., Stark, H. & Peters, J. M. (2009) Structure of the anaphase-promoting complex/cyclosome interacting with a mitotic checkpoint complex. Science 323, 1477-1481.85

Hetzer, M., Meyer, H. H., Walther, T. C., Bilbao-Cortes, D., Warren, G. & Mattaj, I. W. (2001) Distinct AAA-ATPase p97 complexes function in discrete steps of nuclear assembly. Nat Cell Biol 3, 1086-1091.287

Hirota, T., Kunitoku, N., Sasayama, T., Marumoto, T., Zhang, D., Nitta, M., Hatakeyama, K. & Saya, H. (2003) Aurora-A and an interacting activator, the LIM protein Ajuba, are required for mitotic commitment in human cells. Cell 114, 585-598.206

Hirota, T., Lipp, J. J., Toh, B. H. & Peters, J. M. (2005) Histone H3 serine 10 phosphorylation by Aurora B causes HP1 dissociation from heterochromatin. Nature 438, 1176-1180.136

Hiruma, Y., Sacristan, C., Pachis, S. T., Adamopoulos, A., Kuijt, T., Ubbink, M., von Castelmur, E., Perrakis, A. & Kops, G. J. (2015) CELL DIVISION CYCLE. Competition between MPS1 and microtubules at kinetochores regulates spindle checkpoint signaling. Science 348, 1264-1267.75

Holt, L. J., Krutchinsky, A. N. & Morgan, D. O. (2008) Positive feedback sharpens the anaphase switch. Nature 454, 353-357.225

Honda, R., Korner, R. & Nigg, E. A. (2003) Exploring the functional interactions between Aurora B, INCENP, and survivin in mitosis. Mol Biol Cell 14, 3325-3341.103

Howell, B. J., McEwen, B. F., Canman, J. C., Hoffman, D. B., Farrar, E. M., Rieder, C. L. & Salmon, E. D. (2001) Cytoplasmic dynein/dynactin drives kinetochore protein transport to the spindle poles and has a role in mitotic spindle checkpoint inactivation. J Cell Biol 155, 1159-1172.89

Hsu, J. Y., Sun, Z. W., Li, X., Reuben, M., Tatchell, K., Bishop, D. K., Grushcow, J. M., Brame, C. J., Caldwell, J. A., Hunt, D. F. et al. (2000) Mitotic phosphorylation of histone H3 is governed by Ipl1/aurora kinase and Glc7/PP1 phosphatase in budding yeast and nematodes. Cell 102, 279-291.245

Hua, S., Wang, Z., Jiang, K., Huang, Y., Ward, T., Zhao, L., Dou, Z. & Yao, X. (2011) CENP-U cooperates with Hec1 to orchestrate kinetochore-microtubule attachment. J Biol Chem 286, 1627-1638.153

Huang, H., Hittle, J., Zappacosta, F., Annan, R. S., Hershko, A. & Yen, T. J. (2008) Phosphorylation sites in BubR1 that regulate kinetochore attachment, tension, and mitotic exit. J Cell Biol 183, 667-680.232

Huang, H. S. & Lee, E. Y. (2008) Protein phosphatase-1 inhibitor-3 is an in vivo target of caspase-3 and participates in the apoptotic response. J Biol Chem 283, 18135-18146.253

Huang, H. S., Pozarowski, P., Gao, Y., Darzynkiewicz, Z. & Lee, E. Y. (2005) Protein phosphatase-1 inhibitor-3 is co-localized to the nucleoli and centrosomes with PP1gamma1 and PP1alpha, respectively. Arch Biochem Biophys 443, 33-44.203

Hummer, S. & Mayer, T. U. (2009) Cdk1 negatively regulates midzone localization of the mitotic kinesin Mklp2 and the chromosomal passenger complex. Curr Biol 19, 607-612.131

Hurley, T. D., Yang, J., Zhang, L., Goodwin, K. D., Zou, Q., Cortese, M., Dunker, A. K. & DePaoli-Roach, A. A. (2007) Structural basis for regulation of protein phosphatase 1 by inhibitor-2. J Biol Chem 282, 28874-28883.248

Izawa, D. & Pines, J. (2011) How APC/C-Cdc20 changes its substrate specificity in mitosis. Nat Cell Biol 13, 223-233.86

Izawa, D. & Pines, J. (2015) The mitotic checkpoint complex binds a second CDC20 to inhibit active APC/C. Nature 517, 631-634.82

Jang, J. K., Rahman, T. & McKim, K. S. (2005) The kinesinlike protein Subito contributes to central spindle assembly and organization of the meiotic spindle in Drosophila oocytes. Mol Biol Cell 16, 4684-4694.175

Jentsch, S. & Rumpf, S. (2007) Cdc48 (p97): a "molecular gearbox" in the ubiquitin pathway? Trends Biochem Sci 32, 6-11.276

Jeyaprakash, A. A., Basquin, C., Jayachandran, U. & Conti, E. (2011) Structural basis for the recognition of phosphorylated histone h3 by the survivin subunit of the chromosomal passenger complex. Structure 19, 1625-1634.122

Jeyaprakash, A. A., Klein, U. R., Lindner, D., Ebert, J., Nigg, E. A. & Conti, E. (2007) Structure of a Survivin-Borealin-INCENP core complex reveals how chromosomal passengers travel together. Cell 131, 271-285.106

Jia, L., Kim, S. & Yu, H. (2013) Tracking spindle checkpoint signals from kinetochores to APC/C. Trends Biochem Sci 38, 302-311.61

Jia, L., Li, B., Warrington, R. T., Hao, X., Wang, S. & Yu, H. (2011) Defining pathways of spindle checkpoint silencing: functional redundancy between Cdc20 ubiquitination and p31(comet). Mol Biol Cell 22, 4227-4235.94

Jiang, L., Stanevich, V., Satyshur, K. A., Kong, M., Watkins, G. R., Wadzinski, B. E., Sengupta, R. & Xing, Y. (2013) Structural basis of protein phosphatase 2A stable latency. Nat Commun 4, 1699.228

Johnson, J. O., Mandrioli, J., Benatar, M., Abramzon, Y., Van Deerlin, V. M., Trojanowski, J. Q., Gibbs, J. R., Brunetti, M., Gronka, S., Wuu, J. et al. (2010) Exome sequencing reveals VCP mutations as a cause of familial ALS. Neuron 68, 857-864.263

Ju, J. S., Miller, S. E., Hanson, P. I. & Weihl, C. C. (2008) Impaired protein aggregate handling and clearance underlie the pathogenesis of p97/VCP-associated disease. J Biol Chem 283, 30289-30299.307

Ju, J. S. & Weihl, C. C. (2010) p97/VCP at the intersection of the autophagy and the ubiquitin proteasome system. Autophagy 6, 283-285.284

Kaneko, Y., Tamura, K., Totsukawa, G. & Kondo, H. (2010) Phosphorylation of p37 is important for Golgi disassembly at mitosis. Biochem Biophys Res Commun 402, 37-41.305

Kang, J., Chaudhary, J., Dong, H., Kim, S., Brautigam, C. A. & Yu, H. (2011) Mitotic centromeric targeting of HP1 and its binding to Sgo1 are dispensable for sister-chromatid cohesion in human cells. Mol Biol Cell 22, 1181-1190.112

Kapoor, T. M., Lampson, M. A., Hergert, P., Cameron, L., Cimini, D., Salmon, E. D., McEwen, B. F. & Khodjakov, A. (2006) Chromosomes can congress to the metaphase plate before biorientation. Science 311, 388-391.52

Katayama, H., Zhou, H., Li, Q., Tatsuka, M. & Sen, S. (2001) Interaction and feedback regulation between STK15/BTAK/Aurora-A kinase and protein phosphatase 1 through mitotic cell division cycle. J Biol Chem 276, 46219-46224.198

Katoh, H., Harada, A., Mori, K. & Negishi, M. (2002) Socius is a novel Rnd GTPase-interacting protein involved in disassembly of actin stress fibers. Mol Cell Biol 22, 2952-2964.301

Kawashima, S. A., Tsukahara, T., Langegger, M., Hauf, S., Kitajima, T. S. & Watanabe, Y. (2007) Shugoshin enables tension-generating attachment of kinetochores by loading Aurora to centromeres. Genes Dev 21, 420-435.124

Kawashima, S. A., Yamagishi, Y., Honda, T., Ishiguro, K. & Watanabe, Y. (2010) Phosphorylation of H2A by Bub1 prevents chromosomal instability through localizing shugoshin. Science 327, 172-177.125

Kelly, A. E. & Funabiki, H. (2009) Correcting aberrant kinetochore microtubule attachments: an Aurora B-centric view. Curr Opin Cell Biol 21, 51-58.69

Kelly, A. E., Sampath, S. C., Maniar, T. A., Woo, E. M., Chait, B. T. & Funabiki, H. (2007) Chromosomal enrichment and activation of the aurora B pathway are coupled to spatially regulate spindle assembly. Dev Cell 12, 31-43.127

Kemmler, S., Stach, M., Knapp, M., Ortiz, J., Pfannstiel, J., Ruppert, T. & Lechner, J. (2009) Mimicking Ndc80 phosphorylation triggers spindle assembly checkpoint signalling. EMBO J 28, 1099-1110.233

Kim, Y., Holland, A. J., Lan, W. & Cleveland, D. W. (2010) Aurora kinases and protein phosphatase 1 mediate chromosome congression through regulation of CENP-E. Cell 142, 444-455.53

King, E. M., Rachidi, N., Morrice, N., Hardwick, K. G. & Stark, M. J. (2007) Ipl1p-dependent phosphorylation of Mad3p is required for the spindle checkpoint response to lack of tension at kinetochores. Genes Dev 21, 1163-1168.19

Kinoshita, K., Noetzel, T. L., Pelletier, L., Mechtler, K., Drechsel, D. N., Schwager, A., Lee, M., Raff, J. W. & Hyman, A. A. (2005) Aurora A phosphorylation of TACC3/maskin is required for centrosome-dependent microtubule assembly in mitosis. J Cell Biol 170, 1047-1055.212

Kirchner, P., Bug, M. & Meyer, H. (2013) Ubiquitination of the N-terminal region of caveolin-1 regulates endosomal sorting by the VCP/p97 AAA-ATPase. J Biol Chem 288, 7363-7372.281

Kirschner, M. & Mitchison, T. (1986) Beyond self-assembly: from microtubules to morphogenesis. Cell 45, 329-342.49

Kiyomitsu, T. & Cheeseman, I. M. (2012) Chromosome- and spindle-pole-derived signals generate an intrinsic code for spindle position and orientation. Nat Cell Biol 14, 311-317.222

Klein, U. R., Nigg, E. A. & Gruneberg, U. (2006) Centromere targeting of the chromosomal passenger complex requires a ternary subcomplex of Borealin, Survivin, and the N-terminal domain of INCENP. Mol Biol Cell 17, 2547-2558.110

Kondo, H., Rabouille, C., Newman, R., Levine, T. P., Pappin, D., Freemont, P. & Warren, G. (1997) p47 is a cofactor for p97-mediated membrane fusion. Nature 388, 75-78.270

Kong, M., Ditsworth, D., Lindsten, T. & Thompson, C. B. (2009) Alpha4 is an essential regulator of PP2A phosphatase activity. Mol Cell 36, 51-60.334

Kops, G. J., Weaver, B. A. & Cleveland, D. W. (2005) On the road to cancer: aneuploidy and the mitotic checkpoint. Nat Rev Cancer 5, 773-785.37

Kotak, S., Busso, C. & Gonczy, P. (2012) Cortical dynein is critical for proper spindle positioning in human cells. J Cell Biol 199, 97-110.223

Kotak, S. & Gonczy, P. (2013) Mechanisms of spindle positioning: cortical force generators in the limelight. Curr Opin Cell Biol 25, 741-748.217

Krenn, V. & Musacchio, A. (2015) The Aurora B Kinase in Chromosome Bi-Orientation and Spindle Checkpoint Signaling. Front Oncol 5, 225.55

Krenn, V., Overlack, K., Primorac, I., van Gerwen, S. & Musacchio, A. (2014) KI motifs of human Knl1 enhance assembly of comprehensive spindle checkpoint complexes around MELT repeats. Curr Biol 24, 29-39.16

Krenn, V., Wehenkel, A., Li, X., Santaguida, S. & Musacchio, A. (2012) Structural analysis reveals features of the spindle checkpoint kinase Bub1-kinetochore subunit Knl1 interaction. J Cell Biol 196, 451-467.79

Kress, E., Schwager, F., Holtackers, R., Seiler, J., Prodon, F., Zanin, E., Eiteneuer, A., Toya, M., Sugimoto, A., Meyer, H., Meraldi, P., Gotta, M. (2013) The UBXN-2/p37/p47 adaptors of CDC-48/p97 regulate mitosis by limiting the centrosomal recruitment of Aurora A. J Cell Biol 201, 559-575.30

Kubala, M. H., Kovtun, O., Alexandrov, K. & Collins, B. M. (2010) Structural and thermodynamic analysis of the GFP:GFP-nanobody complex. Protein Sci 19, 2389-2401.338

Lampson, M. A. & Cheeseman, I. M. (2011) Sensing centromere tension: Aurora B and the regulation of kinetochore function. Trends Cell Biol 21, 133-140.56

Lampson, M. A., Renduchitala, K., Khodjakov, A. & Kapoor, T. M. (2004) Correcting improper chromosome-spindle attachments during cell division. Nat Cell Biol 6, 232-237.185

Lan, W., Zhang, X., Kline-Smith, S. L., Rosasco, S. E., Barrett-Wilt, G. A., Shabanowitz, J., Hunt, D. F., Walczak, C. E. & Stukenberg, P. T. (2004) Aurora B

phosphorylates centromeric MCAK and regulates its localization and microtubule depolymerization activity. Curr Biol 14, 273-286.160

Lara-Gonzalez, P., Scott, M. I., Diez, M., Sen, O. & Taylor, S. S. (2011) BubR1 blocks substrate recruitment to the APC/C in a KEN-box-dependent manner. J Cell Sci 124, 4332-4345.84

Latif, C., Harvey, S. H. & O'Connell, M. J. (2001) Ensuring the stability of the genome: DNA damage checkpoints. ScientificWorldJournal 1, 684-702.40

Lesage, B., Beullens, M., Pedelini, L., Garcia-Gimeno, M. A., Waelkens, E., Sanz, P. & Bollen, M. (2007) A complex of catalytically inactive protein phosphatase-1 sandwiched between Sds22 and inhibitor-3. Biochemistry 46, 8909-8919.33

Lesage, B., Qian, J. & Bollen, M. (2011) Spindle checkpoint silencing: PP1 tips the balance. Curr Biol 21, R898-903.70

Li, M., Satinover, D. L. & Brautigan, D. L. (2007) Phosphorylation and functions of inhibitor-2 family of proteins. Biochemistry 46, 2380-2389.202

Lipp, J. J., Hirota, T., Poser, I. & Peters, J. M. (2007) Aurora B controls the association of condensin I but not condensin II with mitotic chromosomes. J Cell Sci 120, 1245-1255.140

Liu, D., Vader, G., Vromans, M. J., Lampson, M. A. & Lens, S. M. (2009) Sensing chromosome bi-orientation by spatial separation of aurora B kinase from kinetochore substrates. Science 323, 1350-1353.348

Liu, D., Vleugel, M., Backer, C. B., Hori, T., Fukagawa, T., Cheeseman, I. M. & Lampson, M. A. (2010) Regulated targeting of protein phosphatase 1 to the outer kinetochore by KNL1 opposes Aurora B kinase. J Cell Biol 188, 809-820.5

London, N., Ceto, S., Ranish, J. A. & Biggins, S. (2012) Phosphoregulation of Spc105 by Mps1 and PP1 regulates Bub1 localization to kinetochores. Curr Biol 22, 900-906.76

Luo, X. & Yu, H. (2008) Protein metamorphosis: the two-state behavior of Mad2. Structure 16, 1616-1625.87

Ma, H. T. & Poon, R. Y. (2011) How protein kinases co-ordinate mitosis in animal cells. Biochem J 435, 17-31.38

Machicoane, M., de Frutos, C. A., Fink, J., Rocancourt, M., Lombardi, Y., Garel, S., Piel, M. & Echard, A. (2014) SLK-dependent activation of ERMs controls LGN-NuMA localization and spindle orientation. J Cell Biol 205, 791-799.336

MacKelvie, S. H., Andrews, P. D. & Stark, M. J. (1995) The Saccharomyces cerevisiae gene SDS22 encodes a potential regulator of the mitotic function of yeast type 1 protein phosphatase. Mol Cell Biol 15, 3777-3785.246

Mapelli, M., Filipp, F. V., Rancati, G., Massimiliano, L., Nezi, L., Stier, G., Hagan, R. S., Confalonieri, S., Piatti, S., Sattler, M. et al. (2006) Determinants of conformational dimerization of Mad2 and its inhibition by p31comet. EMBO J 25, 1273-1284.92

Mapelli, M. & Musacchio, A. (2007) MAD contortions: conformational dimerization boosts spindle checkpoint signaling. Curr Opin Struct Biol 17, 716-725.88

McConnell, J. L., Watkins, G. R., Soss, S. E., Franz, H. S., McCorvey, L. R., Spiller, B. W., Chazin, W. J. & Wadzinski, B. E. (2010) Alpha4 is a ubiquitin-binding protein that regulates protein serine/threonine phosphatase 2A ubiquitination. Biochemistry 49, 1713-1718.335

Meadows, J. C., Shepperd, L. A., Vanoosthuyse, V., Lancaster, T. C., Sochaj, A. M., Buttrick, G. J., Hardwick, K. G. & Millar, J. B. (2011) Spindle checkpoint silencing requires association of PP1 to both Spc7 and kinesin-8 motors. Dev Cell 20, 739-750.237

Mehta, G. D., Rizvi, S. M. & Ghosh, S. K. (2012) Cohesin: a guardian of genome integrity. Biochim Biophys Acta 1823, 1324-1342.58

Meyer, H., Bug, M. & Bremer, S. (2012) Emerging functions of the VCP/p97 AAA-ATPase in the ubiquitin system. Nat Cell Biol 14, 117-123.259

Meyer, H. & Weihl, C. C. (2014) The VCP/p97 system at a glance: connecting cellular function to disease pathogenesis. J Cell Sci 127, 3877-3883.275

Meyer, H. H., Kondo, H. & Warren, G. (1998) The p47 co-factor regulates the ATPase activity of the membrane fusion protein, p97. FEBS Lett 437, 255-257.288

Meyer, H. H., Shorter, J. G., Seemann, J., Pappin, D. & Warren, G. (2000) A complex of mammalian ufd1 and npl4 links the AAA-ATPase, p97, to ubiquitin and nuclear transport pathways. EMBO J 19, 2181-2192.271

Meyer, H. H., Wang, Y. & Warren, G. (2002) Direct binding of ubiquitin conjugates by the mammalian p97 adaptor complexes, p47 and Ufd1-Npl4. EMBO J 21, 5645-5652.304

Minnebo, N., Gornemann, J., O'Connell, N., Van Dessel, N., Derua, R., Vermunt, M. W., Page, R., Beullens, M., Peti, W., Van Eynde, A. et al. (2013) NIPP1 maintains EZH2 phosphorylation and promoter occupancy at proliferation-related target genes. Nucleic Acids Res 41, 842-854.11

Minoshima, Y., Kawashima, T., Hirose, K., Tonozuka, Y., Kawajiri, A., Bao, Y. C., Deng, X., Tatsuka, M., Narumiya, S., May, W. S., Jr. et al. (2003) Phosphorylation by aurora B converts MgcRacGAP to a RhoGAP during cytokinesis. Dev Cell 4, 549-560.182

Mitchison, T. & Kirschner, M. (1984) Dynamic instability of microtubule growth. Nature 312, 237-242.48

Moir, D., Stewart, S. E., Osmond, B. C. & Botstein, D. (1982) Cold-sensitive cell-division-cycle mutants of yeast: isolation, properties, and pseudoreversion studies. Genetics 100, 547-563.256

Mora-Bermudez, F., Gerlich, D. & Ellenberg, J. (2007) Maximal chromosome compaction occurs by axial shortening in anaphase and depends on Aurora kinase. Nat Cell Biol 9, 822-831.178

Mori, D., Yano, Y., Toyo-oka, K., Yoshida, N., Yamada, M., Muramatsu, M., Zhang, D., Saya, H., Toyoshima, Y. Y., Kinoshita, K. et al. (2007) NDEL1 phosphorylation by Aurora-A kinase is essential for centrosomal maturation, separation, and TACC3 recruitment. Mol Cell Biol 27, 352-367.209

Morin, X. & Bellaiche, Y. (2011) Mitotic spindle orientation in asymmetric and symmetric cell divisions during animal development. Dev Cell 21, 102-119.216

Morishita, J., Matsusaka, T., Goshima, G., Nakamura, T., Tatebe, H. & Yanagida, M. (2001) Bir1/Cut17 moving from chromosome to spindle upon the loss of cohesion is required for condensation, spindle elongation and repair. Genes Cells 6, 743-763.137

Morrow, C. J., Tighe, A., Johnson, V. L., Scott, M. I., Ditchfield, C. & Taylor, S. S. (2005) Bub1 and aurora B cooperate to maintain BubR1-mediated inhibition of APC/CCdc20. J Cell Sci 118, 3639-3652.18

Murata-Hori, M. & Wang, Y. L. (2002) Both midzone and astral microtubules are involved in the delivery of cytokinesis signals: insights from the mobility of aurora B. J Cell Biol 159, 45-53.168

Murnion, M. E., Adams, R. R., Callister, D. M., Allis, C. D., Earnshaw, W. C. & Swedlow, J. R. (2001) Chromatin-associated protein phosphatase 1 regulates aurora-B and histone H3 phosphorylation. J Biol Chem 276, 26656-26665.133

Musacchio, A. (2011) Spindle assembly checkpoint: the third decade. Philos Trans R Soc Lond B Biol Sci 366, 3595-3604.36

Musacchio, A. (2015) The Molecular Biology of Spindle Assembly Checkpoint Signaling Dynamics. Curr Biol 25, R1002-1018.54

Nakazawa, N., Mehrotra, R., Ebe, M. & Yanagida, M. (2011) Condensin phosphorylated by the Aurora-B-like kinase Ark1 is continuously required until telophase in a mode distinct from Top2. J Cell Sci 124, 1795-1807.142

Nakazawa, N., Nakamura, T., Kokubu, A., Ebe, M., Nagao, K. & Yanagida, M. (2008) Dissection of the essential steps for condensin accumulation at kinetochores and rDNAs during fission yeast mitosis. J Cell Biol 180, 1115-1131.145

Neurohr, G., Naegeli, A., Titos, I., Theler, D., Greber, B., Diez, J., Gabaldon, T., Mendoza, M. & Barral, Y. (2011) A midzone-based ruler adjusts chromosome compaction to anaphase spindle length. Science 332, 465-468.134

Nicklas, R. B. & Koch, C. A. (1969) Chromosome micromanipulation. 3. Spindle fiber tension and the reorientation of mal-oriented chromosomes. J Cell Biol 43, 40-50.184

Nilsson, J., Yekezare, M., Minshull, J. & Pines, J. (2008) The APC/C maintains the spindle assembly checkpoint by targeting Cdc20 for destruction. Nat Cell Biol 10, 1411-1420.95

Nishimura, Y. & Yonemura, S. (2006) Centralspindlin regulates ECT2 and RhoA accumulation at the equatorial cortex during cytokinesis. J Cell Sci 119, 104-114.181

Nishino, T., Takeuchi, K., Gascoigne, K. E., Suzuki, A., Hori, T., Oyama, T., Morikawa, K., Cheeseman, I. M. & Fukagawa, T. (2012) CENP-T-W-S-X forms a unique centromeric chromatin structure with a histone-like fold. Cell 148, 487-501.62

Nozawa, R. S., Nagao, K., Masuda, H. T., Iwasaki, O., Hirota, T., Nozaki, N., Kimura, H. & Obuse, C. (2010) Human POGZ modulates dissociation of HP1alpha from mitotic chromosome arms through Aurora B activation. Nat Cell Biol 12, 719-727.111

Nuytten, M., Beke, L., Van Eynde, A., Ceulemans, H., Beullens, M., Van Hummelen, P., Fuks, F. & Bollen, M. (2008) The transcriptional repressor NIPP1 is an essential player in EZH2-mediated gene silencing. Oncogene 27, 1449-1460.12

O'Connor, D. S., Grossman, D., Plescia, J., Li, F., Zhang, H., Villa, A., Tognin, S., Marchisio, P. C. & Altieri, D. C. (2000) Regulation of apoptosis at cell division by p34cdc2 phosphorylation of survivin. Proc Natl Acad Sci U S A 97, 13103-13107.114

O'Connor, D. S., Wall, N. R., Porter, A. C. & Altieri, D. C. (2002) A p34(cdc2) survival checkpoint in cancer. Cancer Cell 2, 43-54.115

Ogura, T. & Wilkinson, A. J. (2001) AAA+ superfamily ATPases: common structure--diverse function. Genes Cells 6, 575-597.265

Ono, T., Fang, Y., Spector, D. L. & Hirano, T. (2004) Spatial and temporal regulation of Condensins I and II in mitotic chromosome assembly in human cells. Mol Biol Cell 15, 3296-3308.139

Pedelini, L., Marquina, M., Arino, J., Casamayor, A., Sanz, L., Bollen, M., Sanz, P. & Garcia-Gimeno, M. A. (2007) YPI1 and SDS22 proteins regulate the nuclear localization and function of yeast type 1 phosphatase Glc7. J Biol Chem 282, 3282-3292.15

Peggie, M. W., MacKelvie, S. H., Bloecher, A., Knatko, E. V., Tatchell, K. & Stark, M. J. (2002) Essential functions of Sds22p in chromosome stability and nuclear localization of PP1. J Cell Sci 115, 195-206.2

Peng, J., Schwartz, D., Elias, J. E., Thoreen, C. C., Cheng, D., Marsischky, G., Roelofs, J., Finley, D. & Gygi, S. P. (2003) A proteomics approach to understanding protein ubiquitination. Nat Biotechnol 21, 921-926.332

Peset, I., Seiler, J., Sardon, T., Bejarano, L. A., Rybina, S. & Vernos, I. (2005) Function and regulation of Maskin, a TACC family protein, in microtubule growth during mitosis. J Cell Biol 170, 1057-1066.213

Peset, I. & Vernos, I. (2008) The TACC proteins: TACC-ling microtubule dynamics and centrosome function. Trends Cell Biol 18, 379-388.214

Peters, J. M., Walsh, M. J. & Franke, W. W. (1990) An abundant and ubiquitous homo-oligomeric ring-shaped ATPase particle related to the putative vesicle fusion proteins Sec18p and NSF. EMBO J 9, 1757-1767.257

Petersen, J. & Hagan, I. M. (2003) S. pombe aurora kinase/survivin is required for chromosome condensation and the spindle checkpoint attachment response. Curr Biol 13, 590-597.144

Petroski, M. D. & Deshaies, R. J. (2005) Function and regulation of cullin-RING ubiquitin ligases. Nat Rev Mol Cell Biol 6, 9-20.328

Petrovic, A., Pasqualato, S., Dube, P., Krenn, V., Santaguida, S., Cittaro, D., Monzani, S., Massimiliano, L., Keller, J., Tarricone, A. et al. (2010) The MIS12 complex is a protein interaction hub for outer kinetochore assembly. J Cell Biol 190, 835-852.66

Petsalaki, E., Akoumianaki, T., Black, E. J., Gillespie, D. A. & Zachos, G. (2011) Phosphorylation at serine 331 is required for Aurora B activation. J Cell Biol 195, 449-466.128

Pierce, N. W., Lee, J. E., Liu, X., Sweredoski, M. J., Graham, R. L., Larimore, E. A., Rome, M., Zheng, N., Clurman, B. E., Hess, S. et al. (2013) Cand1 promotes assembly of new SCF complexes through dynamic exchange of F box proteins. Cell 153, 206-215.327

Pinsky, B. A., Kotwaliwale, C. V., Tatsutani, S. Y., Breed, C. A. & Biggins, S. (2006) Glc7/protein phosphatase 1 regulatory subunits can oppose the Ipl1/aurora protein kinase by redistributing Glc7. Mol Cell Biol 26, 2648-2660.244

Pinsky, B. A., Kung, C., Shokat, K. M. & Biggins, S. (2006) The Ipl1-Aurora protein kinase activates the spindle checkpoint by creating unattached kinetochores. Nat Cell Biol 8, 78-83.195

Pinsky, B. A., Nelson, C. R. & Biggins, S. (2009) Protein phosphatase 1 regulates exit from the spindle checkpoint in budding yeast. Curr Biol 19, 1182-1187.234

Polioudaki, H., Markaki, Y., Kourmouli, N., Dialynas, G., Theodoropoulos, P. A., Singh, P. B. & Georgatos, S. D. (2004) Mitotic phosphorylation of histone H3 at threonine 3. FEBS Lett 560, 39-44.121

Posch, M., Khoudoli, G. A., Swift, S., King, E. M., Deluca, J. G. & Swedlow, J. R. (2010) Sds22 regulates aurora B activity and microtubule-kinetochore interactions at mitosis. J Cell Biol 191, 61-74.3

Poser, I., Sarov, M., Hutchins, J. R., Heriche, J. K., Toyoda, Y., Pozniakovsky, A., Weigl, D., Nitzsche, A., Hegemann, B., Bird, A. W. et al. (2008) BAC TransgeneOmics: a high-throughput method for exploration of protein function in mammals. Nat Methods 5, 409-415.13

Powers, A. F., Franck, A. D., Gestaut, D. R., Cooper, J., Gracyzk, B., Wei, R. R., Wordeman, L., Davis, T. N. & Asbury, C. L. (2009) The Ndc80 kinetochore complex forms load-bearing attachments to dynamic microtubule tips via biased diffusion. Cell 136, 865-875.146

Przewloka, M. R., Venkei, Z., Bolanos-Garcia, V. M., Debski, J., Dadlez, M. & Glover, D. M. (2011) CENP-C is a structural platform for kinetochore assembly. Curr Biol 21, 399-405.64

Puumalainen, M. R., Lessel, D., Ruthemann, P., Kaczmarek, N., Bachmann, K., Ramadan, K. & Naegeli, H. (2014) Chromatin retention of DNA damage sensors DDB2 and XPC through loss of p97 segregase causes genotoxicity. Nat Commun 5, 3695.323

Pye, V. E., Dreveny, I., Briggs, L. C., Sands, C., Beuron, F., Zhang, X. & Freemont, P. S. (2006) Going through the motions: the ATPase cycle of p97. J Struct Biol 156, 12-28.321

Qian, J., Beullens, M., Lesage, B. & Bollen, M. (2013) Aurora B defines its own chromosomal targeting by opposing the recruitment of the phosphatase scaffold Repo-Man. Curr Biol 23, 1136-1143.166

Qian, J., Lesage, B., Beullens, M., Van Eynde, A. & Bollen, M. (2011) PP1/Repo-man dephosphorylates mitotic histone H3 at T3 and regulates chromosomal aurora B targeting. Curr Biol 21, 766-773.165

Quartuccio, S. M. & Schindler, K. (2015) Functions of Aurora kinase C in meiosis and cancer. Front Cell Dev Biol 3, 50.100

Radulescu, A. E. & Cleveland, D. W. (2010) NuMA after 30 years: the matrix revisited. Trends Cell Biol 20, 214-222.221

Ramadan, K., Bruderer, R., Spiga, F. M., Popp, O., Baur, T., Gotta, M. & Meyer, H. H. (2007) Cdc48/p97 promotes reformation of the nucleus by extracting the kinase Aurora B from chromatin. Nature 450, 1258-1262.172

Raman, M., Sergeev, M., Garnaas, M., Lydeard, J. R., Huttlin, E. L., Goessling, W., Shah, J. V. & Harper, J. W. (2015) Systematic proteomics of the VCP-UBXD adaptor network identifies a role for UBXN10 in regulating ciliogenesis. Nat Cell Biol 17, 1356-1369.306

Regan, J. L., Sourisseau, T., Soady, K., Kendrick, H., McCarthy, A., Tang, C., Brennan, K., Linardopoulos, S., White, D. E. & Smalley, M. J. (2013) Aurora A kinase regulates mammary epithelial cell fate by determining mitotic spindle orientation in a Notch-dependent manner. Cell Rep 4, 110-123.218

Rezvani, K., Teng, Y., Pan, Y., Dani, J. A., Lindstrom, J., Garcia Gras, E. A., McIntosh, J. M. & De Biasi, M. (2009) UBXD4, a UBX-containing protein, regulates the cell surface number and stability of alpha3-containing nicotinic acetylcholine receptors. J Neurosci 29, 6883-6896.300

Rieder, C. L., Cole, R. W., Khodjakov, A. & Sluder, G. (1995) The checkpoint delaying anaphase in response to chromosome monoorientation is mediated by an inhibitory signal produced by unattached kinetochores. J Cell Biol 130, 941-948.71

Rieder, C. L., Khodjakov, A., Paliulis, L. V., Fortier, T. M., Cole, R. W. & Sluder, G. (1997) Mitosis in vertebrate somatic cells with two spindles: implications for the metaphase/anaphase transition checkpoint and cleavage. Proc Natl Acad Sci U S A 94, 5107-5112.239

Riemer, A., Dobrynin, G., Dressler, A., Bremer, S., Soni, A., Iliakis, G. & Meyer, H. (2014) The p97-Ufd1-Npl4 ATPase complex ensures robustness of the G2/M checkpoint by facilitating CDC25A degradation. Cell Cycle 13, 919-927.292

Rischitor, P. E., May, K. M. & Hardwick, K. G. (2007) Bub1 is a fission yeast kinetochore scaffold protein, and is sufficient to recruit other spindle checkpoint proteins to ectopic sites on chromosomes. PLoS One 2, e1342.81

Ritz, D., Vuk, M., Kirchner, P., Bug, M., Schutz, S., Hayer, A., Bremer, S., Lusk, C., Baloh, R. H., Lee, H. et al. (2011) Endolysosomal sorting of ubiquitylated caveolin-1 is regulated by VCP and UBXD1 and impaired by VCP disease mutations. Nat Cell Biol 13, 1116-1123.22

Rosenberg, J. S., Cross, F. R. & Funabiki, H. (2011) KNL1/Spc105 recruits PP1 to silence the spindle assembly checkpoint. Curr Biol 21, 942-947.236

Rouiller, I., DeLaBarre, B., May, A. P., Weis, W. I., Brunger, A. T., Milligan, R. A. & Wilson-Kubalek, E. M. (2002) Conformational changes of the multifunction p97 AAA ATPase during its ATPase cycle. Nat Struct Biol 9, 950-957.266

Ruchaud, S., Carmena, M. & Earnshaw, W. C. (2007) Chromosomal passengers: conducting cell division. Nat Rev Mol Cell Biol 8, 798-812.116

Salimian, K. J., Ballister, E. R., Smoak, E. M., Wood, S., Panchenko, T., Lampson, M. A. & Black, B. E. (2011) Feedback control in sensing chromosome biorientation by the Aurora B kinase. Curr Biol 21, 1158-1165.163

Samejima, K., Platani, M., Wolny, M., Ogawa, H., Vargiu, G., Knight, P. J., Peckham, M. & Earnshaw, W. C. (2015) The Inner Centromere Protein (INCENP) Coil Is a Single alpha-Helix (SAH) Domain That Binds Directly to Microtubules and Is

Important for Chromosome Passenger Complex (CPC) Localization and Function in Mitosis. J Biol Chem 290, 21460-21472.188

Santaguida, S. & Musacchio, A. (2009) The life and miracles of kinetochores. EMBO J 28, 2511-2531.189

Santaguida, S., Tighe, A., D'Alise, A. M., Taylor, S. S. & Musacchio, A. (2010) Dissecting the role of MPS1 in chromosome biorientation and the spindle checkpoint through the small molecule inhibitor reversine. J Cell Biol 190, 73-87.17

Santaguida, S., Vernieri, C., Villa, F., Ciliberto, A. & Musacchio, A. (2011) Evidence that Aurora B is implicated in spindle checkpoint signalling independently of error correction. EMBO J 30, 1508-1519.192

Saurin, A. T., van der Waal, M. S., Medema, R. H., Lens, S. M. & Kops, G. J. (2011) Aurora B potentiates Mps1 activation to ensure rapid checkpoint establishment at the onset of mitosis. Nat Commun 2, 316.73

Schleiffer, A., Maier, M., Litos, G., Lampert, F., Hornung, P., Mechtler, K. & Westermann, S. (2012) CENP-T proteins are conserved centromere receptors of the Ndc80 complex. Nat Cell Biol 14, 604-613.65

Schuberth, C. & Buchberger, A. (2008) UBX domain proteins: major regulators of the AAA ATPase Cdc48/p97. Cell Mol Life Sci 65, 2360-2371.258

Schuberth, C., Richly, H., Rumpf, S. & Buchberger, A. (2004) Shp1 and Ubx2 are adaptors of Cdc48 involved in ubiquitin-dependent protein degradation. EMBO Rep 5, 818-824.325

Screpanti, E., De Antoni, A., Alushin, G. M., Petrovic, A., Melis, T., Nogales, E. & Musacchio, A. (2011) Direct binding of Cenp-C to the Mis12 complex joins the inner and outer kinetochore. Curr Biol 21, 391-398.63

Shepperd, L. A., Meadows, J. C., Sochaj, A. M., Lancaster, T. C., Zou, J., Buttrick, G. J., Rappsilber, J., Hardwick, K. G. & Millar, J. B. (2012) Phosphodependent recruitment of Bub1 and Bub3 to Spc7/KNL1 by Mph1 kinase maintains the spindle checkpoint. Curr Biol 22, 891-899.77

Shibata, Y., Oyama, M., Kozuka-Hata, H., Han, X., Tanaka, Y., Gohda, J. & Inoue, J. (2012) p47 negatively regulates IKK activation by inducing the lysosomal degradation of polyubiquitinated NEMO. Nat Commun 3, 1061.342

Song, C., Wang, Q. & Li, C. C. (2003) ATPase activity of p97-valosin-containing protein (VCP). D2 mediates the major enzyme activity, and D1 contributes to the heat-induced activity. J Biol Chem 278, 3648-3655.267

Starita, L. M., Lo, R. S., Eng, J. K., von Haller, P. D. & Fields, S. (2012) Sites of ubiquitin attachment in Saccharomyces cerevisiae. Proteomics 12, 236-240.333

Stolz, A., Hilt, W., Buchberger, A. & Wolf, D. H. (2011) Cdc48: a power machine in protein degradation. Trends Biochem Sci 36, 515-523.311

Suijkerbuijk, S. J., van Dam, T. J., Karagoz, G. E., von Castelmur, E., Hubner, N. C., Duarte, A. M., Vleugel, M., Perrakis, A., Rudiger, S. G., Snel, B. et al. (2012) The vertebrate mitotic checkpoint protein BUBR1 is an unusual pseudokinase. Dev Cell 22, 1321-1329.72

Sumara, I., Quadroni, M., Frei, C., Olma, M. H., Sumara, G., Ricci, R. & Peter, M. (2007) A Cul3-based E3 ligase removes Aurora B from mitotic chromosomes, regulating mitotic progression and completion of cytokinesis in human cells. Dev Cell 12, 887-900.171

Suzuki, M., Otsuka, T., Ohsaki, Y., Cheng, J., Taniguchi, T., Hashimoto, H., Taniguchi, H. & Fujimoto, T. (2012) Derlin-1 and UBXD8 are engaged in dislocation and degradation of lipidated ApoB-100 at lipid droplets. Mol Biol Cell 23, 800-810.340

Tada, K., Susumu, H., Sakuno, T. & Watanabe, Y. (2011) Condensin association with histone H2A shapes mitotic chromosomes. Nature 474, 477-483.143

Tanaka, K. (2013) Regulatory mechanisms of kinetochore-microtubule interaction in mitosis. Cell Mol Life Sci 70, 559-579.50

Tanenbaum, M. E., Macurek, L., van der Vaart, B., Galli, M., Akhmanova, A. & Medema, R. H. (2011) A complex of Kif18b and MCAK promotes microtubule depolymerization and is negatively regulated by Aurora kinases. Curr Biol 21, 1356-1365.161

Terada, Y., Uetake, Y. & Kuriyama, R. (2003) Interaction of Aurora-A and centrosomin at the microtubule-nucleating site in Drosophila and mammalian cells. J Cell Biol 162, 757-763.210

Terrak, M., Kerff, F., Langsetmo, K., Tao, T. & Dominguez, R. (2004) Structural basis of protein phosphatase 1 regulation. Nature 429, 780-784.250

Thoma, C. R., Toso, A., Gutbrodt, K. L., Reggi, S. P., Frew, I. J., Schraml, P., Hergovich, A., Moch, H., Meraldi, P. & Krek, W. (2009) VHL loss causes spindle misorientation and chromosome instability. Nat Cell Biol 11, 994-1001.32

Tien, J. F., Umbreit, N. T., Gestaut, D. R., Franck, A. D., Cooper, J., Wordeman, L., Gonen, T., Asbury, C. L. & Davis, T. N. (2010) Cooperation of the Dam1 and Ndc80 kinetochore complexes enhances microtubule coupling and is regulated by aurora B. J Cell Biol 189, 713-723.156

Toure, A., Mzali, R., Liot, C., Seguin, L., Morin, L., Crouin, C., Chen-Yang, I., Tsay, Y. G., Dorseuil, O., Gacon, G. et al. (2008) Phosphoregulation of MgcRacGAP in mitosis involves Aurora B and Cdk1 protein kinases and the PP2A phosphatase. FEBS Lett 582, 1182-1188.183

Toyoshima, F. & Nishida, E. (2007) Integrin-mediated adhesion orients the spindle parallel to the substratum in an EB1- and myosin X-dependent manner. EMBO J 26, 1487-1498.31

Tresse, E., Salomons, F. A., Vesa, J., Bott, L. C., Kimonis, V., Yao, T. P., Dantuma, N. P. & Taylor, J. P. (2010) VCP/p97 is essential for maturation of ubiquitin-containing autophagosomes and this function is impaired by mutations that cause IBMPFD. Autophagy 6, 217-227.282

Trinkle-Mulcahy, L., Andersen, J., Lam, Y. W., Moorhead, G., Mann, M. & Lamond, A. I. (2006) Repo-Man recruits PP1 gamma to chromatin and is essential for cell viability. J Cell Biol 172, 679-692.164

Trinkle-Mulcahy, L., Andrews, P. D., Wickramasinghe, S., Sleeman, J., Prescott, A., Lam, Y. W., Lyon, C., Swedlow, J. R. & Lamond, A. I. (2003) Time-lapse imaging reveals dynamic relocalization of PP1gamma throughout the mammalian cell cycle. Mol Biol Cell 14, 107-117.21

Trinkle-Mulcahy, L. & Lamond, A. I. (2006) Mitotic phosphatases: no longer silent partners. Curr Opin Cell Biol 18, 623-631.224

Trowitzsch, S., Bieniossek, C., Nie, Y., Garzoni, F. & Berger, I. (2010) New baculovirus expression tools for recombinant protein complex production. J Struct Biol 172, 45-54.344

Tsai, M. Y. & Zheng, Y. (2005) Aurora A kinase-coated beads function as microtubule-organizing centers and enhance RanGTP-induced spindle assembly. Curr Biol 15, 2156-2163.215

Tsujimoto, Y., Tomita, Y., Hoshida, Y., Kono, T., Oka, T., Yamamoto, S., Nonomura, N., Okuyama, A. & Aozasa, K. (2004) Elevated expression of valosin-containing protein (p97) is associated with poor prognosis of prostate cancer. Clin Cancer Res 10, 3007-3012.316

Tsukahara, T., Tanno, Y. & Watanabe, Y. (2010) Phosphorylation of the CPC by Cdk1 promotes chromosome bi-orientation. Nature 467, 719-723.126

Uchiyama, K., Jokitalo, E., Lindman, M., Jackman, M., Kano, F., Murata, M., Zhang, X. & Kondo, H. (2003) The localization and phosphorylation of p47 are important for Golgi disassembly-assembly during the cell cycle. J Cell Biol 161, 1067-1079.297

Uchiyama, K., Totsukawa, G., Puhka, M., Kaneko, Y., Jokitalo, E., Dreveny, I., Beuron, F., Zhang, X., Freemont, P. & Kondo, H. (2006) p37 is a p97 adaptor required for Golgi and ER biogenesis in interphase and at the end of mitosis. Dev Cell 11, 803-816.290

Vader, G., Cruijsen, C. W., van Harn, T., Vromans, M. J., Medema, R. H. & Lens, S. M. (2007) The chromosomal passenger complex controls spindle checkpoint function independent from its role in correcting microtubule kinetochore interactions. Mol Biol Cell 18, 4553-4564.190

Vader, G., Kauw, J. J., Medema, R. H. & Lens, S. M. (2006) Survivin mediates targeting of the chromosomal passenger complex to the centromere and midbody. EMBO Rep 7, 85-92.108

Valle, C. W., Min, T., Bodas, M., Mazur, S., Begum, S., Tang, D. & Vij, N. (2011) Critical role of VCP/p97 in the pathogenesis and progression of non-small cell lung carcinoma. PLoS One 6, e29073.319

van der Waal, M. S., Saurin, A. T., Vromans, M. J., Vleugel, M., Wurzenberger, C., Gerlich, D. W., Medema, R. H., Kops, G. J. & Lens, S. M. (2012) Mps1 promotes rapid centromere accumulation of Aurora B. EMBO Rep 13, 847-854.74

Vanoosthuyse, V. & Hardwick, K. G. (2009) A novel protein phosphatase 1-dependent spindle checkpoint silencing mechanism. Curr Biol 19, 1176-1181.235

Vazquez-Novelle, M. D. & Petronczki, M. (2010) Relocation of the chromosomal passenger complex prevents mitotic checkpoint engagement at anaphase. Curr Biol 20, 1402-1407.196

Verdecia, M. A., Huang, H., Dutil, E., Kaiser, D. A., Hunter, T. & Noel, J. P. (2000) Structure of the human anti-apoptotic protein survivin reveals a dimeric arrangement. Nat Struct Biol 7, 602-608.113

Vigneron, S., Prieto, S., Bernis, C., Labbe, J. C., Castro, A. & Lorca, T. (2004) Kinetochore localization of spindle checkpoint proteins: who controls whom? Mol Biol Cell 15, 4584-4596.194

Vong, Q. P., Cao, K., Li, H. Y., Iglesias, P. A. & Zheng, Y. (2005) Chromosome alignment and segregation regulated by ubiquitination of survivin. Science 310, 1499-1504.170

Vulsteke, V., Beullens, M., Waelkens, E., Stalmans, W. & Bollen, M. (1997) Properties and phosphorylation sites of baculovirus-expressed nuclear inhibitor of protein phosphatase-1 (NIPP-1). J Biol Chem 272, 32972-32978.347

Walczak, C. E. & Heald, R. (2008) Mechanisms of mitotic spindle assembly and function. Int Rev Cytol 265, 111-158.47

Wan, X., O'Quinn, R. P., Pierce, H. L., Joglekar, A. P., Gall, W. E., DeLuca, J. G., Carroll, C. W., Liu, S. T., Yen, T. J., McEwen, B. F. et al. (2009) Protein architecture of the human kinetochore microtubule attachment site. Cell 137, 672-684.187

Wang, Y., Satoh, A., Warren, G. & Meyer, H. H. (2004) VCIP135 acts as a deubiquitinating enzyme during p97-p47-mediated reassembly of mitotic Golgi fragments. J Cell Biol 164, 973-978.303

Watts, G. D., Wymer, J., Kovach, M. J., Mehta, S. G., Mumm, S., Darvish, D., Pestronk, A., Whyte, M. P. & Kimonis, V. E. (2004) Inclusion body myopathy associated with Paget disease of bone and frontotemporal dementia is caused by mutant valosin-containing protein. Nat Genet 36, 377-381.262

Wei, R. R., Al-Bassam, J. & Harrison, S. C. (2007) The Ndc80/HEC1 complex is a contact point for kinetochore-microtubule attachment. Nat Struct Mol Biol 14, 54-59.67

Welburn, J. P., Grishchuk, E. L., Backer, C. B., Wilson-Kubalek, E. M., Yates, J. R., 3rd & Cheeseman, I. M. (2009) The human kinetochore Ska1 complex facilitates microtubule depolymerization-coupled motility. Dev Cell 16, 374-385.157

Welburn, J. P., Vleugel, M., Liu, D., Yates, J. R., 3rd, Lampson, M. A., Fukagawa, T. & Cheeseman, I. M. (2010) Aurora B phosphorylates spatially distinct targets to differentially regulate the kinetochore-microtubule interface. Mol Cell 38, 383-392.152

Winkler, C., De Munter, S., Van Dessel, N., Lesage, B., Heroes, E., Boens, S., Beullens, M., Van Eynde, A. & Bollen, M. (2015) The selective inhibition of protein phosphatase-1 results in mitotic catastrophe and impaired tumor growth. J Cell Sci 128, 4526-4537.9

Wojcik, C., Yano, M. & DeMartino, G. N. (2004) RNA interference of valosin-containing protein (VCP/p97) reveals multiple cellular roles linked to ubiquitin/proteasome-dependent proteolysis. J Cell Sci 117, 281-292.341

Wolf, D. H. & Stolz, A. (2012) The Cdc48 machine in endoplasmic reticulum associated protein degradation. Biochim Biophys Acta 1823, 117-124.278

Wurzenberger, C. & Gerlich, D. W. (2011) Phosphatases: providing safe passage through mitotic exit. Nat Rev Mol Cell Biol 12, 469-482.57

Wurzenberger, C., Held, M., Lampson, M. A., Poser, I., Hyman, A. A. & Gerlich, D. W. (2012) Sds22 and Repo-Man stabilize chromosome segregation by counteracting Aurora B on anaphase kinetochores. J Cell Biol 198, 173-183.4

Xu, G., Paige, J. S. & Jaffrey, S. R. (2010) Global analysis of lysine ubiquitination by ubiquitin remnant immunoaffinity profiling. Nat Biotechnol 28, 868-873.331

Yamagishi, Y., Honda, T., Tanno, Y. & Watanabe, Y. (2010) Two histone marks establish the inner centromere and chromosome bi-orientation. Science 330, 239-243.120

Yamagishi, Y., Yang, C. H., Tanno, Y. & Watanabe, Y. (2012) MPS1/Mph1 phosphorylates the kinetochore protein KNL1/Spc7 to recruit SAC components. Nat Cell Biol 14, 746-752.78

Yamamoto, S., Tomita, Y., Hoshida, Y., Iizuka, N., Kidogami, S., Miyata, H., Takiguchi, S., Fujiwara, Y., Yasuda, T., Yano, M. et al. (2004) Expression level of valosin-containing protein (p97) is associated with prognosis of esophageal carcinoma. Clin Cancer Res 10, 5558-5565.313

Yamamoto, S., Tomita, Y., Hoshida, Y., Sakon, M., Kameyama, M., Imaoka, S., Sekimoto, M., Nakamori, S., Monden, M. & Aozasa, K. (2004) Expression of valosin-containing protein in colorectal carcinomas as a predictor for disease recurrence and prognosis. Clin Cancer Res 10, 651-657.318

Yamashiro, S., Yamakita, Y., Totsukawa, G., Goto, H., Kaibuchi, K., Ito, M., Hartshorne, D. J. & Matsumura, F. (2008) Myosin phosphatase-targeting subunit 1 regulates mitosis by antagonizing polo-like kinase 1. Dev Cell 14, 787-797.238

Yang, M., Li, B., Tomchick, D. R., Machius, M., Rizo, J., Yu, H. & Luo, X. (2007) p31comet blocks Mad2 activation through structural mimicry. Cell 131, 744-755.91

Ye, Q., Rosenberg, S. C., Moeller, A., Speir, J. A., Su, T. Y. & Corbett, K. D. (2015) TRIP13 is a protein-remodeling AAA+ ATPase that catalyzes MAD2 conformation switching. Elife 4.96

Ye, Y. (2006) Diverse functions with a common regulator: ubiquitin takes command of an AAA ATPase. J Struct Biol 156, 29-40.254

Ye, Y., Meyer, H. H. & Rapoport, T. A. (2003) Function of the p97-Ufd1-Npl4 complex in retrotranslocation from the ER to the cytosol: dual recognition of nonubiquitinated polypeptide segments and polyubiquitin chains. J Cell Biol 162, 71-84.268

Yeung, H. O., Kloppsteck, P., Niwa, H., Isaacson, R. L., Matthews, S., Zhang, X. & Freemont, P. S. (2008) Insights into adaptor binding to the AAA protein p97. Biochem Soc Trans 36, 62-67.274

Yu, H. (2007) Cdc20: a WD40 activator for a cell cycle degradation machine. Mol Cell 27, 3-16.83

Yuan, X., Simpson, P., McKeown, C., Kondo, H., Uchiyama, K., Wallis, R., Dreveny, I., Keetch, C., Zhang, X., Robinson, C. et al. (2004) Structure, dynamics and interactions of p47, a major adaptor of the AAA ATPase, p97. EMBO J 23, 1463-1473.294

Yuce, O., Piekny, A. & Glotzer, M. (2005) An ECT2-centralspindlin complex regulates the localization and function of RhoA. J Cell Biol 170, 571-582.180

Zachos, G., Black, E. J., Walker, M., Scott, M. T., Vagnarelli, P., Earnshaw, W. C. & Gillespie, D. A. (2007) Chk1 is required for spindle checkpoint function. Dev Cell 12, 247-260.129

Zhang, L., Qi, Z., Gao, Y. & Lee, E. Y. (2008) Identification of the interaction sites of Inhibitor-3 for protein phosphatase-1. Biochem Biophys Res Commun 377, 710-713.247

Zhang, S., Guha, S. & Volkert, F. C. (1995) The Saccharomyces SHP1 gene, which encodes a regulator of phosphoprotein phosphatase 1 with differential effects on glycogen metabolism, meiotic differentiation, and mitotic cell cycle progression. Mol Cell Biol 15, 2037-2050.23

Zhang, X., Shaw, A., Bates, P. A., Newman, R. H., Gowen, B., Orlova, E., Gorman, M. A., Kondo, H., Dokurno, P., Lally, J. et al. (2000) Structure of the AAA ATPase p97. Mol Cell 6, 1473-1484.310

Abbreviations

aa	amino acid
AAA	ATPases associated with diverse cellular activities
ALS	amyotrophic lateral sclerosis
APC/C	anaphase promoting complex / cyclosome
ATP	adenosine 5‘-triphosphate
ATPase	adenosine 5‘-triphosphatase
AurB	Aurora B
BAC	bacterial artificial chromosome
BCA	bicinchoninic acid
BIR	baculovirus IAP repeat
BS1	binding site 1
Bub	budding uninhibited by benomyl
BubR1	Bub-related 1
C	Conalbumin
CA	Carbonic anhydrase
Cand1	cullin-associated and neddylation-dissociated protein 1
CCAN	constitutive centromere-associated network
Cdc	cell division cycle
CDK	Cyclin-dependent kinase
cDNA	complementary DNA
CENP	centromere protein
CPC	Chromosomal passenger complex
CRL	Cullin-RING E3 ubiquitin ligase
DAPI	4',6-diamidino-2-phenylindole
DMEM	*Dulbecco's Modified Eagle Medium*
DNA	deoxyribonucleic acid
DOX	doxycycline
DTT	dithiothreitol
DUB	deubiquitinating enzyme
EC	error correction
ECL	enhanced chemiluminescence
EDTA	ethylenediaminetetraacetic acid

EMCCD	Electron-multiplying Charge-coupled Device
ER	Endoplasmic Reticulum
ERAD	ER-associated degradation
ERM	ezrin/radixin/moesin
FCS	fetal calf serum
FHA	ForkHead Associated
FPLC	fast protein liquid chromatography
FRET	fluorescence resonance energy transfer
FT	flowthrough
GFP	green fluorescent protein
Glc	GLyCogen
GST	*Glutathione* S-transferase
GTP	*guanosine*-5'-*triphosphate*
GTPase	*guanosine*-5'-*triphosphatase*
H	histone
HA	hemagglutinin epitope tag
HEK 293	Human Embryonic Kidney 293 cells
HeLa	Henrietta Lacks human cervical carcinoma cell line
HEPES	4-(2-hydroxyethyl)-1-piperazineethanesulfonic acid
HMW	high molecular weight
HP1	heterochromatin protein 1
HSC	heat shock cognate protein
HSP	heat shock protein
IAP	inhibitor of apoptosis
IBMPFD	inclusion body myopathy associated with Paget's disease of the bone and frontotemporal dementia
IF	immunofluorescence
INCENP	inner centromere protein
IP	immunoprecipitation
Ipl1	Increase in PLoidy 1
KMN	KNL1, Mis12, Ndc80
KNL1	kinetochore null protein 1
LAP	Localization and Affinity Purification tag
LMW	low molecular weight

LRR	leucine-rich repeats
Luc	luciferase
Mad	mitotic arrest deficient
MBP	myelin basic protein
MCAK	mitotic centromere-associated kinesin
MCC	mitotic checkpoint complex
Mis12	missegregation 12
MKLP2	mitotic kinesin-like protein 2
MPF	maturation-promoting factor
Mps1	monopolar spindle protein1
mRNA	messenger RNA
mRNP	mRNA-protein complex
MT	microtubule
MTOC	microtubule-organizing centers
MTS	3-(4,5-dimethylthiazol-2-yl)-5-(3-carboxymethoxyphenyl)-2-(4-sulfophenyl)-2H-tetrazolium)
Mypt1	myosin phosphatase-targeting subunit 1
Ndc80	nuclear division cycle 80
NEBD	nuclear envelope breakdown
NER	nucleotide excision repair
NHS	N-hydroxysuccinimide
NIPP1	Nuclear Inhibitor of PP1
NLS	nuclear localization signal
Npl4	*nuclear protein localization* protein 4
NSF	N-ethylmaleimide sensitive fusion *protein*
NuMA	nuclear mitotic apparatus *protein*
PAGE	polyacrylamide gel electrophoresis
PCM	pericentriolar matrix
PCR	polymerase chain reaction
PiP	PP1 interacting protein
PLK1	polo-like kinase 1
PP	protein phosphatase
PPP	phosphoprotein phosphatases
PTPA	PP2A phosphatase activator

PUB	peptide N-glycosidase / ubiquitin-associated
PUL	PLAA, Ufd3 and Lub1
R	Ribonuclease A
Repo-Man	Recruits PP1 Onto Mitotic Chromatin at Anaphase
RNA	ribonucleic acid
RNAi	RNA interference
SAC	spindle assembly checkpoint
SCF	Skp1, cullin and F box
SDS	*sodium dodecyl sulfate*
SEP	Shp1, eyes closed and p47
SH	Strep-HA
Shp1	suppressor of high-copy PP1
siRNA	small interfering RNA
SNARE	soluble NSF attachment protein receptor
SRH	second region of homology
Strep	streptavidin affinity tag
TACC	transforming acidic coiled-coil containing proteins
TE	Tris EDTA
Tris	Tris(hydroxymethyl)-aminomethan
Ub	ubiquitin
UBA	ubiquitin-associated
UBX	ubiquitin-regulatory X
UBXD	UBX domain-containing protein
UBXN-2	UBX-containing protein in Nematodes 2
Ufd1	ubiquitin fusion degradation protein 1
UPS	ubiquitin-proteasome system
VBM	VCP-binding motif
VCP	valosin containing protein
VIM	VCP-interacting motif
Ypi1	Yeast phosphatase inhibitor 1

Acknowledgements

First and foremost, I would like to thank Hemmo for giving me the opportunity to work on this exciting project and for his guidance, constant support and advice during the course of my work. Especially, I have to thank you for your patience during the writing period.

I would like to thank Mathieu Bollen and Andrea Musacchio for valuable discussions and insights concerning PP1 and mitosis and for supporting us with invaluable ideas and material. In this context, I would also like to thank the whole Bollen and Musacchio groups, especially Monique Beullens, Bart Lesage, Claudia Winkler, Veronika Krenn and Ivana Primorac.

Many thanks also to Monica Gotta, Elsa Kress, Patrick Meraldi and all the others involved in the UBXN-2/p37/p47 story for the opportunity to take part in this project.

Special thanks go to all the Very Cool People (i.e. the whole Mayer lab) for the amazing work atmosphere and all the fun we had and have inside and outside the lab. I would like to separately thank Annika and Matthias for the great collaboration within the PP1 subgroup.

I am especially thankful to my parents and brothers for their everlasting support and encouragement. Finally, I would like to thank Joy for her love and support and for the great time we've been having for the last 10 years and many more to come.

Curriculum vitae

Der Lebenslauf ist in der Online-Version aus Gründen des Datenschutzes nicht enthalten.

Affidavits / Erklärungen

Erklärung:

Hiermit erkläre ich, gem. § 6 Abs. (2) f) der Promotionsordnung der Fakultäten für Biologie, Chemie und Mathematik zur Erlangung des Dr. rer. nat., dass ich das Arbeitsgebiet, dem das Thema „Regulation and mitotic functions of the PP1 interactors SDS22 and Inhibitor-3“ zuzuordnen ist, in Forschung und Lehre vertrete und den Antrag von Jonas Seiler befürworte und die Betreuung auch im Falle eines Weggangs, wenn nicht wichtige Gründe dem entgegenstehen, weiterführen werde.

Essen, den _____ _____

Unterschrift eines Mitglieds der Universität Duisburg-Essen

Erklärung:

Hiermit erkläre ich, gem. § 7 Abs. (2) c) + e) der Promotionsordnung der Fakultäten für Biologie, Chemie und Mathematik zur Erlangung des Dr. rer. nat., dass ich die vorliegende Dissertation selbständig verfasst und mich keiner anderen als der angegebenen Hilfsmittel bedient habe.

Essen, den _____ _____

Unterschrift des/r Doktoranden/in

Erklärung:

Hiermit erkläre ich, gem. § 7 Abs. (2) d) + f) der Promotionsordnung der Fakultäten für Biologie, Chemie und Mathematik zur Erlangung des Dr. rer. nat., dass ich keine anderen Promotionen bzw. Promotionsversuche in der Vergangenheit durchgeführt habe und dass diese Arbeit von keiner anderen Fakultät/Fachbereich abgelehnt worden ist.

Essen, den _____ _____

Unterschrift des/r Doktoranden/in